UNIVERSITY OF
NEWCASTLE UPON TYNE

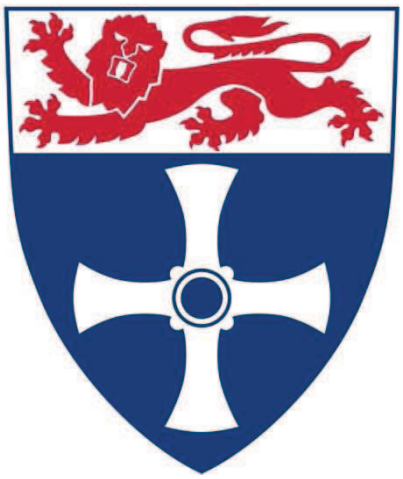

Wnt/Wg pathway activation in medulloblastoma and disease risk stratification

Hisham Megahed

Thesis submitted in partial fulfilment of the requirements

for the degree of Doctor of Philosophy

Newcastle University

Faculty of Medical Sciences

Northern Institute for Cancer Research

June 2010

Abstract

Despite improvements in the diagnosis and therapy of medulloblastoma (MB), the most common malignant paediatric brain tumour, survival rates are still only 40-60% for high-risk patients, and surviving patients offer suffer life-long therapy-associated late effects. Improving the current clinical disease risk classification may provide opportunities to tailor therapy to disease-risk more accurately, aiming to improve survival whilst minimizing late effects. The overall aim of this study was to identify and validate clinicopathological and molecular markers of prognostic significance in a large cohort of cases derived from the PNET3 clinical trial, which could be used in improved disease stratification schemes.

Initial investigations focussed on defects of chromosome 17, the most common chromosomal aberrations identified in MB, which have been associated with adverse outcome in some previous studies. During this initial study, methods for testing for regions of genetic loss in DNA samples extracted from routinely collected and stored pathology material were developed and validated. Using these methods, 17p loss was assessed in 284 cases overall, but did not show an association with poor prognosis. 17p loss was rare in patients <3 years at diagnosis (1/21 cases) compared to children aged >3 years (21/59, p=0.009), supporting the notion that infants with MB may represent a biologically distinct disease subgroup. During the course of this study, evidence of a microsatellite instability phenotype was also found in one case (1/29; 3.8%), suggesting a role for this phenomenon in a small subset of medulloblastomas.

Previous studies have identified MBs with activation of the Wnt/Wg signalling pathway to be associated with a favourable outcome. Three independent molecular markers of Wnt/Wg activation in medulloblastoma (β-catenin nuclear localization, *CTNNB1* mutation and chromosome 6 loss) have recently been identified, and were therefore assessed in the PNET3 cohort to examine their inter-relationships and relative prognostic utilities. β-catenin nuclear localization was detected in 34/207 (16.4%) cases, *CTNNB1* mutation in 20/197 (10.1%), and chromosome 6 LOH in 20/190 (10.5%); all three markers were highly associated with each other (p=0.001). Univariate survival analysis showed significant associations between clinicopathological (gender, pathology, M stage and extent of tumour resection) and molecular variables (β-catenin nuclear localization and *CTNNB1* mutation) with survival (all 'p' values <0.03) in the PNET3 cohort. Multivariate survival analysis and Cox proportional regression hazard analysis identified M stage, large cell / anaplastic pathology, gender and β-catenin nuclear staining to be significantly associated with prognosis (p<0.04), with hazard ratios of 1.924, 3.338, 0.57 and 0.215, respectively. Finally, combined models for disease risk prediction were constructed using the prognostically significant clinicopathological and molecular variables identified, including models to precisely classify the overall disease hazard for individual cases based on their clinical, pathological and molecular profile. In summary, Wnt/Wg pathway activation was associated with favourable outcome and can be most accurately identified using β-catenin nuclear staining. Combined models which incorporate Wnt/Wg status alongside other prognostically significant clinical and pathological indices validated in this study provide schemes for improved disease risk prediction in medulloblastoma, which should now be tested prospectively in large clinical trials.

Table of Contents

		Page
Contents		
	Abstract	
	Acknowledgement	
	Dedication	
	Table of contents	i
	List of Tables	ix
	List of Figures	xiii
	List of abbreviation	xvii
Chapter 1 :	Introduction	1
Chapter 2 :	Materials and methods	67
Chapter 3 :	The clinicopathological implications of chromosome 17p loss in medulloblastoma	118
Chapter 4 :	Wnt/Wg pathway activation in medulloblastoma: detection of β-catenin nuclear localization by immunohistochemistry	163
Chapter 5 :	Mechanisms of Wnt/Wg pathway activation in medulloblastoma: Mutation analysis of the *CTNNB1* gene	179
Chapter 6 :	Molecular correlates of Wnt/Wg pathway activation: analysis of chromosome 6 loss in medulloblastoma	195
Chapter 7 :	Assessment of the prognostic significance of clinicopathological and molecular disease features of the PNET3 cohort in univariate survival analysis	213
Chapter 8 :	Combination of clinical, histopathological and molecular markers for disease risk stratification in medulloblastoma	257
Chapter 9 :	Discussion	288
Chapter 10:	References	317
Chapter 11:	Appendices	331

Acknowledgement

I would like to thank everyone at the NICR who helped me during my study especially my colleagues in the molecular biology laboratory. In particular, I would like to express my deep gratitude and thanks to my supervisor, Professor Steven Clifford for his extensive guidance, support and help in almost every aspect of my work during the past four years. His unlimited help and patience in writing and revising my thesis is very well appreciated. His outstanding energy and wide knowledge were most inspiring and encouraging. Also, I would like to thank Dr. Simon Bailey for his kind supervision throughout my study, enlightened me with his knowledge, outstanding kindliness, support and helping in revising my thesis.

I would like to thank Dr. Meryl Lusher in particular for her technical guidance. Special thanks also, to Sarah Nicholson for her help in preparing and analysing the immunohistochemical studies.

I would like to thank the Egyptian government for funding my PhD for the last four years.

Finally, special thanks to my parents who have and still supporting me in every aspect of my life and their continuous believe in me.

Dedication

I would like to dedicate this thesis to my parents who have been a constant support and encouragement for me through out m whole life. Thank you for all the love and patience you provided me and keeping up with my swinging mood during the past years, I could never thank you enough.

To my sister, who also provided me with a lot of support and encouragement, especially when things seemed to be going the wrong way, her advice was of great value.

CONTENTS

	Page
Chapter 1: Introduction	1
1.1. Introduction to cancer	2
1.1.1. Oncogenes	6
1.1.2. Tumour suppressor genes	6
1.2. Childhood cancer	9
1.2.1. Incidence of childhood cancer	10
1.2.2. Brain tumours	11
1.3. Medulloblastoma	12
1.3.1. Incidence	13
1.3.2. Pathological features	13
1.3.3. Current diagnosis and management	19
1.3.3.1. Clinical presentation	19
1.3.3.2. Diagnosis of medulloblastoma	20
1.3.3.3. Current clinical classification and its influence on therapy decision	22
1.3.3.4. Limitations of the current clinical disease classification	24
1.3.3.5. Management of standard-risk medulloblastoma patients	25
1.3.3.6. Management of high-risk medulloblastoma patients	26
1.3.3.7. Management of medulloblastoma in very young patients	26
1.3.3.8. Treatment of relapsed medulloblastoma patients	27
1.3.3.9. Long-term treatment sequelae	28
1.3.3.10. Novel trials and therapeutic approaches	29
1.3.4. The molecular genetics of medulloblastoma	30
1.3.4.1. Chromosomal abnormalities in medulloblastoma	31
1.3.4.2. Familial cancer syndromes associated with medulloblastoma development	32
1.3.4.3. Disregulated cell-signalling pathways in medulloblastoma	35
1.3.4.4. Epigenetic mechanisms in medulloblastoma	38
1.4. The function and development of the cerebellum and relationships to medulloblastoma pathogenesis	40
1.4.1. Stem cells in medulloblastoma	46
1.5. Potential improvement of patients' outcome through the use of prognostic molecular markers for medulloblastoma	50

1.5.1. Requirements and difficulties facing the development and validation of molecular indices for prognostication in medulloblastoma 52
1.6. Role of the Wnt/Wg pathway in cancer development 53
1.6.1. Wnt/Wg pathway activation and medulloblastoma development 60
1.6.2. Clinical significance of Wnt/Wg pathway activation in medulloblastoma 63
1.7. Summary of this project 65
1.8. Aims of the project 65

Chapter 2: Materials and Methods 67
2.1. Materials 68
2.1.1. The NMB cohort of primary medulloblastomas 68
2.1.2. The PNET3 cohort of primary medulloblastoma samples 73
2.1.3. PNET3 primary medulloblastomas FFPE material 76
2.1.4. Medulloblastoma cell lines 82
2.2. Methods 83
2.2.1. DNA extraction 83
2.2.1.1. DNA extraction from tumour tissue and blood 83
2.2.1.2. DNA extraction from FFPE sections and curls 83
2.2.1.3. Assessment of DNA yielded and purity 84
2.2.2. Polymerase Chain Reaction (PCR) 87
2.2.2.1. PCR protocol used in this project 90
2.2.2.2. Primer design protocol used in this project 91
2.2.3. Analysis of PCR products using agarose gel electrophoresis 92
2.2.4. Detection of Loss of Heterozygosity (LOH) 93
2.2.4.1. Loss of heterozygosity (LOH) and cancer development 93
2.2.4.2. Analysis of LOH using the CEQ 8000 system 94
2.2.4.3. Interpretation of LOH results assessed by polymorphic microsatelitte markers 95
2.2.4.4. Analysis of LOH using the HOMOD method 99
2.2.4.5. Analysis of LOH using the conventional LOH (cLOH) method 101
2.2.5. Mutation analysis using direct DNA sequencing 107
2.2.5.1. Sequencing method 109
2.2.5.2. PCR for β-catenin gene (*CTNNB1*) 110
2.2.6. Immuno-histochemistry 111

2.2.6.1. Types of antibodies used 112
2.2.6.2. The direct method for antigen detection 113
2.2.6.3. The indirect method for antigen detection 113
2.2.6.4. Immunohistochemistry method used in this project 115
2.2.7. Statistical Analysis 117

Chapter 3 : The clinicopathological implications of chromosome 17p loss in medulloblastoma 118
3.1. Introduction 119
3.2. Aims 124
3.3. Materials and methods 125
3.3.1 Materials 125
3.3.1.1. The NMB cohort 125
3.3.1.2. The PNET3 cohort 125
3.3.2. Methods 125
3.3.2.1. DNA extraction 125
3.3.2.2. Polymerase chain reaction (PCR) 126
3.3.2.3. Agarose gel electrophoresis 126
3.3.2.4. Loss of heterozygosity analysis 126
3.3.2.5. Statistical analysis 126
3.4. Results 128
3.4.1. Validation of the HOMOD method by cLOH and aCGH 128
3.4.1.1. Validation of HOMOD by cLOH 128
3.4.1.2. Validation of HOMOD by aCGH 134
3.4.2. Evidence of MSI in the NMB cohort 137
3.4.3. Analysis of chromosome 17p LOH status in the NMB cohort 140
3.4.3.1. The incidence of chromosome 17p LOH status in the NMB cohort 140
3.4.3.2. Assessment of relationship between chromosome 17p LOH and clinicopathological variables in the NMB cohort 141
3.4.4. Analysis of chromosome 17p LOH status in the PNET3 cohort 146
3.4.4.1. The incidence of chromosome 17p LOH in the PNET3 cohort 146
3.4.4.2. Correlations of chromosome 17p LOH with clinical and pathological variables 146

3.4.4.3. Analysis of chromosome 17p LOH in the PNET3 cohort; survival analysis 151
3.5. Discussion 153
3.5.1. Validation of HOMOD as a method for the detection of genetic losses in FFPE tumour material 153
3.5.2. MSI in medulloblastoma 155
3.5.3. Chromosome 17p LOH in medulloblastoma and its clinico-pathological significance 157
3.5.4. Relationship between chromosome 17p LOH status and patients' outcome 160
3.6. Summary and conclusions 162

Chapter 4 : Wnt/Wg pathway activation in medulloblastoma: detection of β-catenin nuclear localization by Immunohistochemistry 163
4.1. Introduction 164
4.2. Aims 168
4.3. Materials and Methods 169
4.3.1. The PNET3 cohort 169
4.3.2. Detection of β-catenin nuclear immuno-reactivity by IHC 169
4.4. Results 170
4.4.1. β-catenin immuno-reactivity 170
4.4.2. Relationship to clinicopathological disease features 170
4.5. Discussion 176
4.6. Conclusions 178

Chapter 5: Mechanisms of Wnt/Wg pathway activation in medulloblastoma: Mutation analysis of the *CTNNB1* gene 179
5.1. Introduction 180
5.2. Aims 185
5.3. Materials and methods 186
5.3.1. The PNET3 cohort 186
5.3.2. DNA extraction and quality control 186
5.3.3. Polymerase chain reaction (PCR) 186
5.3.4. Mutation analysis of exon 3 of the *CTNNB1* gene 186
5.4. Results 187

5.4.1. Assessment of *CTNNB1* mutations 187
5.4.2. Assessment of the clinicopathological significance of *CTNNB1* mutations 187
5.5. Discussion 192
5.6. Conclusions 194

Chapter 6 : Molecular correlates of Wnt/Wg pathway activation: analysis of chromosome 6 loss in medulloblastoma 195
6.1. Introduction 196
6.2. Aims 200
6.3. Materials and methods 201
6.3.1. The PNET3 cohort 201
6.3.2. DNA extraction and quality control 201
6.3.3. Polymerase chain reaction (PCR) 201
6.3.4. Loss of heterozygosity analysis, using the HOMOD method 201
6.4. RESULTS 203
6.4.1. Assessment of chromosome 6 loss 203
6.4.2. The correlation between chromosome 6 status and clinicopathological disease features 203
6.5. Discussion 210
6.6. Conclusions 212

Chapter 7: Assessment of the prognostic significance of clinicopathological and molecular disease features of the PNET3 cohort in univariate survival analyses 213
7.1. Introduction 214
7.1.1. The prognostic significance of disease histopathology in medulloblastoma 214
7.1.2. The potential prognostic significance of patients' gender in medulloblastoma 218
7.2. Aims 220
7.3. Material and methods 222
7.3.1. PNET3 cohort, clinical, pathological and molecular variables 222
7.3.2. Statistical analysis 222
7.4. Results 224

7.4.1. Assessment of correlations between clinical and histopathological variables 224
7.4.2. Univariate survival analysis for the clinico-pathological features of the PNET3 cohort 226
7.4.2.1. OS and EFS characteristics of the PNET3 cohort 226
7.4.2.2. Assessment of relationships between age and survival 229
7.4.2.3. Relationships between other clinicopathological disease features and survival 230
7.4.3. Analysis of molecular variables 235
7.4.3.1. *CTNNB1* mutations 236
7.4.3.1.1. Incidence in the PNET3 cohort and its clinicopathological association 236
7.4.3.1.2. Univariate survival analysis 236
7.4.3.2. β-catenin nuclear localization 238
7.4.3.2.1. Incidence in the PNET3 cohort and clinicopathological associations 238
7.4.3.2.2. Univariate survival analysis 238
7.4.3.3. Chromosome 6 LOH 241
7.4.3.3.1. Incidence in the PNET3 cohort and clinicopathological associations 241
7.4.3.3.2. Univariate survival analysis 242
7.4.3.4. Correlations between molecular variables 244
7.4.3.5. Correlations between β-catenin nuclear localization, *CTNNB1* mutation and chromosome 6 LOH: Impact on patient survival 247
7.5. Discussion 250
7.5.1. Correlations between clinicopathological disease features 250
7.5.2. Correlations between molecular markers and clinicopathological disease features 250
7.5.3. Correlation between the molecular marker 251
7.5.4. Univariate survival analysis 252
7.5.4.1. Correlation between clinicopathological features and survival 252

7.5.4.2. Correlations between molecular markers and survival 253
7.6. Conclusions 255

Chapter 8: Combination of clinical, histopathological and molecular markers for disease risk stratification in medulloblastoma 257
8.1. Introduction 258
8.2. Aims 262
8.3. Materials and Methods 263
8.3.1. The PNET3 cohort 263
8.3.2. Statistical analysis 263
8.3.3. Variables used in multivariate survival analysis and their categorization 263
8.4. Results 265
8.4.1. Classification of cases using current clinical criteria 265
8.4.2. Investigation of statistical models based on combined clinical, pathological and molecular markers 266
8.4.2.1. A combination model for the prediction of disease risk based on 5 variables 268
8.4.2.2. A combination model for the prediction of disease risk based on 4 significant variables 269
8.4.2.3. A combined model for predicting disease risk based on 3 significant variables 272
8.4.2.4. Kaplan-Meier survival estimates applied to a model based on 3 variables 275
8.4.2.5. Interaction between Wnt/Wg subtype tumours and high-risk disease markers 277
8.4.2.6. Effect of gender and extent of tumour resection on survival in β-catenin positive cases 278
8.4.2.7. Interesting cases 280
8.5. Discussion 281
8.6. Conclusions 287

Chapter 9: Discussion 288
9.1. Introduction 289

9.2. Limitations of the current clinical classification in medulloblastoma 290
9.3. The initial aims of this study 290
9.4. Using an initial cohort to develop and validate the HOMOD method 291
9.5. Assessment of microsatellite instability in medulloblastoma 293
9.6. Age at diagnosis may define a distinct molecular subgroup of medulloblastomas 294
9.7. Assessment of the Wnt/Wg pathway in medulloblastoma 295
9.8. Molecular indices associated with Wnt/Wg pathway activation 295
9.9. The role of Wnt/Wg activation in disease risk stratification 297
9.10. The molecular bases of favourable prognosis in the Wnt/Wg subgroup medulloblastomas 298
9.11. The significance of chromosome 6 loss in medulloblastoma 298
9.12. The role of chromosome 17p LOH in medulloblastoma risk stratification 303
9.13. Further molecular markers in medulloblastoma 303
9.14. Development of clinico-biological models for medulloblastoma risk prediction 307
9.15. Constructing disease risk combination models for the prediction of hazard ratios in medulloblastoma 309
9.16. Incorporation of other prognostic biological markers in future disease risk stratification and practical challenges 311
9.17. The current study provides a better disease risk prediction model compared to the models reviewed in the literature 313
9.18. Applying similar disease risk assessment in medulloblastoma patients aged <3 years at diagnosis 314
9.19. Summary of the project 315

Chapter 10: References 317

Chapter 11: Appendices 331

List of Tables

		Page
Chapter 1: Introduction		
Table 1.1.	The biological functions and mechanisms of 6 common oncogenes in cancer	8
Table 1.2.	Common TSGs and associated cancers	9
Table 1.3.	World Health Organization classification of embryonal tumours (including medulloblastoma), 1993-2007	15
Table 1.4.	Chang Staging System for medulloblastoma	23
Table 1.5.	Medulloblastoma Risk Staging	24
Table 1.6.	Medulloblastoma in hereditary cancer syndromes	34
Table 1.7.	Genetic defects reported in medulloblastoma	39
Table 1.8.	Molecular and histopathological markers of disease-risk stratification in medulloblastoma	51
Table 1.9.	Known and putative regulators of β-catenin signalling	59
Chapter 2: Materials and Methods		
Table 2.1.	Clinical data of the NMB cohort of 72 medulloblastoma tumour tissue sample	72
Table 2.2.	Descriptive analysis of the NMB cohort: clinical and pathological variables	73
Table 2.3.	Detailed individual clinical data for the PNET3 cohort	77
Table 2.4.	Descriptive statistics for age follow up period, time to recurrence and event free survival of the PNET3 cohort	81
Table 2.5.	Descriptive analysis of clinical variables for the PNET3 cohort	81
Table 2.6.	Medulloblastoma cell lines	82
Table 2.7.	Tumour tissue DNA extraction, showing DNA concentration, yield and volume	85
Table 2.8.	Blood DNA extraction, showing DNA concentration, yield and volume	86
Table 2.9.	Standard PCR reaction reagents and concentrations.	90
Table 2.10.	The sequence of the forward and reverse specific primers used for amplification of exon 3 of *CTNNB1*	110
Table 2.11.	PCR reaction used for amplification of *CTNNB1* gene	111
Table 2.12.	PCR program used for amplifying *CTNNB1* gene	111

Chapter 3: The clinicopathological implications of chromosome 17p loss in medulloblastoma

Table 3.1. The incidence of chromosome 17p LOH and its correlation to survival in the studies reported in the literature. 124

Table 3.2. Chromosome 17p microsatellite primers 127

Table3.3. Comparison of chromosome 17p LOH status, assessed by cLOH and HOMOD in 26 samples 129

Table 3.4. Comparison between the Analysis of chromosome 17p LOH status using Array CGH and HOMOD 135

Table 3.5. Assessment of MSI in the 5 cases which showed evidence of MSI during validation of HOMOD, using additional microsatellite markers 137

Table 3.6. Chromosome 17p LOH analysis in the PNET3 cohort using HOMOD 148

Table 3.7. Correlation between Chromosome 17p LOH and clinicopathological variables in the PNET3 cohort (n= 190) 150

Chapter 4: Wnt/Wg pathway activation in medulloblastoma: detection of β-catenin nuclear localization by Immunohistochemistry

Table4.1. Results of different studies and the current study of β-catenin nuclear localization by IHC in medulloblastoma, and methodologies used. 167

Table 4.2. Degree of β-catenin immuno-reactivity in 207 cases assessed 175

Table 4.3. Correlation between β-catenin nuclear localization and clinicopathological variables in 207 medulloblastomas 175

Table 4.4. The clinicopathological profile of the 4 cases with positive β-catenin IHC and M2/3 metastatic stage 175

Chapter 5: Mechanisms of Wnt/Wg pathway activation in medulloblastoma: Mutation analysis of the *CTNNB1* gene

Table 5.1. Frequencies of *CTNNB1* mutations reported in the literature and the current study. 184

Table 5.2. *CTNNB1* nucleotide mutations and corresponding amino acid alterations detected in the PNET3 cohort (n= 20) 189

Table 5.3. Correlation between *CTNNB1* status and clinicopathological variables 191

Chapter 6: Molecular correlates of Wnt/Wg pathway activation: analysis of chromosome 6 loss in medulloblastoma

Table 6.1. Incidence of chromosome 6 LOH in different studies 199

Table 6.2. Polymorphic microsatellite markers used for the analysis of chromosome 6 LOH 202

Table 6.3. Complete data of chromosome 6 LOH status analysis in the PNET3 cohort using 6 microsatellite markers 207

Table 6.4. Correlation between chromosome 6 LOH and clinicopathological variables in the PNET3 cohort (n= 190) 209

Chapter 7: Assessment of the prognostic significance of clinicopathological and molecular disease features of the PNET3 cohort in univariate survival analyses

Table 7.1. Inter-correlation matrix for clinicopathological variables within the PNET3 cohort 224

Table 7.2. Correlation between extent of tumour resection, pathology and metastatic stage at time of diagnosis in the PNET3 cohort 225

Table 7.3. Survival analysis for age grouped in 2 year intervals 230

Table 7.4. Summary of overall survival analyses for clinicopathological variables (Log-rank test) 231

Table 7.5. Summary of event free survival analysis for clinicopathological variables (Log-rank test) 231

Table 7.6. Correlations between β-catenin immuno nuclear reactivity patterns and *CTNNB1* mutation status 245

Table 7.7. Assessment of associations between *CTNNB1* mutations, β-catenin nuclear staining, Chromosome 6 LOH and Chromosome 17p LOH status. 245

Table 7.8. Correlations between β-catenin nuclear localization and *CTNNB1* mutations, Chromosome 6 status and chromosome17p statuses 246

Table 7.9. Correlations between chromosome 6 status and chromosome 17p Status β-catenin nuclear localization status and *CTNNB1* mutation status 246

Table 7.10. Summary of cases displaying combinations of Wnt/Wg associated molecular markers. 248

Chapter 8: Combination of clinical, histopathological and molecular markers for disease risk stratification in medulloblastoma

Table 8.1. Survival analysis using current clinical stratification based on metastatic stage and extent of tumour resection 265

Table 8.2. Summary of Cox regression univariate survival analyses for clinical and molecular variables 267

Table 8.3. Cox proportional regression hazard model incorporating 5 variables 269

Table 8.4. Multiple multivariate Cox proportional hazard regression model incorporating β-catenin status, pathology, gender and metastatic stage at time of diagnosis 270

Table 8.5. Multiple Cox proportional regression hazard models based on 4 variables; β-catenin, pathology, metastatic stage and gender applied on the PNET3 cohort 271

Table 8.6. Multiple multivariate Cox proportional hazard regression modelincorporating β-catenin status, pathology and metastatic stage at time of diagnosis 273

Table 8.7. Multiple Cox proportional regression model based on β-catenin status, M-stage and pathology groupings applied on the PNET3 274

Table 8.8. Survival analysis for risk groups defined by β-catenin nuclear localization, metastatic stage and pathology variables 276

Table 8.9. Survival analysis for metastatic stage and pathology variables in cases with β-catenin nuclear positivity 277

Table 8.10. The clinicopathological profile of cases with β-catenin nuclear localization and had interesting outcome 280

List of Figures

	Page
Chapter 1: Introduction	
Figure 1.1. The 20 most common causes of death from cancer in UK 2008	2
Figure 1.2. Number of deaths from cancer in the UK 2006	4
Figure 1.3. Acquired capabilities of cancer cells	5
Figure 1.4. Annual average number of deaths from malignancy in children under 15, diagnosed with cancer, by diagnostic group and sex in Great Britain, 1997-2001	10
Figure 1.5. Number of new cases and rates, by age and sex, all malignant neoplasms UK 2006	11
Figure 1.6. The percentage of patients alive 5 years after diagnosis, childhood cancers in Great Britain, 1992-1996	12
Figure 1.7. Histopathological variants of medulloblastoma	19
Figure 1.8. MRI of a child with medulloblastoma	21
Figure 1.9. Precursor cell population in the developing and adult cerebellum	43
Figure 1.10. Potential cellular and molecular origins of medulloblastoma subtypes	44
Figure 1.11. The role of SHH pathway in normal development of the cerebellum	45
Figure 1.12. Medulloblastoma can arise as an aberration of cerebellar development	46
Figure 1.13. Potential cellular origin of medulloblastoma	48
Figure 1.14. Developing targeted therapies for medulloblastoma	53
Figure 1.15. Summary of the canonical Wnt signalling pathway	56
Figure 1.16. Diagram of β-catenin and the mutations identified in cancer	58
Chapter 2: Materials and Methods	
Figure 2.1. Age at diagnosis of the NMB cohort distributed in one year intervals.	70
Figure 2.2. Age distribution of the PNET3 cohort in 2 year intervals.	76
Figure 2.3. Polymerase chain reaction (PCR).	89
Figure 2.4. Polymorphic microsatellite markers demonstrating different patterns of homozygosity	97
Figure 2.5. Polymorphic microsatellite markers demonstrating different	98

patterns of heterozygosity.
Figure 2.6. Polymorphic microsatellite markers for 17p LOH analysis using HOMOD. 100
Figure 2.7. (A-D). Assessment of chromosome 17p LOH using PCR-based polymorphic microsatellite markers using cLOH. 102
Figure 2.8. Automated DNA sequence analysis using the Sanger direct DNA Sequencing method. 108
Figure 2.9. Direct method of IHC staining 113
Figure 2.10. The indirect method. 114

Chapter 3: The clinicopathological implications of chromosome 17p loss in medulloblastoma

Figure 3.1. Analysis for chromosome 17p LOH status using cLOH and HOMOD methods in 26 medulloblastoma samples 129
Figure 3.2. (A-D) Assessment of chromosome 17p LOH using PCR-based polymorphic microsatellite markers using cLOH 130
Figure 3.3. Array CGH analysis of chromosome 17 status 135
Figure 3.4. Chromosome 17p microsatellite instability status 138
Figure 3.5. Analysis of 17p LOH status in 76 cases from the NMB cohort using HOMOD 140
Figure 3.6. Chromosome 17p LOH status in age stratified risk groups (n=72) 141
Figure 3.7. Analysis of the distribution of chromosome 17p LOH status with age. cases are shown grouped in one year intervals 142
Figure 3.8. Assessment of the relationship between 17p LOH analysis and gender 143
Figure 3.9. The correlation between 17p LOH and histopathological Subtypes in 72 medulloblastoma cases 144
Figure 3.10. Assessment of correlation between 17p LOH and metastatic stage at time of diagnosis (67 cases) 145
Figure 3.11. Survival analysis for chromosome 17p LOH status in the PNET3 cohort 152

Chapter 4. Wnt/Wg pathway activation in medulloblastoma: detection of β-catenin nuclear localization by Immunohistochemistry

Figure 4.1. Immuno-histochemical assessment of β-catenin in 171

medulloblastoma

Chapter 5. Mechanisms of Wnt/Wg pathway activation in medulloblastoma: mutation analysis of the *CTNNB1* gene

Figure 5.1. Chromosome 3 and corresponding *CTNNB1* gene 181

Figure 5.2. PCR amplification of *CTNNB1* gene exon 3 189

Figure 5.3. Direct sequencing of *CTNNB1* in medulloblastoma demonstrating:(A) *CTNNB1* sequence analysis showing wild-type sequence of exon 3 residues 30-40 in forward direction (B) *CTNNB1* sequence analysis showing wild-type sequence of exon 3 residues 50-40 in reverse direction (C) Mutation at codon 33 (TCT>TTT) in forward direction and 33 (AGA>AAA) in reverse direction (arrows) 190

Chapter 6: Molecular correlates of Wnt/Wg pathway activation: analysis of chromosome 6 loss in medulloblastoma

Figure 6.1. Assessment of chromosome 6 LOH by HOMOD using PCR-based polymorphic microsatellite markers 204

Figurer 6.2. Illustration analysis of chromosome 6 LOH markers using HOMOD in PNET3 cases 206

Chapter 7 Assessment of the prognostic significance of clinicopathological and molecular disease features of the PNET3 cohort in univariate survival analyses

Figure 7.1. Kaplan-Meier survival analysis for overall survival of the PNET3 cohort (n=208) 227

Figure 7.2. Kaplan-Meier analysis for event free survival for the PNET3 cohort 227

Figure 7.3. Overall survival analysis for treatment 228

Figure 7 4. Kaplan-Meier survival curves for age grouped in 2 year intervals 229

Figure 7.5. Overall survival analysis for clinicopathological variables 232

Figure 7.6. Event free survival analysis for clinicopathological variables 234

Figure 7.7. Kaplan Meier survival estimate for *CTNNB1* mutated and wild-type cases in the PNET3 cohort 237

Figure 7.8. overall survival (A) and event free survival(B) for β-catenin nuclear localization by immuno-histochemistry, positive cases versus negative cases 240

Figure 7.9. Kaplan Meier estimates of survival associations with the degree of β-catenin immuno-reactivity observed in cases with positive nuclear reactivity 241
Figure 7.10. Relationship between chromosome 6 status and overall survival (OS) (A) and Event free survival (B) 243
Figure 7.11. Venn diagram showing the correlation between *CTNNB1* mutations, β-catenin nuclear localization and chromosome 6 LOH in 184 cases from the PNET3 cohort 248
Figure 7.12. Survival analysis for Wnt/Wg associated marker groupings shown in Table 7.10 249

Chapter 8: Combination of clinical, histopathological and molecular markers for disease risk stratification in medulloblastoma

Figure 8.1. Survival analysis based on clinical stratification variables 266
Figure 8.2. Survival analysis for favourable (blue), standard (green) and high (red) risk groups defined by β-catenin nuclear localization, metastatic stage and pathology variables 276
Figure 8.3. Kaplan Meier survival curves for M-stage and pathology variables in cases with positive β-Catenin nuclear positivity 278
Figure 8.4. Kaplan Meier survival curves for gender variable in cases with β-catenin nuclear positivity 278
Figure 8.5. Survival analysis for extent of tumour resection in cases with positive nuclear β-catenin 278

List of Abbreviations

ALL	Acute lymphoblastic leukaemia
AMP	Antigen machinery process
APC	Adenomatous Polyposis Coli
ATCC	American type Culture Collection
ATP	Adenose triophosphates
AXIN1	Axix inhibitory gene
BCC	Basal cell carcinoma
BCR-ABL	Philadelphia chromosome (oncogene fusion protein)
β-2m	Beta 2- microglobulin
Bp	Base pairs
BRCA1	Breast cancer-1 gene
BRCA2	breast cancer-2 gene
BTRC	Beta-transducin repeat-containing protein
C	Classic
CASP8	Apoptosis-related cysteine protease 8 gene
CpG	Guanine-phosphate-diester-cystine
CBP	CREB-binding protein
CCNU	1-(2-chloroethyl)-3-cyclohexyl-1-nitrosourea
CCLG	Childrens Cancer Leukaemia Group
CDK	Cyclin dependent kinase
CGH	Comparative genomic hybridisation
Ci	Cubitus interruptus
cLOH	Conventional loss of heterozygosity
CNS	Central nervous system
COBRA	combined bisulphite restriction analysis
COL1A2	Collagen, type 1, α2 gene
Cos2	costal 2
CSA	Cranio spinal axis
CSC	Cancer stem cells
CSF	Cerebrospinal fluid
CSI	Craniospinal irradiation
CSS	Coffin-Siris syndrome

CSRT	Cranio spinal radiotherapy
CT	Computed tomography
CTL	Cytotoxin T lymphocytes
CTNNB1	β-catenin gene
DAB	Diaminobenzidine
dATP	Deoxyadenosine triphosphate
dCTP	Deoxycytosine triphosphate
dGTP	Deoxyguanosine triphosphate
DHH	Desert Hedgehog
DHPLC	Denaturing high performance liquid chromatography
DMEM	Dulbecco's modified Eagle's medium
DMSO	Dimethylsulphoxide
DNA	deoxyribonucleic acid
DNMT	DNA methylytransferases
dNTP	Deoxynucleotide triphosphate
dTTP	Deoxythymine triphosphate
EDTA	Ethylenedinitrilo tetraacetic acid
EGER	Epidermal growth factor receptor
EGL	External granule layer
Emboss	The European Molecular Biology Open software suite
ERBB2	Erythroblastic leukaemia viral oncogenes homolg 2
EFS	Event free survival
ERH	Extended regions of homozygosity
ERK	Extracellular signal-regulated kinase
FACS	Fluorescent-activated cell sorting
FAP	Familial adenomatous Polyposis syndrome
FBS	Phosphate buffered saline
FCS	Foetal calf serum
FFPE	Formalin fixed-paraffin embedded
FISH	fluorescence in situ hybridisation
FU	Fused
GLI	Glioma-associated homolog
GNPC	Granule neurone precursor cell
***GSK3*-β**	Glycogen synthase kinase 3β
HCL	Hydrochloric acid

HDAC	Histone deactylase
HDCT	High dose chemotherapy
HERT	Hyper-fractionated radiotherapy
Hh	Hedgehog
HICl	Hypermethylated in cancer 1
HIP	Hedgehog interacting protein
HLA	Human leukocyte antigen
His	Histidine
H & E stain	Haematoxylin and eosin stain
HOMOD	Homozygous Mapping Of Deletions
HNPCC	Hereditary Non Polyposis Colorectal cancer syndrome
HT	Heterozygosity
h-TRT	Human telomerase reverse transcriptase
IGL	Internal granular layer
IGF2	Insulin-like growth factor 2
IMEMZO	Improved minimal essential medium with zinc option
KDa	Kil Daltons
LC/A	Large cell/Anaplastic
LEF	Lymphoid enhancer-binding factor
LOH	Loss of heterozygosity
MB	Medulloblastoma
MBEN	Medulloblastoma with extensive nodularity
MCR	Mutation cluster region
MDBP	Methyl-CpG binding domain
MDM2	Mdm2-transformed 3T3 cell double minute2, P53 binding protein
MECP2	Methyl-CpG-binding protein 2
MHC	Major histocompatability complex
m-iRNA	micro-RNA
MRI	Magnetic resonance image
MRS	Magnetic resonance spectroscopy
mRNAL	Messenger RNA
MMR	Mismatch repair
MRS	Magnetic resonance spectroscopy
MSI	Microsatellite instability
M S	Metastatic staging

MSP	Methylation specific polymerase chain reaction
MYCC	Human homolog of V-MYC Avian myelcytomatosis viral oncogen
NI	Non informative
NICR	Northern Institute for Cancer Research
NMBT	Newcastle medulloblastoma tumour
ND	Nodular desmoplastic
N2	Neural cell growth supplement
NBCCS	Naevoid basal cell carcinoma syndrome
ncRNA	non-coding RNA
NEB	New England Biolabs
Ng	Nanogram
OS	Overall survival
PCR	Polymerase chain reaction
PDGFR-β	Platelet-derived growth factor receptor beta polypeptide
RAS	Res protein gene
REP	RNA binding protein
RET	Retention of heterozygosity
PI3K	Phosphatidyl enositol 3-kinase
PNET	Primitive neuroectodermal tumour
PTCH/PTCH1	Human Patched gene
Ptc/Ptch	Drosophila/mouse homolog of the Patched gene
PTEN	Phosphate and tensin homolog
RASSFIA	RAS association domain family 1
RB	Retinoblastoma protein
RBI	Retinoblastoma gene
RELP	Restriction fragment length polymorphism
RNA	Ribonucleic acid
Rpm	Revolutions per minute
RTK	Receptor tyrosine kinase
RTS	Rubensteinn-Taybi syndrome
SD	Standard deviation
SE	Standard error
SHH	Sonic Hedgehog
SIOP	International Society for Pediatric Oncology
SLS	Sample loading solution

SMO/Smo	Smoothened
Spect	Single photon emission computed tomography
SSCP	Single stranded conformational polymorphism
Std	Standard size marker
SUFU	Human Suppressor of Fused
Su(Fu)SuFu	Drosophila/Mouse homolog suppressor of fused
SVZ	Sub ventricular zone
TAP	Transporter associate with antigen processing
TBE	Tris Boric acid
TBS	Tri-buffered saline
TE	Tri-EDTA buffer
Tris	Tris (hydroxymethyl) aminomethan
TP53	Tumour protein 53 gene
TRCF	Transforming growth factor receptor
TS	Turcot's syndrome
TS1	Turcot's syndrome type1
TS2	Turcot's syndrome type 2
TSG(s)	Tumour suppressor gene(s)
USS	Unstained sections
UKCCSG	United Kingdom Children's Cancer Study Group
UV	Ultraviolet
VHL	von Hippe1-Lindau
VZ	Ventricular zone
WHO	World Health Organization
Wnt/Wg	Wingless signalling pathway

Chapter 1

Introduction

1.1. Introduction to cancer

Cancer can be described as rapid, uncontrolled cell growth which exceeds its normal boundaries. Cancer cells have the capability to spread locally, and may invade adjacent tissues, through the lymphatic or blood systems. Cancer is one of the leading causes of death worldwide, accounting for 7.9 million deaths in 2007 (World Health Organization, 2007).

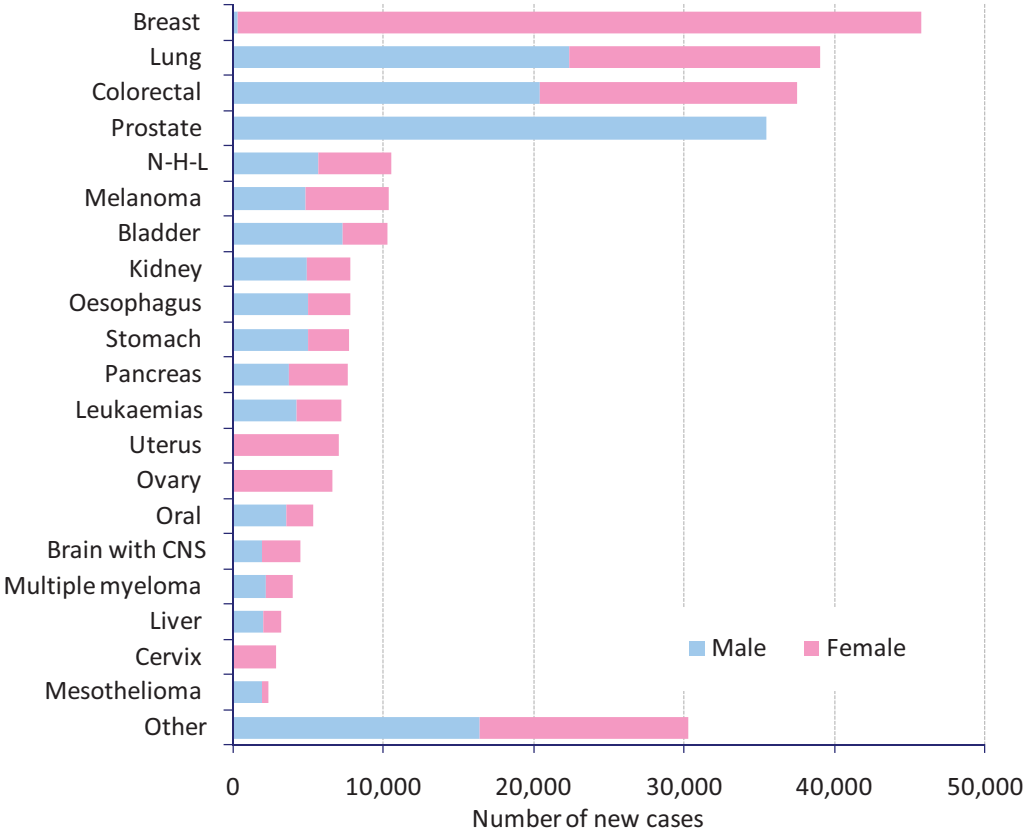

Figure 1.1. The 20 most common new cases caused from cancer in the UK, 2008 (Adapted from, www.cancer recearchuk.org).

Almost any organ in the human body can be affected by cancer, however breast, lung, colorectal and prostate cancer are the most common in the UK (Figure 1.1), together accounting for 47% of all cancer deaths (Figure 1.2). The frequency and incidence of cancer among the human population seems to be increasing over the last few decades; a number of factors may contribute, including increases in the degree of exposure to DNA damaging agents which increase the chance for accumulation of DNA defects leading to mutations and eventually cancer development. These hazardous agents include radiation and carcinogens incorporated in chemicals, food additives, preservatives and tobacco smoke, however, while some strong association do exist (e.g. between tobacco smoke and various cancers, or radiation and melanoma) many of these potential hazards have not been significantly linked to specific types of cancer and research is ongoing to clarify these risks. One clear factor for the apparent increase in cancer rates is the advancements in the methods by which better detection and early diagnosis can now be generally achieved (Packer et al 1999).

It is believed that one in every 3 people will develop one kind of cancer in their life time. In the UK, cancer is considered the second most common cause of death, representing 26% of deaths in 2003 (King and Robins 2006). The highest death rates occur from lung, colorectal and breast cancers respectively.

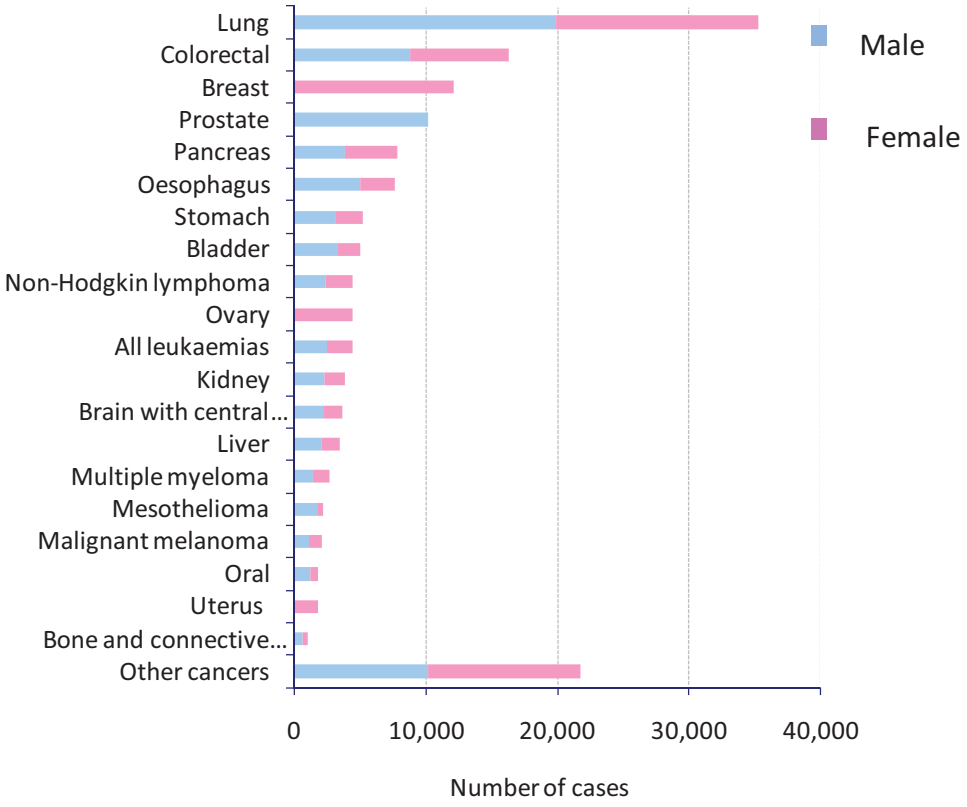

Figure 1.2. Number of cases from cancers in the UK in 2008 (adapted from www.info.cancer research uk.org/cancerstats).

Carcinogenesis occurs as a result of DNA mutations of a single originating cell. These changes can be due to external agents (e.g. chemicals or irradiation) or inherited genetic causes. In order for a normal cell to convert into a cancerous cell, at least six successive mutations have been postulated as necessary to occur. Since the chance of a single cell undergoing six successive independent mutations is almost impossible, two major mechanisms have been identified which may permit such an accumulation of events to happen. First, certain mutations allow cell proliferation, which provide an expanded target cell population favouring a second mutation. Secondly, certain

mutations affect the stability of the genome at the DNA or chromosomal level, which increases the general mutation rate (Strachan and Reed 2004).

The six fundamental and functional properties which are believed to be necessary to all cancer cells, and which allow for their immortality are; (i) self-sufficiency from growth signals, (ii) insensitivity to anti-growth signals, (iii) overcoming apoptosis, (iv) unrestrained replicative potential, (v) sustained angiogenesis and (vi) tissue invasion and metastasis (Strachan and Reed 2004, King and Robins 2006) (Figure 1.3).

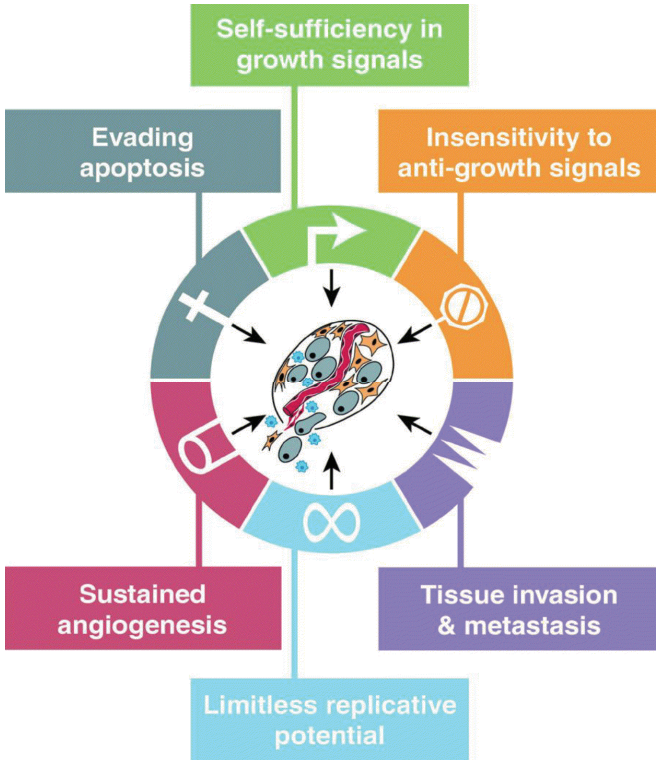

Figure 1.3. Acquired capabilities of cancer cells. Most cancer cells acquire the same set of functional capabilities during their development (Figure taken from Hanahan and Weinberg, 2000).

Mutations in certain specific gene classes have been proven to drive cells to become cancer cells; these genes include oncogenes and tumour suppressor genes (TSGs). In addition, TSGs may be further sub-classified as caretakers (encoding proteins which stabilize the genome preventing accumulation of mutations) and gatekeepers (encoding proteins that prevent growth of potential cancer cells and cellular proliferation). Landscaper genes (encoding proteins which contribute to tumorigenesis when mutated), also play roles in tumour development (King and Robins 2006). These gene classes are reviewed in the following sections.

1.1.1. Oncogenes

Proto-oncogenes are the normal non-mutated form of oncogenes, which act dominantly through gain of function mutations to promote the cancer phenotype. Five main classes of oncogenes have been identified which control cellular functions. These functions have been shown to be disrupted in cancer (Table 1.1). These include; secreted growth factors, cell surface receptors, intracellular signal transduction systems, DNA-binding nuclear proteins and the components of the cyclin network of cell cycle control, including cyclin-dependent kinases and kinase inhibitors (Strachan and Reed 2004).

1.1.2. Tumour suppressor genes

Tumour suppressor genes inhibit cell proliferation, promote apoptosis and stabilize the genome ensuring DNA replication and repair. In 1971, Knudson proposed the two-hit hypothesis through his studies on retinoblastoma (Knudson, 2001). This led to the theory that loss of function and inactivation of the two copies of tumour suppressor

genes is required for cancer development. Tumour suppressor genes can become inactivated through several genetic mechanisms including gene conversion, recombination, DNA point mutation and homozygous deletion. Loss of one of the alleles of a TSG usually leads to loss of heterozygosity of the locus containing that TSG, a hallmark which can allow the identification of loci which may harbour TSGs. Examples of common TSGs are shown in Table 1.2.

Oncogenes	Location	Function	Mechanism of activation	Cancer associated
PDGFB	22q13.1	Growth factor	Translocation to transcriptionally active region (Col1A1) Point mutation	Dermatofibrosarcoma (skin cancer), fibroblastoma
EGFR	7p12	Growth factor receptor	Amplification point mutation	Glioma, NSCLC
HRAS	11p15.5	Component of signal transduction pathway	Point mutation amplification	Colorectal, bladder, rhabdomyosarcoma
MYCC	8q24.1	DNA binding transcription factor	Translocation to transcriptionally active region (IGH,*BCL*5) Amplification Transcriptional activation Point mutations	Burkitt's lymphoma, B-CLL, breast, prostate, colorectal
BCL-2	18q21.3	Anti-apoptotic	Translocation to transcriptionally active region Transcriptional activation	N-H-L, CLL, melanoma breast, prostate, lung
BCR-ABL	t(9;22) (q34;q11)	Novel tyrosine kinase	Translocation creating a novel chimeric gene	CML, ALL

Table 1.1. The biological functions and mechanisms of activation of 6 common oncogenes in cancer. N-H-L= Non Hodgkin-Lymphoma; CLL= Chronic lymphoblastic leukaemia; CML= Chronic myelogenous leukaemia; IGH= Immunoglobulin heavy chain locus; B-CLL= B cell chronic lymphocytic leukaemia; ALL= Acute lymphoblastic leukaemia; NSCLC= Non-small-cell lung cancer. Data collected from the Cancer Genome Project, Welcome Trust Sanger Institute; (www.sanger.ac.uk/genetics/CGP/Census/:www.en.wikipedia.org;Strachan and Reed 2004).

Tumour suppressor gene	Chromosomal location	Function	Associated tumours
APC	5q21-22	Loss of β-catenin function Altered cell migration and chromosome instability	Familial adenomatosis polyposis, colorectal carcinoma
BRCA1	17q12-21	DNA repair	Breast and ovarian carcinoma
DCC	18q21	Induce apoptosis	Colon carcinoma
RB1	13q14	Inhibit cell cycle progression	Retinoblastoma, osteosarcoma, breast, bladder and lung carcinomas, others
TP53	17p13.1	DNA repair Induce cell growth arrest Initiate apoptosis	Breast, colon and lung carcinomas, osteosarcoma, astrocytoma, others
WT1	11p12	Control transcriptional factors Induce apoptosis and differentiation	Wilms tumour

Table 1.2. Common TSGs and associated cancers. Adapted from (Franks and Teich 1997).

1.2. Childhood cancers

The most common cancer affecting the paediatric population, accounting for 30% of childhood cancer cases, is leukaemia, followed by brain tumours, which account for 20% of cases. Figure 1.4 shows the death rates from cancers in children below 15 years of age in the UK between 1997 and 2. Advancements in diagnostic and therapeutic methodologies over the last few decades have resulted in a dramatic improvement in survival rates for children with cancer overall. Survival rates for patients with acute lymphoblastic leukaemia (ALL), the most common type of leukaemia in childhood, have now reached 80% (Tubergen et al 1993), while other

cancers including brain tumour still carry significantly worse overall survival rates of approximately 65%.

1.2.1. Incidence of childhood cancer

The incidence of cancer in the population overall is directly proportional to the patients' age, since with a longer life-span, the higher the chance for cells' exposure to various carcinogens and mutations to occur. However, children are at risk of developing cancers, particularly within certain organs systems (mainly leukaemia, lymphomas, CNS tumours, embryonal tumours and bone tumours) (Figure 1.5). Over 1500 newly diagnosed cancers are reported within childhood in the UK every year.

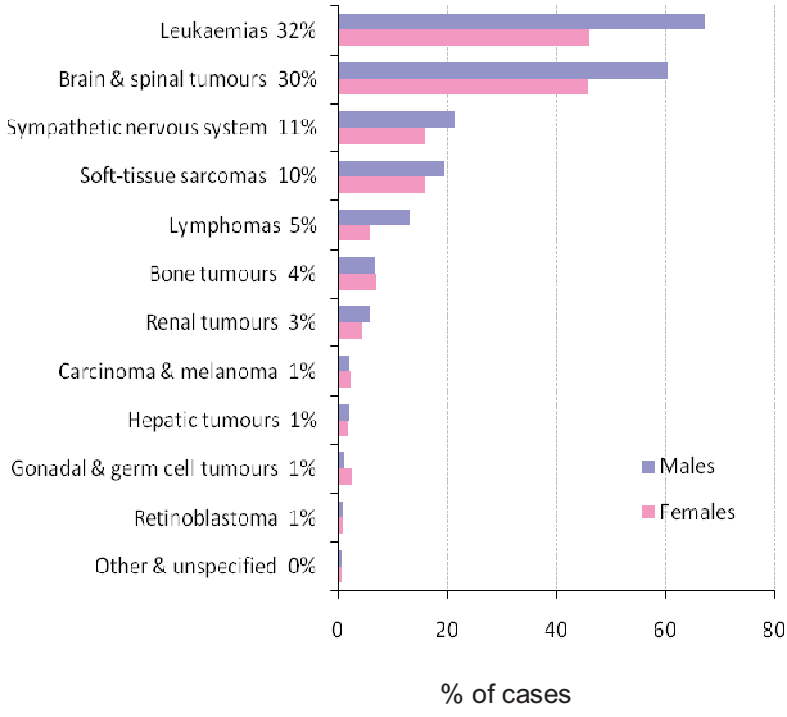

Figure 1.4. Annual average number of deaths from malignancy in children aged under 15, diagnosed with cancer, by diagnostic group and sex in Great Britain, 1997-2001. (Adapted from www.info.cancer research uk.org/cancerstats).

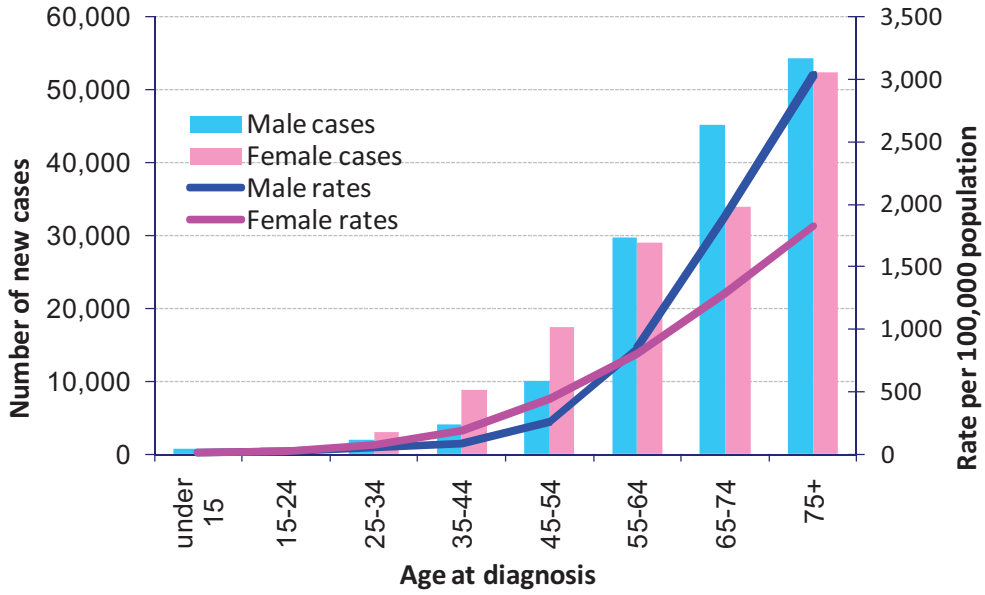

Figure 1.5. Number of new cases and rates, by age and sex, for all malignant neoplasms, UK, 2006 (adapted from www.info.cancer research uk.org/cancerstats).

1.2.2. Brain tumours

CNS tumours within the paediatric population are the second most frequent tumour type and the most common form of childhood solid tumour. They account for 22% and 10% of all malignancies among children aged up to 14 years and 15-19 years, respectively (Figure 1.6) (Potter et al 1998). This entity of tumours includes astrocytomas (approximately 50%), primitive neuroectodermal tumours (PNETs) (approximately 20%) and ependymomas (approximately 10%), where PNET represent the most prevalent malignant brain tumours in childhood. This subgroup of tumours was previously defined as one single entity due to their similar histology and presumed common cellular origin, but recent immunohistochemical and genetic profiling studies have provided evidence that some PNETs represent distinct entities, including medulloblastoma (Sarkar et al 2005).

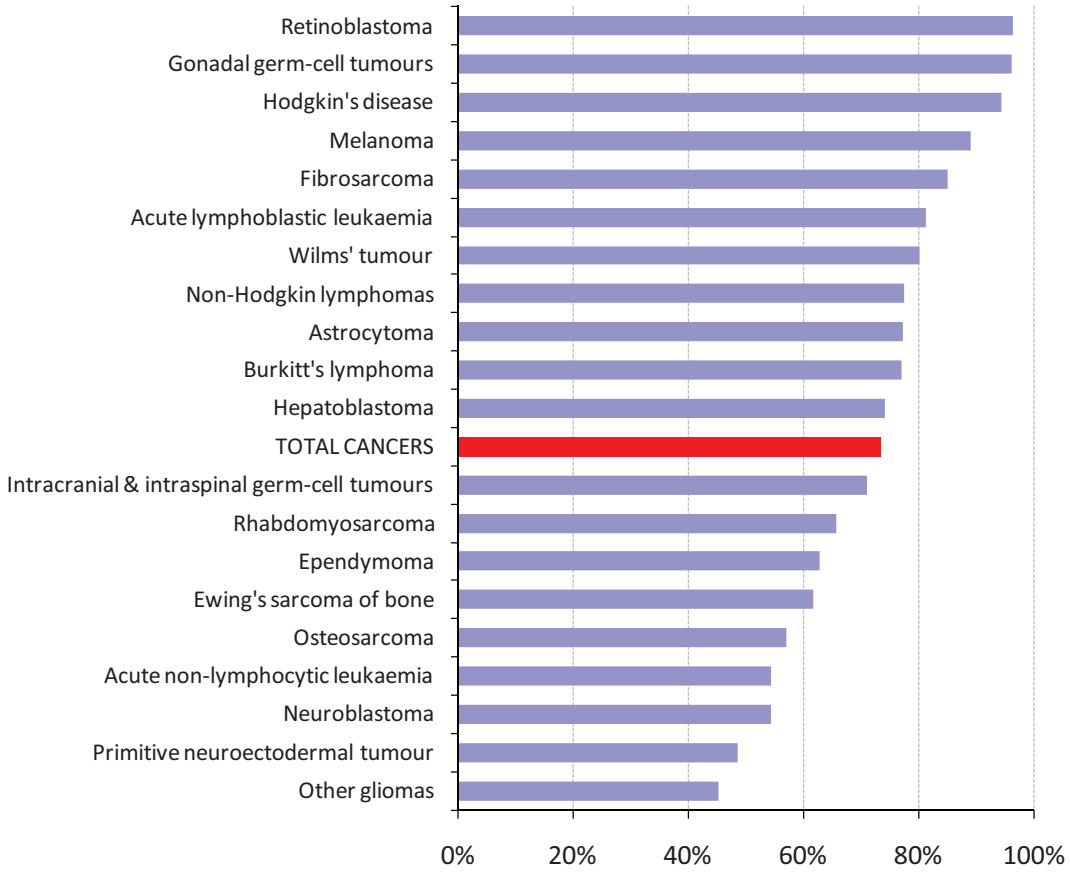

Figure 1.6. Percentage of patients alive 5 years after diagnosis, childhood cancers, Great Britain 1992-1996 (UK Childhood Cancer Research Group, National Registry of Childhood Tumours 2004) (adapted from cancerresearchuk.org/cancerstats/childhoodcancer/survival/index.htm).

1.3. Medulloblastoma

Medulloblastoma was initially described by Bailey and Cushing (1925) and was defined as an invasive embryonal tumour of the CNS arising from undifferentiated neuroepithelial cells in the cerebellum. The term medulloblastoma has always been in place since Cushing and Bailey's in 1925. Later, medulloblastoma and histologically similar tumours occurring outside the posterior fossa come under the umbrella term primitive neuroectodermal tumour (PNET) of the posterior fossa (Rorke 1983). It is

however, increasingly recognized that the so called supratentorial PNETs are histologically different from medulloblastoma.

1.3.1. Incidence

Medulloblastoma is the most common paediatric primary malignant intra-cranial neoplasm, accounting for 20-25% of all childhood brain tumours. It is a distinctive embryonal brain tumour and accounts for 40% of posterior fossa tumours. It occurs mainly in the cerebellar vermis. It can locally infiltrate the brain stem and/or the fourth ventricle and may spread along the cerebro-spinal pathway. The incidence of medulloblastoma is approximately 7 per million in children between 5-10 years of age and a peak incidence is seen around 7 to 8 years of age. The male to female ratio is 1.6: 1. Medulloblastoma may occur in adults, comprising no more than 1% of all adult primary CNS tumours (reviewed by Ellison et al 2006).

1.3.2. Pathological features

Medulloblastoma is classified as a grade IV tumour by the WHO, which is the most severe grade. In 2007 a modified WHO classification for brain tumours was introduced (Louis et al 2007). The new classification was based on the consensus of an international working group of 25 pathologists, geneticists and more than 70 international experts (Table 1.3). The international classification of disease for oncology (ICD-O) was established more than 30 years ago. The fourth edition of ICD-O was published in 2007 and was based on distinctive morphology, location, age distribution and biological behaviour, and not simply by an unusual histopathological

pattern. Thus variants were defined as being reliably identified histologically and having same relevance for clinical outcome.

New variants were introduced in the new classification where there was evidence that a particular morphological pattern is associated with a different biological or clinical behaviour. Other variants were merged if their morphological differences do not appear to play part in their clinical outcome. Macroscopically, medulloblastoma is typically a midline tumour which arises in the region of the cerebellar vermis but can also arise in the cerebellar hemispheres. It is a poorly defined pale-pink or grey soft tissue growth that may contain foci of haemorrhages, necrosis or calcification (Kleihues and Cavenee 2000).

Embryonal tumors

1993
Medulloepithelioma
Neuroblastoma
  Ganglioneuroblastoma
Ependymoblastoma
Primitive neuroectodermal tumors (PNETs)
  Medulloblastoma
    Variants:
    Desmoplastic medulloblastoma
    Medullomyoblastoma
    Melanotic medulloblastoma

2000
Medulloepithelioma
Ependymoblastoma
Medulloblastoma
  Desmoplastic medulloblastoma
  Large-cell medulloblastoma
  Medullomyoblastoma
  Melanotic medulloblastoma
Supratentorial PNET
  Neuroblastoma
  Ganglioneuroblastoma
Atypical teratoid/rhabdoid tumour

2007
Medulloepithelioma
Ependymoblastoma
Medulloblastoma
  Desmoplastic medulloblastoma
  Medulloblastoma with extensive nodularity
  Large-cell medulloblastoma
  Anaplastic medulloblastoma
Supratentoirial PNET
  Cerebral neuroblastoma
  Ganglionneuroblastoma
Atypical teratoid/rhabdoid tumour

Table 1.3. World Health Organization classification of embryonal tumours (including medulloblastoma), 1993-2007 (Louis et al 2007).

Five distinct histopathological variants of medulloblastoma are now recognized; classic medulloblastoma; desmoplastic/nodular medulloblastoma (N/D); medulloblastoma with extensive nodularity (MBEN); anaplastic medulloblastoma and large cell medulloblastoma (Louis et al 2007).

(i) Classic medulloblastoma

This is the most common variant, accounting for about 80% of medulloblastomas. Classic medulloblastomas grow as sheets of densely-packed cells with round to oval or carrot-shaped hyperchromatic nuclei, surrounded by scant cytoplasm. There is a high nuclear-cytoplasmic ratio and a capacity to invade adjacent structures and leptomeninges. They can form rosettes (Homer-Wright) with pallisading patterns in approximately 40% of the cases. Neuronal differentiation, which is characterized by a reduced nuclear: cytoplasmic ratio, is common, but glial differentiation is unusual (McManamy et al 2003) (Figure 1.7A).

(ii) Desmoplastic / nodular

This variant, together with MBEN, accounts for 15% of medulloblastomas. It shows a distinctive architecture composed of nodules, reticulin-free zones or "pale islands". These are surrounded by densely packed mitotically active cells with hyperchromatic and moderately pleomorphic nuclei which produce a dense intercellular reticulin-positive network of fibres. The nodules represent zones of neuronal maturation and they have a reduced nuclear: cytoplasmic ratio. They also have low mitotic activity and increased apoptosis (Ellison 2002) (Figure 1.7B1).

(iii) Medulloblastoma with extensive nodularity (MBEN)

This variant was previously designated as "cerebellar neuroblastoma". It has an expanded nodular architecture, while the internodular region is markedly reduced compared to the desmoplastic / nodular type. Cells within the nodules exhibit neuronal differentiation. This represents the most differentiated form of the desmoplastic / nodular medulloblastoma. It typically occurs in children below three

years of age and has been associated with a favourable prognosis (Giangaspero et al 1999, Louis et al 2007, McManamy et al 2007) (Figure 1.7B2). It is proposed that both desmoplastic /nodular medulloblastoma and MBEN share the same international disease classification (ICD-O 971/3).

(iv) Large cell / anaplastic medulloblastoma

In the current WHO grading, the large cell and anaplastic medulloblastoma share the same code, since they have considerable cytological overlap and have some patterns that can coexist. The large cell /anaplastic variant represents 2-4 % of medulloblastomas. The large cell histological subtype includes cells with large, round, vesicular nuclei containing prominent nucleoli, abundant mitotic figures and numerous apoptotic bodies. These tumours are usually associated with poor outcome (Giangaspero et al 1992). While the anaplastic medulloblastoma subtype shared elevated cell size, mitotic rate and apoptotic frequency with large cell tumours, they also have cells that are pleomorphic, angular and anaplastic rather than round as in the large cell medulloblastoma. Because large cell and advanced anaplastic cell changes often co-mingle in individual tumours they were combined into a single subtype (LC/A) in the previous WHO classification (Figure 1.7C). In the current WHO classification for brain tumours (Louis et al 2007) the large cell and anaplastic medulloblastoma subtypes were classified as two separate entities but share the same ICD-O (9474/3) because their clinical implication is still debatable.

Anaplastic medulloblastoma, first described by Brown et al 2000), varies in severity (mild, moderate and severe) and spread (focal and diffuse) (Eberhart et al 2002). The prognostic significance of anaplasia showed inconsistent correlation with

survival. Eberhart et al 2002 and Giangaspero et al 2006 found anaplasia to be associated with poor prognosis. The details of their studies are detailed in pages 211 and 212).

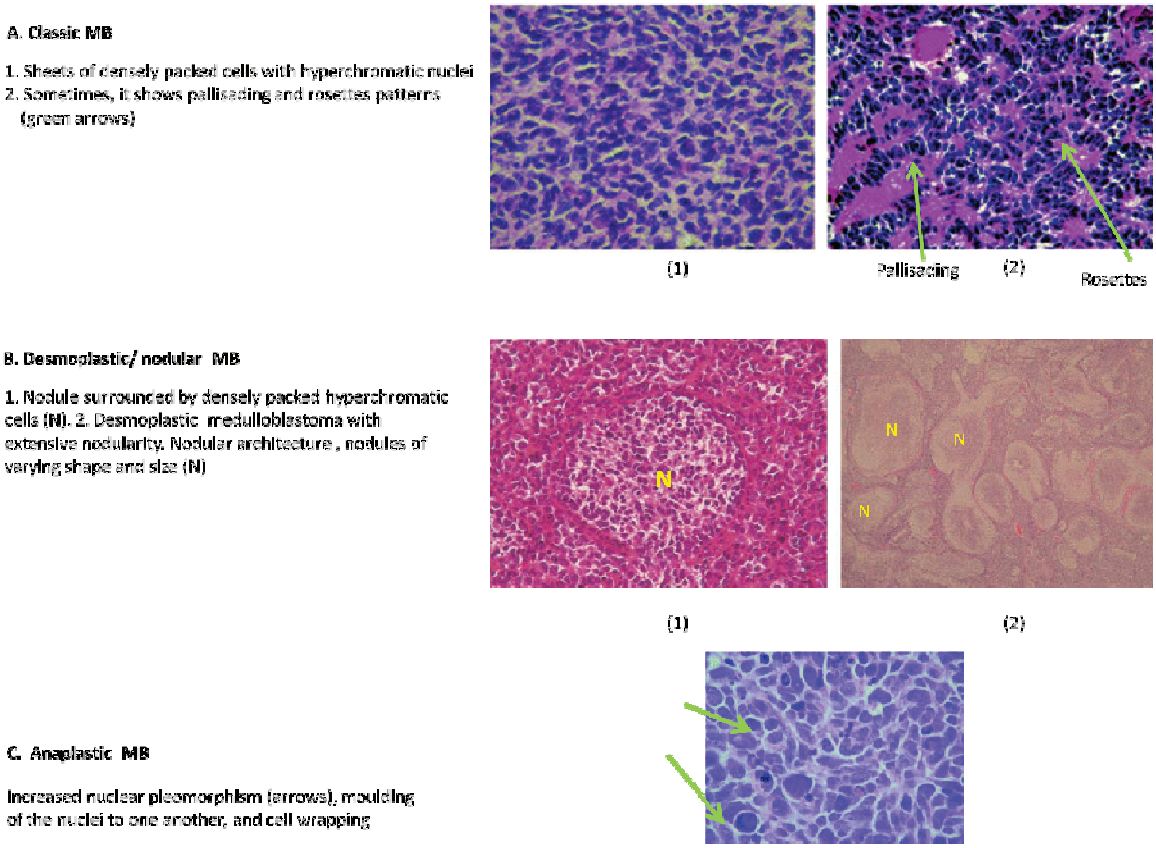

Figure 1.7. Histopathological variants of medulloblastoma (Adapted from Ellison 2002).

1.3.3. Current diagnosis and management

1.3.3.1. Clinical presentation

Children with medulloblastoma usually present with signs of increased intracranial pressure (vomiting, headache, visual disturbances) due to obstruction of cerebro-spinal fluid (CSF) flow. Early in the course of illness, these symptoms may be subtle. Diagnosis is usually made within three months of the appearance of symptoms (Packer et al 1999). With progression of the tumour, there may be progressive truncal ataxia and cranial nerve dysfunction. Abducent nerve palsy may be affected early in the course of the disease due to increased intracranial pressure rather than brain stem

infiltration. The presentation of stiff neck and head tilt usually suggest cerebellar tonsilar herniation, less frequently head tilt may be due to trochlear nerve palsy (Hill et al 2005). Infants may present with macrocephaly, intermittent vomiting and signs of increased intra-cranial pressure (Crawford et al 2007).

1.3.3.2. Diagnosis of medulloblastoma

Imaging plays a primary role in the diagnosis of medulloblastoma. Nowadays, magnetic resonance imaging (MRI) is increasingly being used instead of traditional computed tomography (CT) scans, since MRI is a superior diagnostic tool with higher resolution than CT.

On CT, medulloblastoma is usually a homogeneous, hyperintense midline mass, surrounded by hypodense areas denoting vasogenic oedema. Approximately 10-20% of patients will have calcification in non-contrast CT, also cystic or necrotic areas are frequent. After contrast enhancement, the majority of tumours will show homogeneous enhancement (although a degree of heterogeneity have been observed).

On MRI, medulloblastoma usually presents as a midline inferior vermian lesion filling the fourth ventricle. It typically appears as a hypodense mass in T1-weighted MR images (Figure 1.8). On sagittal MRI examination, compression and displacement of the brain stem ventrally and metastasis of the tumour into the spinal cord can be visualized (Bühring et al 2002). Following administration of gadolinium, T1-weighted images typically show a homogeneously enhancing hyperintense mass with

surrounding areas of oedema. MRI is also effective in visualizing metastatic lesions. Metastases usually show as nodular or diffuse, contrast enhancing, lesions in the leptomeninges on contrast-enhanced T1 weighted images (Vezina and Packer 1994).

Other imaging modalities including Magnetic Resonance Spectroscopy (MRS) and Single Photon Emission Computed Tomography (SPECT) are used in the management of medulloblastoma, most commonly as a clinical aid to distinguish tumour recurrence from post-therapy necrosis (Crawford et al 2007).

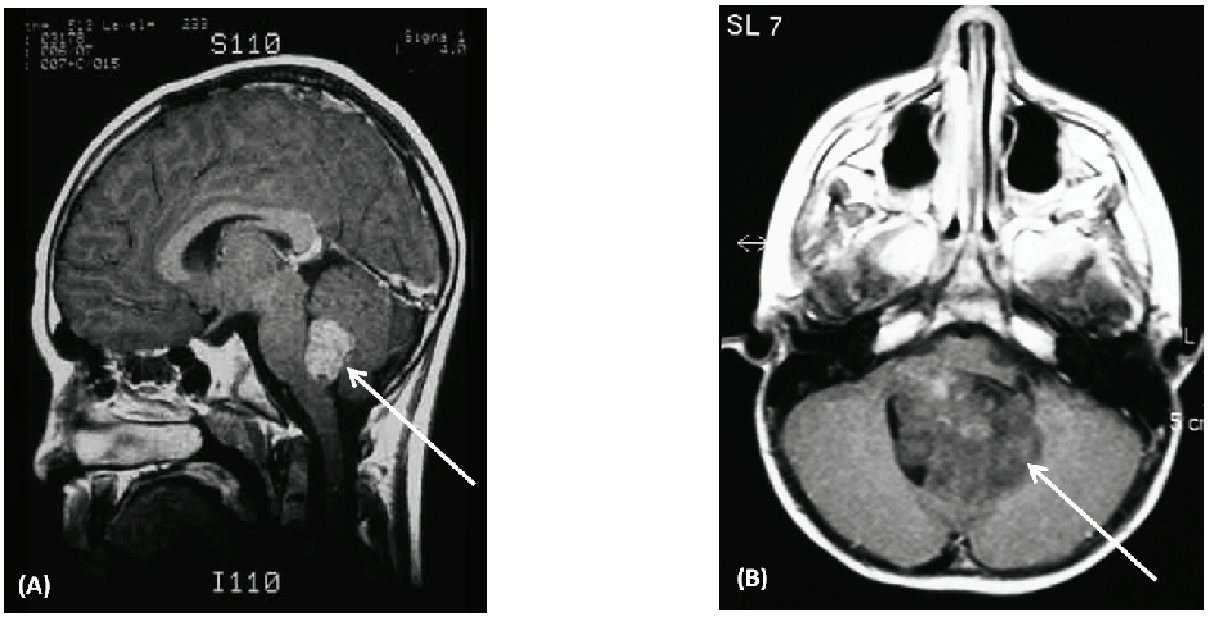

Figure 1.8. MRI of a children with medulloblastoma (A) Sagittal section of the brain demonstrating tumour in the posterior fossa (B) Axial section of the brain showing a medulloblastoma tumour (Arrows), (Figures taken from www.emedicine.medscape.com/articles).

1.3.3.3. Current clinical classification and its influence on therapy decision

Patients with medulloblastoma are currently classified as standard-risk and high-risk according to three criteria; age, extent of tumour resection and the presence or absence of metastasis at diagnosis. Since it is now generally accepted that the residual tumour volume after surgery is a more important predictive factor than the initial tumour size, the older T-staging system (T0-T4, (Chang et al 1969)), which was an intra-operative staging system based on the determination of the size and location of the tumour by the surgeons during the operation, has been abandoned. The extent of dissemination (M0-M4) is determined by CSF cytology examination, and pre-operative and postoperative imaging system (Table 1.4). The first post-operative MRI is done 72 hours after surgery to document the extent of tumour resection. Consecutive MRIs can be done to assess tumour response to adjuvant therapy, and to detect any recurrence or complications. Therefore, clinical staging of medulloblastoma patients is now limited to the diagnosis of standard-risk and high-risk patients using the criteria shown in Table 1.5.

Average-risk patients are defined as children of three years of age or older, who had total resection of the primary tumour or $\leq$ 1.5 cm^2 of residual tumour following surgery and there is no evidence of metastasis based on gadolinium-enhanced MRI of the whole neuroaxis and negative CSF cytology obtained 15 days post-operatively. High-risk patients are defined as children younger than three years of age and/or who have the presence of $\geq$ 1.5 cm^2 of residual tumour at the primary site, and/or there is evidence of metastatic disease in the neuroaxis based on gadolinium MRI study and

positive CSF cytology 15 days post-operatively. Patients who present with metastasis at diagnosis more commonly die from their disease (Gilbertson et al 2001, Lamont et al 2004, McManamy et al 2007). Also, due to the neuro-cognitive and neuro-endocrine adverse effects of radiotherapy on patients younger than 3 years, radiotherapy is usually delayed in this group of patients and this may contribute to the poor outcome of these youngsters (Crawford et al 2007).

Classification	Description
T1	Tumour less than 3 cm in diameter and limited to the classic midline position in the vermis, the roof of the fourth ventricle, and, less frequently, to the cerebellar hemispheres.
T2	Tumour 3 cm or greater in diameter, further invading one adjacent structure or partially filling the fourth ventricle.
T3	Divided into T3a and T3b: **T3a**: Tumour further invading two adjacent structures or completely filling the fourth ventricle with extension into the queduct of Sylvius, foramen of Magendie, or foramen of Luschka, producing marked internal hydrocephalus. **T3b**: Tumour arising from the floor of the fourth ventricle or brain stem and filling the fourth ventricle.
T4	Tumour further spreading through the aqueduct of Sylvius to involve the third ventricle or midbrain or tumour extending to the upper cervical cord.
M0	No evidence of gross subarachnoid or haematogenous metastasis.
M1	Microscopic tumour cells formed in cerebrospinal fluid.
M2	Gross nodular seedling demonstrated in cerebellar, cerebral subarachnoid space, or in the third or lateral ventricles.
M3	Gross nodular seedling in spinal subarachnoid space.
M4	Metastasis outside the cerebrospinal axis

Table 1.4. Chang staging system for medulloblastoma (Chang et al 1969).

	Standard-risk	High-risk
Extent of resection	$\leq$ 1.5 cm^2 residual tumour	> 1.5 cm^2 residual tumour
Age at operation	3 years or greater	Younger than 3 years
Dissemination	Negative CSF cytology Normal neuroaxis MRI with gadolinium enhancement.	Positive CSF cytology Positive neuroaxis MRI with gadolinium enhancement.

Table 1.5. Medulloblastoma risk staging.

1.3.3.4. Limitations of the current clinical disease classification

Despite advancements in chemotherapeutic regimens, irradiation delivery methods and surgical procedures (see following sections), the survival rate for patients with standard-risk and high-risk medulloblastoma assessed using clinical indices, remains 70-80% and 40-60% respectively (Gilbertson et al 2001). Moreover, 20% of standard-risk patients will experience relapse of their disease while over 40 % of high risk-patients are successfully cured. Treatment protocols, especially radiotherapy, cause devastating intellectual, neurological and endocrinal remote side effects, in particular for young children < 3-6 years at diagnosis. A significant factor in this inaccurate prediction of patients' outcome is the current disease classification, which is based only on 3 clinical parameters. Both histopathological and molecular variables are not included in this disease classification, while a lot of research has recently identified them as significant factors associated with prognosis (Gilbertson et al 2001, 2004). Adding histopathological and molecular criteria to the current clinical classification

may allow for better and more individualized disease staging leading to tailored therapeutic protocol, which may increase survival whilst minimizing the adverse effects of therapy.

1.3.3.5. Management of standard-risk medulloblastoma patients

Total or near-total tumour excision followed by both chemotherapy and radiotherapy form the mainstay of treatment for this subgroup of patients. Advancement in the techniques of radiotherapy administration allows delivery of boost radiation to the posterior fossa while minimizing the exposure of the supratentorial brain through the use of 3-dimentional conformal approaches. Chemotherapy proved to be a significant therapeutic element in the treatment of medulloblastoma. The European SIOP PNET3 study demonstrated that patients with standard-risk medulloblastoma had 79% EFS with intensive pre-irradiation chemotherapy compared to a 64% EFS in patients who only received radiotherapy (Taylor et al 2003).

Children older than 3-5 years at diagnosis with standard-risk medulloblastoma currently typically undergo surgery to achieve maximum tumour excision followed by reduced dose radiotherapy (23.4 Gy CSRT augmented up to 54-55.8 Gy dose to the posterior fossa). Patients then receive maintenance chemotherapy, typically using the 'Packer' regimen which consists of 8 courses of Vincristine, Lomustine and Cisplatin. This regimen provides 5 year EFS of around 81% (Paker et al 2006) in this patient group.

1.3.3.6. Management of high-risk medulloblastoma patients

Metastatic high risk medulloblastoma patients typically receive the conventional therapy composed of surgery, chemotherapy and craniospinal radiotherapy (CSRT) at an increased dose of 35-36 Gy, however this modality of treatment only achieves a 30-40% cure rate for M2/3 patients (Friedman et al 1986, Bacha et al 1986). Therefore, several clinical trials have taken place or are ongoing in order to achieve a better survival including the St. Jude Medulloblastoma 96 trials, which involve the administration of cycles of cyclophosphamide-based, dose intensive chemotherapy followed by radiotherapy at a dose higher than 35-36 Gy and these protocols have achieved 5 year survival rates of >60% in M2/3 patients within both trials (Gajjar et al 2006).

Other studies performed by European groups have assessed the utilization of altered hyperfractionated radiotherapy (HART), administered twice daily along with high-dose sequential chemotherapy. These protocols have achieved 5 year survival rates of 70% (Gandola et al 2009). A study by COG is currently evaluating the use of radiotherapy concomitantly with carboplatin in patients with metastatic disease and reported a 3 year EFS of 60% (Jakacki et al 2007).

1.3.3.7. Management of medulloblastoma in very young patients

Patients below the age of 3 years at diagnosis represent a challenging subgroup, since there are devastating intellectual, endocrine and neurological late side effects resulting from the use of radiotherapy on these youngsters compared to older children with medulloblastoma. Therefore, chemotherapy-based therapeutic protocols

are currently widely used in order to delay or avoid CSRT. However, recent advancements in radiotherapy delivery methods allow tightly controlled radiation for the posterior fossa, which has been reintroduced in the initial management of medulloblastoma in infant patients, achieving 50-60% survival in non-metastatic cases (Crawford et al 2007).

The 'Baby Brain` study used prolonged low-dose chemotherapy and achieved around 30% EFS by both UK and French groups, the latter group showed a significant difference between patients who had total tumour resection versus patients who had subtotal excision of the tumour (reviewed by Pizer and Clifford 2009). Moderate intensity chemotherapy including intraventricular methotrexate has been used by German researchers achieved, and 82% achieved EFS in non-metastatic medulloblastoma patients who underwent total tumour excision, while those with metastatic disease and residual tumour achieved a 5 year EFS of 33% and 50% respectively (Rutkowski et al 2005).

1.3.3.8. Treatment of relapsed medulloblastoma patients

Deciding the best therapeutic regimen to apply to patients who experience relapse of their tumours is still a difficult and challenging process, mainly due to a lack of prospective clinical trials that compare patients' responsiveness and outcome following different treatments. One major consideration is to ensure that the benefit of any extra therapy overweighs the toxic side effects, especially among younger patients.

Infants who did not initially receive radiotherapy and whose tumour relapse is localized may benefit form tumour re-excision followed by local irradiation with or without high dose chemotherapy (HDCT) (Ridola et al 2000). While metastatically relapsing tumours will require HDCT associated with CSRT, this treatment approach inevitably results in devastating neurocognitive and endocrine side effects (Gajjar et al 1994).

Patients who have already been treated using conventional protocols and experience minimal tumour recurrence can be salvaged using HDCT, but in cases with macroscopic tumour recurrences HDCT may be ineffective. Generally, patients who receive both radiotherapy and chemotherapy during their initial treatment have less chance to benefit from HDCT to overcome their relapsed disease (reviewed by Pizer and Clifford 2009).

1.3.3.9. Long-term treatment sequelae

Neurocognitive defects represent some of the most pervasive of all long term effects and occur across all age groups. Specific neurocognitive defects in verbal, spatial memory and attention have been found amongst medulloblastoma survivors. Both IQ and specific neurocognitive function tests show that severe defects are associated with total dose of radiotherapy and age at treatment. In one study of 18 patients under 3 years of age at diagnosis receiving radiotherapy, 14 had an IQ scores of <90 and 7 had IQ scores of <70 (Skowronsk-Gardas 1999), highlighting the profound effect of radiotherapy on young patients. Less commonly, patients are at increased risk

of stroke which is presumed to be secondary to radiation-induced vasculitis (Bowers et al 2006).

Furthermore, surgery has been shown to induce neurological defects. Peri-operative and operative factors such as the presence of hydrocephalus, incision of the vermis and infections, have been associated with cerebellar mutism, reduced hand skills and reduced verbal IQ scores (Fossati 2009). In addition, a multitude of medical problems have been identified in medulloblastoma survivors treated with certain chemotherapeutic agents, including ototoxicity and infertility (Packer and Vezina 2008).

Studies have also revealed a wide range of endocrine dysfunction following cranio-spinal radiotherapy affecting the hypothalamic-pituitary region (Voute et al 2005). The most common impairment is growth failure due to growth hormone deficiency. Hypothyroidism may also occur leading to poor liner growth, learning difficulties and lethargy.

1.3.3.10. Novel trials and therapeutic approaches

Few novel therapeutic regimens are currently being tested which, focus on targeting the disease at the molecular level. The concept of using molecular markers to identify subsets of tumours that can be targeted using novel therapies aimed at certain critical biological pathways, have shown successful results in certain cancers. These therapeutic methodologies include identification of the Philadelphia chromosome (BCR-ABL) in chronic myeloid leukaemia, where cases harbouring this translocation

show significant improved survival using Imatinib (Barr 2010). Similarly, breast cancer patients with positive HER2 show a significant response to the anti-cancer drug Herceptin (Murphy and Fornier 2010) when added to adjuvant chemotherapy. However, such approaches have not been widely undertaken in medulloblastoma to date.

1.3.4. The molecular genetics of medulloblastoma

Medulloblastoma is a heterogeneous disease at the molecular level and so far no specific diagnostic cytogenetic or molecular aberrations have been identified. A number of major non-random molecular genetic abnormalities have been identified in the human disease, which have increased our understanding of the molecular mechanisms involved in the pathogenesis of medulloblastoma and raise the possibility for improving the current disease stratification and treatment protocols through the development of risk stratification biomarkers and the identification of novel therapeutic targets. Insights into the aberrations that occur in medulloblastoma have been derived from four main areas of investigation, (1) the identification and mapping of chromosomal aberrations in medulloblastoma, (2) the investigation of inherited cancer syndromes associated with medulloblastoma formation, (3) the analysis of defects in candidate tumour suppressor genes or oncogenes and, (4) the identification of cell-signalling systems which are dysregulated in medulloblastoma (Ellison et al 2003).

1.3.4.1. Chromosomal abnormalities in medulloblastoma

The most commonly observed chromosomal abnormalities in MB affect chromosome 17, where isochromosome 17q is seen in about 30-50% of medulloblastomas and isolated 17p loss is found in approximately another 20% (Lamont et al 2004). Genetic losses affecting 17p have been associated with classic or large-cell variants, metastasis and subsequently adverse clinical outcome (Batra et al 1995, Scheurlen et al 1998, Gilbertson et al 2001, Lamont et al 2004), however these correlations are not consistent between different studies and some researchers did not find 17p loss to be associated with bad prognosis (Emadian et al 1996, Biegel et al 1997, Pan et al 2005). Additionally more than 40% of medulloblastoma cases show gain of chromosome 7, while 30% of the patients show non-random loses of chromosomes 8, 9, 10q, 11 and 16q (reviewed by Pizer & Clifford 2009).

The specific genetic targets of most of these chromosomal abnormalities are not well recognized and are still under investigation. While mutations in *PTCH* (at 9q22.3), *SUFU* (10q24.3) and *TP53* (17p13.1) have each been identified in approximately 10% of tumours, mutations of these genes occur at a lower frequency than loss of the corresponding chromosomal locus. Therefore, alternative mechanisms may be responsible for their inactivation (e.g. epigenetic defects) or alternative tumour suppressor genes (TSGs) may be present nearby (reviewed by Pizer & Clifford 2009).

Genetic amplification is seen in approximately 10% of medulloblastomas. The most commonly amplified chromosomal regions (each occurring in 5-15% of

medulloblastomas) are 2p24 and 8q24, which harbour the *MYCN* and *MYC* oncogenes, respectively. *MYCN* and *MYC* amplification have been associated with the large cell / anaplastic medulloblastoma variant and a poor clinical outcome (Brown et al 2000, Eberhart et al 2002, Lamont et al 2004; Hoff et al 2010). Other loci showing gene amplification at a lower frequency in medulloblastoma include *OTX2, NOTCH2, hTERT, MYCL1, PDGFRA, KIT, MYB, PPMID* and *CDK6* (Fan et al 2003, Boon et al 2005 and reviewed by Pizer & Clifford 2009).

1.3.4.2. Familial cancer syndromes associated with medulloblastoma development

Approximately 5% of medulloblastomas occur as part of inherited cancer syndromes, however many of the genetic defects underlying these syndromes have shown to play a part in the pathogenesis of sporadic medulloblastoma. The most commonly identified mutations in sporadic medulloblastoma are of *TP53, APC,* and *PTCH,* which also predispose to Li-Fraumeni, Turcot and Gorlin (NBCC) syndromes, respectively, of which medulloblastoma is seen as a feature. Both the *APC* and *PTCH* genes are major components of the Wnt/Wg and Sonic Hedgehog (SHH) cell signalling pathways, respectively. Less commonly, medulloblastoma is seen as part of Rubenstein-Taybi (RTS) and Coffin-Siris (CSS) syndromes, however further studies are needed to support and validate the involvement of both RTS and CSS, and their associated genes, in the development of medulloblastoma (Table 1.6).

Li-Fraumeni syndrome is an autosomal dominant disorder characterised by multiple cancer formation, including primary brain tumours. Germ line mutations of

the *TP53* TSG underlie this disorder. This TSG resides on 17p13.1 and plays major role in regulation of the cell cycle and apoptosis. Mutations of *TP53* lead to its inactivation and allow cells to bypass control cell cycle check-points and escape apoptosis, leading to the accumulation of genetic defects and immortalization of cancer cells. Up to 14% of tumours associated with Li-Fraumeni syndrome are brain tumours, of which 10% are medulloblastoma (Malkin et al 1990, Srivastava et al 1990). Around 10% of sporadic medulloblastomas show mutations in *TP53* (Ellison 2002).

Turcot's syndrome (TS) is another familial cancer disorder characterised by the formation of adenomatous colorectal polyps, colorectal carcinomas and neuro-epithelial tumours. Two types of TS exist, TS type 1 (TS1) and TS type 2 (TS2). Both types are associated with an increased chance (up to 92%) to develop brain tumours. In TS2, there are mutations in the *APC* gene. Patients develop familial adenomatous polyps (FAP) and have an increased risk to develop medulloblastoma. TS1 is associated with mutations in DNA mismatch repair genes, development of hereditary non polyposis colorectal cancer (HNPCC) and the development of gliomas (Hamilton et al 1995, Paraf et al 1997, Ellison 2002). Studies have shown that *APC* is mutated in <5% of sporadic medulloblastoma. The *APC* gene is a major component of the Wnt/Wg pathway, which is involved in cell cycle progression through expression of proteins including cyclin D1 as well as in cell growth and differentiation (reviewed by Gilbertson and Ellison 2008).

Gorlin syndrome (named after Gorlin and Goltz who first described it in 1960) or Nevoid basal cell carcinoma (NBCCS) is another autosomal dominant syndrome

where patients develop basal cell carcinomas and show developmental abnormalities, and skeletal anomalies including jaw cysts (Gorlin 1987, Evans et al 1991). NBCCS is caused by mutations in the *PTCH1* gene on chromosome 9q22.3-q31. Approximately 4% of patients with Gorlin syndrome develop medulloblastoma and germ line mutations in the *PTCH1* gene are responsible for this tumour group. Medulloblastomas associated with Gorlin syndrome tend to be of the nodular/desmoplastic histopathological subtype and mainly affect children above 3 years of age. *PTCH1* was thus considered a potential TSG for medulloblastoma and studies have since shown that approximately 10% of medulloblastomas have mutations in this gene (reviewed by Ellison 2002).

Syndrome	OMIM	Gene	Locus	Tumour susceptibilities	Risk
Brain tumour-polyposis syndrome 2 / Turcot syndrome type 2	175100	*APC*	5q21-q22	Medulloblastoma Multiple colorectal adenomas	79% 100
Naevoid basal cell carcinoma syndrome (NBCCS) Gorlin syndrome	109400	*PTCH*	9q22.3	Medulloblastoma Basal cell carcinoma	3-5% 100%
Li-Fraumeni syndrome	151623	*TP53*	17p13.1	Medulloblastoma Multiple primary neoplasm	~2% 3-25%
Fanconi anemia (FA) subtype 'D1' Fanconi anemia (FA) subtype 'N'	605724 610832	*BRCA2* *PALB2*	13q12.3 16q12.1	Medulloblastoma Wilms tumour Neuroblastoma Haematalogical malignancies (paediatric kindred members) Breast cancer (adult kindred members)	High
Rubenstein-Taybi syndrome	180849	*CREBBP*	16p 13.3	Medulloblastoma Other nervous system tumours Neural crest tumours	Rare Rare Rare
Coffin-Siris syndrome	135900			Medulloblastoma	Rare

Table1.6. Medulloblastoma in hereditary cancer syndromes (adapted from Gajjar and Clifford, 2010).

1.3.4.3. Disregulated cell-signalling pathways in medulloblastoma

The Hedgehog Sonic (SHH) signalling pathway

The SHH signalling pathway has a vital role in the development of the normal cerebellum, where the Purkinje neurones secrete SHH ligand which in turn promotes mitogenesis in the external granule layer (EGL) progenitor cells during the early stages of development (reviewed by Pizer and Clifford 2009). The SHH signal is under the control of 2 trans-membrane protein receptors (PTCH and SMO), both of which transactivate the GLI family of transcription factors. Activating mutations in the SHH pathway occur in at least 15% of medulloblastomas which may occur as a result of mutations within several components of the pathway including *PTCH1* (10%) (Zurawel et al 2000); *SMO* (approximately 5%) (Kallassy et al 1997) and *SUFU* (0-10%) (Taylor et al 2002, Koch et al 2004). Illustration of SHH pathway are shown in Figure 1.15.

Two studies by Thompson et al (2006) and Kool et al (2008) identified a subgroup of medulloblastomas displaying distinct SHH-related gene expression profiles, which were consistent with SHH activation and *PTCH1* mutations in about 25% of medulloblastoma cases. This subgroup was highly associated with mutations in components of the SHH pathway and is mainly associated with the desmoplastic histopathological variant and patients of young age. This association is supported by the fact that medulloblastoma occurring in NBCC is mainly of the nodular/desmoplastic subtype, and mutations in *PTCH* gene as well as deletions of chromosome 9q, and gene-expression profiles associated with SHH pathway activation, occur in 30-40% of

sporadic nodular/desmoplastic medulloblastoma (Pietsch et al 1997, Thompson et al 2006, Kool et al 2008).

The Wnt/Wg pathway

Wnt/Wg signalling plays an important role in normal development particularly determination of neural cell fates. This role is mediated through regulation of the levels of intra-cellular β-catenin, a key transcriptional activator. The inactive form, β-catenin, is bound in a multimeric protein complex targeting it for proteosomal degradation through the BTRC protein. While activation of the pathway leads to dissociation of β-catenin from the APC protein complex and translocation to the nucleus, where it transactivates TCF/LEF transcriptional factors, which in turn activate downstream target genes associated with cell proliferation (e.g. *MYC, Cyclin D1)*. Activation of the Wnt/Wg pathway can occur as a result of activating mutations of *CTNNB1* at the regulatory regions affecting the *GSK3*-β phosphorylation domain (Morin, 1999). Mutations in *APC* and *CTNNB1* have been identified in 5% and 6% of medulloblastomas, respectively, while other components of the Wnt/Wg pathway, including *AXIN1,* have been identified as mutated in another 5% of medulloblastomas. Thus, mutations in components of the Wnt/Wg pathway account for approximately 15% of sporadic medulloblastoma (reviewed by Gilbertson et al 2002, 2004). Investigation of this pathway represents the main theme of this project and, therefore, more details of the mechanisms controlling this pathway are discussed later in this chapter.

TP53 and related pathways

Since chromosome 17p loss is reported to occur in up to 50% of medulloblastomas, research has focused on identifying TSGs located at or in the vicinity of this region. *TP53* is located on 17p 13.1 and plays an important role in regulating the cell cycle and apoptosis and its disruption has been identified in a number of cancers. *TP53* becomes stabilized in response to cellular stress through $p14^{ARF}$ which sequesters *MDM2* (a negative regulator of *TP53*). *TP53* stabilization allows cell cycle arrest or apoptosis, preventing cells from accumulating further genetic defects. Destabilization of *TP53* and subsequent disruption of its pathway may occur as a result of mutations in *TP53* itself, $p14^{ARF}$ inactivation (by mutations, deletions or epigenetic hypermethylation) or *MDM2* oncogene amplification (reviewed by Pizer and Clifford 2009). *TP53* mutations have been identified in approximately 10% of sporadic medulloblastoma, while mutually exclusive genetic alterations in *ARF* affect another 10%, implicating *TP53* with medulloblastoma development in approximately 20% of cases. Some studies have correlated medulloblastomas with *TP53* disruption with the large cell/ anaplastic subtype and an adverse clinical outcome (Woodburn et al 2001, Ray et al 2004). However, to date, *MDM2* amplification does not seem to play a role in the pathogenesis of medulloblastoma.

Other cell signalling pathways disrupted in medulloblastoma

Approximately 5% of sporadic medulloblastomas harbour mutations in *PIK3CA*, which is a member of the phosphatidylinositol 3'-kinase (PI3K) family signalling

pathway, suggesting this pathway may play a role in the pathogenesis of medulloblastoma (Broderic et al 2004).

Furthermore, gene expression studies have identified other signalling pathways associated with medulloblastoma development including the PDGFR, neurotrophin and ERBB2 receptor families, but the exact mechanisms involved in their over-expression, and their role in medulloblastoma tumourigenesis, are not fully clear and remain under investigation (reviewed in Pizer and Clifford 2009).

1.3.4.4. Epigenetic mechanisms in medulloblastoma

Epigenetic mechanisms may also deregulate genes in medulloblastoma as an alternative to genetic mechanisms. The most commonly described mechanism by which epigenetic gene silencing can occur is hypermethylation of promoter-associated CpG islands. This causes re-modelling of the chromatin structure without alterations in the DNA nucleotide sequences and can lead to transcriptional silencing (Lindsey et al 2005). Three genes have demonstrated strong and consistent evidence of DNA methylation in medulloblastoma and may play a role in tumour pathogenesis, namely; *RASSF1A* (in >90% of cases), *CAPS8* (35-40%) and *HIC1* (35-40%). Epigenetic events have shown associations with clinicopathological features of medulloblastoma and patients' outcome, which makes them candidate prognostic biological markers. *CAPS8* has been associated with non-desmoplastic medulloblastoma (Pingoud-Meier 2003), *COL1A2* methylation rarely occurs in desmoplastic medulloblastoma arising in infants (Anderton et al., 2008), while *HIC1* hypermethylation was reported to be an independent poor prognostic factor (Anderton, 2008).

Notably, gene silencing by hypermethylation is a reversible process, through treatment with agents such as DNA methyltransferase inhibitors, which may provide a potential therapeutic strategy for medulloblastomas with evidence of hypermethylation of target genes (Egger et al 2004). Examples of genetic defects reported in medulloblastoma are shown in table 1.7.

Gene	Locus	Frequency (%)	Clinical association/comments
Gene amplifications			
MYC	8q24	5-15	Associated with large cell/anaplastic tumou
MYCN	2p24	5-15	
OTX2	14q22.3	Isolated cases[a]	
NOTCH2	1p13-p11	Isolated cases[a]	
hTERT2	5p15.33	Isolated cases[a]	
Sonic hedgehog (SHH) pathway genes			
Gene-specific defects			
PTCH1	Mutation	~ 10	Associated with nodular/desmoplastic tum
SMO	Mutation	~5	
SUFU	Mutation	0-10	
Wingless (Wnt/Wg) pathway genes			
CTNNB1	Mutation	5-15	
APC	Mutation	~2.5	
AXIN1	Mutation	~2.5	
TP53 and associated genes			
TP53	Mutation	~10	Associated with large cell/anaplastic tumours
P14^{ARF}	Homozygous deletion, Hypermethylation	~10	
Other genes			
PIK3CA	Mutation	~5	P13K signalling pathway protein kinase
CASP8	Hypermethylation	~35	
HIC-1	Hypermethylation	~35	
RASSF1A	Hypermethylation	~90	

[a]Defects reported in isolated cases: further investigations are required to establish incidence.

Table 1.7. Genetic defects reported in medulloblastoma (Adapted from Ellison et al, 2006).

1.4. The function and development of the cerebellum and relationship to medulloblastoma pathogenesis

The cerebellum plays key roles in the control of tone, posture and multiple muscle activation required to support fine movements. While the brain determines where to move, the cerebellum implements its proper timing and modulates the force given to every motor command. Therefore, the cerebellum plays an important role in coordination, fine movement and equilibrium. However, modern research has shown that the cerebellum also has a role in a number of cognitive functions including attention and processing of language (Wang and Zoghbi 2001).

Medulloblastoma was first considered to originate from neural precursor cells of the cerebellum, however to date the exact cellular origin of medulloblastoma is still not entirely clear. The cerebellum consists of a nuclear structure, typical of subcortical regions and a covering laminar cortex, typical of the cerebrum. Convincing research suggests that oncogenic aberrations in different cells and signalling pathways that participate in cerebellar development may be responsible for the pathogenesis of different subtypes of medulloblastomas (reviewed by Gilbertson and Ellison, 2008).

The normal cerebellum develops within the roof of the embryonic metancephalic brain from 2 distinct germinal zones namely; (i) glutamatergic projection neurones of deep nuclei arising from the rhombic lip at approximately embryonic stage E 10.5-E 12.5 in mice and (ii) GABAergic projection neurones which include the Purkinje cells and Golgi neurones (Figure 1.9A) (reviewed by Gilbertson and

Ellison 2008). Another germinal zone develops within the rhombic lip comprising the granule neurone precursor cells (GNPCs) which produce the external germinal layer (EGL) which in-turn migrates inwards to form the mature granule cell neurones of the internal germinal layer (IGL). The EGL persists until postnatal stage P 15 in mice and into the second postnatal year in humans (Figure 1.9B). Recently, stem cell populations were identified within the post-natal white matter of the brain which expresses the neural stem cell markers, CD133 and Nestin. These cells are capable of self renewal and are multipotent, generating astrocytes, oligodendrocytes and neurones, but not granule cells. As a result, 3 distinct pools of progenitor cells may possess a potential source of cells for different subtypes of medulloblastoma (Gilbertson and Ellison, 2008). Gilbertson and Ellison (2008) proposed that these 3 distinct pools of neuronal precursors may be regulated by different signalling pathways. Neural precursor cells in the cerebellum are influenced by mutations within these pathways and may result in the formation of different subtypes of medulloblastoma. These signalling pathways regulate the development of the normal cerebellum and defects within them may indicate that different medulloblastoma subtypes arise from distinct cell lineages (Figure 1.10). The Wnt/Wg signalling pathway is controlled by the cytosolic /nuclear β-catenin levels, and early cerebellar multipotent precursor cells are dependent on the Wnt/Wg signalling pathway (details of this pathway in medulloblastoma have been further discussed in section 1.6).

The SHH pathway plays a key role in the development of the normal cerebellum, where activation of this pathway occurs in the EGL promoting cell growth and proliferation while inactivation takes place in the IGL inducing differentiation

(Figure 1.11). A subset of medulloblastoma appears to show constitutive activation of this pathway leading to continuous growth of cells within the EGL. In vivo studies showed that *ptch* +/- mice develop cerebellar tumours which resemble the nodular / desmoplastic medulloblastoma, and human cerebellar tumours that display a dysfunction in the SHH pathway are usually of the nodular/ desmoplastic medulloblastoma (Schofield et al 1995).

Negative regulators of the SHH pathway include the transmembrane protein PTCH. Mutations in *PTCH* have been identified in 10% of medulloblastoma. Normally, SHH ligands bind to *PTCH*, removing the suppression form the co-receptor Smoothened (SMOH) activating the GLI family of transcription factors and other genes of cell growth and proliferation (e.g. *MYCN* and *Cyclin D1*) (Figure 1.12.). While absence of SHH-PTCH interaction promotes transportation of GLI family members from the nucleus to the cytoplasm by the suppressor of fussed (SUFU) homologue where, they are degraded by proteosomal system including the β-transducin repeat-containing protein (β-TRCP). The SHH pathway in medulloblastoma has already been discussed in section 1.3.4.3.

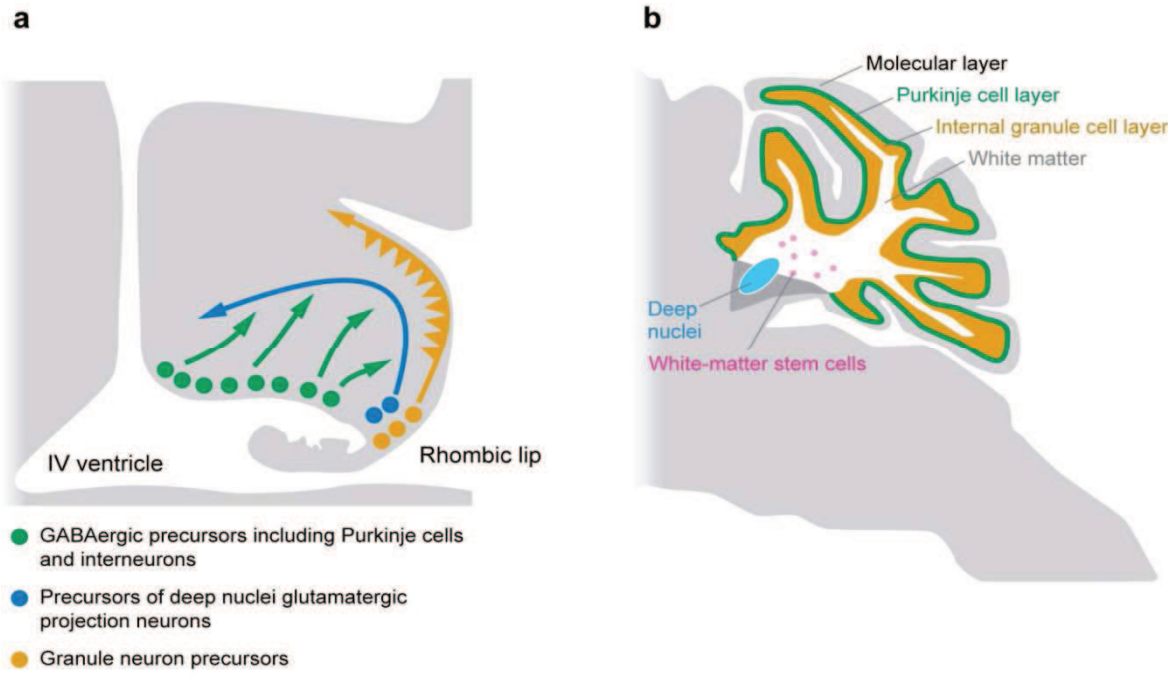

Figure 1.9. Precursor cell population in the developing and adult cerebellum
(a) Embryonic cerebellum: precursor cells of the GABAergic neurons, including Purkinje cells and interneurons, are located within the primary germinal zone in the roof of the IV ventricle. Glutamatergic neurons of the deep cerebellar nuclei arise within the rhombic lip and migrate to form the nuclei via the nuclear transitory zone. Granule neuron precursor cells also arise within the rhombic lip, but migrate across the surface of the cerebellar anlage to form the external germinal layer. Granule neuron precursor cells proliferate within the external germinal layer before migrating inward to from the glutamatergic granule neuron of the internal granule layer, (b) The final position in the adult cerebellum of cells generated by the precursor cells shown in panel (a). A third population of stem / precursors cells has been identified in the white matter of the adult cerebellum (Adapted from Gilbertson & Ellison 2008).

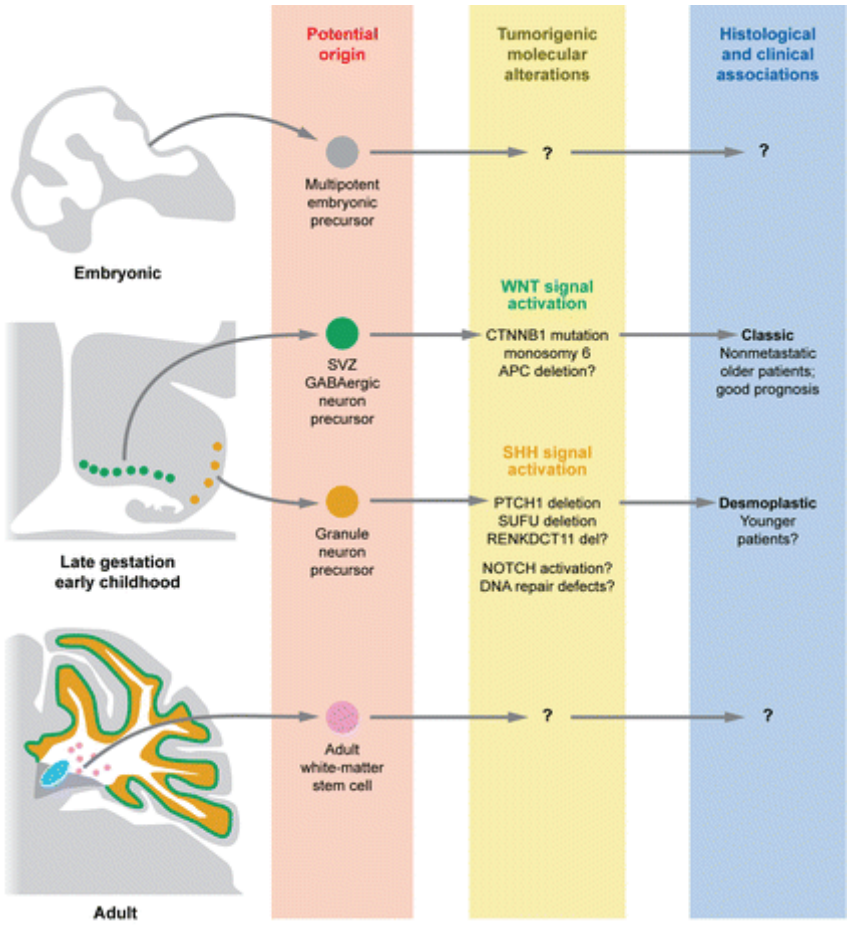

Figure 1.10. Potential cellular and molecular origins of medulloblastoma subgroups (Adapted from Gilbertson and Ellison 2008).

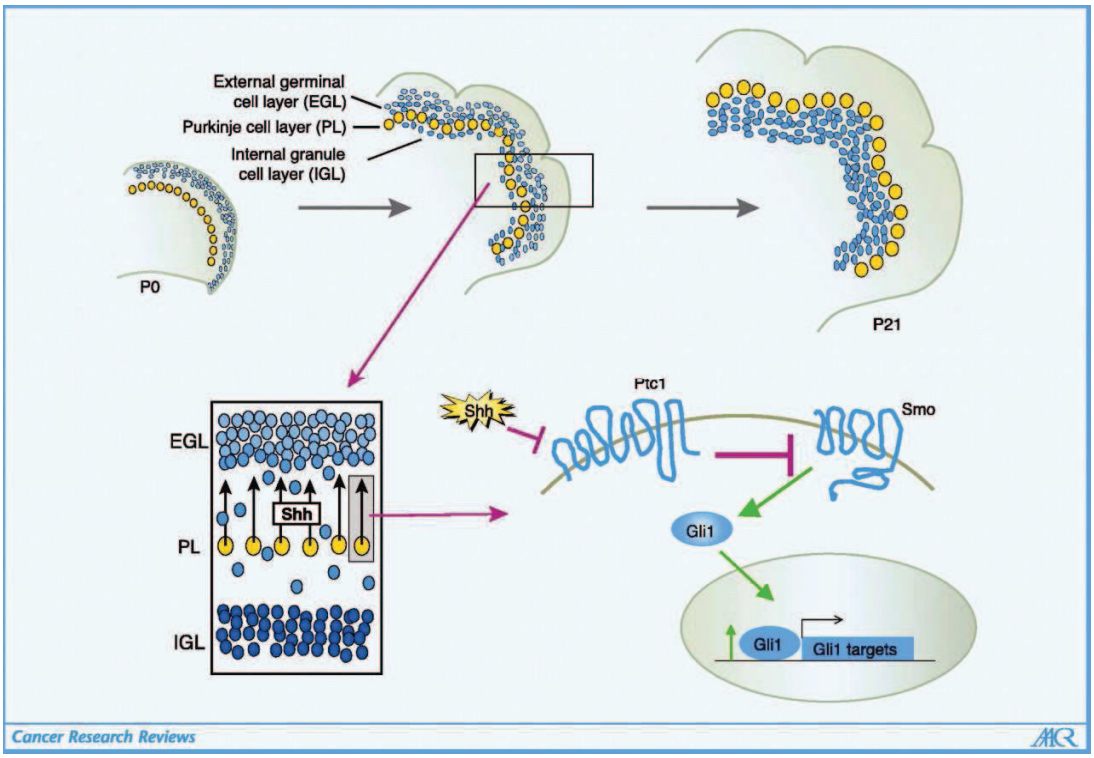

Figure 1.11. The role of SHH pathway in normal development of the cerebellum. SHH released from the Purkinje cells acts on overlying GNP cells in the EGL, leading to proliferation. After this period of Shh-dependent proliferation, granule neurons exit the cell cycle, begin to differentiate, and migrate inwards, past the Purkinje cell layer to reside in the IGL in the mature cerebellum (adapted from Romer and Curran, 2005).

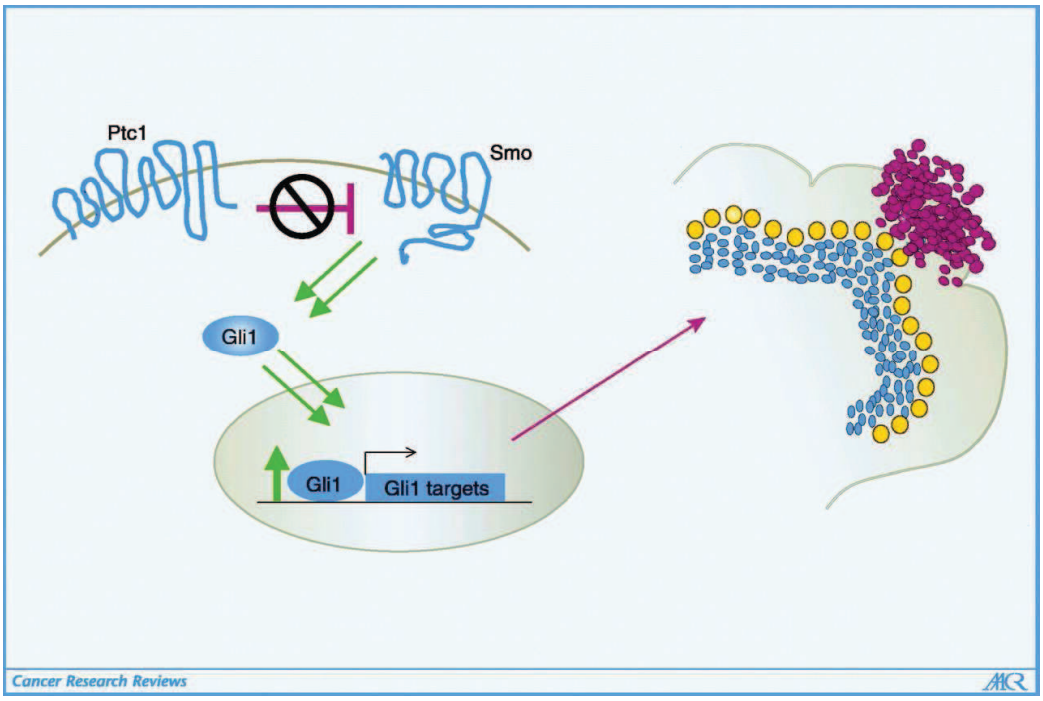

Figure 1.12. Medulloblastoma can arise as an aberration of cerebellar development, when a GNP cell fails to exit the cell cycle and remains proliferating in the EGL. Somatic mutations in different components of the Shh pathway, including PTCH1 and SMOH may contribute to sporadic medulloblastoma and germ line mutations of *PTCH1* gene underlie tumours arising in patients with Gorlin syndrome (adapted from Romer and Curran, 2005).

1.4.1. Stem cells in medulloblastoma

Singh et al (2004) identified that 1-21% of cells in freshly resected medulloblastomas to express CD133, a marker of stem cells. These cells are hypothesised to be capable of self renewal and generating heterogeneous lineages of cancer cells that comprise a tumour, therefore capable of recapitulating all the elements of a tumour. Previous research suggested that cancer stem cells (CSCs) may arise from precursor cells, especially in the CNS, where in the case of medulloblastoma, CSCs may arise from cerebellar precursor cells. This fact raises the question whether different medulloblastoma subtypes are associated with CSCs, and whether they arise from different cerebellar precursor cell populations.

The common primitive undifferentiated stem-or progenitor like appearance of medulloblastoma cells has supported the idea that medulloblastomas arise from CNS stem cells. If this theory is true then stem-like cells within medulloblastoma must be removed in order for patients to be cured. Research has been focused to understand the mechanisms which provide this subset of cells with self renewal capabilities leading to a more aggressive phenotype of the disease and its propagation.

As previously described, the potential origin of medulloblastoma from cerebellar stem and progenitor cells may come from 2 primary germinal epithelia of the cerebellum; deep-seated ventricular zone (VZ) and the superficial external germinal layer (EGL) which give rise to neuronal and glial cells as well as cerebellar granular cells, respectively. The latter type of cells is the most numerous class of neurons in the entire brain (Fan and Eberhart 2008). Additionally, other cerebellar stem cells have been described and could also give rise to medulloblastoma, including CD133 positive cells (Lee et al 2005) and novel stem / progenitor cell populations in the rhombic lip, which gives rise to nuclei of the deep cerebellar white matter (Wang et al 2005). Medulloblastoma of the classic (non-nodular) subtype are believed to originate from the VZ and express Calbindin-D marker associated with this zone, while the nodular / desmoplastic medulloblastoma commonly express the EGL marker p75 presumed to originate from this region. This hypothesis has been supported by murine models, which show aberrant activation of SHH in medulloblastomas of EGL origin (Figure 1.13) (reviewed by Fan and Eberhart 2008).

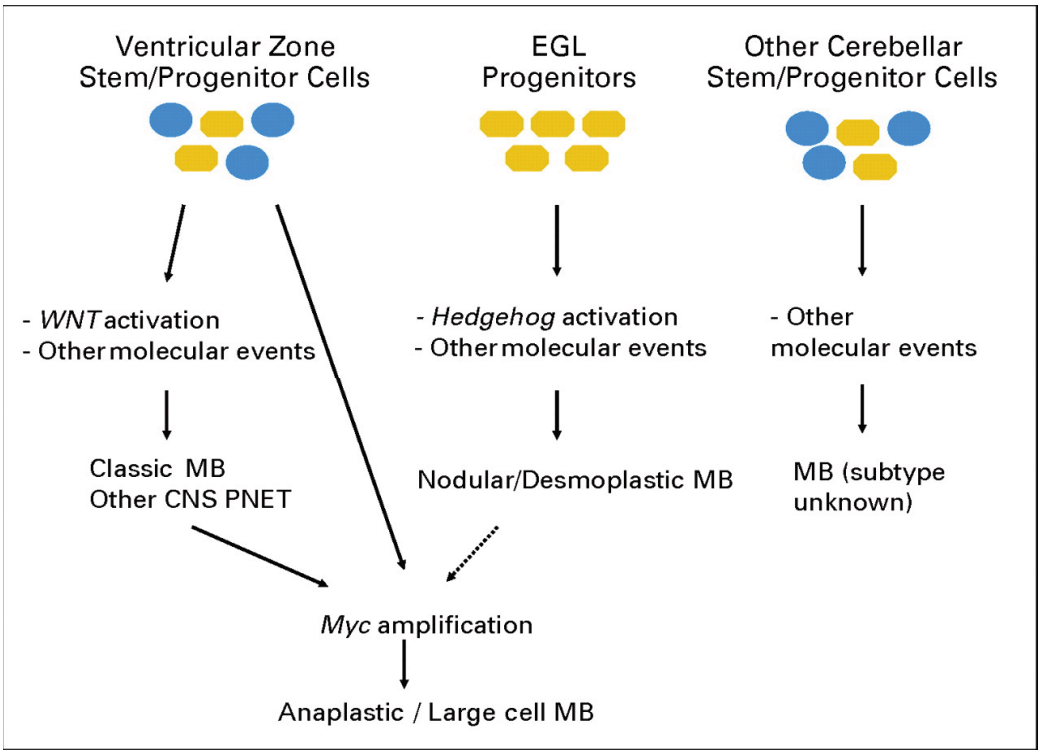

Fig 1.13. Potential cellular origins of medulloblastoma. Mutations activating Wnt have been identified primarily in the classic medulloblastoma subtype, which is thought to derive primarily from stem and /or progenitor cells of the ventricular zone. The external germinal layer (EGL), in contrast, is thought to give rise to nodular/desmoplastic medulloblastoma commonly associated with Hedgehog (Hh) pathway activation. Other cerebellar stem and progenitor cells have been described and may also give rise to medulloblastoma. MB= medulloblastoma; PNET= primitive neuroectodermal tumour (adapted from Fan & Eberhart, 2008).

Several signalling pathways aberrantly activated in medulloblastoma are also required in neural stem cells, including the SHH pathway, which regulates neural stem-cell development and cerebellar EGL. Granule cell precursors from the EGL have been shown to transform into medulloblastoma-like tumours in transgenic mice displaying loss of *ptch*. The Wnt/Wg pathway regulates the proliferation of stem and progenitor cells within the foetal VZ, post natal SVZ and hippocampus but does not seem to regulate EGL precursors which is consistent with why the Wnt/Wg pathway is activated in medulloblastoma of the classic subtype supporting the fact that this variant may

arise from stem / progenitor cells outside EGL (e.g. VZ) (reviewed by Fan and Eberhart 2008). Activation of the pathway appears to be mutually exclusive from tumours with aberrations in SHH and chromosome 17, thus, the role of Wnt/Wg activation is not confirmed to play an important role in cancer stem cells-derived medulloblastoma.

Notch signalling also regulates neural stem and progenitor cells in the embryonic VZ and rhombic lip and their equivalent post natal SVZ and EGL. Activation of Notch promotes proliferation and / or survival of stem cells during CNS development whilst inhibiting differentiation. This is a complex pathway which displays idiosyncrasy, where Notch2 promotes proliferation of cerebellar granular neurone progenitors, while Notch1 expression is associated with cell cycle exit and differentiation (Fan et al 2004). Over expression of Notch2 is associated with primary medulloblastoma and tumour proliferation, while Notch1 was undetectable and appears to suppress tumour growth supporting this notion of the association between chromosomal gain of Notch2 locus and poor clinical outcome. Two of the mechanisms which may promote neural stem cell proliferation via Notch signalling and medulloblastoma formation are SHH activation and hypoxia.

There is controversy around the percentage of stem-like cancer cells within tumours which are capable of unlimited self renewal. In cases of medulloblastoma, only a small fraction of stem-like cancer cells show this property and are responsible for tumour growth and metastasis, while the rest of the neoplasm is usually formed of progenitors of limited but relatively rapid proliferation rates or well differentiated cells

(Reviewed by Wang et al 2005). Those latter cells may transform into cancerous cells, followed by acquiring stem-like properties after their transformation.

1.5. Potential improvement of patients' outcome through the use of prognostic molecular markers for medulloblastoma

Medulloblastoma patients are currently stratified based only on clinical criteria (age, metastatic stage at diagnosis and extent of tumour resection) into average risk and high-risk groups. However, as previously described, their clinical outcome does not absolutely follow this classification and 20% of standard risk patients experience disease relapse while over 40% of high-risk patients may be cured. Neither histopathological nor molecular criteria are currently taken in account. A significant amount of research and investigation has therefore focused on the investigation and validation of such variables, in order to assess their potential use in disease classification, which may provide more accurate, individualized disease stratification and tailoring of treatment.

Although numerous molecular markers have been tested to date in order to allow better disease stratification, only a few have shown consistent and significant results and have the potential to be taken into clinical practice. These include molecular markers (e.g. β-catenin nuclear localization and *MYC* gene amplification) and tumour pathology subtypes (Table 1.8).

Tumours with Wnt/Wg pathway activation, optimally detected through nuclear immunoreactivity of β-catenin, have been consistently associated with good prognosis

in multiple studies (Clifford, 2006; Ellison, 2005). On the other hand, amplification of the *MYC* oncogene, defects of chromosome 17 and expression of ERBB2 receptor tyrosine kinase have been associated with a poor outcome (Ray et al 2004), although the latter 2 markers have not been consistently reported as significant in isolated studies. Other less consistently reported prognostic biological markers also include expression of the *MYC* oncogene, TRKC neurotrophin receptor and *MYCN* oncogene amplification. So far, activation of the SHH pathway and chromosome 9q deletions have not shown associations with prognosis (reviewed in Pizer and Clifford 2009).

At the histopathological level, large cell/ anaplastic medulloblastoma has been repeatedly associated with a poor prognosis (Brown et al 2000, Eberhart et al 2002, Lamont et al 2004, Gajjar et al 2004 and 2006, Giangaspero et al 2006), while MBEN, which occurs mainly in infancy, is associated with a favourable outcome (Ellison 2002). The desmoplastic / nodular variant has been associated with favourable outcome in infant patients with medulloblastoma, while this significant association is lost among older children with the disease (McManamy 2007).

	Disease marker	**Clinical trials**
Favourable risk	WNT pathway activation (β-catenin nuclear stabilization)	PNET3 (Ellison et al 2005), SJMB96 (Gajjar et al 2006)
	Desmoplastic/nodular histology (in infants ≤3 yrs)	HIT-SKK'92 (Rutkowski et al 2005), CNS9204 (McManamy et al 2007)
Adverse risk	*MYC* gene amplification	PNET3 (Lamont et al 2004), HIT '91(Rutkowski et al 2007)
	Large-cell or severe anaplastic histology	SJMB96 (Gajjar et al 2006), PNET3 (McManamy et al 2007)

Table I.8. Molecular and histopathological markers of disease-risk stratification in medulloblastoma, showing disease features which have displayed consistent associations with prognosis in ≥2 clinical trials-based studies (adapted from Pizer and Clifford 2009).

1.5.1 Requirements and difficulties facing the development and validation of molecular indices for prognostication in medulloblastoma

Several issues must be addressed before routine application of histopathological and molecular criteria in disease classification can be put into practice. So far, assessment of these markers reported has generally been undertaken in small, retrospectively collected, heterogeneously treated cohorts; therefore the collection of fresh frozen tumour samples is a necessity to allow analysis of target biological markers. Multi-centre collaborations may provide the opportunity to collect large number of fresh frozen and for FFPE samples, ideally in the context of clinical trials, which have been subjected to standardized protocols of treatment to allow the impact of molecular markers to be accurately assessed. Methodologies must also be developed for the robust assessment and quality control of any molecular measurements taken, ideally in routinely collected FFPE tumour material. Finally, the relative utility and interaction between multiple prognostic markers must be considered in order to define optimal models for disease risk prediction.

New understanding of medulloblastoma molecular genetics may help identify new therapeutic targets

The most commonly investigated approach uses small molecule inhibitors against pathways constitutively mutated in medulloblastoma (e.g. SHH, Wnt/Wg, *ERBB2*, PDGFR and the RAS/MAPK pathways). Inhibitors of the SHH pathway are the most widely investigated agents and have shown promising results in pre-clinical trials

in both xenograft models and transgenic mice with medulloblastoma (Figure 1.14) (reviewed by Pizer and Clifford, 2009).

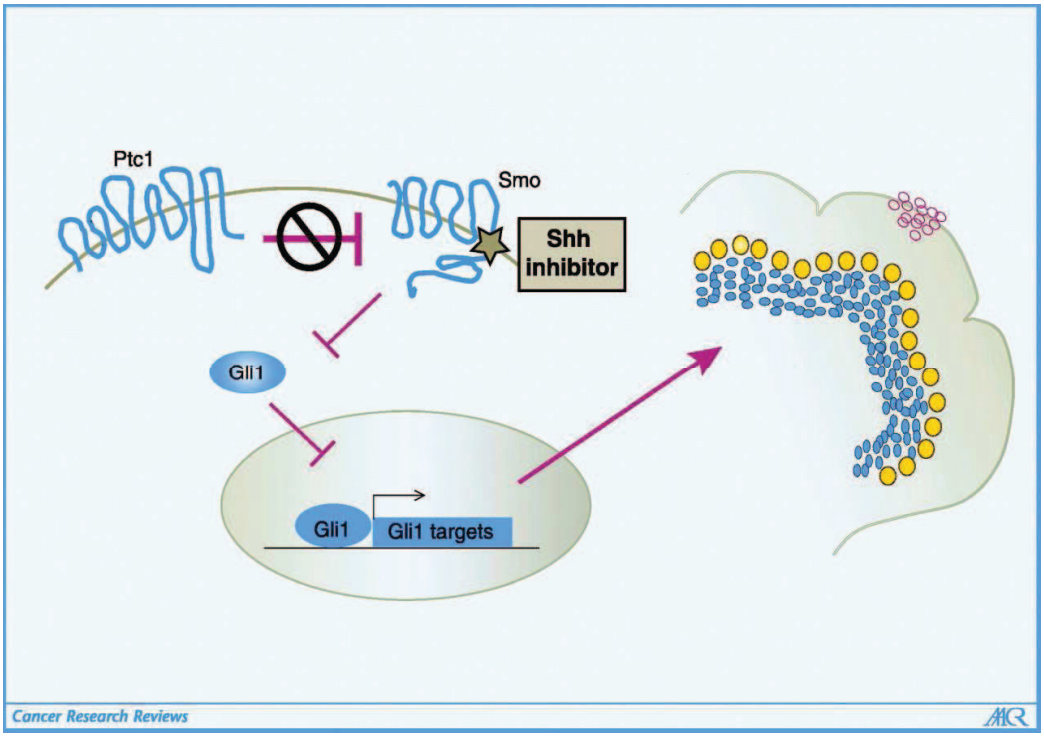

Figure 1.14. Developing targeted therapies for medulloblastoma The link between the Shh pathway and medulloblastoma led to investigate whether suppressing Shh signalling in these tumours in vivo could be therapeutic. Using small molecule inhibitor of the Shh pathway *(HhAntag-691, a Smo* inhibitor) in a mouse model of medulloblastoma showed that treating mice with the Smo inhibitor suppressed the Shh pathway and led to the elimination of tumours. This was accompanied by a decrease in tumour cell proliferation and increase in apoptosis. Importantly, long-term treatment prolonged tumour-free survival of the mice. This experiment underlines the importance of developing relevant animal models in which to test new cancer therapies (adapted from Romer and Curran, 2005).

1.6. Role of the Wnt/Wg pathway in cancer development

Assessment of the role of the Wnt/Wg pathway as a prognostic indicator forms the major theme of this thesis. The Wnt/Wg signalling pathway has been highly conserved during evolution. Together, Wnt/Wg and other signalling systems (Hedgehog, Notch, TGFβ, and receptor tyrosine kinase) are the most recognized

molecular mechanisms involved in embryonic development. They function as morphogens, being secreted from one cell or tissue while activate surface receptors, signal transduction components and transcription factors within nearby cells or tissues, regulating cell proliferation, apoptosis and differentiation. During normal development, these signalling pathways are tightly regulated while their disruption can lead to the development of several diseases including cancers. Oncogenes can develop as a consequence of gain-of-function mutations of a signalling component which normally functions transiently during development. On the other hand, tumour suppressor genes lose their inhibitory effects as a result of loss-of-function mutations (Klaus and Brichmeier 2008) and may lead to pathway activation. Genes in the Wnt/Wg pathway were initially thought to function transiently in development however, many of them later appeared to act as oncogenes and tumour suppressor genes when they become deregulated, contributing to cancer development. Members of the β-catenin dependent canonical Wnt pathway include; *CTNNB1, APC, BTRC, AXIN, GSK3*-β*, CBP, Groucho, Conductin* and *TCF,* while *c-MYC* and C*yclin D1* act as key downstream transcriptional targets for this pathway.

As previously described in section (1.3.4.3.), the canonical Wnt/Wg pathway regulates intra-cellular and cytoplasmic β-catenin, which is a key transcriptional activator in normal development. In the normal inactive pathway, β-catenin associates with a multiprotein cytoplasmic complex including APC*,* GSK3-β and AXIN 1, which allow phosphorylation and degradation of β-catenin through the ubiquitin-dependent proteasome. Activation of the Wnt/Wg pathway destabilizes the APC, GSK3-β and AXIN 1 complex, leading to nuclear translocation and accumulation of β-catenin which

results in transactivation of TCF/LEF transcriptional complexes which persistently up-regulate downstream target genes (e.g. *cyclin D1* and *MYC*) associated with cell proliferation and tumorigenesis (Taipale and Beachy 2001) (Figure 1.15).

The Wnt/Wg pathway regulates β-catenin stability and context-dependent transcription. This signalling pathway controls many processes including cell fate determination, cell proliferation and self renewal of stem and progenitor cells. As well as its role as a transcriptional activator controlled by Wnt/Wg signalling, β-catenin is also involved in regulating cell-cell adhesion.

Deregulation of β-catenin signalling is involved in a number of malignancies including colon cancer, melanoma, ovarian cancer, hepatocellular carcinoma, endometrial cancer, pilomatricomas and prostatic cancer (reviewed in Morin 1999).

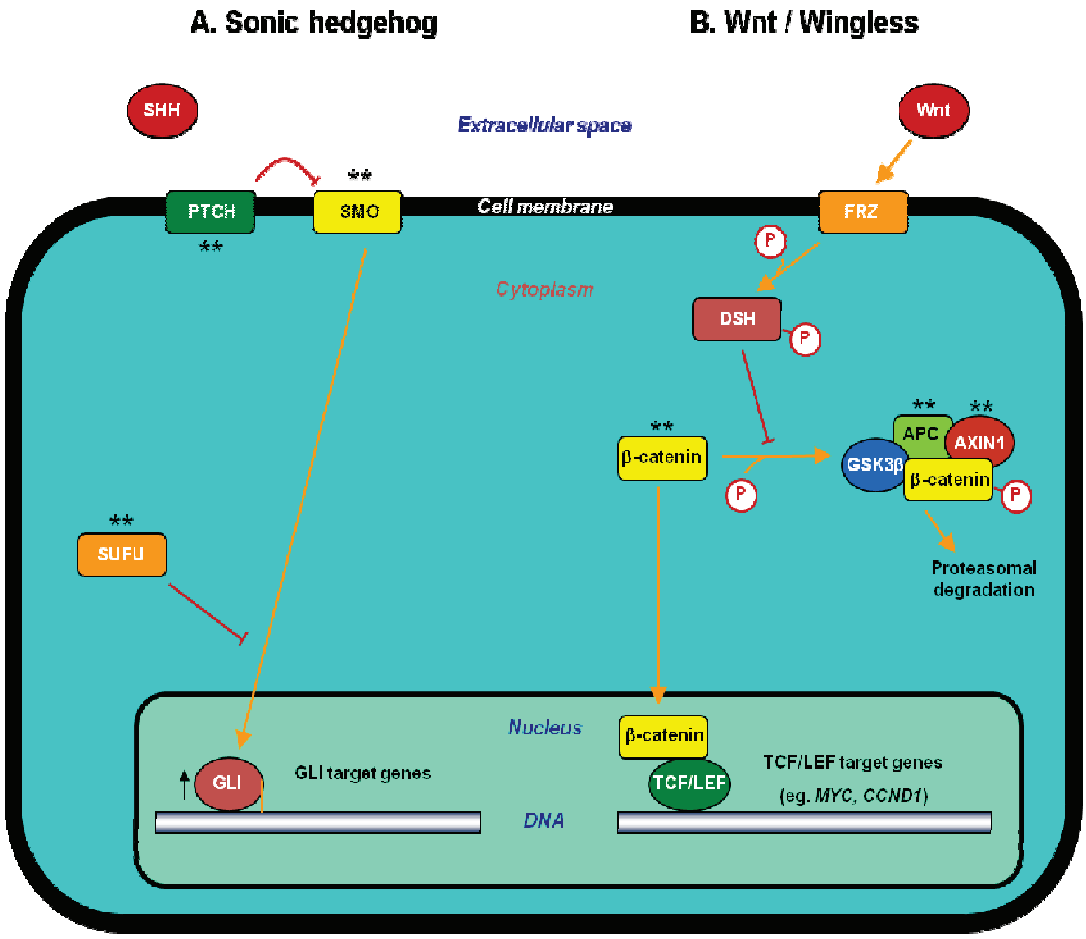

Figure 1.15. Summary of the canonical Wnt signaling pathway (right) Activation of Frizzeled by Wnt activates Dishevelled which anatagonizes the multiprotein complex that contains *APC, AXIN1* and glycogen synthase kinase-3β and prevents phosphorylation and degradation of β-catenin. This leads to to its upregulation and translocation to the nucleus, where it acts as a co-activator for transcriptional factors (e.g. *MYC* and *CCND1*). (left) SHH pathway includes common negative regulators with Wnt/Wg pathway (e.g. β-TRCP, SUFU) (see text for explanations). "Double stars" represent pathway components, which are mutated in medulloblastoma causing pathway activation. (Adapted from Pizer and Clifford 2009).

β-catenin appears to play a role in 2 distinct functions in cancer development; its involvement in tumour invasion and metastasis as well as its oncogenic properties in tumorigenesis. The former function is mediated through its role in cell adhesion, where β-catenin, α and γ catenins associate with the cytoplasmic region of E-cadherin,

a transmembrane protein, promoting homotypic cell-contact. Binding of β-catenin with E-cadherin occurs through the conserved armadillo repeat region of β-catenin. The second function of β-catenin is independent of cell adhesion properties and involves its signalling activity in the canonical Wnt/Wg pathway. It is the monomeric β-catenin form that is involved in this (while large molecular weight protein is involved in cell adhesion function) (Morin 1999).

The tumorigenic function of β-catenin results from deregulation of the Wnt/Wg pathway, and subsequently improper activation of down stream transcriptional target genes involved in cell proliferation and differentiation (reviewed by Morin 1999). The function of β-catenin in Wnt/Wg signalling depends on the ratio of cytoplasmic / nuclear protein available. Free cytoplasmic β-catenin level is crucially controlled by a multi-protein complex formed of *APC, AXIN1* and *GSK3*-β, which leads to its degradation by the ubiquitin-proteasomal pathway. Association between β-catenin and this multimeric protein complex depends on phosphorylation of β-catenin by the serine-threonine kinase *GSK3*-β at the ubiquitination motif, which exists along a stretch of 3 serines and one threonine, each separated by 3 residues (Figure 1.16). Mutations in cancer that prevent phosphorylation of these residues prevent ubiquitination and degradation of β-catenin leading to its accumulation and translocation into the nucleus. Additionally, β-catenin can be degraded by β-TRCP, which binds β-catenin in a phosphorylation-dependant manner directing it into the ubiquitin ligase complex (reviewed by Morin 1999).

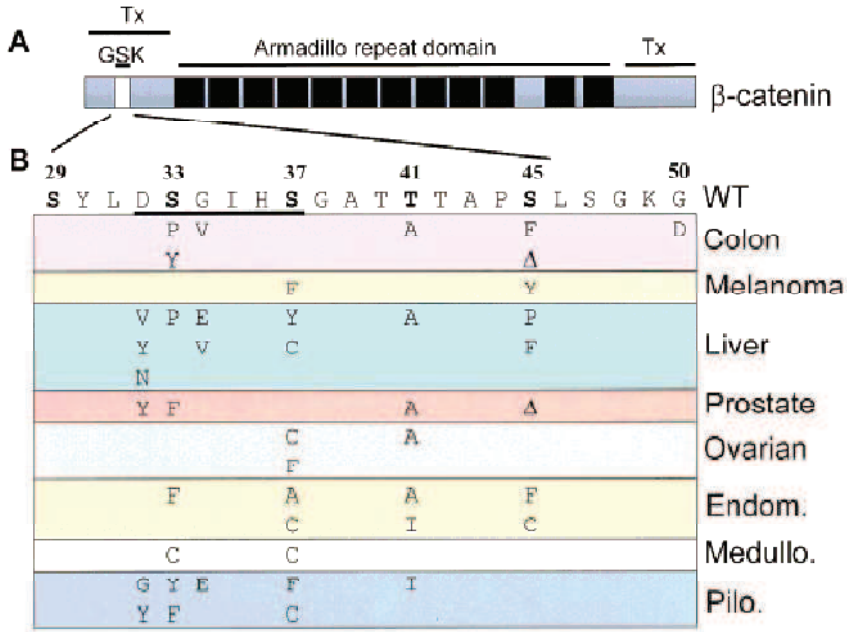

Figure 1.16. Diagram of β-catenin and the mutations identified in cancer A: Diagram of the β-catenin protein showing the armadillo repeats (black boxes) and the N-terminal consensus *GSK3*-β phosphorylation domain (GSK).The two transcriptional activation domains (Tx) are indicated. B: Amino acid sequence of the regulatory region of wild-type (WT) β-catenin and predicted changes reported in the various tumor types are indicated. The residues of the ubiquitination motif are underlined and the putative *GSK3*-β phosphorylation residues are indicated in bold. Endom= endometrial cancer; Medullo= medulloblastoma; Pilo=pilomatricoma. Deletions involving exon 3 have been identified in several of these tumours (adapted from Morin, 1999).

The TSG *APC* plays a major role in controlling levels of β-catenin, where it forms part of the multimeric protein complex responsible for its degradation. *APC* binds to the armadillo repeat region of β-catenin, this is important for the tumour suppressive function of *APC*. The interaction between *GSK3*-β, *APC* and β-catenin is a complex one, where *GSK3*-β initially phosphorylates the 20 amino acids repeat of *APC,* which favours the association between it and β-catenin. The main down regulators of β-catenin include TSG *APC, GSK3*-β, *AXIN1* (and to a lesser extent *AXIN2*), β-*TRCP* (Table 1.9). Down-regulation of β-catenin (mainly the free form) results in absence of signalling and inactivation of the Wnt/Wg pathway due to its degradation and inability to

associate with TCF family of genes with subsequent transcription of down stream target genes (e.g. *CMYC* and *Cyclin D1*). Other regulators of β-catenin are listed in Table 1.9 and include Wnt itself and *Akt;* the latter is an oncogene with serine / threonine kinase activity, which inactivates *GSK3*-β by phosphorylation. *Frat1* and its homologue *GBP*, both oncogenes, can also inactivate *GSK3*-β (reviewed by Morin 1999).

Regulators of β-catenin signalling		
Protein	**Description**	**Presumed effect of β-catenin signalling**
APC	Colon tumour suppressor	Downregulation
GSK3-β	serine/theronine kinase	Downregulation
WNT	Secreted glycoprotein first isolated as a mouse oncogen Morphogen	Upregulation
HGF	Cytokine acting as a nitrogen and motility factor	Upregulation
AXIN	Encoded by the mouse fused locus. Regulates embryonic axis formation	Downregulation
Conductin/Axil	Homologue of Axin	Downregulation
β-TRCP	Part of ubiquuitination machinery	Downregulation
GBP	Homologue of the Frat1 oncogene (mouse T-cell lymphoma).Interacts and Downregulates GSK3-β	Upregulation
AKt	Oncogene with serine theornine kinase activity	Upregulation
c-erbB-2	Receptor-like tyrosine kinase	Unknown
PP2A	Protein phosphatase	Downregulation
Presenilin-1	Mutated in familial Alzheimer's disease	Downregulation

Table 1.9. Known and putative regulators of β-catenin signalling (Adapted from Morin 1999).

1.6.1. Wnt/Wg pathway activation and medulloblastoma development

Eighteen to 30 % of sporadic medulloblastomas show aberrant Wnt/Wg pathway activation. Approximately 10% of the 30% contain oncogenic mutations in the *CTNNB1* gene, which encodes β-catenin. These mutations affect the *GSK3*-β phosphorylation domain, leading to desensitization of β-catenin to phosphorylation and degradation. These tumour-causing mutations result in inappropriate stabilization of β-catenin. Accumulated β-catenin then translocates to the nucleus and upregulates tumorigenic target genes. Other components of the Wnt/Wg pathway including *APC, AXIN1* and *AXIN2* each show mutations in about 2.5%, however, to date, no mutations were detected in *GSK3*-β (Zurawel et al 1998, Eberhart et al 2000, Dahmen et al 2001, Baeza et al 2003). β-catenin nuclear accumulation may be detected using IHC techniques, 60-70% of clinical samples showing β-catenin nuclear accumulation by IHC also harbour *CTNNB1* mutations (Eberhart et al 2000). Although mutations in *AXIN2* are rare, they have been associated with β-catenin nuclear stabilization (Koch, 2007), while so far there is no clear relation between either *APC* or *AXIN1* with β-catenin nuclear stabilization. Therefore, β-catenin nuclear stabilization appears to be a marker of pathway activation, and cases which show β-catenin accumulation with no evidence of *CTNNB1* mutations may harbour mutations in other components of the Wnt/Wg pathway or different mechanisms of genetic or epigenetic activation may be driving the nuclear accumulation of β-catenin.

Medulloblastomas which show activation of the Wnt/Wg pathway appear to form a unique molecular subgroup of the disease defined by distinct gene expression

profiles, genomic features and clinical outcome. Medulloblastoma with Wnt/Wg activation are mostly of the classic histological subtype, and develop in older children in approximately 75% of these cases harbour *CTNNB1* mutations (Eberhart et al 2000, Koch et al 2001; Ellison et al 2005). The gene expression signature displayed by the Wnt/Wg active subgroup of medulloblastoma is mutually exclusive from the gene expression signature displayed by medulloblastomas with SHH pathway activation (Thompson et al 2006; Kool et al 2008). At the genomic level, the former subgroup shows significant association with loss of one copy of chromosome 6. This subgroup also is mutually exclusive from medulloblastomas which harbour aberrations on chromosome 17, which is the most common chromosomal abnormality seen in medulloblastoma (Clifford et al 2006; Thompson et al 2006; Kool et al 2008; Fattet et al 2009). Medulloblastomas with mutations in the SHH signalling pathway components (*PTCH1, SUFU* or *RENKDT11*) are commonly but not exclusively of the desmoplastic histological subtype (Ellison 2002, Di-Marcotullio et al 2004, Thompson et al 2006). These data suggest that Wnt/Wg and SHH signalling pathways drive the pathogenesis of 2 distinct subtypes of medulloblastoma with different clinical and morphological patterns. However, these 2 mechanisms only involve 30-50% of medulloblastoma in total and other pathways are likely to be responsible for the tumorigenisis of the remaining tumours (Offit et al 2003, Fan et al 2004).

In a study by Clifford et al (2006), 19 medulloblastoma were initially assessed for Wnt/Wg activation by testing for β-catenin immuno-reactivity, *CTNNB1* and *APC* mutation analysis as well as a genome-wide analysis by array-CGH to delineate genomic copy-number aberrations. 3 (16%) cases showed *CTNNB1* mutations affecting

the *GSK3*-β phosphorylation residues; 2 of those cases had strong combined cytoplasmic and nuclear β-catenin immuno-reactivity. Those 3 cases also had a unique genomic profile showing a complete loss of chromosome 6 in the absence of other significant genomic defects. Unsupervised hierarchical cluster analysis of the aCGH data for the whole cohort arranged them into 3 groups; Group "A" characterized the Wnt/Wg active group, which showed a low number of other independent genomic defects, were exclusively significantly associated with *CTNNB1* mutations, β-catenin nuclear immuno-reactivity and chromosome 6 loss. Group "B" was characterized by genomic defects previously proved to be associated with medulloblastoma (gain of chromosome 7, 17q, losses of chromosome 8, 10p, 11p/q, 17p and 19q). Aberrations on chromosome 17, the most common chromosomal defect in MB, were exclusively present in group B and mutually exclusive from group A cluster (p= 0.021, Fisher's exact test). Group "C" was not associated with any specific gene expression profile. Clifford et al (2006) then validated their findings by assessing the relationship between Wnt/Wg pathway status and specific chromosomal aberrations using a wider cohort of medulloblastoma samples of known Wnt/Wg active status. 13 Wnt/Wg active tumour samples (9 of which had *CTNNB1* mutations) and 19 Wnt/Wg negative tumour samples (control samples) were tested for chromosome 6 loss and 17p loss. A statistically significant portion of the Wnt/Wg active tumour samples (62%, 8/13) had loss of an entire copy of chromosome 6, but this was not observed in other cases, while 17p loss was only detected in the Wnt/Wg negative tumour samples, suggesting these events are mutually exclusive. Other studies by Thompson et al 2006; Kool et al 2008 and

Fattet et al 2009 have also investigated the correlation between chromosome 6 loss and other Wnt/Wg pathway makers, and these studies are discussed in chapter 6.

1.6.2. Clinical significance of Wnt/Wg pathway activation in medulloblastoma

Thus, three different molecular correlates of the Wnt/Wg medulloblastoma subgroup have been identified to date; β-catenin nuclear stabilization, *CTNNB1* mutation and chromosome 6 loss. Activation of the Wnt/Wg pathway in medulloblastoma has proven to be an independent marker of favourable prognosis in multiple studies. A first study by Ellison et al (2005), showed that medulloblastoma with Wnt/Wg pathway activation had 5 years OS of 92.3% compared to 65.3% for those without Wnt/Wg activation. Other studies by Gajjar et al 2006; Fattet et al 2009, have confirmed the above findings and are discussed extensively in chapters 4, 5 and 6. Wnt/Wg activation may therefore identify a favourable risk group of cases which could be treated differently with the goal of reducing late effects within this group. The relationship between the different Wnt/Wg pathway markers and their relative utility for the identification of Wnt/Wg pathway activation, have not however been addressed. Moreover, the prognostic significance of *CTNNB1* mutation and chromosome 6 loss has not been assessed to date, nor the relative utility of these markers for the prediction of disease prognosis. Finally, all markers require assessment in extensive trials cohorts, alongside other molecular and clinical markers of prognostic significance, before they can be considered for clinical use. The work in this project have addressed and assessed those points. It is worth noting that in this project all

analysis were performed irrespective of the metastatic stage for the PNET3 cohort, which allowed assessment of all clinicopathological and molecular variables on the cohort without being influenced by the metastatic stage.

1.7. Summary

Previous studies have indicated that Wnt/Wg pathway activation occurs in a significant subset of medulloblastoma (15-30%). This is associated with a favourable prognosis and therefore could potentially be used as a molecular marker for therapeutic stratification. However, before incorporating this marker in clinical practice, further validation and testing on wider clinically controlled cohorts must be done. Furthermore, the interrelationship between markers used to identify Wnt/Wg activation (β-catenin nuclear localization, *CTNNB1* mutation and chromosome 6 loss) need to be further assessed in wider cohorts, especially to understand the significance of *CTNNB1* mutation, chromosome 6 loss and prognosis. Improving the current clinical disease stratification may then potentially be achieved by adding validated molecular markers to current clinical markers. Finally, the routine assessment of molecular markers will require the development of robust assays which can be engaged in routinely collected tumour biopsy material.

1.8. Aims of the project

The major aim of this project is:

To investigate the biological role and the prognostic significance of Wnt/Wg activation in medulloblastoma, and its utility for the prediction of disease course alongside existing clinical and pathological risk markers, in a large cohort of patients derived from the PNET3 clinical trial.

Subsidiary aims are:

1. To assemble a large cohort of medulloblastoma from the PNET3 clinical trial, as a basis for investigation.

2. To develop methodologies for the routine assessment of molecular markers in routinely collected FFPE tumour material.

3. To assess alternative molecular markers of Wnt/Wg pathway activation (chromosome 6 loss; β-catenin IHC and *CTNNB1* mutation), their inter-relationship and prognostic significance.

4. To use these data to determine the optimal means of assessing Wnt/Wg pathway activation in medulloblastoma.

5. To investigate the prognostic significance of chromosome 17p loss in medulloblastoma, and whether a mutually exclusive relationship exists between chromosome 17p loss and Wnt/Wg pathway activation.

6. To investigate the prognostic significance of medulloblastoma clinical and pathological disease features in the PNET3 cohort.

7. To determine any relationship between molecular, clinical and pathological disease features assessed in this cohort.

8. To combine these data to develop optimal models for disease risk stratification in medulloblastoma, based on molecular, clinical and pathological variables.

Chapter 2

Materials and Methods

2.1. Materials

2.1.1. The NMB cohort of primary medulloblastomas

The Newcastle medulloblastoma (NMB) cohort consisted of 76 randomly selected primary medulloblastoma tumour DNA samples. These DNA samples were collected from the medulloblastoma bank at the Northern Institute for Cancer Research, Newcastle University. 26 cases had matched constitutional DNA available. 37 of these cases were originally kindly provided by the U.K. Children's Cancer Study Group (UKCCSG) tumour bank and by Prof. HK Ng, Department of Anatomical and Cellular Pathology, the Chinese University of Hong Kong, Hong Kong, China. 21 cases (RJG) samples were kindly provided by Dr. Richard Gilbertson, Department of Developmental Neurobiology, St. Jude Children's Research Hospital Memphis, Tennessee, USA. All these samples were provided in the form of genomic DNA and were stored at – 80 ^{o}C.

Eighteen further cases (EGY) were kindly provided by Prof. Amina Hindawy, Paediatric Neurology Department, Specialized Paediatric Hospital, Cairo University, Egypt. These were in the form of fresh frozen tissue samples, accompanied by 5 ml of matched blood. These fresh samples were collected during surgical resection and were put immediately in RNAlater solution (Applied Biosystems, U.K.) as protocol and stored at -20^{0}C. Informed consent and ethical approval for research was obtained for all samples investigated.

Clinical data was not available for 4 patients, so the remaining 72 samples formed the core of this study. The available clinical data for this cohort were; age at time of diagnosis (72 cases), gender (72 cases), histopathology of the tumour tissue (72 cases), metastatic stage at time of diagnosis (67 cases), period of follow up and the current status of the patients (64 cases). The data for treatment protocol, event of recurrence and progression free survival time were not available (Table 2.1).

There were 47 (65.3%) males and 25 (34.7%) females. Their ages ranged from 0.7 to 19 years with a mean age of 7.25 years. Thirteen samples were from patients less than 3 years old, and 59 were from patients ≥ 3 years of age. Figure 2.1 shows the age distribution in one year intervals for all patients in this cohort. The duration of the follow up period for the 64 cases with available data ranged from 0.1 month to 204 months, with a mean of 43 months. At the end of the study 43 cases (67.2%) were censored and 21 (32.8%) were dead. The metastatic stage of the tumours at time of diagnosis according to Chang's classification (Chang et al 1969) was 39 cases (58.2%) stage M0/1 and 28 cases stage M2/3 (41.8%).

The histopathological subtypes of all the cases were reviewed by Prof. David Ellison, Newcastle General Hospital, Newcastle upon Tyne (Now Department of Pathology St. Jude children's hospital, Memphis, Tennessee, USA). Histopathological classification according to WHO (2007) criteria (Louis et al 2007) showed that 44 cases (61.1%) were classic subtype, 22 cases (30.6%) were nodular/desmoplastic medulloblastoma, while the remaining 6 cases (8.3%) showed large cell/ anaplastic pathology. Descriptive clinical and pathological variables for the cohort are summarized in Table 2.2.

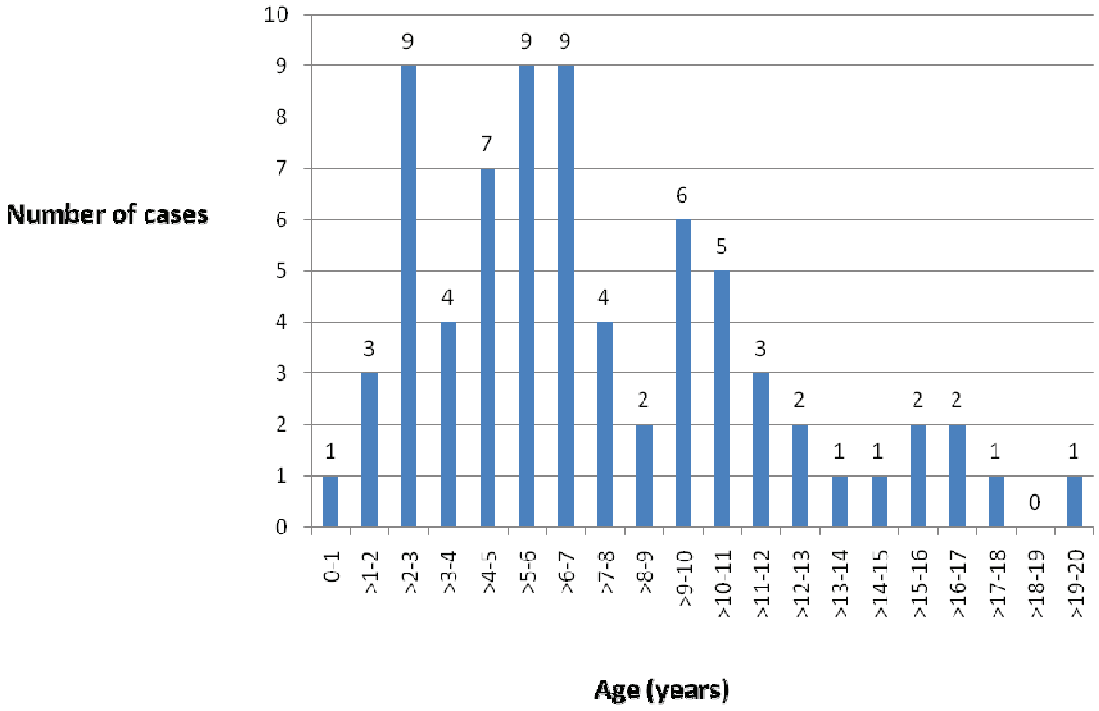

Figure 2.1. Age at diagnosis of the NMB cohort distributed in one year intervals.

	Cohort	Pt. No.	Sex	Age (years)	Path.	M-stage	Follow up (months)	Current Status
1	NMB	NMB 20	M	6.6	C	M0/1	28.1	Dead
2	NMB	28	M	6.3	C	M0/1	108	Alive
3	NMB	38	M	9.8	C	M0/1	18.3	Dead
4	NMB	43	M	10	C	M0/1	62.4	Alive
5	NMB	45	M	12.6	C	M0/1	66.6	Alive
6	NMB	46	M	5.1	C	M0/1	52.9	Alive
7	NMB	51	M	6.8	C	M0/1	59.1	Alive
8	NMB	52	F	8.6	C	M0/1	50.4	Alive
9	NMB	59	M	6.6	LCA	M0/1	13.5	Dead
10	NMB	60	M	5	C	M0/1	1	Dead
11	NMB	61	M	10.3	C	M0/1	5.2	Alive
12	NMB	63	M	11.5	C	M0/1	51.5	Alive
13	NMB	64	F	1.5	MBEN	M0/1	0.5	Dead
14	NMB	65	M	9.3	C	M0/1	3.5	Alive
15	NMB	66	M	4.9	C	M0/1	0.1	Dead
16	NMB	68	F	6.8	C	M0/1	2.5	Alive
17	NMB	69	M	7.9	C	M0/1	99.7	Alive
18	NMB	70	F	3.3	C	M0/1	85.2	Alive
19	NMB	71	M	16.1	C	M0/1	41.5	Dead
20	NMB	74	M	5.9	C	M0/1	11.8	Alive
21	NMB	76	M	7.5	C	M0/1	2.3	Dead
22	NMB	78	M	5.5	C	M2/3	0.3	Dead
23	NMB	79	F	3.5	C	M2/3	90	Alive
24	NMB	80	F	10.2	C	M0/1	23.7	Alive
25	NMB	81	F	14.2	ND	M0/1	45.8	Alive
26	NMB	82	M	5.4	C	M0/1	19.5	Alive
27	NMB	84	F	15	C	M2/3	13.2	Alive
28	NMB	87	M	2.5	C	NA	NA	NA
29	NMB	88	F	17	C	NI	NA	NA
30	NMB	89	F	4.6	C	M0/1	91.7	Alive
31	NMB	90	F	3	C	NA	NA	NA
32	NMB	93	M	10	C	NA	NA	NA
33	NMB	94	F	9	C	NA	NA	NA
34	RJG	112	F	0.7	ND	M0/1	16.4	Dead
35	RJG	113	M	2.5	LC/A	M2/3	204	Alive
36	**RJG**	**114**	**M**	**2.9**	**C**	**M0/1**	**13.2**	Dead

Table 2.1. (See following page for legend)

Table 2.1. (continued)

	Cohort	Pt. No	Sex	Age (yeas)	Path.	M-stage	Follow up (months)	Current status
37	RJG	115	M	4.6	C	M0/1	187.8	Alive
38	RJG	116	M	19	ND	M0/1	185.6	Alive
39	RJG	117	M	12.8	C	M2/3	40.7	Dead
40	RJG	118	F	2.6	C	M2/3	175.3	Alive
41	RJG	121	M	4.1	LCA	M0/1	166.2	Alive
42	RJG	122	M	2.5	LCA	M0/1	21.3	Dead
43	RJG	123	F	15.4	C	M0/1	145.6	Alive
44	RJG	124	M	6.3	ND	M2/3	29.3	Dead
45	RJG	126	M	2.6	ND	M2/3	124.4	Alive
46	RJG	127	F	4.8	ND	M0/1	114.3	Alive
47	RJG	129	M	11.5	C	M0/1	28.0	Dead
48	RJG	131	F	5.7	ND	M2/3	11	Dead
49	RJG	132	F	11.6	LCA	M0/1	38.3	Dead
50	RJG	133	M	16.7	LCA	M2/3	61.7	Dead
51	RJG	135	F	3.6	C	M0/1	73.8	Alive
52	RJG	136	M	2.9	ND	M0/1	73.4	Alive
53	RJG	141	F	9.8	C	M0/1	56.5	Alive
54	RJG	142	F	1	ND	M0/1	8.8	Dead
55	EGY	192	M	4.5	ND	M0/1	8	Alive
56	EGY	193	M	5	ND	M2/3	3	Alive
57	EGY	194	F	1.5	ND	M0/1	13	Alive
58	EGY	195	M	2.5	C	M0/1	8	Dead
59	EGY	205	F	7	ND	M0/1	13	Alive
60	EGY	206	M	4	ND	M0/1	3	Alive
61	EGY	207	M	5	ND	M0/1	4	Alive
62	EGY	208	M	10	ND	M0/1	12	Alive
63	EGY	211	F	2	MBEN	M0/1	10	Alive
64	EGY	212	M	6	C	M2/3	11	NA
65	EGY	213	M	7	C	M2/3	13	Dead
66	EGY	214	M	8	ND	M2/3	3	Alive
67	EGY	215	F	5	ND	M0/1	5	NA
68	EGY	216	M	6	ND	M0/1	2	Alive
69	EGY	217	M	9	ND	M0/1	2	Alive
70	EGY	218	M	6	C	M0/1	3	Alive
71	EGY	219	M	9	C	M0/1	15	NA
72	EGY	220	M	13	ND	M0/1	8	Alive

Table 2.1. Clinical data of the NMB cohort of 72 medulloblastoma tumour tissue sample
M = male, F = female; pathology: C = classic, ND = nodular/desmoplastic, MBEN = medulloblastoma with extensive nodularity, LC/A = large cell/ anaplastic; M stage = metastatic stage; NA= not available

	Number of cases		%
Gender	Male	47	65.3%
	Female	25	34.7%
	Total	72	
Age	< 3 years	13	18%
	≥ 3 years	59	82%
Pathology	Classic	44	61.1%
	Nodular/ desmoplastic	22	30.6%
	Large cell/ anaplastic	6	8.3%
	Total	72	
Metastatic stage	Metastatic stage 0/1	39	58.2%
	Metastatic stage 2/3	28	41.8%
	Total	67	
Current status	Alive	43	67.2%
	Dead	21	32.8%
	Total	64	

Table 2.2. Descriptive analysis of the NMB cohort: clinical and pathological variables

2.1.2. The PNET3 cohort of primary medulloblastoma samples

The PNET3 cohort was derived from patients randomized into the International Society of Paediatric Oncology/ United Kingdom Children's Cancer Study Group (SIOP/UKCCSG) trial of sandwich chemotherapy followed by radiotherapy versus radiotherapy alone for medulloblastoma. Tumour material was provided in the form of FFPE sections and curls. It was conducted between March 1992 and January 2000, and involved several European countries (Taylor et al 2003). At the initial stages of the study metastatic stage was determined on radiological basis, without obtaining definitive data for CSF cytology. This led to the following estimation of the metastatic stage; M0/1: includes patients clearly defined with M0 and those with M1 disease. M0/1: also includes patients whom there was no M2/3 disease but in whom a CSF was not analyzed. Patients with metastatic tumours did not receive a randomized

treatment through out the study, and combined chemotherapy and radiotherapy was allocated for these patients as soon as their metastatic stage was confirmed.

The PNET3 cohort, used in this project, consists of 208 samples (in the form of FFPE tumour tissue material) from patients with medulloblastoma with ages ranging from 3 to 16 years. This subset of medulloblastoma samples constitutes about a third of the whole original PNET3 cohort. All the correlations, survival and statistical analysis in this project were undertaken on this subset and this may explain the difference between the results produced in this project and those reported in the original study (Taylor et al. 2003, 2005). The mean and median ages at diagnosis were 8.8 and 8.4 years respectively. The patients' age distributed in 2 year intervals is shown in Figure 2.2. The detailed clinical data for the cohort is shown in Table 2.3.The period of follow up ranged from 0.1 to 14.9 years with a mean and median of 7.6 and 8.8 years, respectively. Overall survival (OS) was 67.3% (140 cases), 68 died 32.7%; actuarial 5 year OS was 75.2%. Event free survival (EFS) was 65.4% (136 cases), actuarial 5 years EFS was 69.4%. Seventy two children had disease recurrence (34.36%) with a mean and median time to recurrence of 2.3 and 1.9 years, respectively. No patients were lost to follow up (Table 2.4).

132 cases (63.5%) were males and 76 (36.5%) were females, with a male to female ratio of 1.7: 1. Histopathological classification according to WHO (2007) (Louis et al 2007) was undertaken by Prof. David Ellison (Newcastle General Hospital, Newcastle upon Tyne, now Department of Pathology St. Jude children's hospital, Memphis, Tennessee, USA). The classic subtype represented 175 (84.1%) cases,

nodular/ desmoplastic 13 cases (6.2%), and large cell/ anaplastic 20 cases (9.6%). At the time of diagnosis, 169 cases (81.3%) were classified as metastatic stage M0/1, and 39 cases (18.8%) M2/3 (Chang et al 1969). Combined radiotherapy and chemotherapy were allocated to 111 cases (53.4%) and radiotherapy alone to 97 of the cases (46.6%) (Taylor et al 2003). One hundred and five of the 202 cases (52%) had a gross total resection (≤1.5 cm^2 residual tumour), and 97 (48%) had a subtotal tumour resection (>1.5 cm^2 residual tumour). At the time of analysis, 134 cases (64.4%) were alive, 133 disease free and 1 alive with disease. Sixty-eight cases (32.7%) died of disease and 6 (2.9%) died of other causes (Tables 2.5).

2.1.3. PNET3 primary medulloblastomas FFPE material

Medulloblastoma samples for the PNET3 cohort were provided as 5 µm FFPE tissue sections or 25 µm FFPE tissue curls. Samples were provided from Children's Cancer Leukaemia Group (CCLG) centres within the U.K. and samples collection and preparation was coordinated by Sara Leigh Nicholson, Cellular pathology, Royal Victoria Infirmary, Newcastle upon Tyne. Slices were subsequently used for all analysis described (DNA extraction, immunohistochemistry, see following sections).

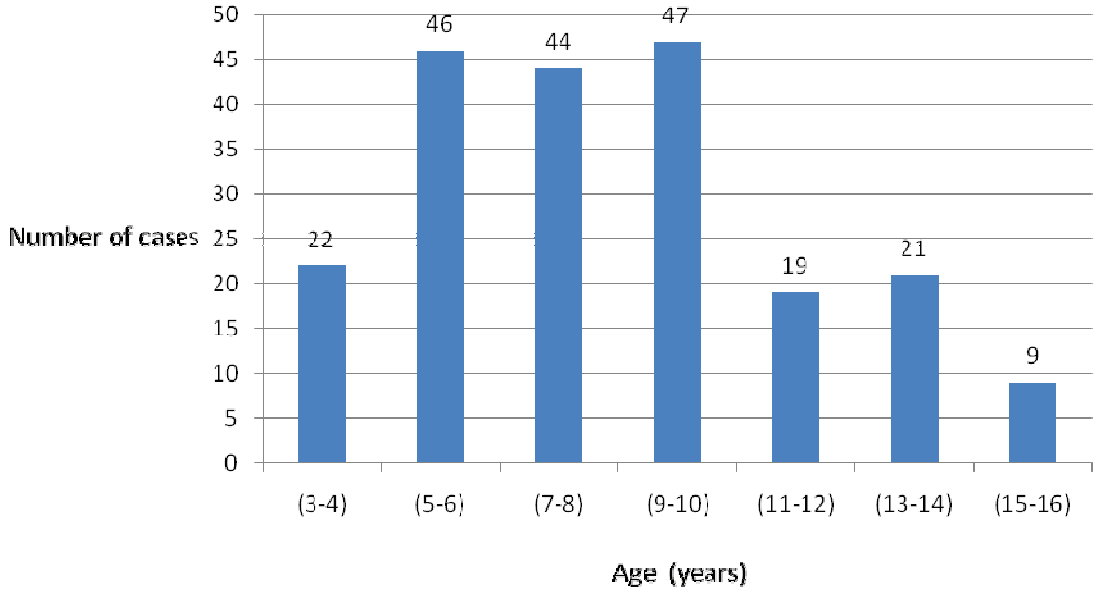

Figure 2.2. Age distribution of the PNET3 cohort in 2 year intervals. Mean, 8.7, Median 8.4 and Mode 6 years. Range, 3-16 years.

PNET3 ID	Age yrs	G.	Path.	M-stage	Treat.	Extent of tumour resection	Rec.	Time to recur. (yrs)	EFS (yrs)	Curr. status	Time to current status (yrs)
2	12.8	F	Classic	M0/M1	RTX+CTX	subtotal	N		13	alive	**13**
9	6.3	F	Classic	M0/M1	RTX+CTX	subtotal	N		12.5	alive	**12.5**
12	4.7	M	Classic	M0/M1	RTX+CTX	subtotal	N		9.9	alive	**9.9**
13	9.9	M	Classic	M0/M1	RTX+CTX	subtotal	Y	3.6	3.6	dead	**5.5**
15	12.9	M	Classic	M0/M1	RTX	Total	Y	0.8	0.8	dead	**1.8**
18	3.4	M	Classic	M0/M1	RTX+CTX	Total	N		12.7	alive	**12.7**
19	15.4	M	Classic	M0/M1	RTX	subtotal	Y	0.7	0.7	dead	**1.3**
28	7.2	F	Classic	M2/3	RTX+CTX	subtotal	N		10.8	alive	**10.8**
30	14.6	M	ND	M0/M1	RTX+CTX	Total	Y	5.8	5.8	dead	**8.8**
31	7.2	M	Classic	M0/M1	RTX	Total	Y	2.1	2.1	dead	**3.2**
32	9.7	M	Classic	M0/M1	RTX+CTX	Total	N		10	alive	**10**
33	8.8	F	Classic	M0/M1	RTX	Total	N		12.1	alive	**12.1**
35	11	M	Classic	M0/M1	RTX	subtotal	Y	0.9	0.9	alive	**10.2**
38	10.8	F	LCA	M0/M1	RTX+CTX	subtotal	Y	2	2	dead	**2.3**
39	8.5	F	Classic	M0/M1	RTX	Total	N		8.7	alive	**8.7**
41	7.6	M	Classic	M0/M1	RTX+CTX	Total	N		11.9	alive	**11.9**
43	8.6	F	Classic	M0/M1	RTX+CTX	subtotal	Y	2.2	2.2	dead	**2.7**
44	9.2	M	ND	M0/M1	RTX	Total	N		11.1	alive	**11.1**
47	7.3	M	ND	M0/M1	RTX	Total	N		10.9	alive	**10.9**
48	14.4	M	Classic	M0/M1	RTX+CTX	subtotal	N		11.4	alive	**11.4**
51	7.5	F	Classic	M0/M1	RTX	subtotal	N.		9.8	alive	**9.8**
52	9.4	M	Classic	M0/M1	RTX+CTX	Total	N		10.2	alive	**10.2**
53	6	M	Classic	M0/M1	RTX+CTX	subtotal	Y	3.4	3.4	dead	**4**
54	6.2	M	Classic	M0/M1	RTX+CTX	subtotal	Y	3.4	3.4	dead	**4**
62	6.6	M	Classic	M0/M1	RTX+CTX	subtotal	N		8	alive	**8.1**
63	13	M	Classic	M0/M1	RTX+CTX	subtotal	N		9.9	alive	**9.9**
65	5.7	F	Classic	M0/M1	RTX+CTX	subtotal	N		11.8	alive	**11.8**
66	5.9	M	Classic	M0/M1	RTX	subtotal	Y	1.5	1.5	dead	**2.2**
69	14.8	M	Classic	M0/M1	RTX+CTX	subtotal	N		10.8	alive	**10.8**
72	7.6	F	Classic	M0/M1	RTX+CTX	subtotal	Y	1.5	1.5	dead	**2.4**
75	6.5	F	ND	M0/M1	RTX	subtotal	N		2.1	alive	**2.1**
77	6.6	M	Classic	M0/M1	RTX+CTX	subtotal	N		9.1	alive	**9.1**
78	3.00	M	LCA	M0/1	RTX	Subtotal	N		10.4	Alive	**10.4**
81	7	F	Classic	M0/M1	RTX+CTX	subtotal	N		10.2	alive	**10.2**
82	10.3	M	Classic	M0/M1	RTX+CTX	subtotal	Y	1.9	1.9	dead	**1.9**
83	4.5	F	Classic	M0/M1	RTX	subtotal	N		10.7	alive	**10.7**
90	4.4	M	Classic	M0/M1	RTX	Total	N		11.5	alive	**11.5**
93	6	M	Classic	M0/M1	RTX+CTX	Total	N		12.4	alive	**12.4**
95	11.6	M	Classic	M0/M1	RTX	Total	Y	7.6	7.6	dead	**9.5**
101	12.8	F	Classic	M0/M1	RTX	subtotal	N		11.4	alive	**11.4**
102	9	F	Classic	M0/M1	RTX	subtotal	N		10.9	alive	**10.9**
105	8.3	M	Classic	M0/M1	RTX	subtotal	N		11.1	alive	**11.1**
106	6.4	M	Classic	M0/M1	RTX+CTX	Total	N	1.4	1.4	dead	**1.8**
107	5.9	F	Classic	M0/M1	RTX	Total	N		11.2	alive	**11.2**
111	7.8	M	Classic	M0/M1	RTX	subtotal	N		8.2	alive	**8.2**
112	8.1	F	Classic	M0/M1	RTX+CTX	Total	N		11.4	alive	**11.4**
113	4.1	F	Classic	M0/M1	RTX	subtotal	Y	0.3	0.3	dead	**0.7**
114	5	F	Classic	M0/M1	RTX+CTX	subtotal	N		11.1	alive	**11.1**
116	9.5	M	Classic	M0/M1	RTX	subtotal	N	1.5	1.5	dead	**1.5**
119	15	M	Classic	M0/M1	RTX+CTX	Total	N		5.3	alive	**5.3**
120	6.3	M	Classic	M0/M1	RTX+CTX	Total	N		10.1	alive	**10.1**
121	13.2	M	Classic	M0/M1	RTX	Total	N		11	alive	**11**
124	6.2	F	LCA	M0/M1	RTX	Total	N		10.6	alive	**10.6**
126	8.4	M	Classic	M0/M1	RTX+CTX	Total	Y	2.2	2.2	dead	**3.6**
129	7.9	M	LCA	M2/3	RTX+CTX	Total	Y	1.1	1.1	dead	**1.3**
131	5.4	F	LCA	M0/M1	RTX+CTX	Total	N		5	alive	**5**

Table 2.3 continued..

Table 2.3 (continued)

PNET3 ID	Age (yrs)	G.	Path.	M-stage	Treat.	Extent of tumour resection	Rec.	Time to recur. (yrs)	EFS (yrs)	Curr. status	Time to current status (yrs)
132	5.1	F	Classic	M0/M1	RTX	NA	N		10.5	alive	**10.5**
134	8.4	M	LCA	M0/M1	RTX	subtotal	Y	2.7	2.7	dead	**3.9**
137	13.4	M	LCA	M0/M1	RTX+CTX	Total	N		11.4	alive	**11.4**
139	7.7	Fe	Classic	M0/M1	RTX	total	Y	1.8	1.8	dead	**4.7**
141	6.4	M	Classic	M0/M1	RTX+CTX	subtotal	N		12.4	alive	**12.4**
145	5	M	Classic	M0/M1	RTX	subtotal	Y	1.4	1.4	dead	**3.2**
146	9.3	F	Classic	M0/M1	RTX+CTX	subtotal	Y	2.8	2.8	dead	**4.2**
147	11	F	Classic	M0/M1	RTX	total	N		12.3	alive	**12.3**
148	4.2	M	Classic	M0/M1	RTX+CTX	subtotal	N		10.2	alive	**10.2**
149	8.3	M	Classic	M0/M1	RTX+CTX	total	N		10.2	alive	**10.2**
150	8.9	F	Classic	M0/M1	RTX+CTX	total	N		12.2	alive	**12.2**
152	10.2	F	Classic	M0/M1	RTX+CTX	subtotal	N		0.1	alive	**0.1**
157	6	M	ND	M0/M1	RTX+CTX	total	N		12	alive	**12**
160	8.8	F	ND	M0/M1	RTX+CTX	total	N		9	alive	**9**
161	8.1	M	Classic	M0/M1	RTX	subtotal	N		11.9	alive	**11.9**
164	8.3	F	Classic	M0/M1	RTX+CTX	total	Y	6.2	6.2	dead	**8.6**
165	12.4	M	Classic	M0/M1	RTX	total	N		7.1	alive	**7.1**
166	8.6	M	Classic	M0/M1	RTX+CTX	total	Y	7.1	7.1	dead	**10.5**
169	5.8	M	Classic	M0/M1	RTX+CTX	total	Y	0.6	0.6	dead	**0.6**
171	9.6	M	Classic	M0/M1	RTX	subtotal	Y	6.2	6.2	dead	**7.8**
172	8.4	M	Classic	M0/M1	RTX+CTX	total	N		8.9	alive	**8.9**
175	5.4	F	Classic	M0/M1	RTX	total	N		6.4	alive	**6.4**
178	7.7	M	Classic	M0/M1	RTX	total	N		6	alive	**6**
179	3.5	F	Classic	M0/M1	RTX+CTX	subtotal	N		11.2	alive	**11.2**
180	9.9	M	Classic	M0/M1	RTX	total	N		9.1	alive	**9.1**
182	8.1	M	Classic	M0/M1	RTX+CTX	subtotal	N		7.8	alive	**7.8**
183	3.6	M	Classic	M0/M1	RTX+CTX	total	N		9.1	alive	**9.1**
185	10.3	M	Classic	M0/M1	RTX+CTX	total	N		11.1	alive	**11.1**
186	11.6	F	Classic	M0/M1	RTX	subtotal	N		11.1	alive	**11.1**
189	7	M	Classic	M2/3	RTX+CTX	NA	Y	0.7	0.7	dead	**1.1**
191	7.8	M	LCA	M0/M1	RTX	total	Y	0.6	0.6	dead	**1.1**
193	7.3	F	LCA	M0/M1	RTX+CTX	total	N		8.7	alive	**8.7**
195	6	F	Classic	M0/M1	RTX	total	N		8.9	alive	**8.9**
198	7.5	M	Classic	M0/1	RTX	Total	N		8.7	Alive	**8.7**
199	15.5	F	ND	M0/M1	RTX	total	N		9.4	alive	**9.4**
200	5.2	M	LCA	M0/M1	RTX+CTX	total	Y	0.3	0.3	dead	**0.4**
201	6.6	M	LCA	M0/M1	RTX	total	Y	0.5	0.5	dead	**0.5**
202	9.7	F	Classic	M0/M1	RTX+CTX	total	N		8.8	alive	**8.8**
205	9.2	F	Classic	M0/M1	RTX+CTX	subtotal	N		7	alive	**7**
207	10.6	F	Classic	M0/M1	RTX	subtotal	Y	1.6	1.6	dead	**2.2**
209	10.4	M	Classic	M0/M1	RTX+CTX	subtotal	N		7.5	alive	**7.5**
210	4.6	M	Classic	M0/M1	RTX+CTX	total	N		7.9	alive	**7.9**
214	7	F	Classic	M0/M1	RTX	subtotal	N		8.4	alive	**8.4**
216	12.6	M	Classic	M0/M1	RTX	total	N		8.5	alive	**8.5**
217	7.5	F	Classic	M0/M1	RTX+CTX	subtotal	N		5.9	alive	**5.9**
50001	10.1	M	ND	M0/M1	RTX+CTX	subtotal	N		8.1	alive	**8.1**
50010	5.9	M	Classic	M0/M1	RTX	total	N		11.8	alive	**11.8**
50011	13.4	M	Classic	M0/M1	RTX	total	Y	5.4	5.4	dead	**7.3**
50012	4.2	F	Classic	M2/3	RTX+CTX	total	N		10.9	alive	**10.9**
50014	2	F	Classic	M0/M1	RTX+CTX	total	N		10.9	alive	**10.9**
50015	4.6	F	Classic	M2/3	RTX	subtotal	Y	0.7	0.7	dead	**0.8**
50016	6	F	Classic	M0/M1	RTX	subtotal	Y	2.4	2.4	dead	**2.6**
50017	9.5	F	Classic	M0/M1	RTX+CTX	subtotal	N		12.4	alive	**12.4**
50018	10	M	Classic	M2/3	RTX+CTX	NA	Y	6.3	6.3	dead	**7.8**
50019	15.4	M	Classic	M0/M1	RTX	subtotal	Y	2.1	2.1	dead	**2.2**
50021	14	M	Classic	M2/3	RTX+CTX	subtotal	N		11	alive	**11**

Table 2.3 (continued)

PNET3 ID	Age (yrs)	G.	Path.	M-stage	Treat.	Extent of tumour resection	Rec.	Time to recur. (yrs)	EFS (yrs)	Curr. status	Time to current status (years)
50034	14.3	M	Classic	M0/M1	RTX	total	N		7	alive	**7**
50035	9.9	F	Classic	M0/M1	RTX	total	N		7.1	alive	**7.1**
50040	15.6	M	Classic	M0/M1	RTX	total	Y	5.1	5.1	dead	**6.9**
50041	10.8	M	Classic	M0/M1	RTX+CTX	total	N		10	alive	**10**
50044	8.1	M	Classic	M0/M1	RTX	subtotal	N		10.1	alive	**10.1**
50045	6.8	M	Classic	M0/M1	RTX	total	N		12.1	alive	**12.1**
50047	10	M	Classic	M0/M1	RTX+CTX	subtotal	Y	2.3	2.3	dead	**2.6**
50049	13.1	F	LCA	M2/3	RTX+CTX	NA	Y	2.2	2.2	dead	**2.9**
50056	10.8	M	Classic	M0/M1	RTX	total	N		11.9	alive	**11.9**
50057	14	M	Classic	M0/M1	RTX	total	N		10.1	alive	**10.1**
50058	11.6	M	Classic	M2/3	RTX+CTX	subtotal	N		10.3	alive	**10.3**
50060	10.3	M	LCA	M2/3	RTX+CTX	Subtotal	Y	1.3	1.3	Dead	**1.5**
50063	5.3	F	Classic	M0/M1	RTX	total	N	0.5	0.5	alive	**10.7**
50065	16	F	LCA	M0/M1	RTX+CTX	total	N	0.9	0.9	dead	**1.1**
50068	6.3	F	Classic	M2/3	RTX+CTX	subtotal	N		11.8	alive	**11.8**
50072	10	F	Classic	M2/3	RTX+CTX	subtotal	N		11.7	alive	**11.7**
50075	8	F	Classic	M0/M1	RTX	total	N		11.8	alive	**11.8**
50079	8.1	M	Classic	M0/M1	RTX	total	N		10.9	alive	**10.9**
50080	10.3	M	Classic	M0/M1	RTX+CTX	subtotal	N		10.2	alive	**10.2**
50081	14	M	LCA	M0/M1	RTX+CTX	total	N		9.9	alive	**9.8**
50086	10.4	F	Classic	M2/3	RTX+CTX	subtotal	N		11.8	alive	**11.8**
50088	15.2	F	Classic	M0/M1	RTX	subtotal	N		10.4	alive	**10.4**
50090	10.3	F	Classic	M0/M1	RTX+CTX	total	N		1.4	alive	**1.4**
50091	4.4	M	Classic	M2/3	RTX+CTX	total	Y	1.7	1.7	dead	**1.8**
50092	8	F	Classic	M0/M1	RTX	total	N		10.9	alive	**10.9**
50099	13	F	Classic	M0/M1	RTX+CTX	total	Y	4.5	4.5	alive	**14.1**
50100	12	M	Classic	M0/M1	RTX	total	Y	2.6	2.6	dead	**4.1**
50101	11	F	Classic	M2/3	RTX+CTX	subtotal	N		10.1	alive	**10.1**
50104	5.4	M	LCA	M2/3	RTX+CTX	subtotal	Y	0	0	dead	**0.1**
50106	7.9	F	Classic	M2/3	RTX+CTX	NA	Y	0.8	0.8	dead	**1**
50111	5	M	LCA	M2/3	RTX+CTX	subtotal	N		10	alive	**10**
50113	11	M	Classic	M2/3	RTX+CTX	total	N		9.8	alive	**9.8**
50116	3.8	F	Classic	M0/M1	RTX	total	N		7	alive	**7**
50117	9	M	Classic	M0/M1	RTX	total	N		11.7	alive	**11.7**
50120	13.5	M	Classic	M0/M1	RTX	subtotal	N		14.9	alive	**14.9**
50124	7.1	M	Classic	M2/3	RTX+CTX	subtotal	Y	2.2	2.2	alive	**10.4**
50128	15.4	M	Classic	M0/M1	RTX+CTX	total	N		9.2	alive	**9.2**
50129	10	M	Classic	M0/M1	RTX	subtotal	N		11.2	alive	**11.2**
50132	14.1	M	Classic	M0/M1	RTX	subtotal	N		9.4	alive	**9.4**
50133	9.5	F	Classic	M0/M1	RTX+CTX	subtotal	N		9.4	alive	**9.4**
50136	12.1	M	Classic	M0/M1	RTX	total	N		8.9	alive	**8.9**
50137	6	F	Classic	M0/M1	RTX+CTX	subtotal	Y	5.5	5.5	dead	**5.6**
50142	9.4	F	Classic	M2/3	RTX+CTX	total	Y	1	1	dead	**1.1**
50145	10.2	M	Classic	M2/3	RTX+CTX	total	Y	1.1	1.1	dead	**1.7**
50147	5.3	M	Classic	M0/M1	RTX	subtotal	N		4.9	alive	**4.9**
50150	5.1	M	Classic	M2/3	RTX+CTX	subtotal	Y	1.1	1.1	dead	**1.2**
50152	4	F	Classic	M2/3	RTX	subtotal	N		7.5	alive	**7.5**
50153	9	M	Classic	M0/M1	RTX	total	N		10.4	alive	**10.4**
50154	11	M	Classic	M0/M1	RTX	subtotal	N		10.4	alive	**10.4**
50158	6	M	Classic	M0/M1	RTX	total	N		9.6	alive	**9.6**
50159	8	M	Classic	M0/M1	RTX	total	N		9.7	alive	**9.7**
50161	6.8	F	Classic	M0/M1	RTX	subtotal	Y	2.6	2.6	dead	**8**
50163	6.8	F	Classic	M0/M1	RTX	subtotal	N		10.1	alive	**10.1**
50165	14	F	Classic	M0/M1	RTX	total	N		5.9	alive	**5.9**

PNET3 ID	Age (yrs)	G.	Path.	M-stage	Treat.	Extent of tumour resection	Rec.	Time to recur. (yrs)	EFS (yrs)	Curr. status	Time to current status (yrs)
50166	10.6	M	Classic	M0/M1	RTX	subtotal	Y	3.2	3.2	dead	**6**
50167	6.9	F	Classic	M0/M1	RTX	subtotal	N		10.5	alive	**10.5**
50169	3.1	M	LCA	M2/3	RTX+CTX	subtotal	Y	1.2	1.2	dead	**1.6**
50170	10.9	F	Classic	M2/3	RTX+CTX	total	N		8.7	alive	**8.7**
50172	5.4	M	Classic	M0/M1	RTX	total	N		10.4	alive	**10.4**
50174	12.5	M	Classic	M2/3	RTX+CTX	subtotal	N		7.7	alive	**7.7**
50176	7.8	F	ND	M0/M1	RTX	total	N		9.7	alive	**9.7**
50184	11.8	M	Classic	M0/M1	RTX	total	N		10.2	alive	**10.2**
50189	14.3	M	Classic	M0/M1	RTX	total	N		10	alive	**10**
50193	14.1	F	Classic	M0/M1	RTX+CTX	NA	N		8.1	alive	**8.1**
50197	5.3	M	Classic	M2/3	RTX+CTX	subtotal	Y	0.8	0.8	dead	**1.6**
50198	9.5	M	Classic	M2/3	RTX+CTX	subtotal	Y	4.2	4.2	dead	**7.8**
50204	10.7	M	Classic	M2/3	RTX+CTX	total	N		10.1	alive	**10.1**
50206	5.4	M	LCA	M0/M1	RTX	subtotal	Y	2.1	2.1	dead	**5.7**
50208	9.7	F	Classic	M2/3	RTX+CTX	total	N		9.7	alive	**9.7**
50209	9.1	M	Classic	M0/M1	RTX+CTX	total	YY	4.1	4.1	dead	**6.7**
50212	10.8	M	Classic	M2/3	RTX+CTX	total	N		5.5	alive	**5.5**
50217	9.5	M	Classic	M2/3	RTX+CTX	subtotal	Y	4.9	4.9	dead	**8.8**
50218	3.4	M	ND	M0/M1	RTX+CTX	total	Y	1.6	1.6	dead	**1.8**
50224	14.9	M	Classic	M0/M1	RTX	total	N		5	alive	**5**
50231	5	M	Classic	M0/M1	RTX	total	Y	1.3	1.3	dead	**1.6**
50233	7.6	M	Classic	M0/M1	RTX	total	Y	3.1	3.1	dead	**4**
50236	6.9	M	LCA	M0/M1	RTX	subtotal	Y	1.3	1.3	dead	**1.5**
50241	13.1	M	Classic	M2/3	RTX+CTX	subtotal	Y	2.2	2.2	dead	**2.3**
50244	14.1	M	Classic	M0/M1	RTX	total	N		6.7	alive	**6.7**
50245	7.4	M	Classic	M0/M1	RTX	subtotal	Y	3.2	3.2	dead	**7**
50248	3.9	M	Classic	M0/M1	RTX+CTX	total	N		8.8	alive	**8.8**
50249	11.6	F	Classic	M0/M1	RTX	subtotal	N		5.6	alive	**5.6**
50250	15.8	M	Classic	M0/M1	RTX+CTX	subtotal	Y	2	2	dead	**3.4**
50251	7	M	Classic	M2/3	RTX+CTX	subtotal	N		9.4	alive	**9.4**
50253	9.6	M	Classic	M0/M1	RTX	total	Y	2.4	2.4	dead	**3.7**
50254	5.6	F	Classic	M0/M1	RTX	total	N		9.4	alive	**9.4**
50256	4.2	M	Classic	M2/3	RTX+CTX	subtotal	Y	0.3	0.3	dead	**0.8**
50259	9.1	M	Classic	M2/3	RTX+CTX	subtotal	Y	0.9	0.9	dead	**1.1**
50263	9	M	ND	M0/M1	RTX	total	N		7.9	alive	**7.9**
50268	6	F	Classic	M2/3	RTX+CTX	subtotal	Y	0.9	0.9	dead	**1.2**
50274	4	M	Classic	M0/M1	RTX	total	N		8.6	alive	**8.6**
50276	8.7	M	ND	M0/M1	RTX	total	N		10.2	alive	**10.2**
50284	11.2	M	Classic	M0/M1	RTX	total	N		5.5	alive	**5.5**
50290	9.7	F	Classic	M0/M1	RTX+CTX	total	N		8.4	alive	**8.4**
50291	6.7	M	Classic	M0/M1	RTX+CTX	subtotal	N		11	alive	**11**
50292	3.3	M	Classic	M2/3	RTX+CTX	subtotal	N		7.9	alive	**7.9**

Table 2.3. Detailed individual clinical data for the PNET3 cohort. G = gender, F = female, M = male; Path. = pathology**,** ND = nodular / desmoplastic, LCA= large cell / anaplastic; M-stage = metastatic stage at time of diagnosis; Treat = treatment**,** RTX = radiotherapy, CTX = chemotherapy; NA = not available; Recur = recurrence; EFS = Event free survival; Curr = current, yr = years.

	Age at diagnosis (years)	Time to current status (years)	Time to recurrence (years)	Event free survival (years)
Number	208	208		208
Mean	8.8	7.6	2.3	7
Median	8.4	8.8	1.9	8.4
Mode	6.0	10	2.2	10.2
Range	3-16.0	0.10-14.9	0.0-7.6	0.0-14.9

Table 2.4. Descriptive statistics for age, follow up period, time to recurrence and event free survival of the PNET3 cohort

Clinicopathological features of the PNET3 cohort		Frequency	Percent
Gender	Male	132	63.5
	Female	76	36.5
	Total	208	100.0
Pathology	Classic	175	84.1
	Nodular / desmoplastic	13	6.3
	Large cell / anaplastic	20	9.6
	Total	208	100.0
Metastatic stage	Metastatic stage 0/1	169	81.3
	Metastatic stage 2/3	39	18.8
	Total	208	100.0
Treatment	Radiotherapy + Chemotherapy	111	53.4
	Radiotherapy	97	46.6
	Total	208	100.0
Extent of tumour resection	Total resection	105	52.0
	Subtotal resection	97	48.0
	Total	202	100.0
Recurrence	No recurrence	136	65.4
	Recurrence	72	34.6
	Total	208	100.0
Current status	Alive	140	67.3
	Dead	68	32.7
	Total	218	100.0

Table 2.5. Descriptive analysis of clinical variables for the PNET3 cohort.

2.1.4. Medulloblastoma cell lines

Cell lines were used to optimize methods before application to primary medulloblastoma samples. The sources of the cell lines used are listed in Table 2.6. D425 Med and D458 Med were established from primary and metastatic medulloblastoma cells from the same patient. The establishment of these seven cell lines are described in Langdon et al (2006). Cell lines were provided as genomic DNA (prepared by colleagues in the lab).

Cell line	Derived from	Source
D384 Med	Primary posterior fossa medulloblastoma	American Type Culture Collection
D425 Med	Primary posterior fossa medulloblastoma	Dr. D. Bigner (Duke University, Durham, USA
D458 Med	Metastatic cells of D425 Med in CSF	Dr. D. Bigner (Duke University, Durham, USA
D556 Med	Medulloblastoma	Dr. D. Bigner (Duke University, Durham, USA
MHH-MEDBA	Cerebellar medulloblastoma	Dr. T. Pietsch (University of Bonn Medical Centre, Germany
DAOY	Primary posterior fossa medulloblastoma	American Type Culture Collection

Table 2.6. Medulloblastoma cell lines

2.2. Methods

2.2.1. DNA extraction

2.2.1.1. DNA extraction from tumour tissue and blood

DNA was extracted from fresh frozen tumour tissue samples and matched blood, where available, using Qiagen DNeasy and QIAamp DNA maxi kits, respectively according to manufacture instructions. Briefly, the DNeasy Tissue Kit uses silica-gel-membrane technology for DNA purification and the buffer provided allows optimal conditions for cell lysis followed by selective binding of the DNA to the DNeasy membrane.

The procedure starts with a primary step of adding ATL buffer to the tissue samples. ATL buffer provides optimal conditions for cell lysis and digestion using proteinase K, followed by loading the lysate onto the DNeasy spin column. By several centrifugation processes, the DNA is bound to the membrane as contaminants pass through. DNA is then eluted in water or buffer. The QIAamp blood extraction kit also utilizes a spin column for DNA purification. Both fresh and frozen blood may be used. The steps are similar to the DNeasy kit, without the addition of the ATL buffer.

2.2.1.2. DNA extraction from FFPE sections and curls

DNA was extracted from formalin fixed-paraffin embedded (FFPE) tissues using the QIAamp DNA FFPE Tissue Kit (Qiagen, UK). All FFPE samples in this project were primary medulloblastoma tumours from the PNET3 clinical trial. Dewaxing and

digesting of approximately 1-2 × 25µm curls of FFPE material was initially undertaken according to manufacturer's instructions. Occasionally, DNA was extracted from FFPE 10µm unstained sections (USS) fixed on microscope slides (Nunc, Denmark). In this case, slides were dewaxed in xylene for 5 minutes and rehydrated through a graded series of ethanol (100%, 95%, 90%, and 75%) for 1 minute each. Buffer ATL (QIAamp DNA FFPE Tissue Kit (Qiagen, UK)) was applied to dewaxed sections and the tissue was scraped into a sterile 1.5 ml microfuge tube using the end of a sterile pipette tip (Starlab). Tissue was then digested according to instructions in the QIAamp DNA FFPE Tissue Kit (Qiagen, UK).

Frozen tissue was available for NMB and RJG primary medulloblastoma tumours which were used in this project, and DNA had previously been extracted by members of the group prior to the commencement of this study, from frozen tissue using the TRIzol method (Invitrogen) according to the manufacturer's instructions.

Regardless of extraction method, concentrated DNA extracts stocks were stored at - 80^{o}C and working stocks of 25ng/µl were periodically prepared and stored at -20^{o}C prior to use.

2.2.1.3. Assessment of the DNA yielded and purity

DNA yield and quality was determined using the NanoDrop® ND-100 spectrophotometer (Nanodrop technologies, USA) (Tables 2.7, 2.8).This ratio between optimal density readings taken at 260nm and 280nm (OD_{260}: OD_{280}) provides an estimation for the purity of the nucleic acid. Pure preparations of DNA have an OD_{260}:

OD_{280} value in the range of 1.7 to 2.0, while in cases with significant protein contamination, the OD ratio value will be lower. The protocol of measuring DNA concentration by spectrophotometry is reviewed by Sambrook and Russell (2001).

Sample ID	Date of extraction	Kit used	DNA concentration	Total volume	DNA yield	OD260/OD280 ratio
NMBT 192	3/10/06	Qiagen DNeasy	42 ng/ul	200 ul	8400 ng	NA
NMBT 193	3/10/06	Qiagen DNeasy	47.6 ng/ul	200 ul	9520 ng	1.97
NMBT 194	3/10/06	Qiagen DNeasy	77 ng/ul	200 ul	15400 ng	1.86
NMBE 195	3/10/06	Qiagen DNeasy	162.1 ng/ul	200 ul	32420 ng	1.86
NMBT 205	10/10/06	Qiagen DNeasy	78 ng/ul	100 ul	7800 ng	1.74
NMBT 206	10/10/06	Qiagen DNeasy	83.3 ng/ul	100 ul	8330 ng	1.62
NMBT 207	10/10/06	Qiagen DNeasy	10.7 ng/ul	100 ul	1070 ng	1.74
NMBT 208	10/10/06	Qiagen DNeasy	19.5 ng/ul	100 ul	1950 ng	2.79
NMBT 216	12/10/06	Qiagen DNeasy	26.2 ng/ul	100 ul	2620 ng	1.91
NMBT 217	12/10/06	Qiagen DNeasy	173.5 ng/ul	100 ul	17350 ng	1.90
NMBT 218	12/10/06	Qiagen DNeasy	108 ng/ul	100 ul	10800 ng	1.97
NMBT 219	12/10/06	Qiagen DNeasy	142.3 ng/ul	100 ul	14230 ng	1.91
NMBT 219	17/10/06	Qiagen DNeasy	24.1 ng/ul	200 ul	4820 ng	1.77
NMBT 211	17/10/06	Qiagen DNeasy	98 ng/ul	200 ul	19600 ng	1.92
NMBT 212	17/10/06	Qiagen DNeasy	37.5 ng/ul	200 ul	7500 ng	3.64
NMBT 213	17/10/06	Qiagen DNeasy	195.23 ng/ul	200ul	39046 ng	2.04
NMBT 214	17/10/06	Qiagen DNeasy	181.2 ng/ul	200 ul	36240 ng	1.86
NMBT 215	17.10.06	Qiagen DNeasy	10 ng/ul	200 ul	2000 ng	2.03
NMBT 220	20/10/06	Qiagen DNeasy	33.3 ng/ul	200 ul	6660 ng	1.93
NMBT 216	20/10/06	Qiagen DNeasy	0 ng/ul	200 ul	ng	NA
NMB 217	20/10/06	Qiagen DNeasy	130.9 ng/ul	200 ul	26180 ng	1.85
NMB 218	20/10/06	Qiagen DNeasy	174.1 ng/ul	200 ul	34820 ng	1.95

Table 2.7. Tumour tissue DNA extraction, showing DNA concentration, yield and volume

Sample ID	**Date of extraction**	**Kit used**	**DNA concentration**	**Total volume**	**DNA yield**	**OD260/OD280 ratio**
NMBB207	1/11/06	QIAamp DNA Maxi	24.8 ng/ul	400 ul	9920 ng	1.75
NMBB 208	1/11/06	QIAamp DNA Maxi	35.3 ng/ul	400 ul	14120 ng	2.06
NMBB 211	1/11/06	QIAamp DNA Maxi	123.1	400 ul	49240 ng	2.20
NMBB 212	1/11/06	QIAamp DNA Maxi	45.8 ng/ul	400 ul	18320 ng	0.90
NMBB 213	3/11/06	Qiagen DNeasy	24.3 ng/ul	200 ul	4860 ng	2.45
NMBB 214	3/11/06	Qiagen DNeasy	12.8 ng/ul	200 ul	2560 ng	NA
NMBB 215	3/11/06	Qiagen DNeasy	10.7 ng/ul	200 ul	2140 ng	1.83
NMBB 216	3/11/06	Qiagen DNeasy	8.07 ng/ul	200 ul	1614 ng	1.97
NMBB 206	8/11/06	QIAamp DNA Maxi	82.6 ng/ul	200 ul	16520 ng	1.80
NMBB 217	8/11/06	Qlamp DNA Maxi	46 ng/ul	200 ul	9200 ng	1.72
NMBB 218	8/11/06	QIAamp DNA Maxi	124 ng/ul	200 ul	24800 ng	1.82
NMBB 220	8/11/06	QIAamp DNA Maxi	o ng/ul	200 ul	0 ng	0

Table 2.8. Blood DNA extraction, showing DNA concentration, yield and volume

2.2.2. Polymerase Chain Reaction (PCR)

The PCR technique was initially developed in 1983 by Dr. Kary Mullis (1983). It allows rapid initial exponential amplification of small quantities of defined target DNA sequences present within a DNA sample. The components of a conventional PCR reaction include a small amount of DNA template to be amplified, specific oligonucleotide PCR primers (ideally two 15-25 nucleotide primers are synthetically generated to bind specifically to complementary strands of a target sequence), Taq DNA polymerase enzyme, magnesium chloride, the four deoxynucleotide-triphosphates adenine (dATP), guanine (dGTP), cytosine (dCTP), thymine (dTTP) and the optimal reaction buffer. Details of the PCR primers used in this project are described in the relevant chapters.

The PCR process consists of three main steps known as denaturing, annealing and elongation. Before the first denaturing step, the reaction is heated up to 95^0C to denature the double stranded DNA template into single strand DNA. This is followed by reduction of the temperature to allow the oligonucleotide primers to anneal (Figure2.3). The temperature used in this annealing step depends on the size and composition of the primers and this step typically takes up to 1 minute. Finally, the elongation step involves synthesis of a complementary DNA strand by the *Taq* DNA polymerase, which has optimal activity at 72^0C. These three main steps of the PCR are repeated over usually 25-40 cycles. At this stage, there are usually about 10^5 copies of the specific target sequence in addition to the starting DNA. After all the cycles have been completed a final elongation step is done at 72^0C, to make sure all the single-

stranded DNA has been fully extended. The use of DNA polymerase, isolated from *Thermus aquaticus*, can withstand temperatures up to 110 ^{0}c, and allows automation of the PCR process. A detailed review of the PCR method is available in Strachan and Read (2004).

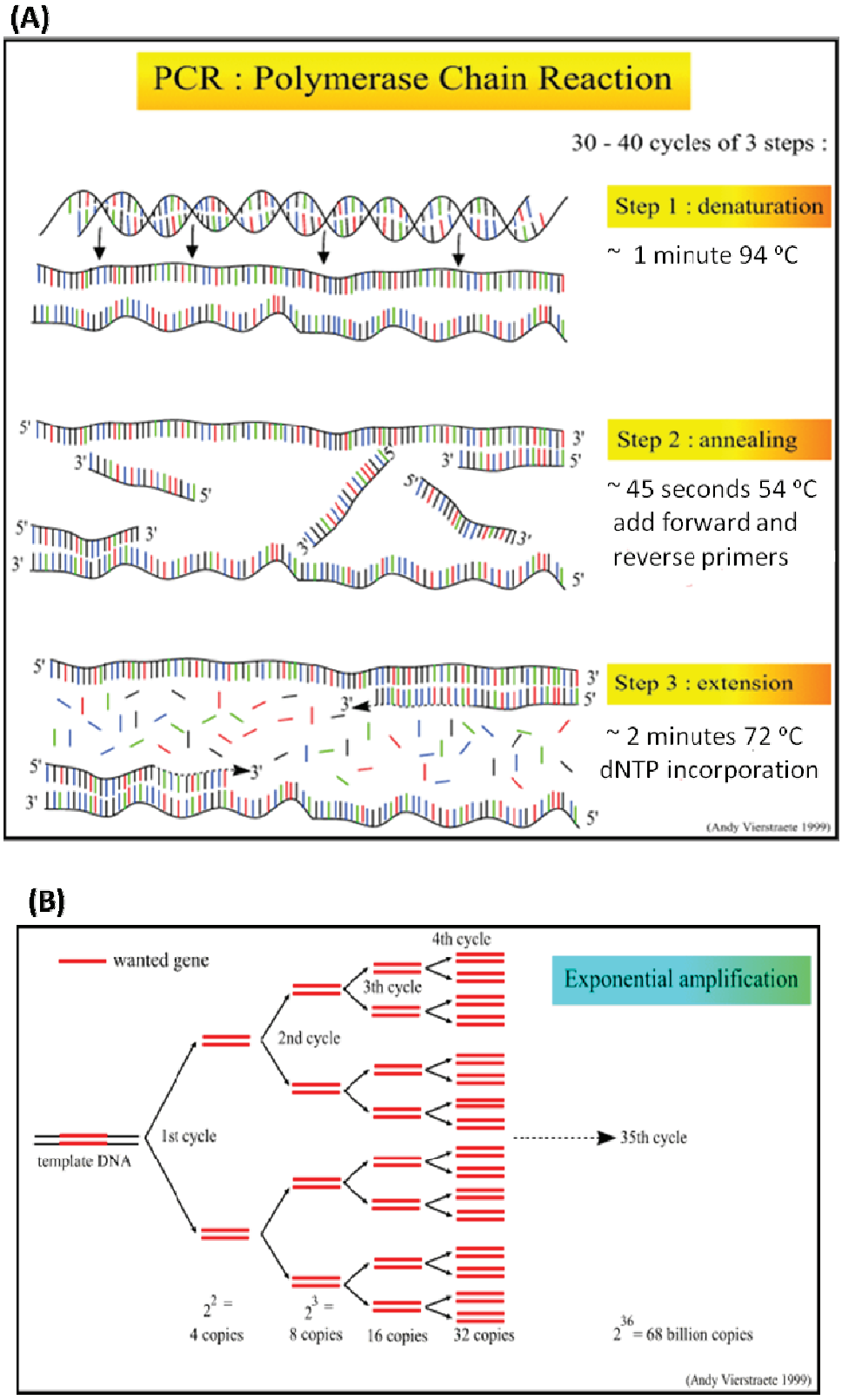

Figure 2.3. Polymerase chain reaction (PCR). (A) The steps of PCR showing denaturation, annealing and extension phases. (B) Illustration of the exponential amplification of DNA target sequences by PCR (adapted from: users.ugent.be/~avierstr/principles/pcrsteps.gif).

2.2.2.1. PCR protocol used in this project

For each standard 20µl PCR reaction, the following reagents were added in individual 0.2ml PCR tubes (Abgene): 2µl (2uM final concentration) each of forward and reverse oligonucleotide PCR primer (Sigma-Proligo, France), 0.2µl Amplitaq enzyme (5U/uL final concentration), 2µl 10x Amplitaq Gold PCR Buffer11 (1x final concentration; Applied Biosystems, UK), 1.2µl $MgCl_2$ (1.5mM final concentration; Applied Biosystems, UK), 0.8 µl dNTPs (Amersham Biosciences), 2µl medulloblastoma tumour or blood DNA (25ng/µl final concentration) and sterile PCR water to a final volume of 20µl. All PCR reactions included a negative control containing all reagents, except the DNA template, to identify any exogenous DNA contamination. Details of the PCR reaction constitution are listed in Table 2.9.

Reagent (stock concentration)	Amount added (µl)	Final concentration	Company
Genomic DNA (25ng/µl)	2	2ng/µl	
10x PCR buffer	2		Applied Biosystems, UK
dNTPs (5mM)	0.8	0.8mM	Amersham Biosciences
Forward primer (10µM)	2	1µM	VHBio, UK
Reverse primer (10µM)	2	1µM	VHBio, UK
Magnesium chloride (25mM)	1.2	1.5mM	Applied Biosystems, UK
Purelab Ultra water	9.8		ELGA, UK
AmpliTaq Gold R (5U/µl)	0.2	0.5U/µl	Applied Biosystems, UK
Total	20		

Table 2.9. Standard PCR reaction reagents and concentrations.

PCR products were generated using the GeneAmp PCR System 9700 thermocycler (Applied Biosystems, UK) using the following PCR program: 95^0C for 10 minutes, followed by 40 cycles of: 95^0C for 1 minute, the optimal annealing

temperature for the specific primers set (55-60^{0}C) for 1 minute and 72^{0}C for 1 minute. On final extension step for 7 minutes at 72^{0}C, was then performed, followed by a holding step at 4^{0}C.

2.2.2.2. Primer design protocol used in this project

Two primers are designed to anneal to both complementary strands of a double-stranded DNA molecule and amplify the sequence of a specific region. One primer anneals to the forward strand and the second primer anneals to the reverse strand of DNA. DNA polymerase binds to the end of each primer and promotes DNA synthesis in the 5' to 3' direction. The specificity of the PCR reaction to amplify a particular region of DNA is highly dependent on the specificity of the primers to bind to the target DNA sequence. Primers that lack sequence specificity can promote the formation of many non-specific PCR products. To increase the specificity of individual primers the following factors need to be considered:

1. Primers should be approximately 20 nucleotides long
2. The G/C content should be approximately 50%
3. Repetitive sequences should be avoided to prevent the formation of hairpin loops
4. The last 5 bases at the 3' end of primers should not contain more than 2×G/C nucleotides
5. Complementary regions between both primers should be avoided

A number of primer design tools are available that can assist in PCR primer design for new and experienced users alike. These tools may reduce the cost and time involved in experimentation by lowering the chances of failed experimentation.

The PCR primers used in this study were designed for particular techniques using a series of software packages that consider the above factors including the free NCBI primer design tool. All primers were BLAST (www.ncbi.nlm.nih.gov) and searched to determine their uniqueness prior to selection.

2.2.3. Analysis of PCR products using agarose gel electrophoresis

This is a method by which linear DNA molecules can be separated according to their molecular sizes (Sambrook and Russell 2001). Agarose gel is composed of polysaccharide molecules and buffer. When subjected to electric current, negatively charged DNA molecules move from the negative cathode to the positive anode. The smaller the molecular size of the DNA the faster and thus further it migrates through the gel. Ethidium bromide (Sigma) is added to the gel, which intercalates with the double-stranded DNA and allows its visualization under UV light. The distance travelled and subsequently the size of each DNA molecule can be determined by comparing it with a known DNA molecular weight marker or ladder, which is loaded in the gel next to the samples.

A 2% agarose gel was routinely used to resolve the PCR products generated. The gel is prepared by heating 100ml 0.5xTBE buffer (Appendix,Table 2) and 2g Ultra Pure® agarose powder (Invitrogen, UK) into a glass flask using a microwave, for approximately 7 minutes. Ethidium bromide is subsequently added (1 drop of a 0.1

mg/ml solution) to the molten agarose after it has cooled down (0.05mg/ml final concentration). Appropriate well-forming combs were placed in the gel and the gel was then left to solidify in a gel-casting tray (GIBCO, California, USA). Gels were placed in a horizontal electrophoresis tank (GIBCO) and submerged with 0.5xTBE buffer.

An electrical current of 120 volts was applied to the gel for approximately 30 minutes, using the Power Pac 3000 (Bio-Rad, Hercules, California, USA). Each PCR product was mixed with a loading buffer (see appendix) and loaded into individual well. Following electrophoresis, DNA was visualized and photographed using a UV transilluminator GelDoc system (Bio-Rad, Hercules, California, USA) and PCR product sizes determined relative to a 100bp DNA ladder (Invitrogen, UK). Further details of protocols for agarose gel electrophoreses are available in Sambrook and Russell (2001).

2.2.4. Detection of Loss of Heterozygosity (LOH)

2.2.4.1. Loss of heterozygosity (LOH) and cancer development

LOH is a common feature of many cancers and analysis of regions of LOH through studying highly polymorphic microsatellite markers has been a key advancement in the identification of regions of genomic loss. Genome-wide scanning approaches using widely spaced polymorphic microsatellite markers, followed by refined mapping through increasing the density of these markers, may identify narrow regions of chromosomal losses and subsequently identify putative candidate TSGs to

be taken forward for more refined analysis (reviewed by Alberts et al 2002; Strachan and Reed 2004; Langdon et al 2006).

Microsatellites are short polymorphic sequences of nucleotide repeats, usually consisting of di, tri or tetra-nucleotide repeats. Since they are polymorphic in nature it is highly possible that the two alleles an individual will inherit will differ in the size of their repeat region. PCR amplification using primers flanking the repeat region allows analysing the sizes of these fragments to determine whether two DNA fragments of different size are present. The presence of only 1 size DNA fragment in a tumour sample (where 2 size fragments are obtained in a matched constitutional DNA from the same individual) denotes that there may be evidence of LOH at that microsatellite marker (reviewed by Alberts et al 2002; Strachan and Reed 2004). The observation of an equivalent single sized DNA fragment in tumour and constitutional DNA indicates the individual is homozygous at that locus, and thus non informative for LOH assessment at that position.

2.2.4.2. Analysis of LOH using the CEQ 8000 System

PCR products generated for investigating microsatellite loci were analysed using the CEQ 8000 Genetic Analysis System according to the manufactures instructions. DNA was amplified using standard PCR as described in section 2.2.2 using the specific PCR primers detailed in chapters 3 and 6, for chromosomes 17p and chromosome 6, respectively. The forward oligonucleotide primer of each set was labelled with a fluorescent dye, WeLLRED, at the 5' end (Sigma-Proligo, France). The dye can then be detected by the CEQ 8000 Genetic Analysis System, through a 4 wave

length laser-induced fluorescence detector. 0.5 µl of each PCR product sample was suspended in 40 µl of sample loading solution (SLS) plus 0.5 µl of standard size marker (Std) (Beckman Coulter) and loaded in the appropriate wells of a 96-well plate compatible with the CEQ 8000 Genetic Analysis System. During electrophoresis using this system, the DNA fragments run past a detector at a fixed point in the gel and the signal emitted by each dye is recorded and analysed by computer software (Strachan and Reed 2004). Up to 3 samples can be added in the same well and analysed together providing markers used can be separately identified e.g. have different dyes or product sizes. Analysis of data to test for LOH can subsequently be done by 2 methods: (i) Conventional LOH (cLOH) analysis or (ii) Homozygous Mapping Of Deletions (HOMOD), depending on whether matched DNA was available or not.

2.2.4.3. Interpretation of LOH results assessed by polymorphic microsatellite markers

Interpretation of the peaks generated by polymorphic microsatellite markers are not always straightforward due to a number of reasons including overlapping of peaks or their close proximity, poor DNA quality specially FFPE tumour material which comprises the sizes of the peaks, inadequate separation during capillary electrophoresis as well as the specific pattern produced by each marker regardless of the appearance of one, two or more peaks in cases showing homozygosity, heterozygosity or MSI respectively. Apart from the last reason, all the above mentioned difficulties can be overcome through re-analyzing and re-running capillary electrophoresis with changing the ejection time of the DNA sample, modifying the DNA quantity in the LOH analysis, purifying the DNA prior to analysis or re-extracting DNA

with better yield from FFPE material. The specific microsatellite patterns also have to be initially recognized, using cell lines during an optimization stage, as well as knowing the specific nucleotide repeats of each marker (e.g. mono, di, tri, or tetra-nucleotide repeats).

Sometimes more than one peak appears and the result is still interpreted as homozygous, since these minor peaks are part of a major peak, which represents this marker at that locus (Figure 2.4). In order to consider a minor peak to be genuine from the larger one (changing the result from homozygous to heterozygous) a minimum of 2, 3, 4, or 5 base-pair repeat difference should appear between the 2 peaks for mono, di, tri or tetra nucleotide repeat markers respectively (Figure 2.5). On the other hand minor and major peaks may still be considered as one even if the intermediate troughs reach the base line.

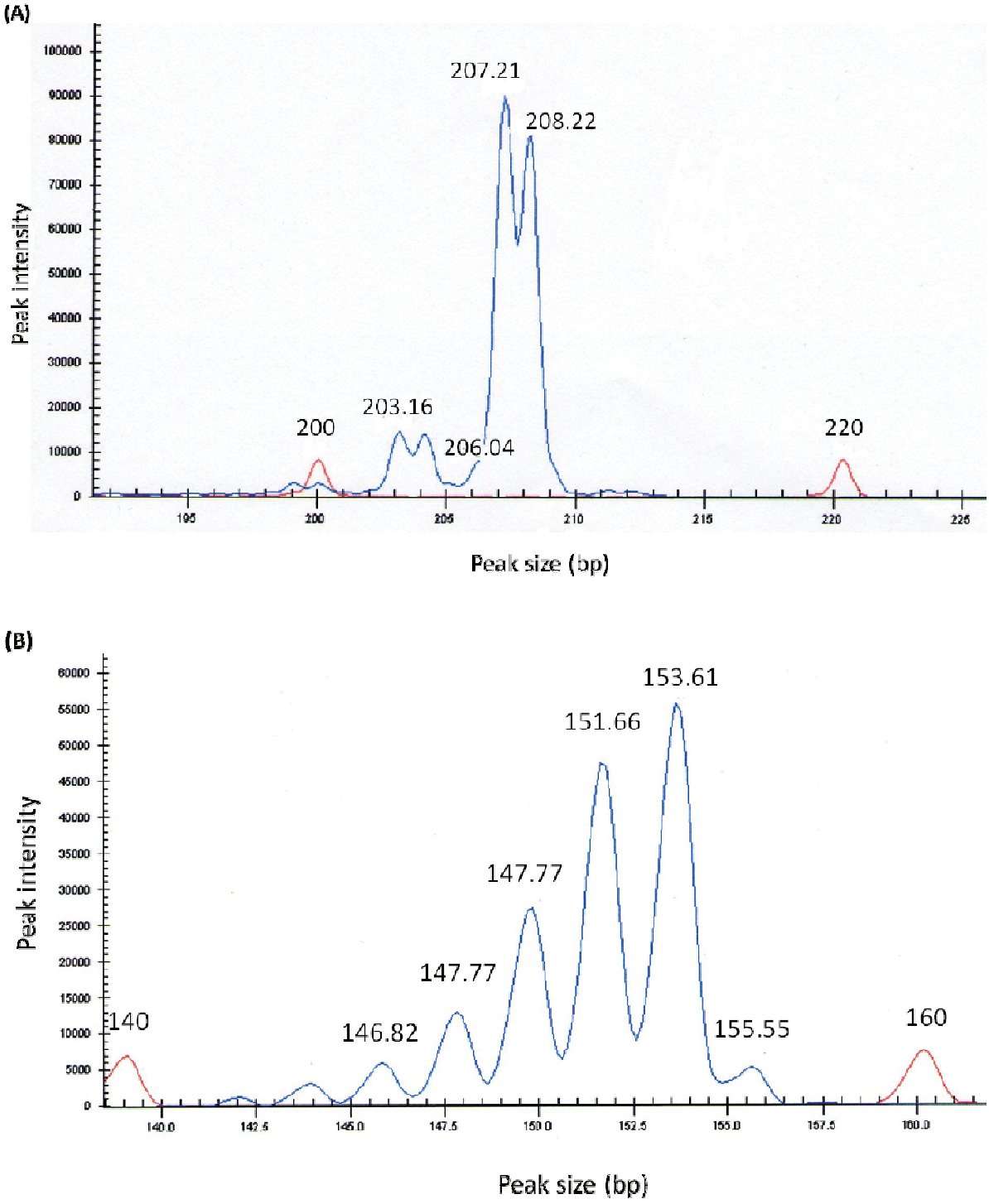

Figure 2.4. Polymorphic microsatellite markers demonstrating different patterns of homozygosity. (A) Homozygosity, using di-nucleotide marker D17S974, showing 2 minor peaks with less than 2 base-pair apart, which is interpreted as one major peak. (B) Homozygosity, using tetra-nucleotide marker D17S1866, showing 5 minor peaks with less than 4 base-pair, which is interpreted as one major. Red peaks represent a standard size marker (std) used in LOH analysis by the CEQ 8000 System

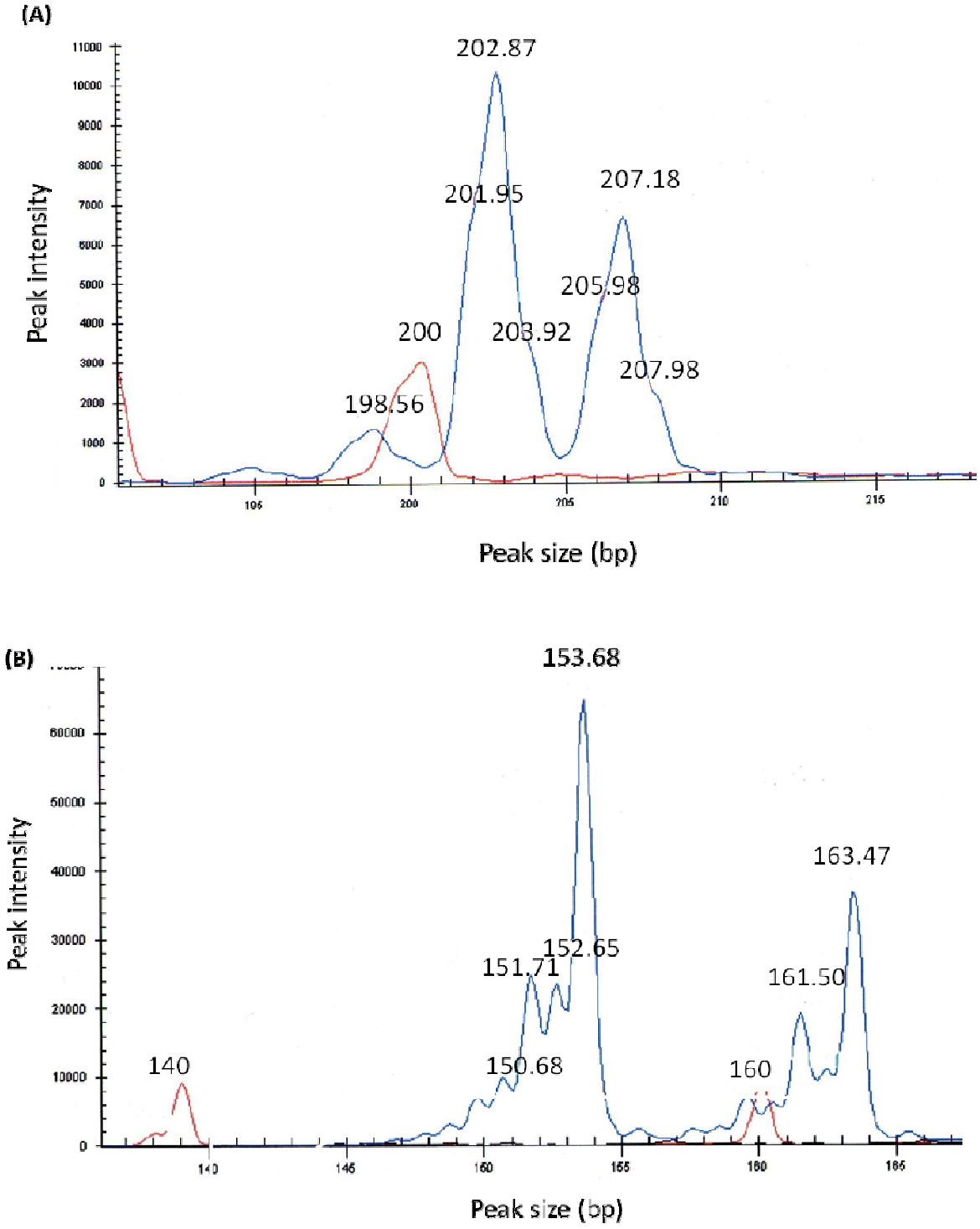

Figure 2.5. Polymorphic microsatellite markers demonstrating different patterns of heterozygosity. (A) Heterozygosity, using di-nucleotide marker D17S974, showing 2 major peaks with more than 4 base-pair apart. (B) Heterozygosity, using tetra-nucleotide marker D17S1866, showing 2 major peaks, more than 4 base-pair apart. Each major peak is composed of several minor peaks with less than 4 base pair-apart and its troughs do not reach the base line. Red peaks represent a standard size marker (std) used in LOH analysis using the CEQ 8000 System.

2.2.4.4. Analysis of LOH using the HOMOD method

The HOMOD method does not require a constitutional blood sample to test for LOH. It detects extended regions of homozygosity (ERH) in tumour DNA samples by identifying 5 or more consecutive microsatellite markers showing homozygosity and statistical analysis. It depends on calculating the statistical probability of adjacent homozygous markers being observed, by multiplying the known homozygosity rates for each marker in areas that appear to be contiguously homozygous, and is thus referred to as of homozygous mapping of deletions (HOMOD). The reported rate of homozygosity for each marker could be obtained from the Centre for Medical Genetics, Marshfield Clinic (www.marshfieldclinic.org/genetics/sets/scrset10.xls).

LOH is recorded when the probability of homozygosity at contiguous markers is ≤0.001, which is typically equivalent to ≥5 adjacent homozygous markers (Goldberg et al 2000). The results for each single marker were scored as follows:

(i) Homozygous (HOM): where only 1 peak was observed or two peaks were observed, with one ≤ 30% of the other.

(ii) Heterozygous (HT): where two 2 peaks were observed with ≤ 50% difference in their heights.

(iii) Non-informative (NI): where peaks are 1 microsatellite repeat unit apart or the difference between their heights is 31-49%, rendering their interpretation difficult.

(iv) Microsatellite instability: where > 2 major peaks were observed.

Typical peak patterns observed for microsatellite markers following electrophoresis on the Beckman CEQ System are shown in Figure 2.6.

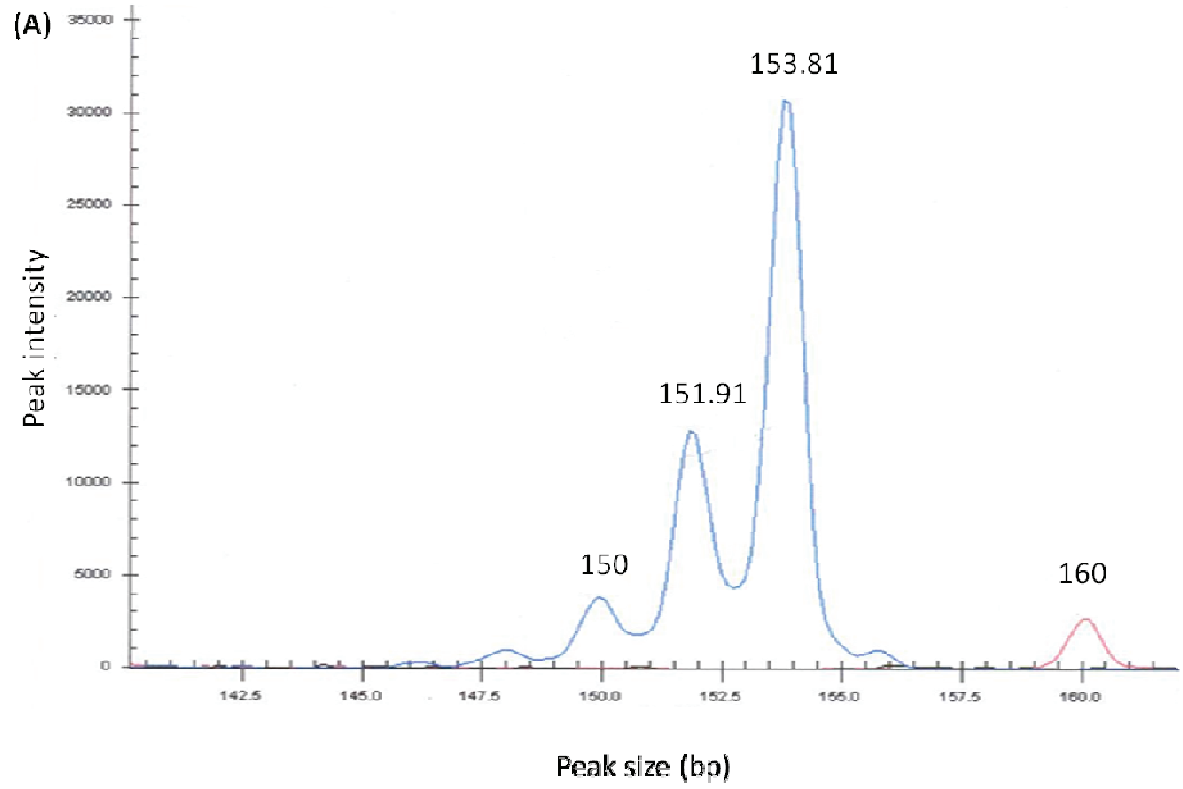
(A)
Peak intensity
35000
30000
25000
20000
15000
10000
5000
0
153.81
151.91
150
160
142.5
145.0
147.5
150.0
152.5
155.0
157.5
160.0
Peak size (bp)

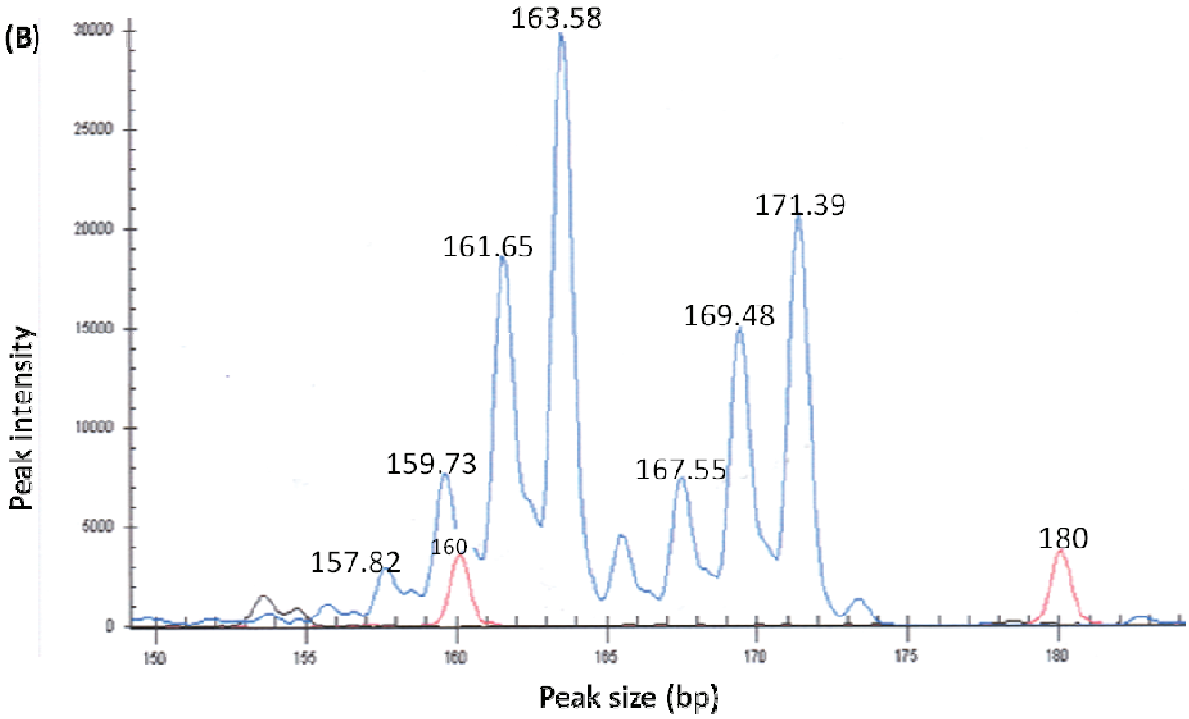
(B)
Peak intensity
30000
25000
20000
15000
10000
5000
0
163.58
161.65
171.39
169.48
159.73
167.55
157.82
160
180
150
155
160
165
170
175
180
Peak size (bp)

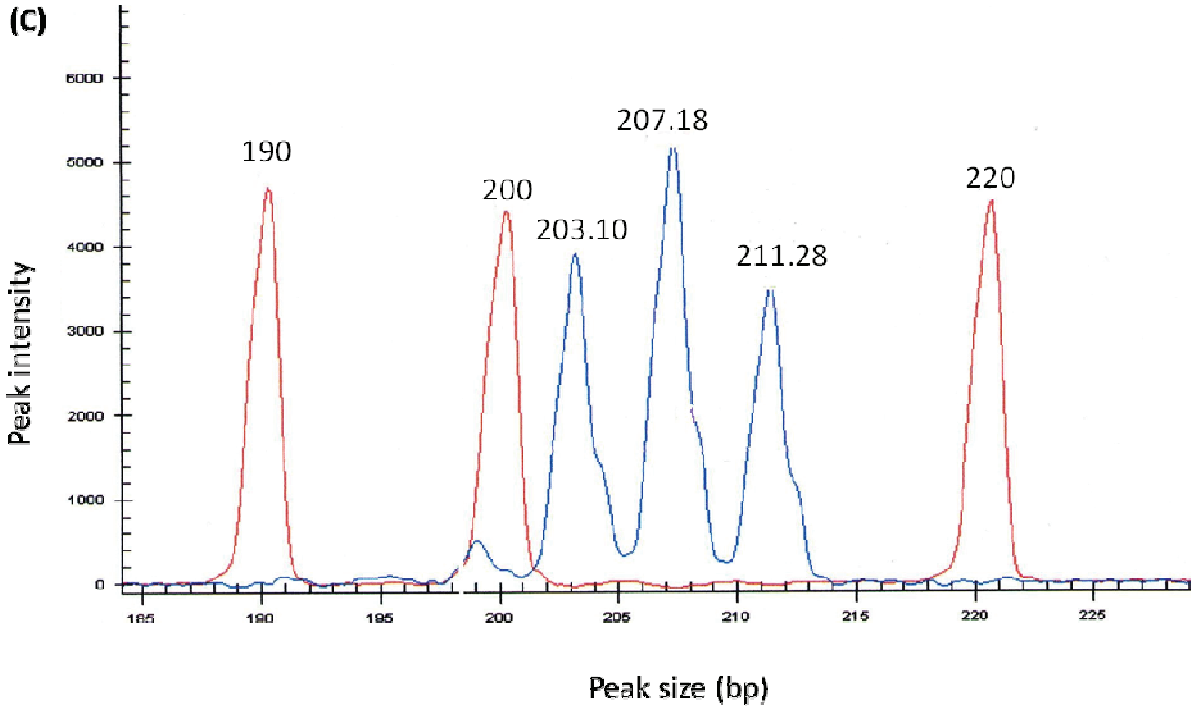

Figure 2.6. Polymorphic microsatellite markers for 17p LOH analysis using HOMOD. (A) Marker D17S1866 showing one major peak = homozygous. (B) Marker D17S1866 showing 2 major peaks = heterozygous. (C) Marker D17S974 showing 3 major peaks (blue) = heterozygous/MSI. Red peaks represent a standard size marker (std) used in LOH analysis using the CEQ 8000 System**.**

2.2.4.5. Analysis of LOH using the conventional LOH (cLOH) method

Where matched blood samples were available, the cLOH method was used to detect LOH relies on comparing allele peak heights in DNA derived from paired tumour tissue and constitutional blood. Thus, unlike HOMOD analysis, which requires information from at least 5 markers, only one marker showing LOH is required to define the case as having LOH (Goldberg et al 2000). The following equation was used to calculate LOH status: Tumour (A1/A2) / Blood (A1/A2), where A1 = Allele 1 peak intensity, A2= Allele 2 peak intensity. Results for cLOH analysis were then scored as follows:

(I) LOH: where 2 major allele peaks appear in the blood but only 1 peak in the tumour, or where 2 peaks are observed in both, and the allele peak ratio of the tumour sample is ≤30% of the blood sample.

(II) Retention of heterozygosity (RET): where two major peaks are observed in both the blood and tumour DNA samples with a difference of ≤ 50%.

(III) Non-informative (NI): where there is homozygosity in the blood sample or if two major allele peaks are observed in the blood and tumour DNA samples, and the difference between the allele peak ratio between the blood and tumour samples is 31-49%, rendering the result difficult to interpret.

(IV) Microsatellite instability (MSI): where the appearance of the major peaks observed in the tumour DNA sample are greater and / or differentially sized compared to the paired blood DNA sample. Illustrative examples of the assessment of LOH using the cLOH method are shown in Figure 2.7.

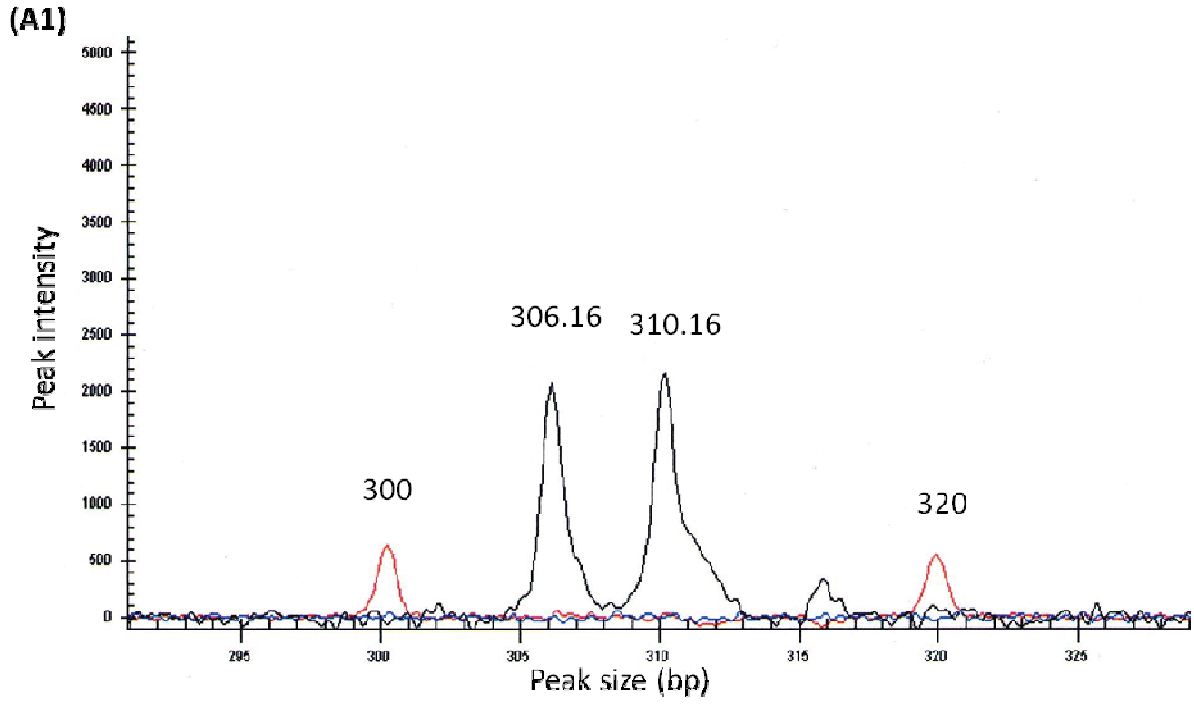

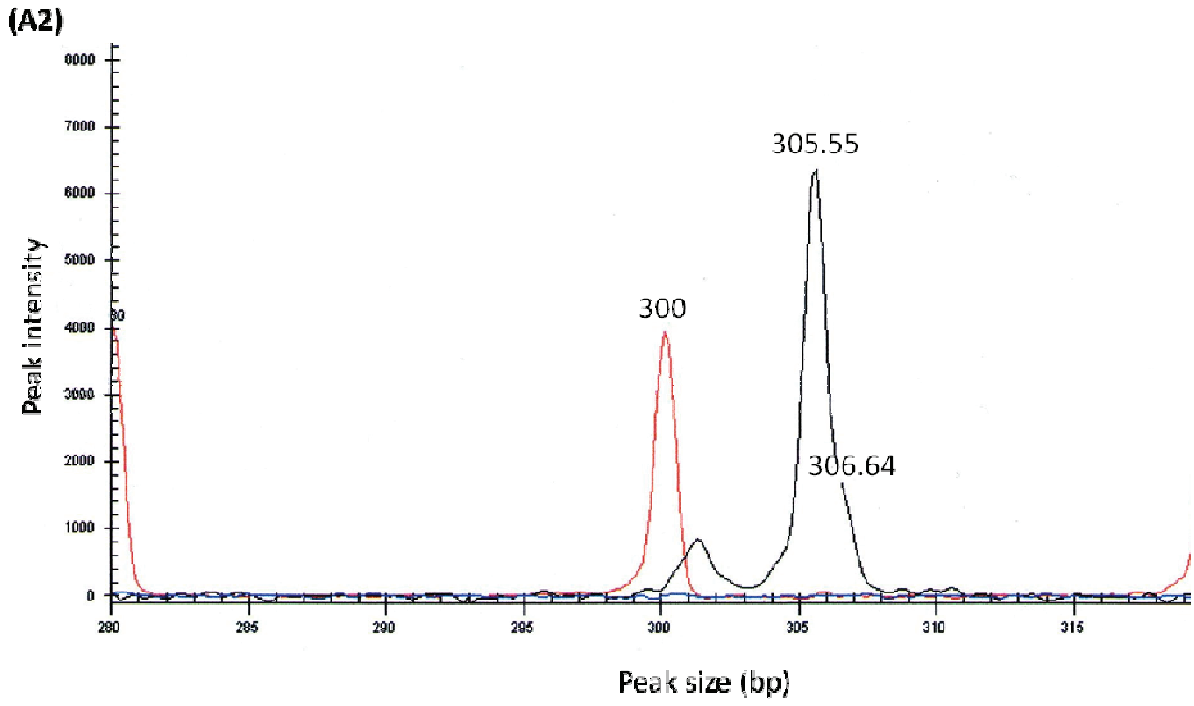

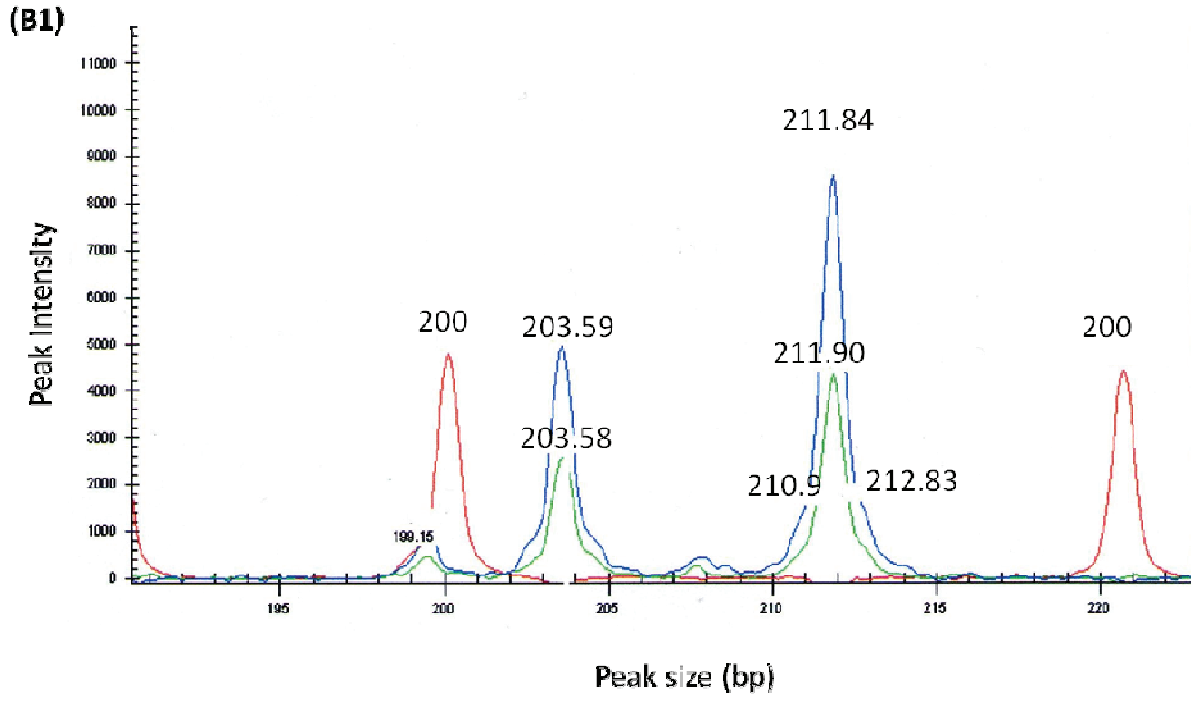

(Figure 2.7 continued)

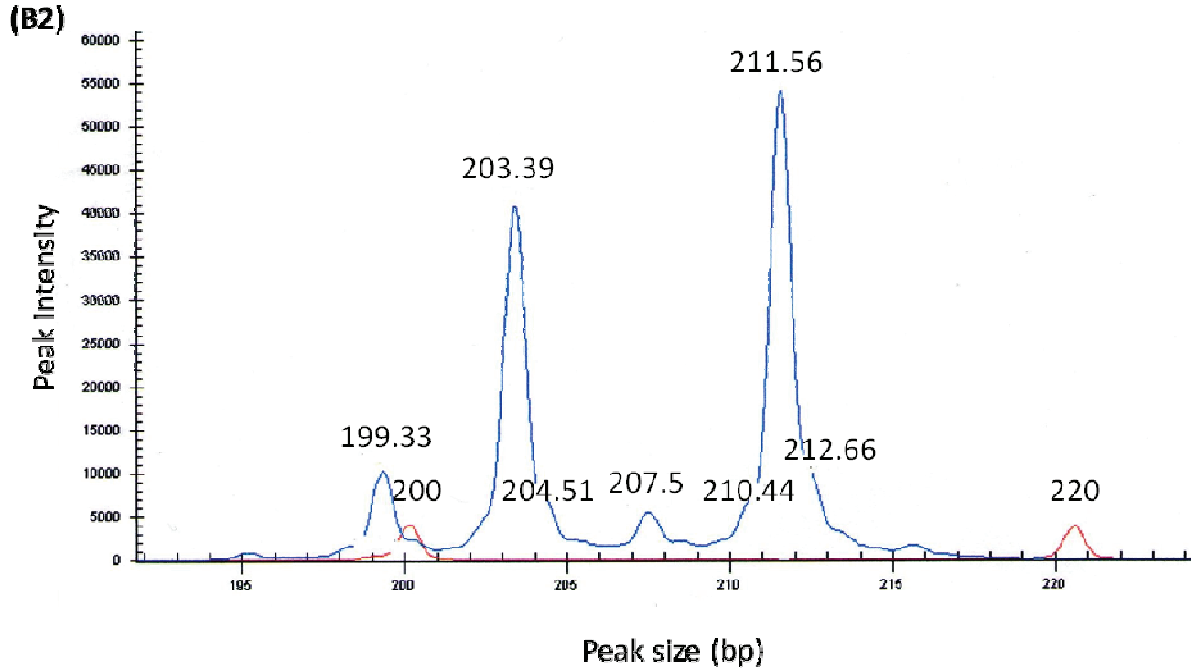

(Figure 2.7. continued)

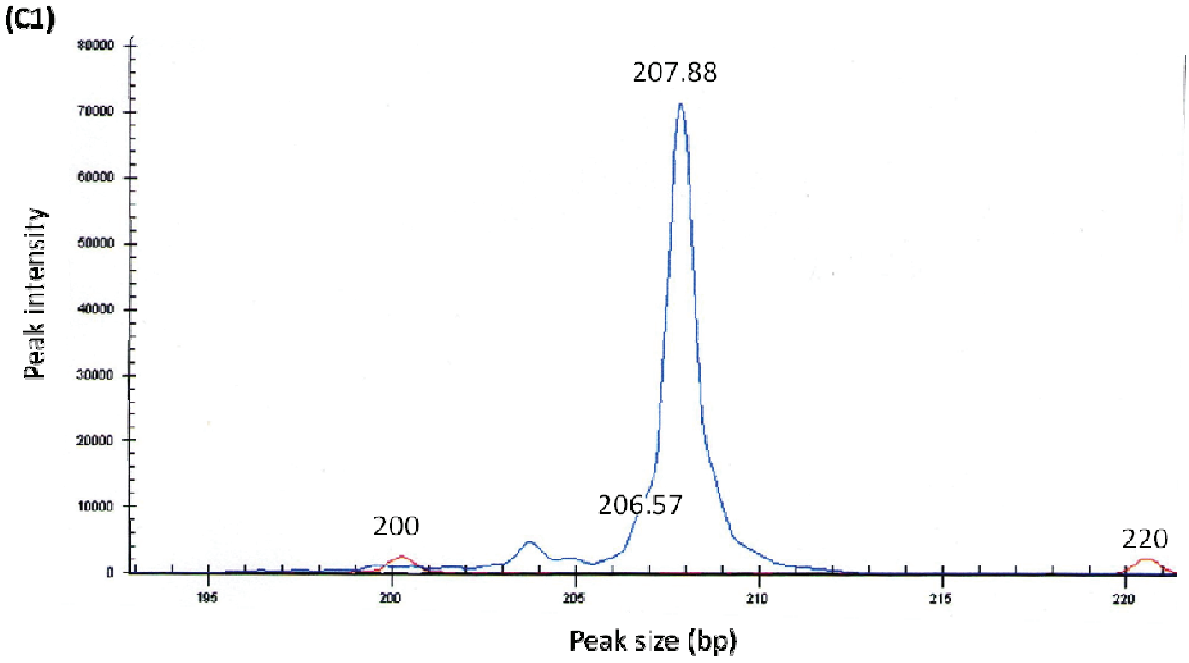

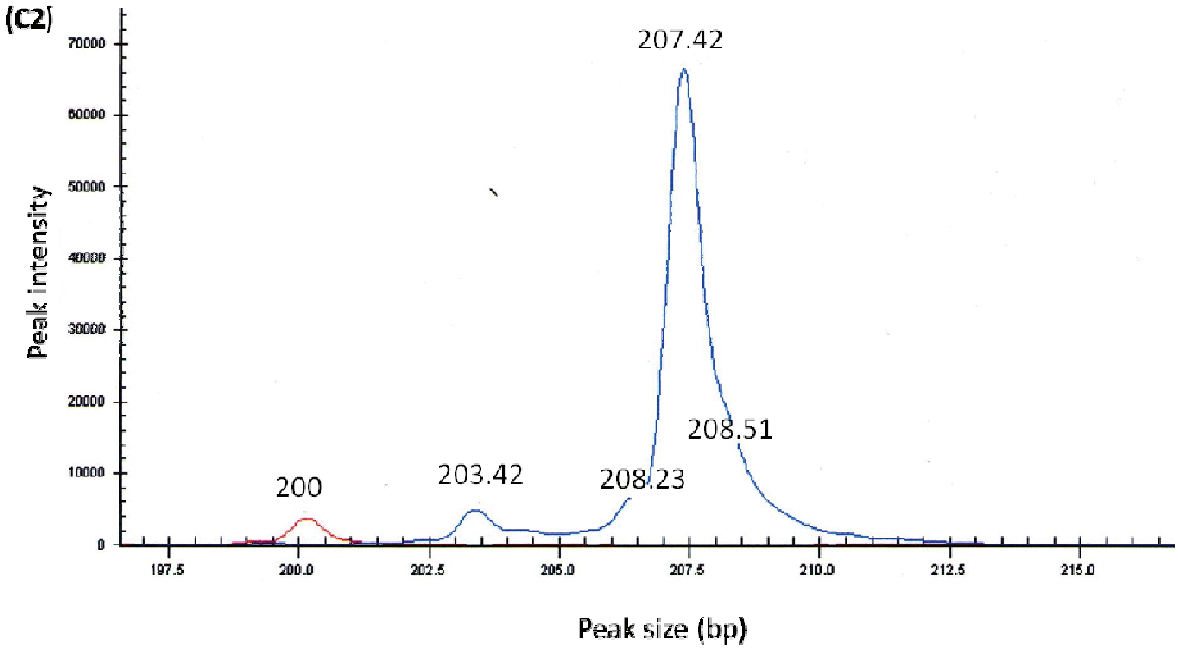

(Figure 2.7. Continued)

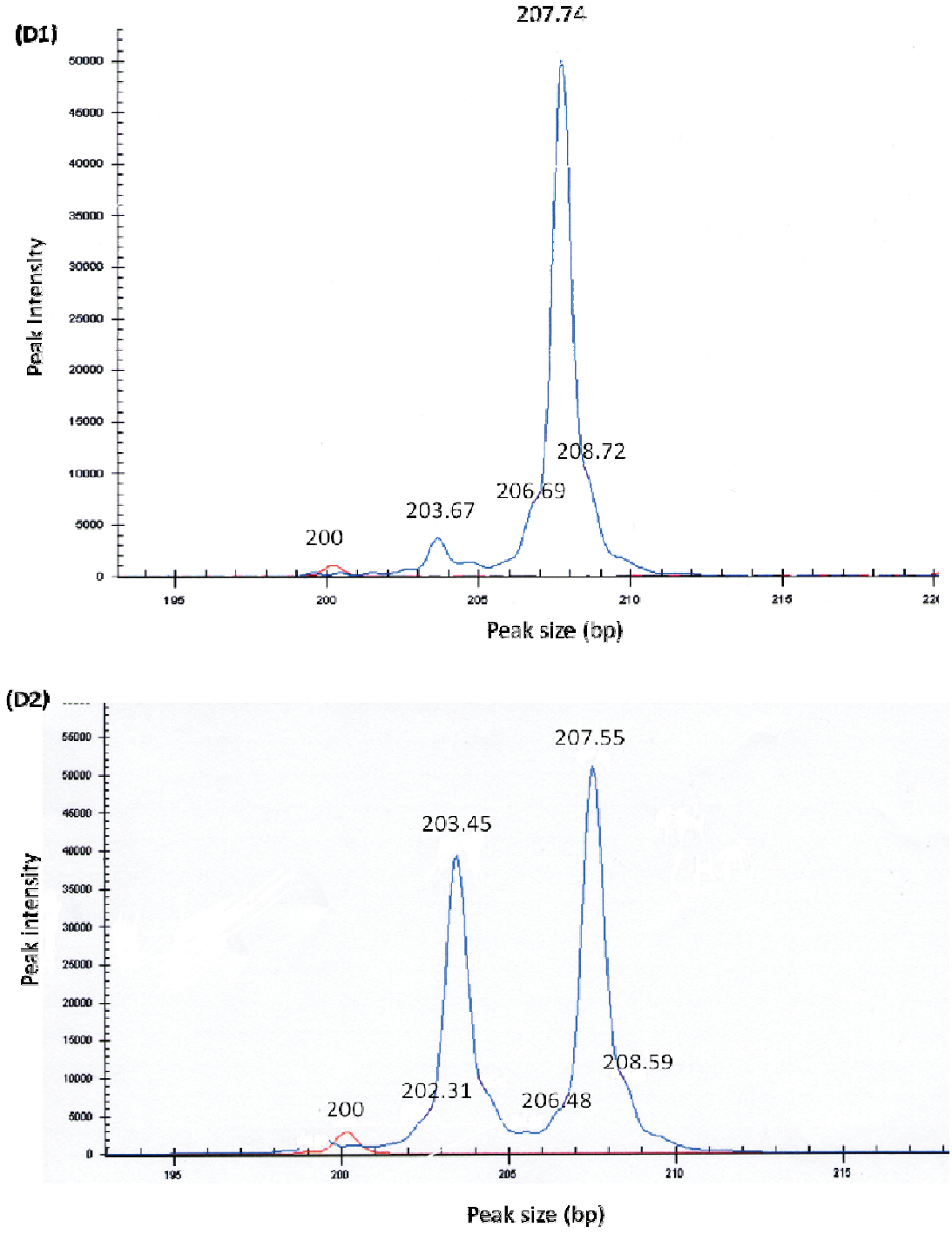

Figure 2.7. (A-D). Assessment of chromosome 17p LOH using PCR-based polymorphic microsatellite markers using cLOH. (A) Shows 17p LOH status, (A1) Blood sample showing heterozygosity = two peaks (A2) tumour sample showing homozygosity = one peak; (B) Shows 17p RET status, (B1) Blood sample showing heterozygosity = two peaks, (B2) Tumour sample showing heterozygosity = two peaks; (C) Shows 17p non informative status, (C1)Blood sample showing homozygosity = one peak, (C2) Tumour sample showing homozygosity = one peak; (D) Shows 17p microsatellite instability status (D1) Blood sample showing homozygosity = one peak, (D2) Tumour sample showing MSI > one peak.

2.2.5. Mutation analysis using direct DNA sequencing

The Sanger dideoxy chain-termination method (Sanger et al 1977) was used to perform direct DNA sequencing in this project. This technique uses dideoxy analogues (ddNTPs) of the normal deoxynucleotide triphosphates (dNTPs), which allow determination of the exact sequence of nucleotides within a DNA strand through acting as specific chain-terminating inhibitors of DNA synthesis. The sequencing reaction utilizes a single strand of the target DNA as a template for a complementary primer, the enzyme DNA polymerase, a combination of the 4 dNTPs (dATPs, dGTPs, dCTPs and dTTPs) and minute amounts of the 4 ddNTPs (ddATPs, ddGTPs, ddCTPs and ddTPs).

Essential components in the sequence reaction are the ddNTPs, which differ from the normal dNTPs by lacking 2 hydroxyl groups at the 3' end. This difference in composition allow ddNTPs to act as base-specific chain terminators, since the random incorporation of a ddNTP nucleotide into a newly synthesized DNA chain prevents further addition of other dNTPs or ddNTPs. The sequencing reaction allows DNA extension up till random incorporation of a ddNTP occurs, thus producing a variety of DNA fragments of different sizes (Figure 2.8, A). In order to visualize and identify the DNA fragments produced, ddNTPs are each fluorescently labelled with a different dye and an automated capillary gel sequencer is used for their analysis. Since each of the ddNTPs is labelled with a different dye, all four reactions may be loaded into a single lane of the capillary electrophoresis sequencer system (Figure 2.8, B).

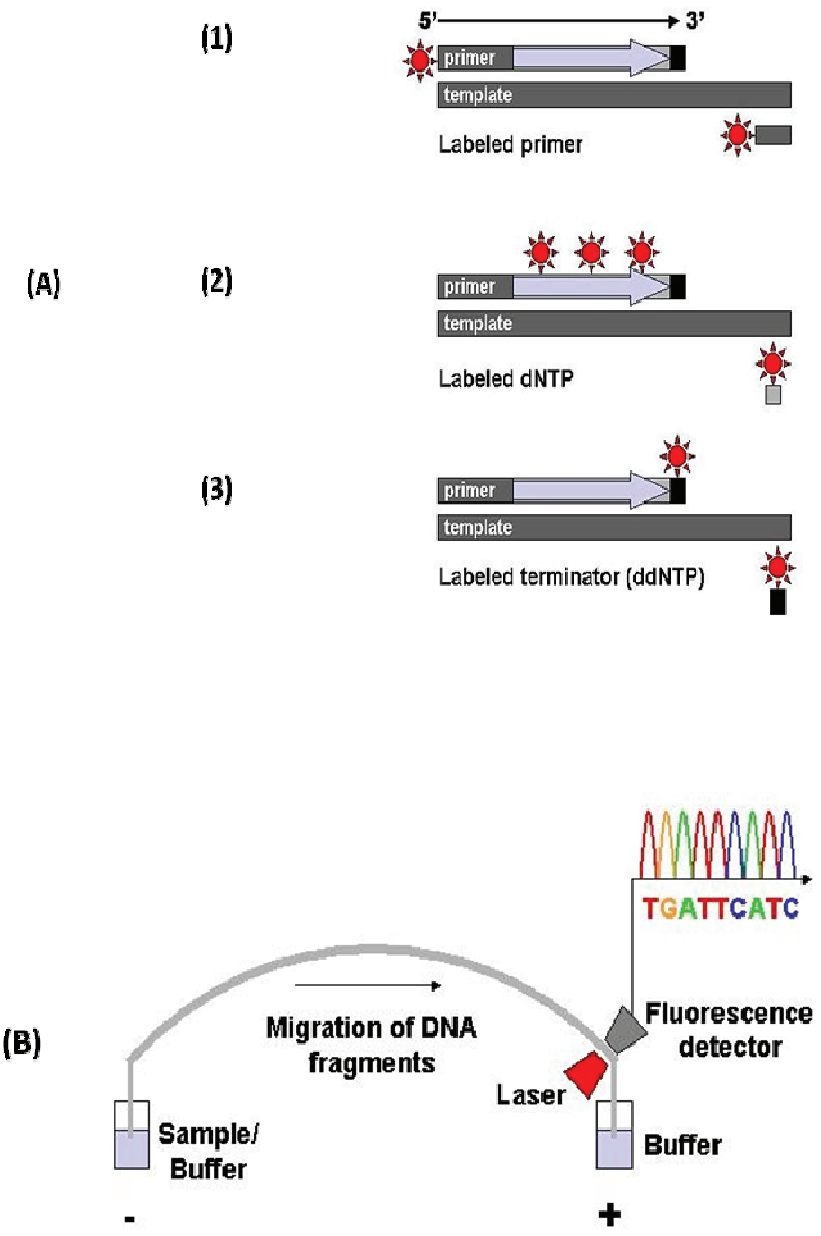

Figure 2.8. Automated DNA sequence analysis using the Sanger direct DNA sequencing method. (A) Four separate fluorescent dye labelled ddNTPs are used as labels for the base-specific DNA polymerase extension reaction. (1) DNA fragments with a fluorescent tag on the primer (2) The new DNA strands with a fluorescent tag labelled dNTP. (3) New DNA strands with fluorescent tag labelled terminator ddNTP. (B) During the electrophoresis run a laser beam is focused at a specific position on the gel. As individual DNA fragments migrate past this position, the laser causes the dyes to fluoresce. Maximum fluorescence occurs at different wavelengths for the 4 dyes, and the information is recorded electronically and interpreted sequence order is recorded (www.wikipedia.org/wiki/DNA_sequencing).

2.2.5.1. Sequencing method

PCR products were used as templates for direct sequence analysis in this project. The PCR reactions were performed as described before in section 2.2.2 and the specific PCR primers for *CTNNB1* are described below. 5µl from the amplified PCR products were run on a gel to ensure that amplification of the specific DNA sequence took place and generated a single specifically sized product. The PCR products were then purified using Invitrogen purification kit (PureLink^{TM} Nucleic Acid Purification Rack) (Invetrogen Ltd. UK), according to the manufacturer's instructions and eluted in the elution buffer provided with the kit and stored at -20^{0}C until their use in subsequent sequencing reactions. The main purpose for DNA purification is to remove excess primers otherwise they may co-anneal with the sequencing primers during the following sequencing reaction steps.

All samples were then sequenced in the forward and the reverse directions. The sequencing reactions were carried out in 0.2ml PCR-tubes (Abgene), which contained 2µl of the forward or reverse primer at 0.25µM final concentration, 8µl of the DTCS Quick Start Master Mix, 4µl of 50ng of purified DNA (PCR product) as a template and Ultra Pure water, to a final volume of 20µl. The DTCS Quick Start Master Mix contains fluorescently labelled ddNTPs, dNTPs and DNA polymerase enzyme. The reaction was performed using GeneAmp®9700 PCR system according to protocol (Applied Biosystem, UK). DNA sequences produced were assessed visually for evidence of sequence variants.

2.2.5.2. PCR for β-catenin gene (*CTNNB1*)

The primers shown in Table 2.10 amplify a 293bp fragment of exon 3 of the gene *CTNNB1* (Genebank accession number X89579), forward primer (nucleotides 780 – 803) and reverse primer (1050 – 1073). 50ng/µl PNET3 DNA (paraffin extracted) or 25ng/µl of other DNA PCR products were amplified using the PCR reaction detailed below (Tables 2.11, 2.12). 5µl of the PCR product was run on gel to check if the PCR amplification has worked. Purify the remaining PCR reaction by Invitrogen columns and the product from the columns was eluted in 30µl elution buffer and stored at -20^{0}C. Clearly labelled 5-10µl DNA (purified PCR product) in suitable tube or plate was sent with forward and reverse primers at 10uM for sequencing by an external provider (currently Durham University, Biosciences).

Sequencing reactions using β-catenin PCR products was performed as protocol using 4µl DNA (if PCR band is strong and clearly visible or if the band is weak then add more DNA to the reaction (max 8µl)), 2µl (of 10uM) of reverse or forward β-catenin primer, 6µl water (or volume required to make final volume of 20µl) and 8µl CEQ Master mix (thaw and mix well before use).

Primers; product size: 293 bp	
β-cat fragment G forward	TCCAATCTACTAATGCTAATACTG
β-cat fragment G reverse	TAAGGCAATGAAAAATAATACTC

Table 2.10. The sequence of the forward and reverse specific primers used for amplification of exon 3 of *CTNNB1*

PCR reaction		x20	x40
Primer F	2.0	40	80
Primer R	2.0	40	80
Buffer x 10	2.0	40	80
Mg (25mM)	1.5	30	60
dNTP (5mM)	0.8	16	32
TAQ	0.2	4	8
DNA (25ng/ul)	2.0	-	
Water	9.5	190	380

Table 2.11. PCR reaction used for amplification of *CTNNB1* gene

1 cycle	95C for 10 min
40 cycles	95C for 10 min 53C for 30 sec 72C for 30 sec

Table 2.12. PCR program used for amplifying *CTNNB1* gene

2.2.6. Immuno-histochemistry

Immunohistochemistry (IHC) is a process for localizing antigens (e.g. proteins) in cells' tissue sections exploiting the principle of an antibody binding specifically to an antigen in biological tissues (Ellison et al 2003). Immunohistochemical staining is commonly utilized for the diagnosis of abnormal cells such as those found in cancerous tumours. Specific molecular markers are characteristic of particular cellular events such as proliferation or cell death. IHC is widely used in standard research to comprehend the distribution, localization of biomarkers and differentially expressed proteins in different parts of biological tissues. Visualizing an antibody-antigen interaction can be achieved in a number of ways most commonly by conjugating an

antibody to an enzyme that can catalyze a colour-producing reaction. Alternatively, the antibody can also be tagged to a fluorophore, such as fluorescein, rhodamine, DyLight Fluor or Alexa Fluor (www.innovabiosciences.com).

2.2.6.1. Types of antibodies used

The antibodies used for specific detection can be either polyclonal or monoclonal. Polyclonal antibodies are typically manufactured by injecting animals with peptide antigen, which stimulates a secondary immune response. Antibodies raised can then be isolated from whole serum, and purified if necessary. Thus, polyclonal antibodies are a heterogeneous mix of antibodies that recognize several epitopes.

Monoclonal antibodies are monospecific antibodies that are the same because they are produced by one type of immune cells and they can be created from any given substance and will specifically bind to that substance thus exhibit greater specificity. Antibodies can also be classified as primary or secondary. Primary antibodies are raised against an antigen of interest and are usually unlabelled (unconjugated), while secondary antibodies are raised against primary antibodies. Hence, secondary antibodies identify immunoglobulins of a particular species and are conjugated to either biotin or a reporter enzyme, or fluorescent dyes, such as alkaline phosphatase or horseradish peroxidase (HRP), to facilitate visualisation as described above.

2.2.6.2. The direct method for antigen detection

There are two major methods used to detect antigens in tissue by IHC, the direct and the indirect methods. In both methods, an additional step for antigen unmasking is required.

The direct method (Figure 2.9) is a one-step staining method involving a labelled antibody reacting directly with the antigen in tissue sections. This method uses only one antibody rendering the procedure simple and rapid. However, it can suffer problems with sensitivity due to little signal amplification and is less commonly used than the indirect methods.

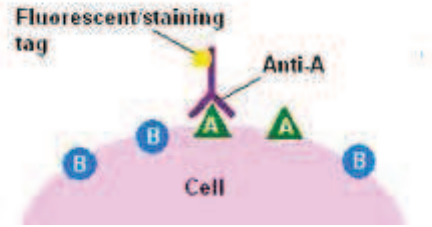

Figure 2.9. Direct method of IHC staining. It uses one labelled antibody (inverted violet Y), which binds directly to the antigen (Green triangles) being stained, (http://en.wikipedia.org/wiki/Immunohistochemistry).

2.2.6.3. The indirect method for antigen detection

The indirect method (Figure 2.10) involves an unlabelled primary antibody as a first layer which reacts with tissue antigen, and a secondary labelled antibody, which reacts with the primary antibody. This method is generally more sensitive due to signal amplification through several secondary antibody reactions with different antigenic sites on the primary antibody. The second layer antibody can be labelled with a

fluorescent dye or an enzyme. A common procedure involves, a biotinylated secondary antibody coupled with streptavidin tagged horseradish peroxidase enzyme. This is reacted with a substrate such as diaminobenzidine (DAB) to produce colorimetric reaction (i.e. brown staining) localized wherever primary and secondary antibodies are attached.

The indirect method, on top of its greater sensitivity, also has the advantage that only a relatively small number of standard conjugated secondary antibodies need to be generated. For example, a labelled secondary antibody raised against rabbit IgG, which can be purchased "off the shelf," is useful with any primary antibody raised in rabbit. On the other hand with the direct method, it is necessary to manufacture custom labelled antibodies against every antigen of interest.

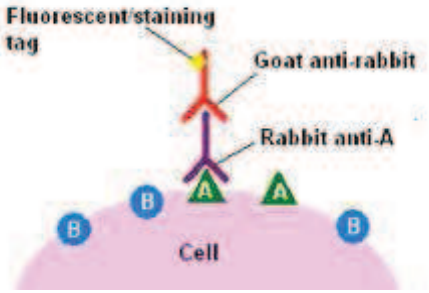

Figure 2.10. The indirect method. A labelled secondary antibody (red inverted Y) reacts with a primary antibody (violet inverted Y) which reacts with the antigen in the tissues (green triangle). (http://en.wikipedia.org/wiki/Immunohistochemistry)

2.2.6 4. Immunohistochemistry method used in this project

Nuclear β-catenin is an immuno-histochemical marker for Wnt/Wg pathway activation, which could be identified by using primary anti-sera on tissue sections by immunohistochemistry technique.

Procedure:

1- Microwave antigen retrieval:

Samples were organized in a plastic rack and immersed into citrate buffer solution in a plastic container, ensuring that all the slides are covered (330 ml.). The lids of the containers are placed in a position allowing ventilation of the slides. The containers are heated in a microwave, set on the highest power, for 5 minutes for 2 periods (2X5 minutes).The citrate buffer should be topped up if needed between the 5 minutes time period making sure that the slides are completely covered during the whole period of antigen retrieval. Next, the slides in the container were allowed to cool for 20 minutes.

2- Immuno-histochemistry-Menapth ^{TM}polymer-HRP IHC Detection kit:

The slides were put under tap water, washed well, and quenched with 3% hydrogen peroxide (95 ml distilled water, 5 ml hydrogen peroxide) for 20 minutes. Then the sections were washed well in water and rinsed in TBS and tween. Excess fluid around the sections were wiped off and primary antiserum (β-catenin BD Transduction labs 610154) was applied (1:600 dilution) and left for 60 minutes. The slides were washed again in TBS with a final wash in TBS and tween. Excess solution around the sections was wiped off and Menapath universal probe (Yellow) was applied for 30

minutes. Slides were washed in TBS followed by a final wash in TBS and tween and wiping off excess solution around the sections.

Menapath HRP-polymer (Orange) was then applied to the sections for 30 minutes then washed well in running water for 20 minutes.

In a designated visualisation area DAB was prepared by adding 1 drop of chromagen liquid DAB to 1 ml of DAB diluent, dropped onto the slides and left for 3-4 minutes. The slides were then washed in water. Slides were counter-stained lightly by immersing them in haematoxylin for few seconds then left to dehydrate. Any excess fluid was wiped off and the sections were mounted in DPX. After the sections had been mounted, they were issued to a central reviewing pathologist where β-catenin outcome was recorded for positivity and quality assessment of sections. All the details of the immuno-histochemical preparations and date of issue were logged into the central database in Newcastle.

2.2.7. Statistical Analysis

The results of all molecular analysis underwent statistical analysis to investigate associations with clinical and pathological features (e.g. patients' age at diagnosis, gender, pathology, metastatic stage at diagnosis, extent of surgical resection and clinical risk group) using t-tests, Fisher's exact tests. Overall survival in clinical and molecular subgroups was calculated using Kaplan-Meier plots and Log-rank statistical tests. Overall survival (OS) was measured from the date of diagnosis to date of death of disease or last contact and event free survival (EFS) was calculated from the date of diagnosis till the date of first event, which was either recurrence or death from any

cause. Statistical tests were prepared using the statistical package for the social science (SPSS) version 16 (IBM company).

All observed prognostic variables were tested individually in Cox proportional regression hazards model. Those shown to be significant ($p < 0.05$) were entered into a multivariate multiple Cox proportional regression hazard ratio model in a stepwise procedure taking a ‘p` value of < 0.05 to enter and > 0.05 to be removed.

Chapter 3

The clinicopathological implications of chromosome 17p loss in medulloblastoma

3.1. Introduction

It is generally accepted now that it is vital to attempt to improve the current disease classification of medulloblastoma by exploring the possible combination of established clinical criteria with prognostic molecular markers. Aberrations on chromosome 17 are the most common chromosomal abnormalities in medulloblastoma, with isolated deletions on 17p frequently affecting the entire chromosomal arm (occurring in 20%) and i(17q) occurring in another 30-50% of cases (Griffin et al, 1988, Gilbertson et al, 2001, Jung et al, 2004, reviewed by Pizer and Clifford, 2009) suggesting the presence of TSGs on 17p or oncogenes on 17q. Since *TP53*, located on 17p13.1 is mutated in less than 10% of medulloblastomas, it is logical to speculate that other TSGs reside on 17p telomeric to 17p13.1 (Cogen et al 1992, McDonald et al 1994, Emadian et al 1996, Biegel et al 1997).

One of the obstacles to the progress of research in medulloblastoma is the shortage of samples, especially those with high quality DNA derived from fresh frozen samples, required for genomic analysis, and their matched DNA, which has frequently precluded the conduct of large, group wide studies. HOMOD (Homozygous Mapping Of Deletions) is a method to overcome this obstacle. It allows testing large numbers of samples and cell lines for evidence of genetic loss (LOH) within FFPE material without the need for matched DNA. The protocol of this method and interpretation of its results are detailed in chapter 2 (Goldberg et al 2000, Langdon et al 2006).

The reported associations between chromosome 17p loss and survival are inconsistent between different studies. Cogen et al (1990) examined 11 medulloblastoma specimens, taken from 9 patients (one patient had 3 surgical procedures in the same year because of tumour recurrence), using RFLP. Allelic losses of DNA sequences of the distal part of chromosome 17p loss were identified in 4/9 (45%) of the samples. Further analysis identified that the common allelic loss targeted 17p11.2-13.3. None of the 4 cases had a good response to treatment despite that 3 of them were clinically classified as low-risk. Four of the other 5 cases without 17p loss were alive during the last follow up. However, the small number of cases in this study weakened its statistical significance. Batra et al (1995) in a cohort of 28 cases of primary medulloblastoma found 8/28 (29%) cases with evidence of chromosome 17p LOH and these were significantly associated with poor survival (p=0.045). Conventional LOH detection methods which compare allelic status in tumour and matched constitutional DNA were used, but their cut-off criteria to record a result as LOH was an observation of reduction by 80% of the allelic intensity in the tumour compared to the constitutional blood sample.

Emadian et al (1996) in a study on a cohort of 21 cases of primary medulloblastoma reported that 10/21 (48%) of the cases showed chromosome 17p LOH. Survival analysis did not show a significant association between chromosome 17p LOH and patients' outcome (p= 0.77). Biegel et al (1997), analysed 56 patients with primary medulloblastoma, where chromosome 17p LOH was detected in 23 cases (41%), and found no significant association with 5 years event free survival (p= 0.25). Scheurlen et al (1998) examined 30 primary medulloblastoma tumours and 6 CSF

metastatic specimens, and reported LOH on chromosome 17p13.1 in 14/30 and 6/6 cases, respectively (collectively, 20/36 (55.6%). No cases with chromosome 17p LOH had desmoplastic pathology and 12/15 cases (80%) with metastasis had chromosome 17p LOH. Survival analysis showed that chromosome 17p loss was associated with a significant poorer outcome ($p< 0.01$). The significant association between chromosome 17p LOH with metastasis and bad prognosis may be influenced by the fact that this centre mainly received patients with metastasis as well as the incorporation of CSF metastatic specimens in their cohort.

Gilbertson et al (2001) reported the results of a study which looked at 41 primary medulloblastoma samples. Chromosome 17p loss was seen in 20/41 (49%) of the cases, with isolated 17p loss seen in 8/20 (40%, in total 8/41 (20%)) and i(17q) in 12/20 (60%, in total 12/41(29%)). Isolated 17p loss was associated with poor prognosis; 7/8 (88%) died of disease, 5/7 within 3 years of diagnosis. Analysis of patients with isolated 17p loss and normal chromosome 17p (21/41) cases showed a significant difference in survival between these 2 groups ($p= 0.003$). Noticeably, i(17q) showed bad prognosis during short term follow up (2 years post operative), but had no influence on survival during long term follow up, and the authors suggested that this may indicate that the 2 groups represent distinct subgroups of medulloblastoma with different clinical and biological backgrounds.

Lamont et al (2004), in a study of 87 cases with primary medulloblastoma, found that 29 cases had chromosome 17p loss (i(17q) was present in 23 cases and isolated loss of 17p in 6 cases). Cases showing 17p loss and i(17q) had significantly

poor outcome, (p= 0.003 and 0.048, respectively) they also occurred at higher frequency in tumours with metastatic disease however, this association did not reach statistical significance. Isolated loss of 17p or i(17q) was not detected in cases with nodular / desmoplastic pathology.

Pan et al (2005), in a study of 35 cases of primary medulloblastoma using CGH found 10/35 (29%) cases with isolated chromosome 17p loss and 12/35 cases had 17q gain, both groups were not associated with poor OS or EFS (p= 0.14 and p= 0.15; p= 0.73 and p= 0.7, respectively). On the other hand, the 5/35 cases which showed i(17q) had shorter OS and EFS (p= 0.03 and p= 0.04, respectively). The 4 infants in his cohort did not show chromosome 17p aberrations, 3/4 died of disease, this supports the theory that medulloblastoma arising in infants may represent a distinct subset of this tumour.

Pfister et al (2009) assessed 2 independent cohorts of 80 and 260 primary medulloblastoma samples using aCGH and FISH techniques, respectively. In the first cohort, no cases with 17p loss were detected. Cases with i(17q) (31/80, 39%) and cases with 17q gain (7/80, 9%) showed a significant poor outcome (5 years OS, p= 0.009 and p= 0.003, respectively). In the second cohort 17p loss was detected in 18/260 cases (7%) and this did not show a significant correlation with survival (5 years OS, p= 0.1) while 43/260 cases (17%) with 17q gain and 77/260 cases (30%) with i(17q) showed a significant poor outcome (5 years OS, p< 0.001). The group, concluded that 17q gain and i(17q) were better predictors than isolated 17p deletion for poor OS survival.

The incidence of chromosome 17p LOH and its correlation with survival in different studies in the literature are summarized in Table 3.1. In conclusion, although a number of studies in the literature have correlated chromosome 17p loss with significant adverse outcome, other studies have failed to detect such significant association. Most studies mentioned above involved small numbers of cases, or have employed a variety of techniques with different sensitivities for detection, where sometimes only isolated 17p loss was analysed, while others tested the whole chromosome 17. These factors render different studies difficult to compare. The examination of larger cohorts of homogeneously treated patients using equivalent methods, are required to precisely define the clinical significance of 17p loss in medulloblastoma. Such analysis is undertaken in the present study, where 208 cases of primary medulloblastoma derived from the PNET3 clinical trial are analysed for chromosome 17p loss, and its correlation to clinicopathological variables, as well as to patients' survival.

	No. of cases	No. of cases with 17p LOH	Log-rank test, 'p` value
Cogen et al (1990)	9	4 (44.4%)	No statistical analysis was done because of the small number of cases, 3/4 cases had recurrence and died
Batra et al (1995)	28	8 (28.5%)	OS, 0.045
Emadian et al (1996)	21	10 (47%)	OS, 0.77
Biegel et al (1997)	56	23 (41%)	EFS, 0.25
Scheurlen et al (1998)	30	14 (46.6)	OS,<0.01
Gilbertson et al (2001)	41	20 (49%) Isolated 17p loss, 8 cases. Additional gain of i(17q) 12 cases	OS, 0.003
Lamont et al (2004)	87	29 (37%) Isolated 17p loss, 6 cases. i(17q) 23 cases	OS, 0.003 OS, 0.048
Pan et al (2005)	35	10 (29%) Isolated 17p loss 10 cases i(17q) 5 cases	OS (0.14), EFS (0.15) OS (0.03), EFS (0.04)
Pfister et al (2009)	80 260	17p loss 0 17q gain 7 i(17q) 31 17p loss 18 17q gain 43 i(17q) 77	5 years OS= (0.003) (0.009) (0.1) (<0.001) (<0.001)

Table 3.1. The incidence of chromosome 17p LOH and its correlation to survival in the studies reported in the literature

3.2. Aims

The specific aims of this chapter are:

1. To develop and validate the HOMOD method to test for LOH in tumour samples which do not have matched DNA.

2. To investigate the incidence of 17p LOH in medulloblastoma.

3. To investigate if chromosome 17p LOH status is associated with patients' disease characteristics, survival and clinical outcome.

4. To see if chromosome 17p LOH can be used as a prognostic factor in medulloblastoma and improve the current disease risk classification.

3.3. Materials and methods

3.3.1 Materials

3.3.1.1. The NMB cohort

Two cohorts of patients were analyzed in the work described in this chapter. The NMB cohort consisted of 76 randomly selected primary medulloblastoma tumour samples which were collected from the medulloblastoma bank at the Northern Institute for Cancer Research, Newcastle University. The details of this cohort are described in chapter 2.

3.3.1.2. The PNET3 cohort

The second cohort of patients was derived from the PNET3 clinical trial and consisted of 208 medulloblastoma samples. Those are patients randomized into the International Society of Paediatric Oncology / United Kingdom Children's Cancer Study Group PNET3 (SIOP/UKCCSG) trial of sandwich chemotherapy followed by radiotherapy versus radiotherapy alone (Taylor et al 2003). The data for this cohort is fully detailed in chapter 2.

3.3.2. Methods

3.3.2.1. DNA extraction

DNA from tumour samples and matched blood DNA was extracted from 76 NMB tumour samples, and 29 constitutional blood samples as per the protocol, detailed in chapter 2, section (2.2.1.1). DNA from 208 PNET3 FFPE tumour samples was extracted according to the protocol, detailed in chapter 2, section (2.2.1.2).

3.3.2.2. Polymerase chain reaction (PCR)

PCR was performed as per the protocol detailed in chapter 2, (section 2.2.2). The specific primers used in the PCR amplification procedure to test for chromosome 17p loss, their specific sequences and product sizes are shown in Table 3.2.

3.3.2.3. Agarose gel electrophoresis

Amplified PCR products were run on a 2% agarose gel to ensure that the amplification was successful. Details of this procedure are described in chapter 2, section (2.2.3).

3.3.2.4. Loss of heterozygosity analysis

26 cases from the NMB cohort were assessed for 17p loss by both cLOH and HOMOD methods and the NMB and PNET3 cohorts were assessed for 17p loss by the HOMOD method. The details of both protocols, and methods for interpreting the results, are provided in chapter 2, section (2.2.4).

3.3.2.5. Statistical analysis

The statistical methods used for analysis of both the NMB and PNET3 cohorts are detailed in chapter 2, section (2.2.7).

Marker	Forward primer (5'-3')	Reverse primer (5'-3')	Product size(bp)	Well RED Dye	Tm^{0}C (F),(R)	NCBI sequence Map/position
D17S2196	CCAATATCTAGAATTATTCAGAATC	ATATTTCAATATTGTAACCAGTCCCC	139-163	D2	(48)(50)	(17p11.2) 17205207-17205343(bp)
D17S936	ATTTGAAACCACAACAGCA	AGGTATATGCCCACCC	93-103	D4	(52)(54)	(17p12-p11.2) 13374009-13374103(bp)
D17S969	ATCTAATCTGTCATTCATCTATCCA	AACTGCAGTGCTGCATCATA	116-140	D2	(49)(58)	(17p12) 11785691-11785822(bp)
D17S974	AGACCCTGTCTCAGATAGATGG	TAAAATAGAAAGTGCCCCTCC	201-217	D4	(49)(50)	(17p13) 10459436-10459639(bp)
D17S1866	TGGATTCTGTAGTCCCAGG	GGTTCAAAGACAACTCCCC	154-185	D4	(58)(58)	(17p13.3) 82571-82745(bp)
D17S1308	TGTGAAACTTTGTCATCACTA	TTGGTGACAAAGAAAGTCTCC	304-318	D2	(50)(48)	(17p13.3) 569917-570218(bp)

Table 3.2. Chromosome 17p microsatellite primers (annealing temperature used for all primers was 55^{0}C)

3.4. Results

3.4.1. Validation of the HOMOD method by cLOH and aCGH

3.4.1.1. Validation of HOMOD by cLOH

In order to validate that the HOMOD is a reliable method to test for LOH, we first assessed 17p LOH status in 26 cases using both conventional LOH (cLOH) and HOMOD. This validation was based on assessment of whether the HOMOD and cLOH generate comparable results for 17p LOH status. 22/26 cases (84.6%) produced equivalent results using both methods. Of these, 14 cases showed 17p LOH, 5 cases showed retention of heterozygosity (RET) and 3 cases showed 17p RET with evidence of microsatellite instability (MSI) by cLOH and 17p RET by HOMOD. Discrepancies between the results obtained using the 2 methods were found in 4 cases (Table 3.3, Figures 3.1 and 3.2). One case showed 17p LOH by cLOH and showed 17p RET by HOMOD, while 3 cases showed 17p LOH + MSI by cLOH and showed 17p RET by HOMOD. Each of the 4 cases interpreted as 17p LOH by cLOH but as RET by HOMOD, showed LOH at only one marker analysed, whereas the surrounding markers were detected as RET. These data indicate that the HOMOD method can robustly detect genetic losses involving the entire p-arm of chromosome 17, but are not able to detect smaller interstitial losses involving lower number of markers.

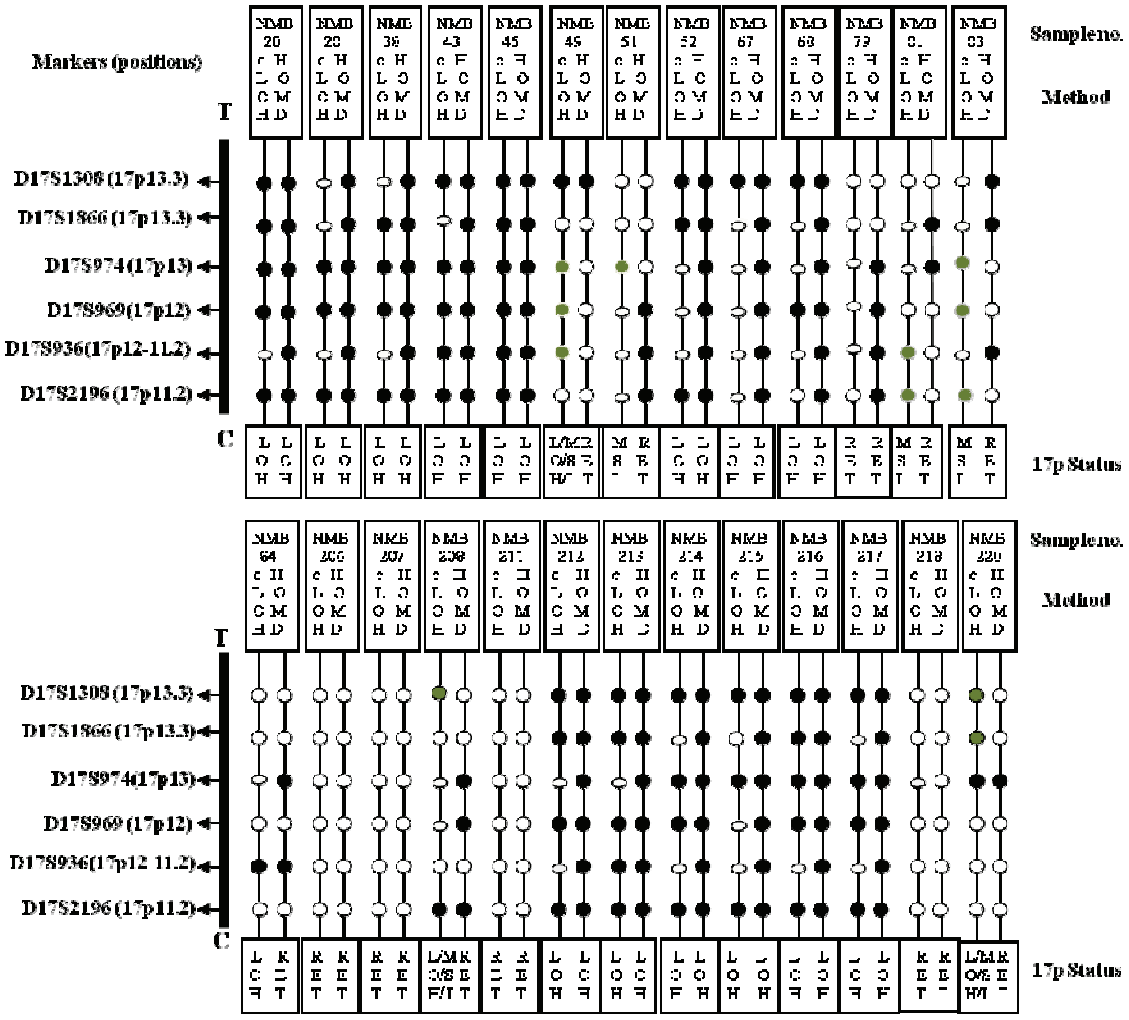

Fig 3.1. Analysis of chromosome 17p LOH status using cLOH and HOMOD methods in 26 medulloblastoma samples

cLOH: LOH● , HET○ , MSI ● , NI =non informative◯ ; HOMOD: HOMO● , HET○
RET= retention of heterozygosity, LOH= loss of heterozygosity, T= Telomere, C= centromere.

Number of cases	17p LOH status by cLOH	17p LOH status by HOMOD
14	LOH	LOH
5 (cases no., 79,206,207,211,218)	RET	RET
3 (cases no., 51,81,83)	RET/MSI	RET
1 (case, 84)	LOH	RET
3 (cases n., 49,208,220)	LOH/MSI	RET

Table 3.3. Comparison of chromosome 17p LOH status, assessed by cLOH and HOMOD in 26 samples

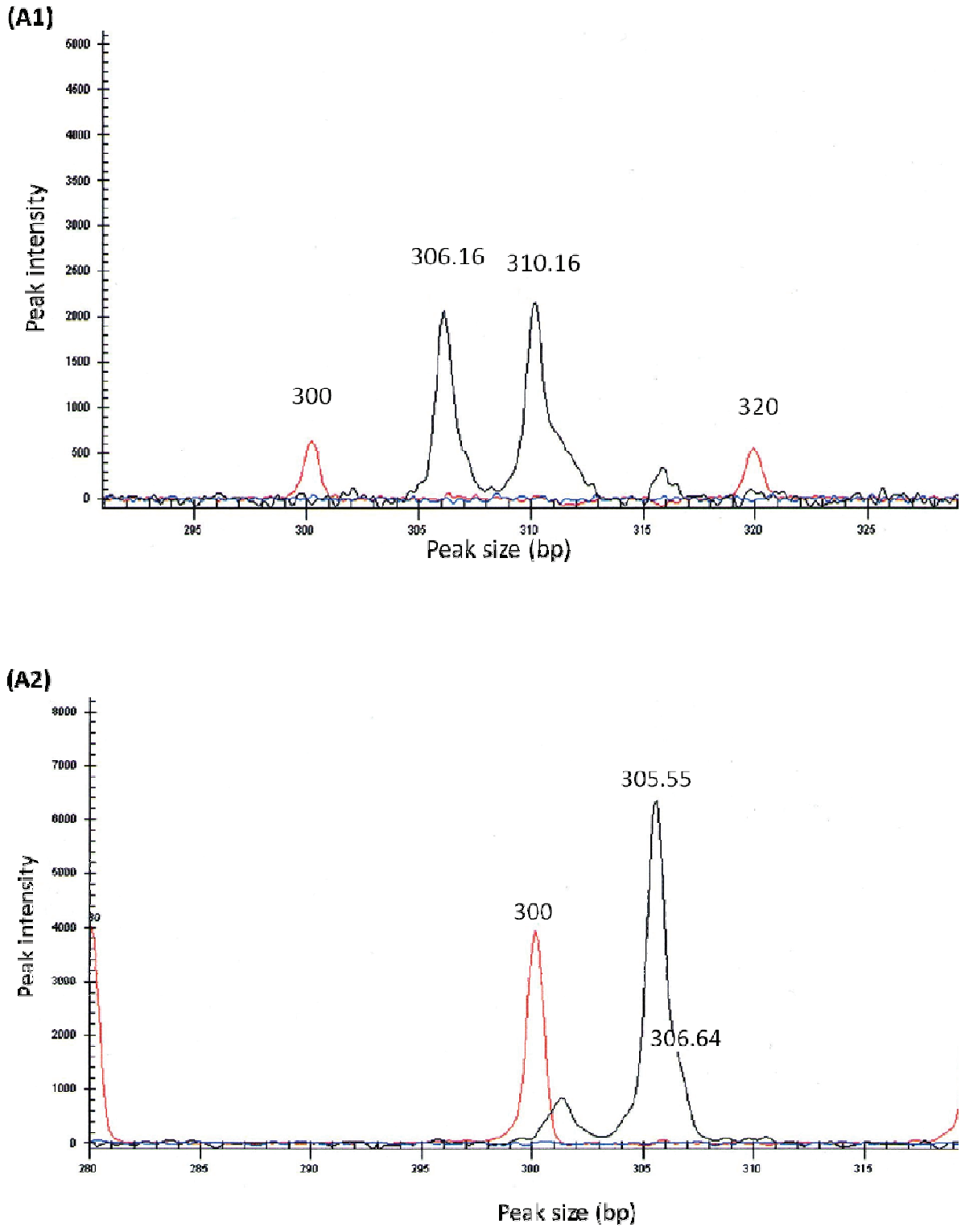
(A1)
Peak intensity
306.16
310.16
300
320
Peak size (bp)
(A2)
Peak intensity
305.55
300
306.64
Peak size (bp)

Figure 3.2.

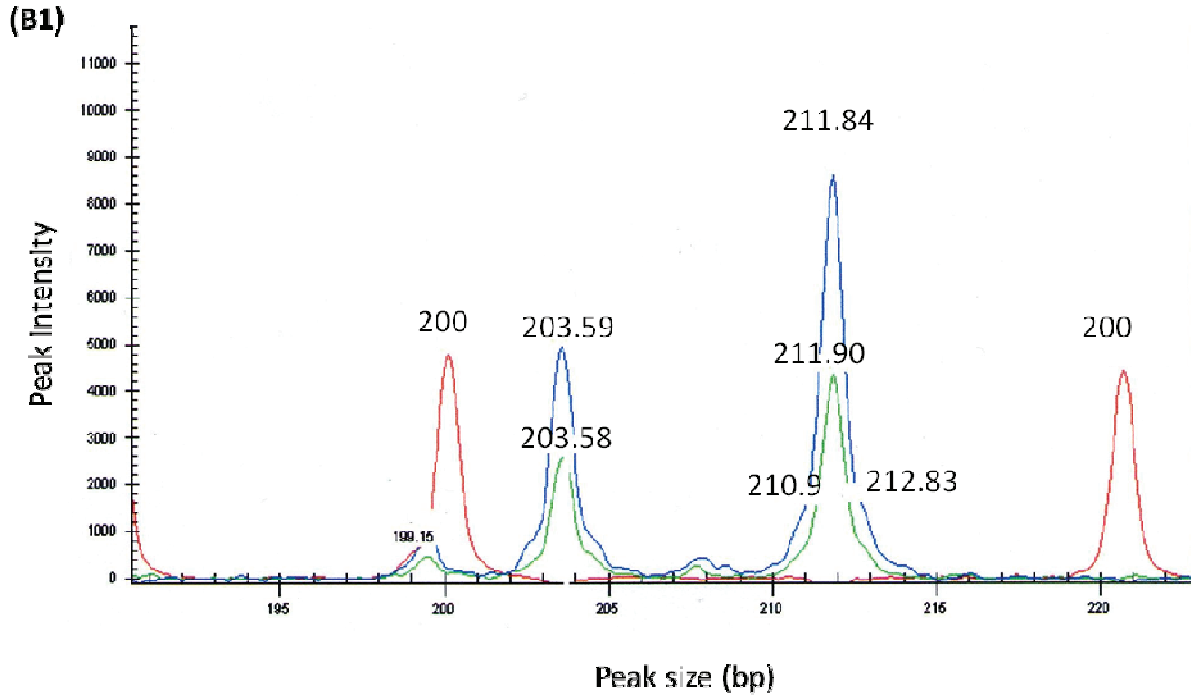

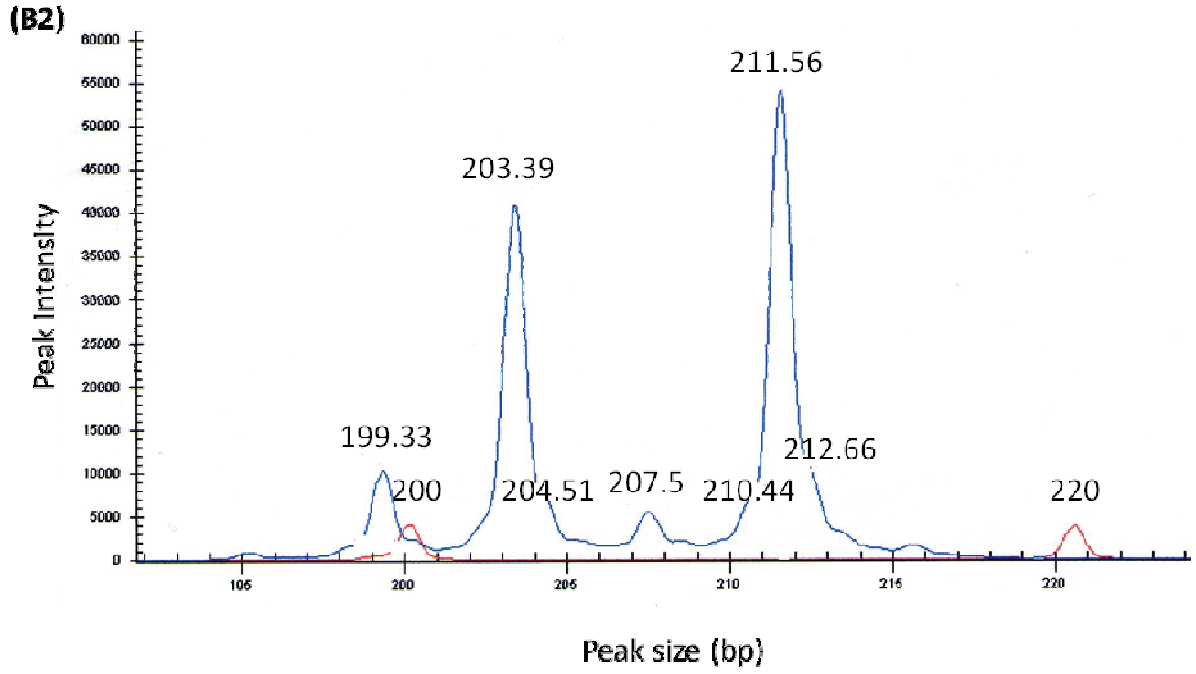

Figure 3.2. (continued)

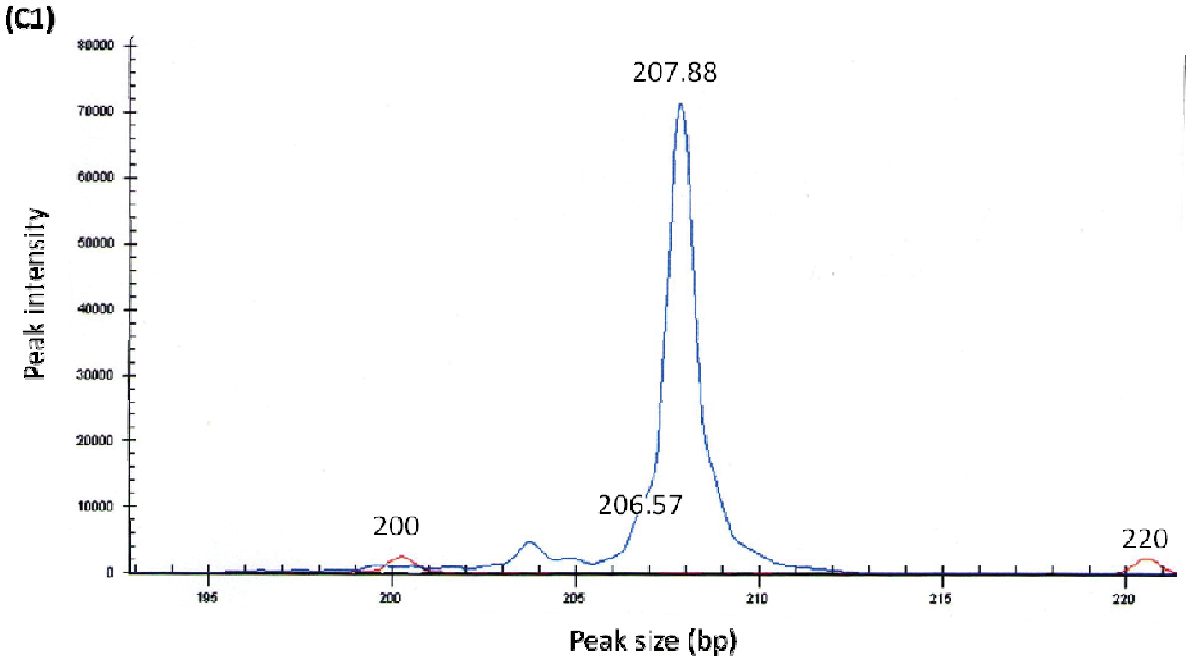

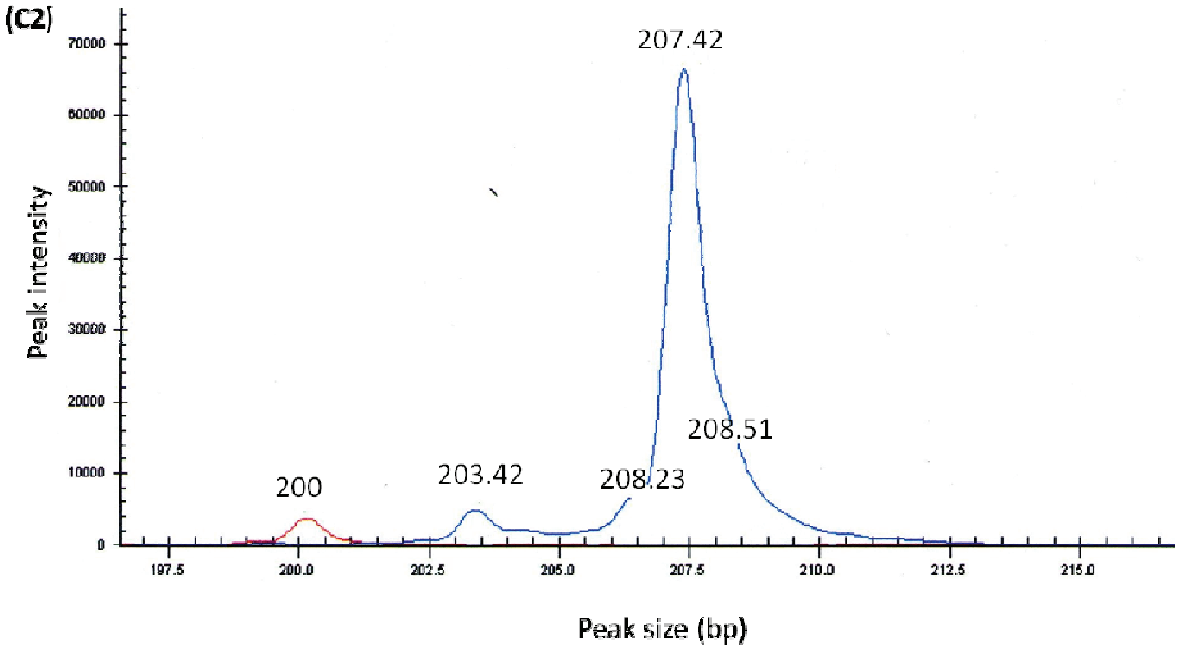

Figure 3.2. (continued)

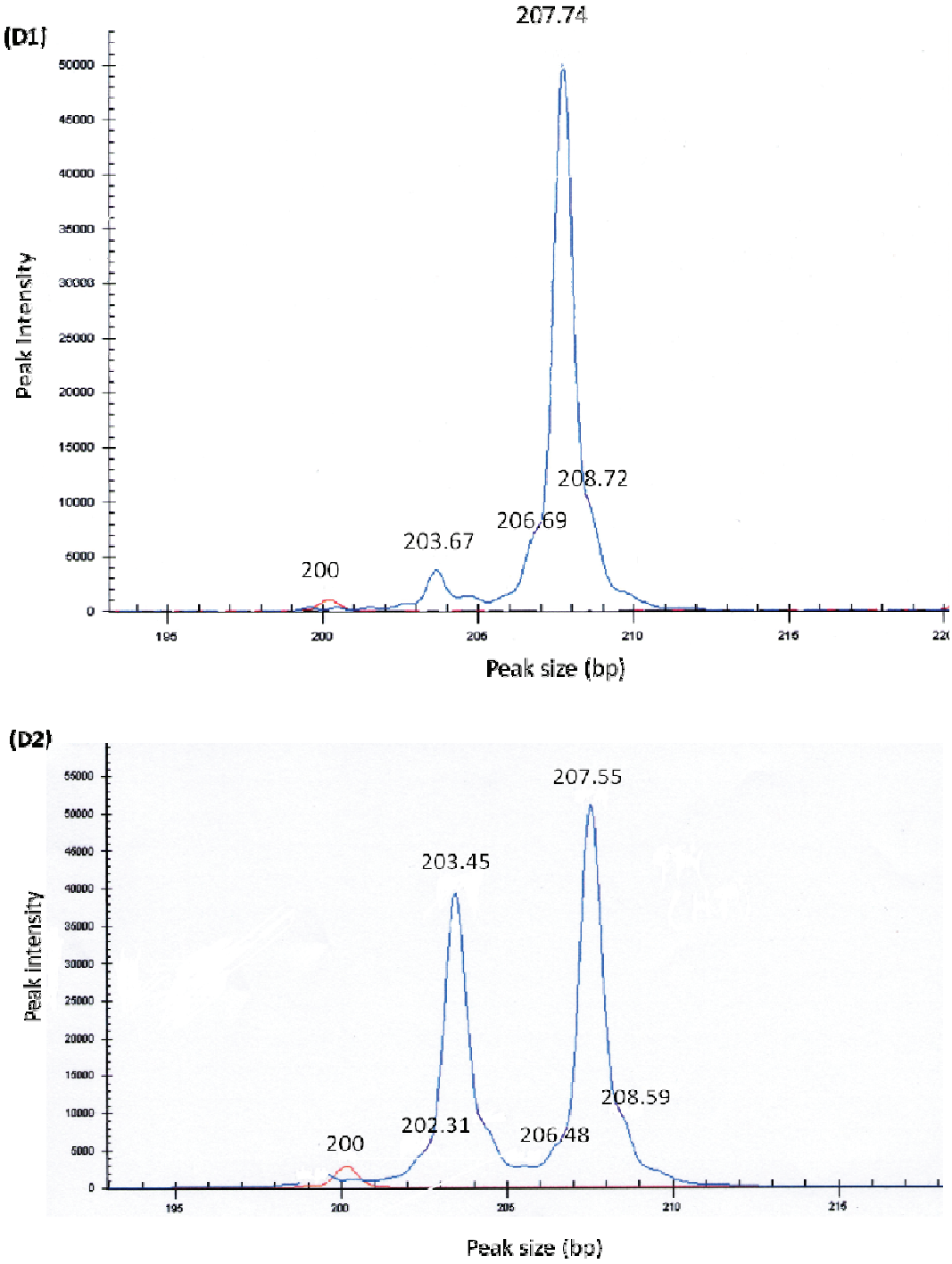

Figure 3.2. (A-D). Assessment of chromosome 17p LOH using PCR-based polymorphic microsatellite markers using cLOH.(A) Shows 17p LOH status, (A1) Blood sample showing heterozygosity = two peaks (A2) tumour sample showing homozygosity = one peak; (B) Shows 17p RET status, (B1) Blood sample showing heterozygosity = two peaks (B2) Tumour sample showing heterozygosity = two peaks; (C) Shows 17p (NI) non informative status, (C1).Blood sample showing homozygosity = one peak (C2) Tumour sample showing homozygosity = one peak; (D) Shows 17p (MSI) microsatellite instability status (D1) Blood sample showing homozygosity = one peak, (D2) Tumour sample showing MSI > one peak.

3.4.1.2. Validation of HOMOD by aCGH

The second method used to validate the HOMOD was aCGH (Figure 3.3). These data were available from a previous study (Langdon et al 2006). In total, 27 cases were assessed for chromosomal losses and gains using aCGH and 17p LOH status by HOMOD. Results showed that there was a very high consistency between the 2 methods. All cases which showed isolated loss of 17p or loss of 17p associated with gain of 17q (consistent with i(17q)) by aCGH were also identified as harbouring 17p LOH by HOMOD. Out of the 11 cases with 17p loss detected by aCGH, 10 cases showed 17p LOH detected by HOMOD. Additionally, 1 case was interpreted as 17p LOH by HOMOD, but did not show chromosome 17p aberrations by aCGH (case number 64). While 1 case (case number 76) showed isolated 17p loss by aCGH and RET by HOMOD (Table 3.4, Figure 3.3). The similar results produced by aCGH and HOMOD further support our confidence that HOMOD can be reliably used to identify regions of LOH in tumour samples without requiring matched blood, and we therefore proceeded to utilise this method to identify regions of genetic losses throughout this project.

NMB case no.	Chromosome 17 status		
	aCGH	HOMOD	
	17p loss / 17q gain {= i(17q)} Isolated 17p loss	17p LOH	17p RET
43	17p loss/ 17q gain	LOH	
45	17p loss/17q gain	LOH	
46	17q gain		RET
51	17q gain		RET
52	17p loss/ 17q gain	LOH	
61	Neutral		RET
63	Neutral		RET
64	Neutral	LOH	
65	17q gain		RET
66	Isolated 17p loss	LOH	
68	17p loss/ 17q gain	LOH	
69	17p loss/ 17q gain	LOH	
71	17p loss/ 17q gain	LOH	
76	Isolated 17p loss		RET
78	17q gain		RET
79	Neutral		RET
81	Neutral		RET
82	Isolated 17p loss	LOH	
83	Neutral		RET
88	17p loss/ 17q gain	LOH	
89	17p loss/ 17q gain	LOH	
90	Neutral		RET
93	Neutral		RET
94	Neutral		RET
112	Neutral		RET
133	Neutral		RET
142	Neutral		RET

Table 3.4. Comparison between the analysis of chromosome 17p LOH status using array CGH and HOMOD.

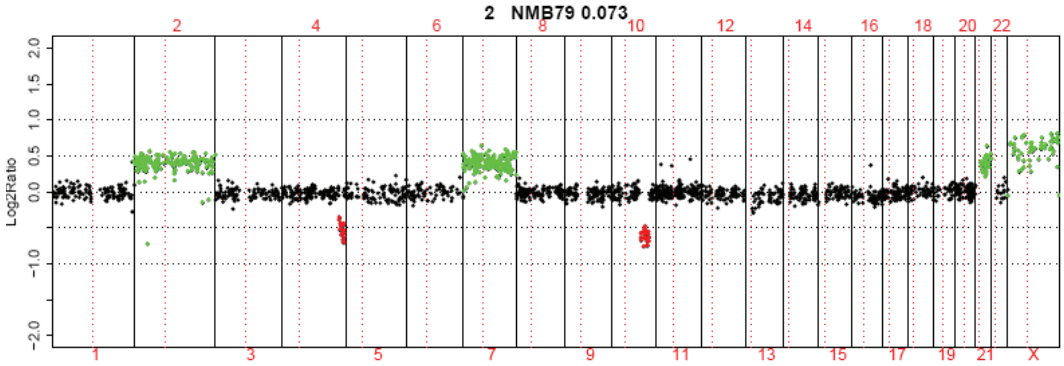

(A) chromosome 17 neutral

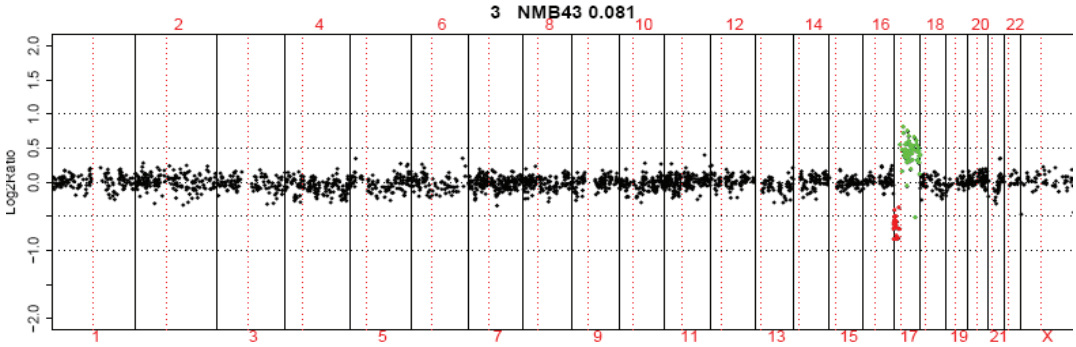

(B) Chromosome 17p loss; 17q gain (i(17q))

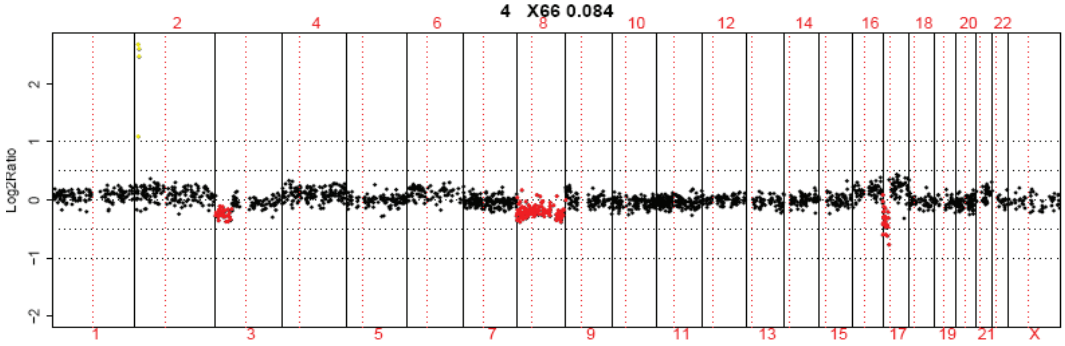

(C) chromosome 17p loss

Figure 3.3. Array CGH analysis of chromosome 17 status. Analysis was previously performed for 27 cases as previously described (Langdon et al 2006).Black dots = neutral; red dots = loss; green dots = gain. Examples of cases displaying, (A) Black dots showing 17p neutral and 17q neutral, (B) Red dots showing 17p loss and green dots showing 17q gain consistent with i(17q) and (C) Red dots showing isolated 17p loss.

3.4.2 Evidence of MSI in the NMB cohort

During the validation of the HOMOD method, we identified 5 cases showing potential evidence of MSI using cLOH analysis (Figure 3.4, Table 3.5). This represents a relatively large percentage of the samples 5/26 (19.2%). Therefore, we tested those 5 samples further for the presence of MSI using 5 additional specific polymorphic microsatellite markers, which were selected from a panel of markers routinely used for the assessment of MSI (Boland et al 1998, Umar et al 2004). Only one case (NMB 49) showed additional evidence of MSI in the di-nucleotide markers D5S346 and D17S250 (Table 3.5, Figure 3.4). Combining the 2 panels of markers, (those used for 17p LOH and the additional microsatellite markers tested), only 1 case (NMB 49) showed evidence of a high level of microsatellite instability (MSI-H ≥2 markers) involving 5 markers out of 11 in total (D17S974, D17S969, D17S936, D5S346 and D17S250). Thus, in summary, MSI affecting multiple markers in our medulloblastoma cohort was seen in one 1/26 (3.8%) case indicating an MSI phenotype may be a feature of a small proportion of medulloblastomas.

	Microsatellite marker status				
Samples	BAT-25	BAT-26	D2S123	D5S346	D17S250
NMB 49	MSS	MSS	MSS	MSI/LOH	MSI/LOH
NMB 51	MSS	MSS	MSS	NI	NI
NMB 81	MSS	NI	MSS	MSS	MSS
NMB 83	MSS	MSS	MSS	MSS	MSS
NMB 220	MSS	MSS	MSS	MSS	MSS

Table 3.5. Assessment of MSI in the 5 cases which showed evidence of MSI during validation of HOMOD, using additional microsatellite markers (MSS= Microsatellite stable; MSI=microsatellite instability; NI=non informative).

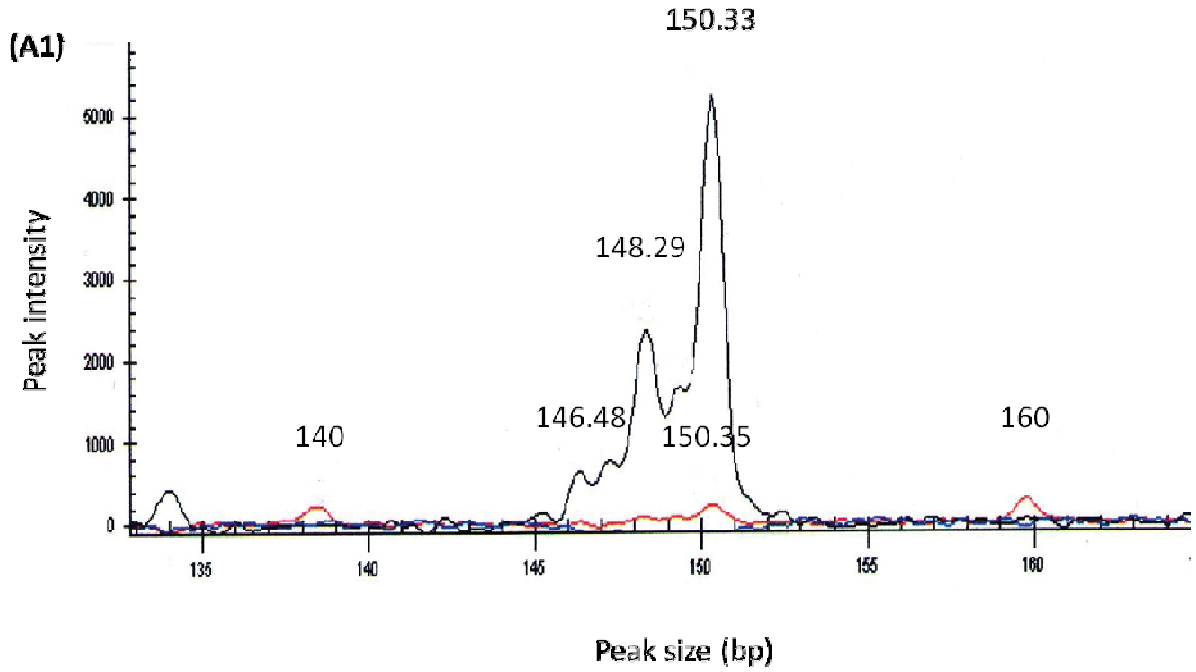
(A1)
150.33
148.29
146.48
150.35
140
160
Peak intensity
Peak size (bp)

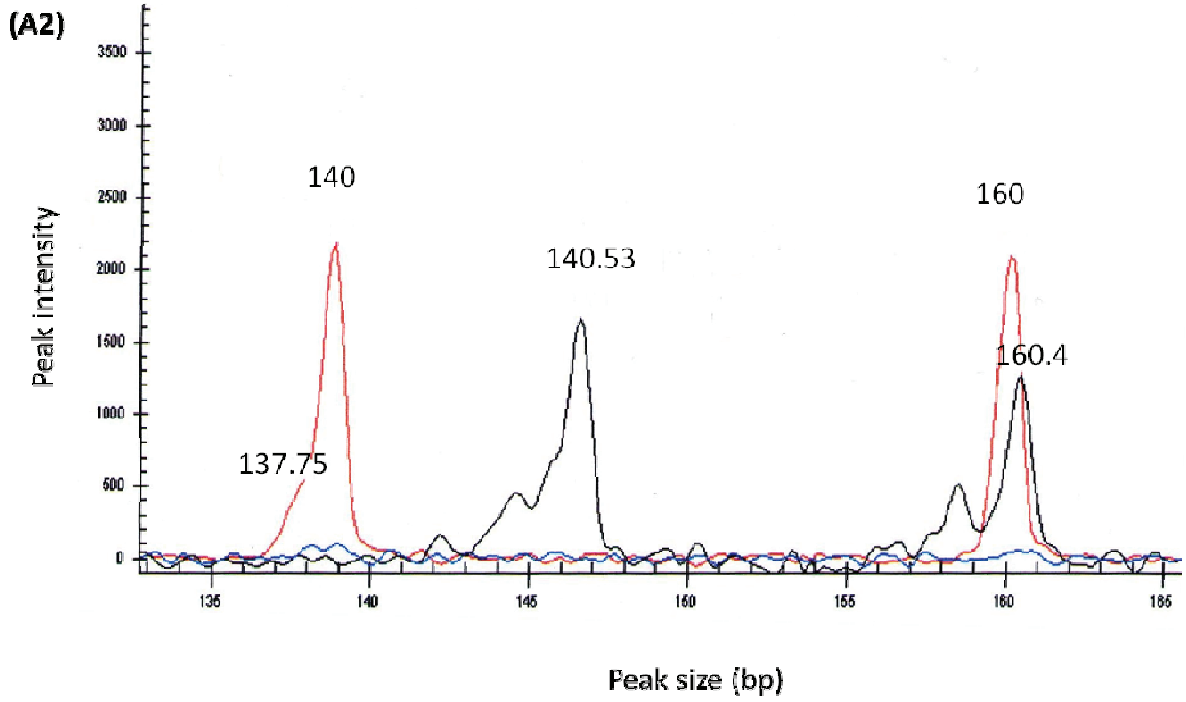
(A2)
140
140.53
160
160.4
137.75
Peak intensity
Peak size (bp)

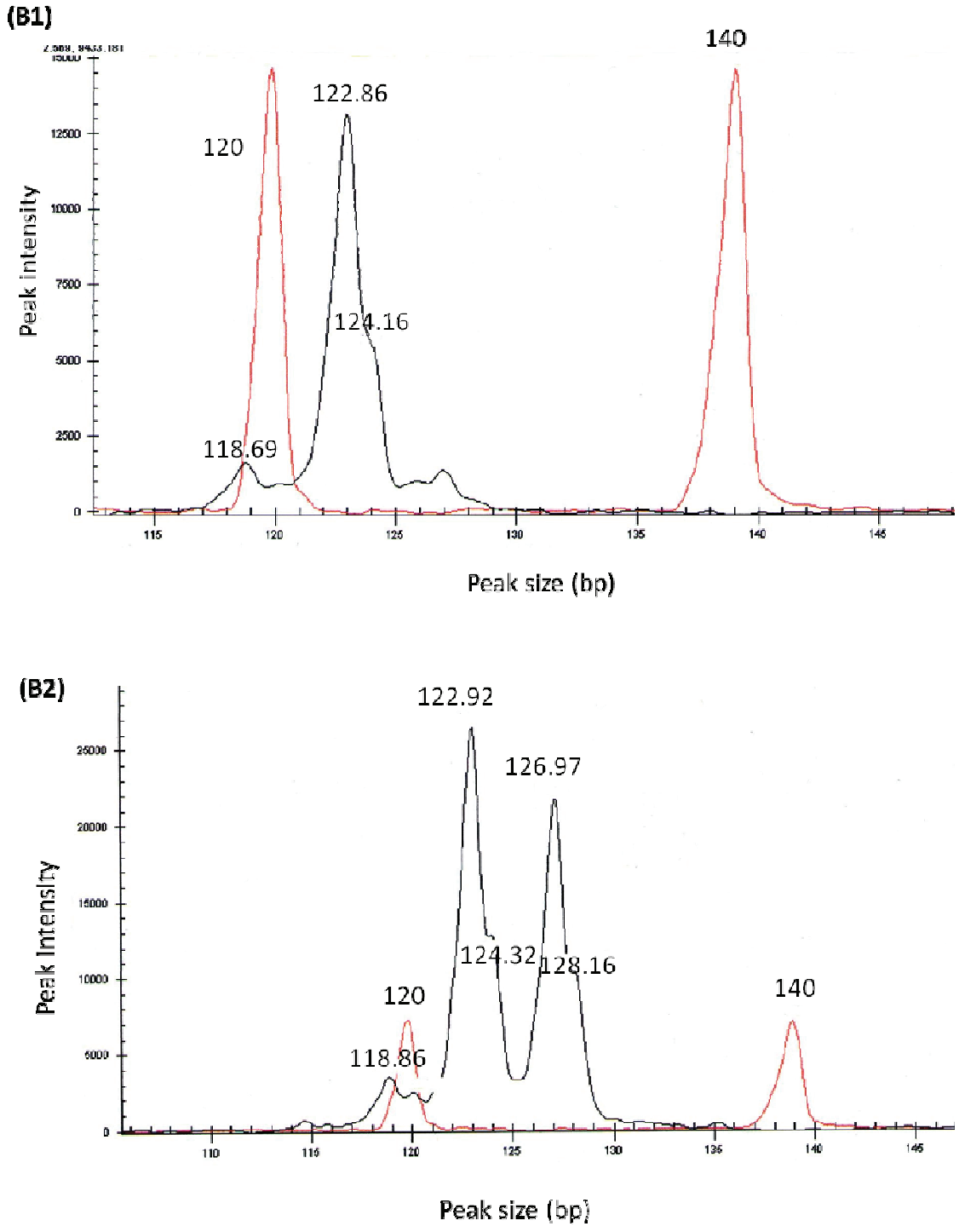

Figure 3.4. Shows 17p microsatellite instability status. (A) Chromosome 17p MSI analysis using the specific MSI marker D17S250 in case NMB49 showing (A1) blood sample showing homozygosity (1 peak), (A2) tumour sample showing heterozygosity (2 peaks); (B) Chromosome 17p LOH analysis using D17S969 marker in case NMB49, (B1) blood sample showing homozygosity (one peak), (B2) tumour sample showing heterozygosity (2 peaks), consistent with MSI.

3.4.3. Analysis of chromosome 17p LOH status in the NMB cohort

3.4.3.1. The incidence of chromosome 17p LOH status in the NMB cohort

Following validation of the HOMOD method, we next tested the 76 NMB samples for 17p LOH status. 23 (30.3%) of the cases showed LOH and 53 (69.7%) showed RET (Figure 3.5)

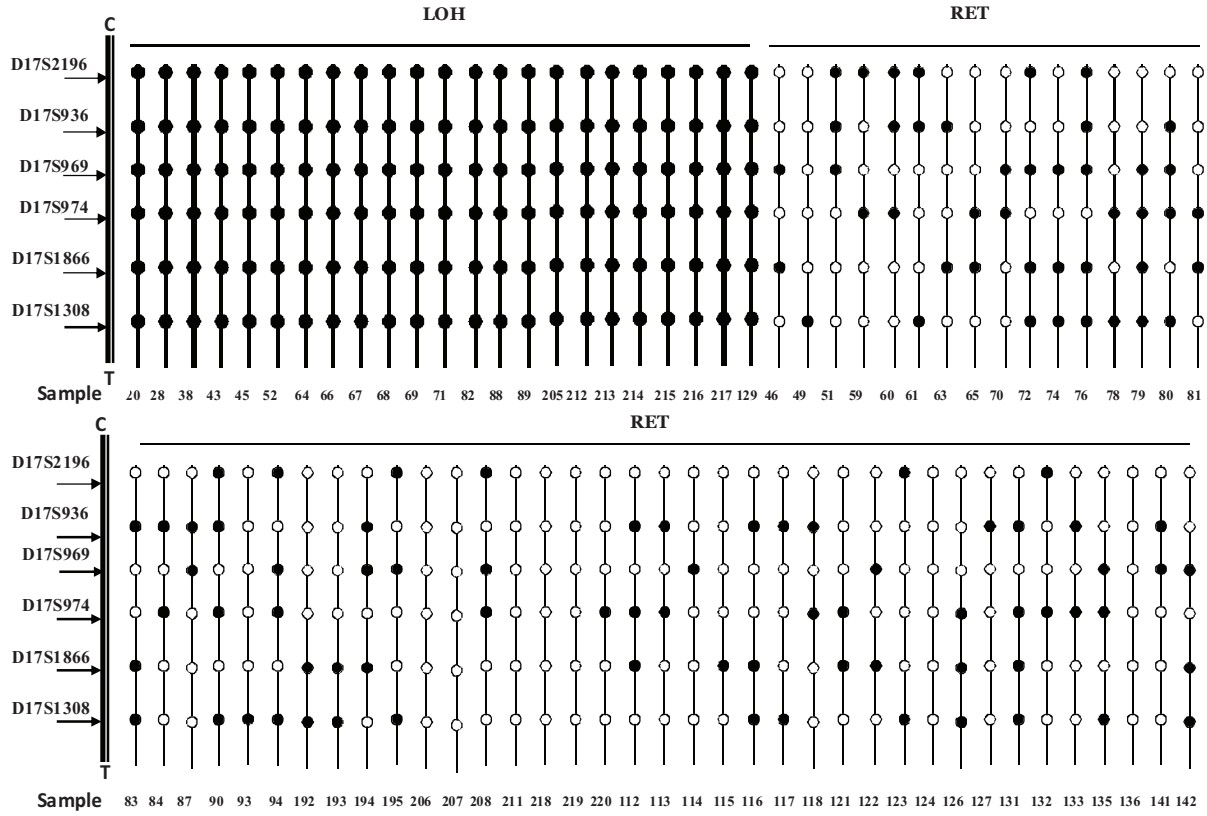

Figure 3.5. Analysis of 17p LOH status in 76 cases from the NMB cohort using HOMOD. C= Centromere, T= Telomere. 17p is represented by the (C-T) thick black line on the left side. The 76 cases analyzed using HOMOD are represented by vertical lines with their NMB number shown below. Results for the six microsatellite markers are plotted. Black dots represent homozygosity, white dots = heterozygosity. Samples with thick black lines are classified as 17p LOH (homozygosity at ≥ 5 continuous markers) or RET. Thick black lines = LOH regions i.e. ≥ 5 homozygous markers).

3.4.3.2. Assessment of relationship between chromosome 17p LOH status and clinicopathological variables in the NMB cohort

Relationship to age at diagnosis

In order to analyze if there is a correlation between 17p LOH and age at diagnosis, our cases were divided into infant cases (i.e. patients < 3 years of age at diagnosis) and non infant patients (i.e. ≥ 3 years of age at diagnosis). Within the 72 cases, 1/13 infants less than 3 years had 17p LOH, while 21/59 patients ≥ 3 years had 17p LOH (Fisher's exact test p= 0.05) (Figure 3.6). However, no significant correlation was found between 17p LOH and age as a continuous variable; mean ages of 8.1 and 6.8 years were observed for cases with 17p LOH versus cases with RET (t-test 0.24). The 17p LOH status distribution by age is shown in Figure 3.7.

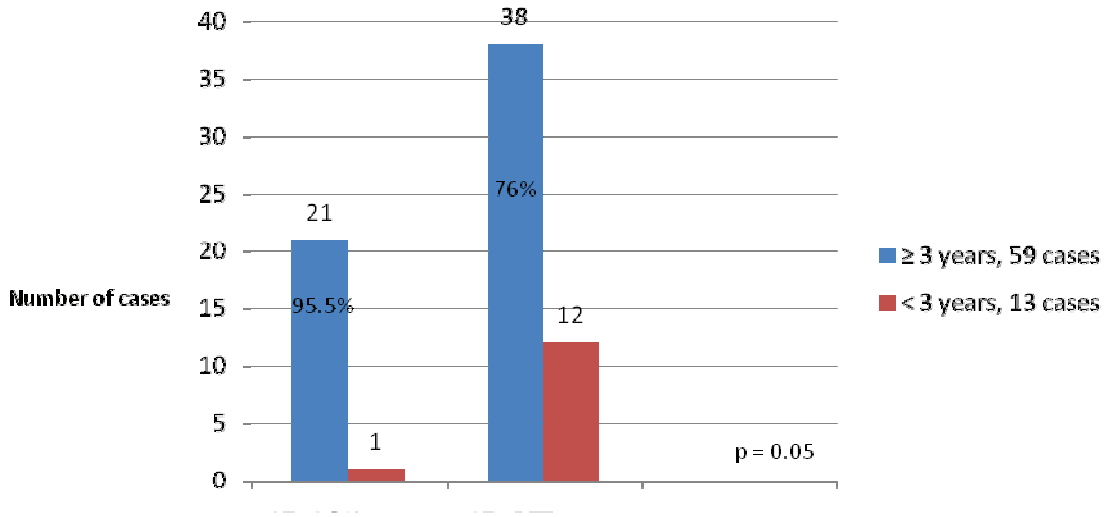

Figure 3.6. Chromosome 17p LOH status in age stratified risk groups (n=72).

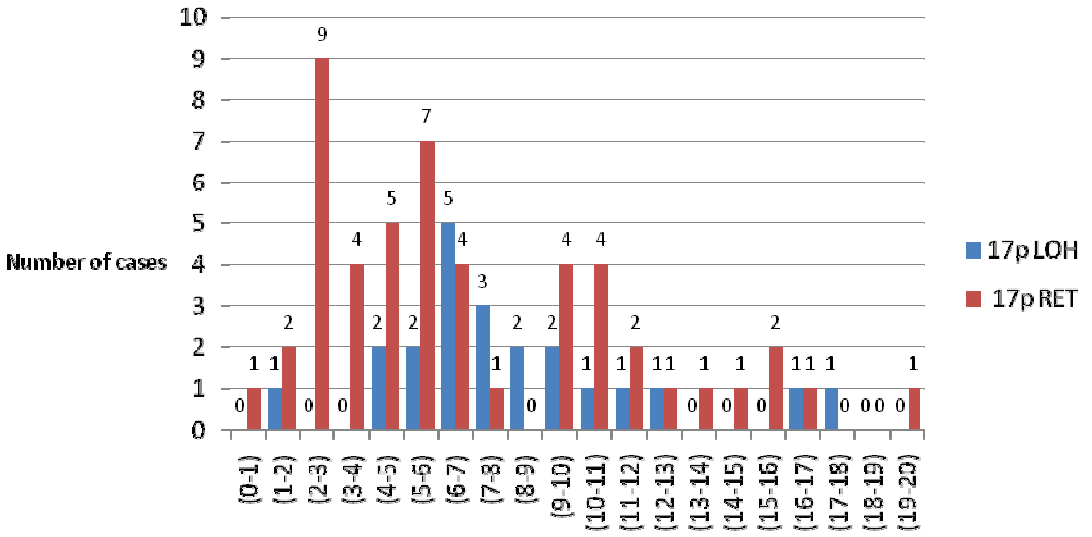

Figure 3.7. Analysis of the distribution of chromosome 17p LOH status with age. Cases are shown grouped in one year intervals**.**

Since age showed a significant correlation with chromosome 17p LOH status (p= 0.05), a wider cohort of medulloblastoma samples was collected from infants (<3 years old at diagnosis, 8 additional cases) to further test this finding. In total, 21 cases less than 3 years of age at diagnosis were tested for 17p LOH status using HOMOD. 20 of them showed 17p RET status and only one case showed LOH compared to the 21/59 of patients ≥ 3 years old which showed 17p LOH. This result was highly significant (p= 0.009, Fisher's exact test).

Relationship between 17p LOH and gender

There was no statistically significant correlation between gender and 17p LOH status (p= 0.79) (Figure 3.8).

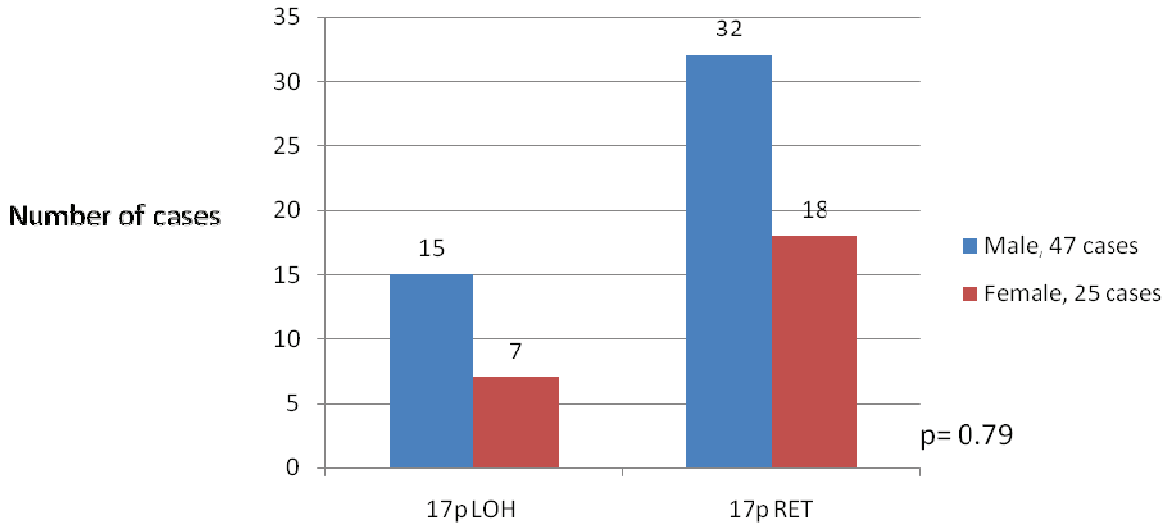

Figure 3.8. Assessment of the relationship between 17p LOH analysis and gender

Relationship to histopathological subtypes

16/22 cases (72.7%) with 17p LOH status were of classic histological subtype, 6 (27.3%) were nodular/desmoplastic and none were of large cell/anaplastic subtype. 28/52 cases (53.8%) with 17p RET were classic variant, 16 desmoplastic (30.7%) and 6 (11.5%) large cell/anaplastic variant. A marginally significant statistical correlation between 17p LOH status and pathological variants was found. All large cell/anaplastic cases displayed 17p RET (p= 0.075, Likelihood ratio test) (Figure 3.9).

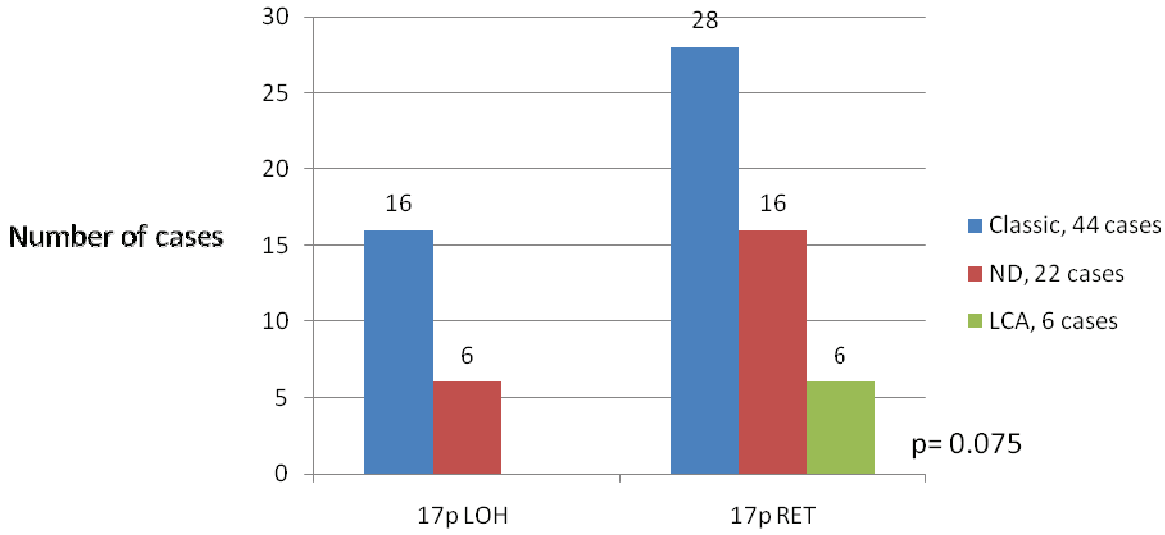

Figure 3.9. The correlation between 17p LOH and histopathological subtype in 72 medulloblastoma cases (Likelihood ratio test; ND = nodular/desmoplastic, LC/A = large cell anaplastic).

Relationship to metastatic stage at time of diagnosis

Data on metastatic stage at time of diagnosis was available for 67 cases only. 18/52 M0/1 cases (34.6%) showed 17p LOH, while 3/15 (20%) M2/3 showed 17p LOH. No statistically significant correlation between 17p LOH status and metastatic stage was found (p= 0.35, Fisher's exact test) (Figure 3.10).

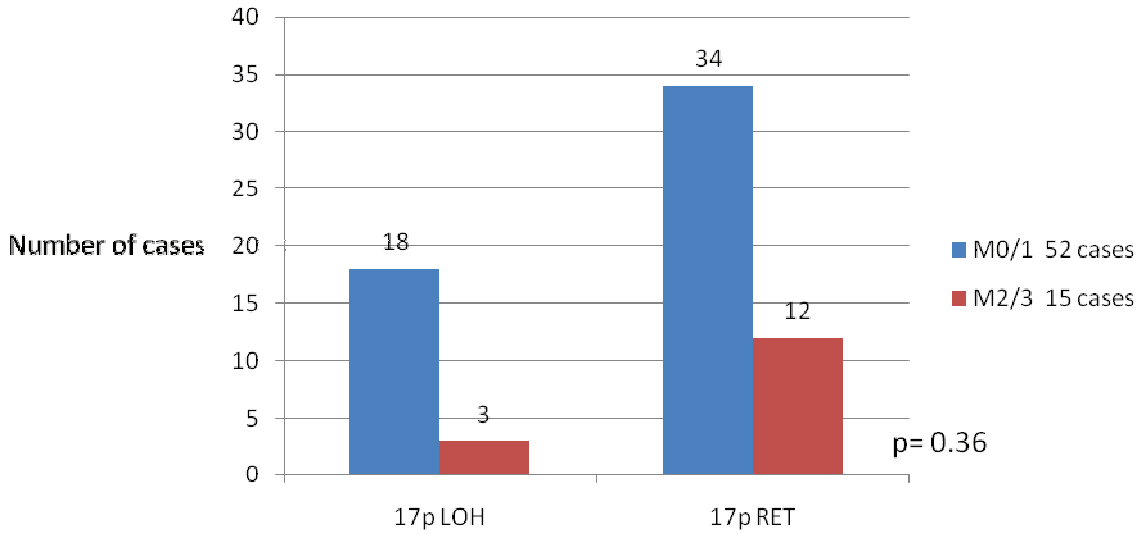

Figure 3.10. Assessment of correlation between 17p LOH and metastatic stage at time of diagnosis (67 cases)

In conclusion, 17p LOH is frequent in older children (>3 years) but is a rare event in infants (p= 0.009). Chromosome 17p LOH had no statistical correlation with any of the clinical variables tested. A marginally significant statistical correlation with pathology (p= 0.075) was observed for further investigation.

3.4.4. Analysis of chromosome 17p LOH status in the PNET3 cohort

The mixed, non-uniformly treated, retrospectively collected nature of the NMB cohort precluded the analysis of relationships to patient survival. We therefore next examined the relationship between 17p LOH status and patient outcome in cases derived from the recent PNET3 clinical trial (Taylor et al 2003).

3.4.4.1. The incidence of chromosome 17p LOH in the PNET3 cohort

The PNET3 cohort consisted of 208 medulloblastoma samples; all were tested for chromosome 17p LOH status using HOMOD. The cohort comprised children aged 3-16 years and its clinical characteristics are detailed in chapter 2, section (2.1.2).

Data reported in this chapter solely focus on the relationship between 17p LOH status and the clinical characteristics and behaviour of this cohort. 190 cases successfully yielded results for chromosome 17p LOH status, 143/190 (75.3%) showed 17p RET and 47 (24.7%) had 17p LOH. These data are shown in Table 3.6.

3.4.4.2. Correlations of chromosome 17p LOH with clinical and pathological variables

Examination of the nature of any relationship between 17p LOH status and clinico-pathological disease features in the PNET3 cohort was undertaken. No significant correlations were observed between chromosome 17p LOH and gender (p= 0.87), metastatic stage (p= 0.38), or the extent of tumour resection (p= 0.4) (Table 3.7), consistent with findings in the NMB cohort. The PNET3 cohort did not contain any infant cases aged < 3 years at diagnosis, and relationship between 17p LOH status and

age was therefore not assessed as a discontinuous variable. The mean age at diagnosis for 17p loss (mean 9.4, range 3-16 years) and 17p RET (mean 8.62, range 3-15.8 years) cases was not significantly different (p= 0.24, t-test). Most notably, a significant relationship between 17p LOH status and histopathological subtype was observed (Table 3.7). While 17p LOH was observed in both classic and large cell/anaplastic subtype tumours, 17p LOH was not a feature of nodular/desmoplastic tumours (p= 0.01).

Study no.	Trial no	Polymorphic microsatellite markers						17p LOH status
		D17S2196	D17S936	D17S969	D17S974	D17S1866	D17S1308	
1	2							
2	9							
3	12							
4	13							
5	15							
6	18							
7	19							
8	28							
9	30							
10	31							
11	32							
12	33							
13	35							
14	38							
15	39							
16	41							
17	43							
18	44							
19	47							
20	48							
21	51							
22	52							
23	54							
24	62							
25	65							
26	66							
27	69							
28	72							
29	75							
30	77							
31	78							
32	81							
33	82		NI					
34	83							
35	90							
36	101							
37	105							
38	106							
39	107							
40	112							
41	113							
42	116							
43	119							
44	120							
45	121							
46	124							
47	126							
48	129							
49	131							
50	132							
51	134							
52	137							
53	139							
54	141							
55	145							
56	146							
57	147							
58	148							
59	149							
60	150							
61	152							
62	157							
63	160							
64	161							
65	164							
66	165							
67	166							
68	169							
69	171							
70	172							
71	175							
72	178							
73	179							
74	180							
75	182							
76	185							
77	186							
78	191							

Table 3.6 (continued)

Study no.	Trial no	Polymorphic microsatellite markers						17p LOH status
		D17S2196	D17S936	D17S969	D17S974	D17S1866	D17S1308	
79	193							
80	195							
81	198							
82	199							
83	201							
84	202							
85	205							
86	207							
87	209							
88	210							
89	214							
90	216							
91	217							
92	50001							
93	50010							
94	50011							
95	50012							
96	50014							
97	50015							
98	50016							
99	50017							
100	50019							
101	50021							
102	50034							
103	50035							
104	50040							
105	5041							
106	50044							
107	50045							
108	50047							
109	50049							
110	50056							
111	50057							
112	50058							
113	50060							
114	50063							
115	50068							
116	50072							
117	50075							
118	50079							
119	50080							
120	50086							
121	50088							
122	50090							
123	50091							
124	50092							
125	50099							
126	50100							
127	50104							
128	50111							
129	50113							
130	50116							
131	50117							
132	50120							
133	50124							
134	50128							
135	50129							
136	50132							
137	50133							
138	50136							
139	50137							
140	50142							
141	50145							
142	50147							
143	50150							
144	50153							
145	50154							
146	50159							
147	50161							
148	50163							
149	50165							
150	50166							
151	50167							
152	50169							
153	50170							
154	50172							
155	50174							
156	50176							
157	50184							
158	50189							

Table 3.7 (continued)								
Study no.	Trial no	Polymorphic microsatellite markers						17p LOH status
		D17S2196	D17S936	D17S969	D17S974	D17S1866	D17S1308	
159	50193							
160	50197							
161	50198							
162	50204							
163	50206							
164	50208							
165	50209							
166	50212							
167	50217							
168	50218							
169	50224							
170	50233							
171	50236							
172	50241							
173	50244							
174	50245							
175	50248							
176	50249							
177	50250							
178	50251							
179	50253							
180	50254							
181	50256							
182	50259							
183	50263							
184	50268							
185	50274							
186	50276							
187	50284							
188	50290							
189	50291							
190	50292							

Table 3.6. Chromosome 17p LOH analysis in the PNET3 cohort using HOMOD. Light blue cell = homozygous; yellow cell = heterozygous; grey cell = retention of heterozygosity ; Red cell = loss of heterozygosity (i.e. homozygous in ≥ 5 contiguous markers); dark blue cells= microsatellite instability; white cell = not done or analysis was unsuccessful.

		Chromosome 17p status		Total	`p` value
		RET	LOH		
Gender	Male	91	29	120	0.87
	Female	52	18	70	
	Total	143	47	190	
Pathology	Classic	121	40	161	0.011
	Nodular /desmoplastic	12	0	12	
	Large cell / Anaplastic	10	7	17	
	Total	143	47	190	
Metastatic stage	Metastatic stage 0/1	115	41	156	0.38
	Metastatic stage 2/3	28	6	34	
	Total	143	47	190	

Table 3.7. Correlation between chromosome 17p LOH and clinicopathological variables in the PNET3 cohort (n=190). Fisher's exact test was used. RET = retention of heterozygosity, LOH = loss of heterozygosity.

3.4.4.3. Analysis of chromosome 17p LOH in the PNET3 cohort; survival analysis

Although cases with chromosome 17p LOH showed a trend towards a worse survival in both analyses, univariate overall (OS) and event free survival (EFS) for chromosome 17p LOH status showed insignificant ‘p` values of 0.31 and 0.21, respectively (log-rank test) demonstrating that 17p LOH status was not associated with a worse prognosis in the PNET3 cohort (Figures 3.11).

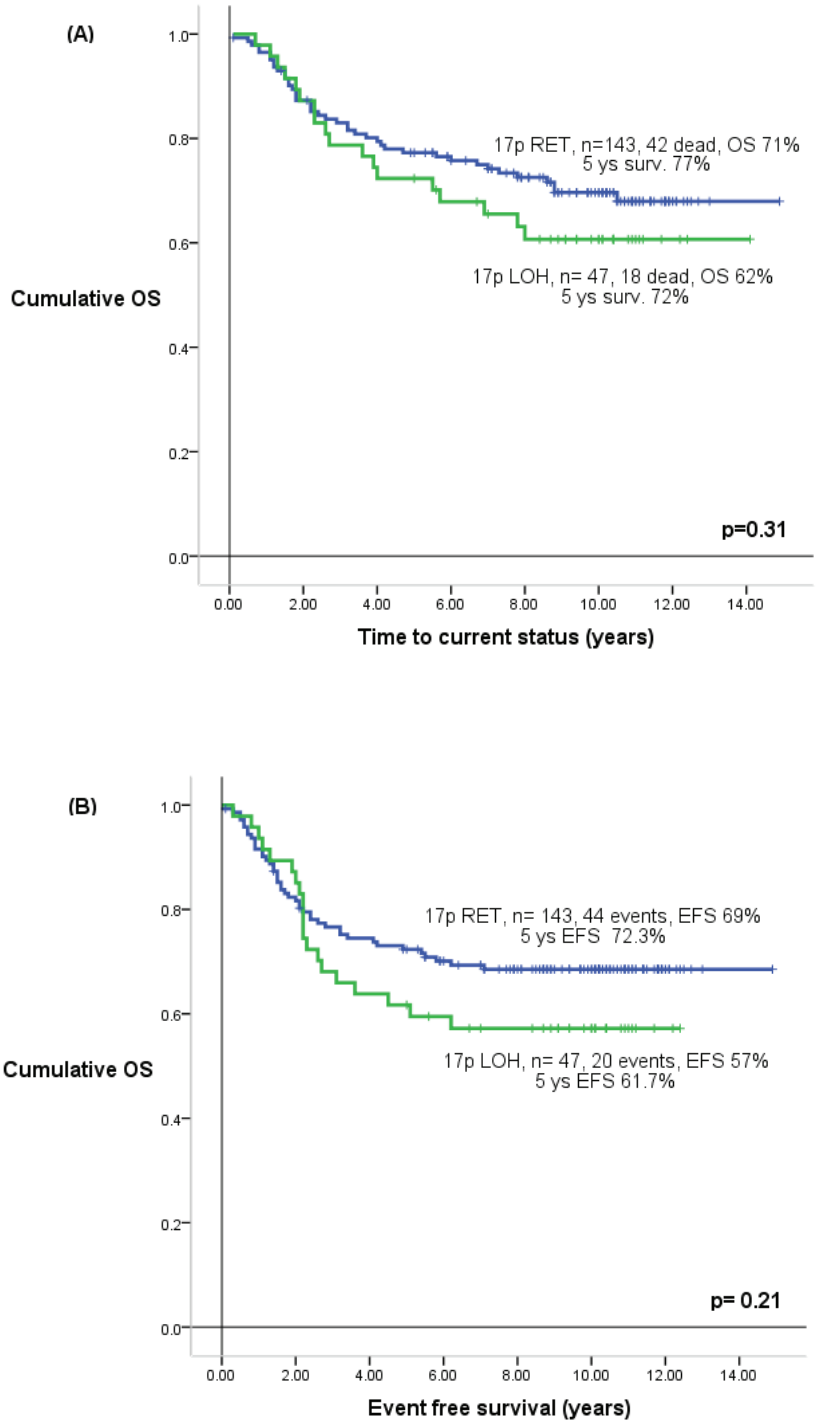

Figure 3.11. Survival analysis for chromosome 17p LOH status in the PNET3 cohort. (A) Overall survival (OS), (B) Event free survival (EFS); LOH= loss of heterozygosity, RET= retention of heterozygosity.

3.5. Discussion

Over the past few years, strategies aiming to improve patients' survival in medulloblastoma started to follow new concepts. Rather than just accentuating therapy, the focus has been on minimizing late side-effects of treatments, by pursuing the optimal balance between the stringency of therapy, side effects, remissions and recurrences. Such balance would benefit hugely from improving the current disease classification, which could more accurately identify favourable and standard-risk patients, as well as high-risk patients, according to a combination of molecular and biological variables. This would allow de-escalating the therapeutic protocols of the former group of patients, while monitoring them closely. On the other hand, 110 the latter group could benefit from novel clinical trials involving more intensified therapies and/or potent drugs.

Since chromosome 17p deletions, whether isolated or as part of i(17q), are the most common chromosomal abnormalities associated with medulloblastoma, we decided to test their incidence and correlations in a pilot study composed of 76 medulloblastoma samples, and assess its potential as a prognostic molecular marker for medulloblastoma in a wider trials-based cohort.

3.5.1. Validation of HOMOD as a method for the detection of genetic losses in FFPE tumour material.

A major limitation in the analysis of DNA-based markers in retrospectively collected and stored tumour samples, in particular cohorts from completed trials, is

that they are often derived from FFPE tumour material, and samples usually lack matched control DNA. We therefore initially developed and validated a method which allows testing for genetic losses in FFPE tumour samples lacking matched DNA. Homozygous Mapping Of Deletion (HOMOD) (Goldberg et al 2000) proved to be a reliable, straight forward method to fulfil this purpose. It depends on identifying ≥ 5 consecutive homozygous polymorphic microsatellite markers, which represent an extended region of homozygosity (ERH), consistent with genetic loss. Another advantage for HOMOD is its utility for the assessment of DNA derived from FFPE samples, giving access to archival, retrospectively collected and stored tissue samples.

We validated the HOMOD method by comparing the results of 17p LOH status generated by HOMOD with those produced using cLOH in 26 medulloblastoma cases, and by aCGH in 27 medulloblastoma cases. Equivalent results were achieved in 85% and 96.2% of cases by both methods, respectively. Of the 4 cases that showed discrepancy in the 17p LOH results produced by HOMOD and cLOH, each had loss affecting only one marker by cLOH analysis. This represented a small deleted region on chromosome 17p, which cannot be picked by HOMOD, since HOMOD depends on detecting extended regions of homozygosity (ERH) covering 5 or more consecutive homozygous markers, in order to be interpreted as LOH. Despite this limitation in the HOMOD method, it was able to detect 85% of cases with 17p LOH, identifying all cases with evidence of genetic loss of the entire p-arm of chromosome 17, missing only cases with very small deletions. Thus it is considered to be a useful and sensitive method for the detection of LOH affecting chromosomal regions in cohorts lacking control constitutional DNA, available in the form of FFPE material. The sensitivity of the

method is dependent on the density of markers used, and higher density of markers could be employed to allow the assessment of smaller chromosomal regions and for specific loci.

3.5.2. MSI in medulloblastoma

MSI is a phenomenon that is most straight forwardly identified by comparing tumour DNA with constitutional DNA. Evidence of MSI was found in 5 cases in a subset of 26 cases assessed for 17p LOH using cLOH. Therefore analysis of these cases was undertaken using a wider panel of markers used for the detection of MSI (Umar et al 2004). We found evidence of MSI in 1/26 cases (3.8%). This low frequency is in agreement with most research investigating defects in mismatch repair genes involved in the pathogenesis of medulloblastoma (Lee et al 1998), suggesting that MSI is not a major feature of this disease.

In a recent study by Viana-Pererira et al (2009), microsatellite instability status was assessed in 36 medulloblastoma samples (21 paediatric samples and 15 adults) using a pentaplex PCR of quasimonomorphic markers (NR 21, NR 24, NR 27, BAT 25 and BAT 26) which allow analysis of MSI status without evaluation of constitutional DNA. The group also assessed the methylation status of MMR genes by MLPA (methylation specific multiplex ligation-dependent probe amplification), as well as determining the expression of *MSH6* (*mutS homolog 6*) using IHC. Pentaplex PCR was then used to determine the mutation status of 10 MSI target genes (*MSH3, TCFBR2, RAD 50, MSH6, BAX, TCF4, XRCC2, MBD4, MREII* and *ATR*). Finally, they assessed the mutation analysis of the hot-spots of 2 oncogenes; exon 3 of *CTNNB1* and *BRAF* (*v-raf*

murine sarcoma viral oncogenes homolog B1) using PCR single-strand conformation polymorphic analysis followed by direct sequencing. They reported that previous studies failed to identify genetic instability in medulloblastoma, however these studies only assessed small number of cases, including non medulloblastoma PNETs using panels of MSI markers with limited capabilities to assess MSI status, while they used a panel of MSI markers which was recommended by the revised Bethesda guidelines for CRC (Umar et al 2004). The study identified 4/36 (11%) of the tumours containing MSI, 1/4 showed MSI-H (≥ 2 markers with instability) and 3/4 MSI-L (one marker with instability) (2 were from adult samples and 2 from paediatric samples) indicating that MSI is not age related in medulloblastoma. A case with evidence of MSI showed hypermethylation in the *MSH6* gene in 75% of cases but was not associated with a lack in protein expression, indicating that this epigenetic mechanism may not be the cause of MSI phenotype. Mutations of MSI target genes was identified in *MBD4* (*methyl CpG binding domain protein 4*) in 2 samples, while both *BRAF* and *CTNNB1* oncogenes did not show mutations in cases with evidence of MSI. The group concluded that MSI and mutations in target genes are involved in the pathogenesis of a small subgroup of medulloblastoma.

In the NMB cohort further assessment of the microsatellite was undertaken in the 26 cases that showed evidence of MSI during the analyses for chromosome 17p LOH using cLOH. We tested cases with evidence of MSI using the reference panel of 5 microsatellite markers standardized by the National Cancer Institute (NCI) for the screening of HNPCC (Umar et al 2004), (namely, the mononucleotide markers BAT 25, BAT 26, and the di-nucleotide markers D2S123, D5S346 and D17S250). DNA amplified

using these markers, in tumours and constitutional blood, was compared and the difference between them was scored. We identified one case only (3.8%) (NMB 49) with MSI-H (MSI-H= ≥ 2 markers with instability, MSI-L= one marker with instability).

Our results were consistent in frequency with those reported by Viana-Pereira et al (2009). Any differences may be due to differences in methods or markers selected for analysis. For instance MMR deficiencies due to mutations in *hMSH* 6 gene cannot be identified by di-nucleotide repeat markers, and could be missed if there is no effect on BAT 25 or BAT 26. Such limitations associated with the reference panel of recommended MSI markers chosen in the Bethesda consensus held in 1997 led to a second Bethesda meeting in 2002, which agreed on using 5 quasimonomorphic mononucleotide MSI markers which provide more accurate and standardized determination of MSI status (Umar et al 2004).

It can be concluded form our study, as well as that by the Portuguese group, that MSI instability may characterize a small subset of medulloblastoma and may play a role in its tumourigenesis. Assessment of the clinicopathological significance of MSI in medulloblastoma will now be of interest, but are likely to be hampered by its low incidence.

3.5.3. Chromosome 17p LOH in medulloblastoma and its clinico-pathological significance

The overall rate of 17p LOH in NMB cohort was 23/76 cases (30.3%). In the NMB cohort, a highly statistically significant association between medulloblastoma

arising in patients less than 3 years old and 17p LOH, where only 1/21 case (5%) had 17p LOH (p= 0.009) compared to 21/59 cases (35.6%) over the age of 3 years. This supports the theory that infantile medulloblastoma patients may represent tumour subgroup with different biological background from non-infantile medulloblastoma (Thompson et al 2006).

There are several indications that medulloblastoma arising in infant patients <3-6 years of age at diagnosis forms a distinct subgroup with different biological back ground and prognosis compared to medulloblastoma arising in patients ≥3 years old. Gilbertson and Ellison (2008) studied the potential cells of origin of medulloblastoma and proposed that tumours in young patients (infants) occur as a result of mutations in the Granule Neuron Precursors (GNP) during late gestation and/or early childhood, which lead to SHH signal activation and consequently the formation of medulloblastoma of the desmoplastic subtype. Also MBEN, a subtype of the desmoplastic variant with an excellent prognosis, predominantly occurs in infants (McManamy et al 2007; Ellison et al 2003).

Methylation mediated gene silencing occurs in *COL1A2* in medulloblastoma and is a frequent process in non-desmoplastic medulloblastomas in patients above and below 3 years at diagnosis, (86% and 83% respectively). However, within the desmoplastic variant, *COL1A2* methylation occurs in 13% of patients <3 years and 90% of patients ≥3 years at diagnosis. Consequently, *COL1A2* expression is significantly higher in infant desmoplastic medulloblastoma compared to desmoplastic medulloblastoma in older children (Anderton et al 2008). This suggests that *COL1A2*

methylation, a gene strongly associated with medulloblastoma development, is not a feature of desmoplastic medulloblastoma arising in infants, and suggest the notion that this tumour group may have a distinct pathology.

Most gene expression studies have associated the Wnt/Wg pathway activation with medulloblastoma in patients ≥3 years at diagnosis (Clifford et al 2006, Thompson et al 2006, Kool et al 2008, Fattet et al 2009). This relationship was not investigated directly in the NMB cohort but suggest a distinct biology for cases arising in infancy.

The large cell/ anaplastic medulloblastoma histological subtype has been associated with a more aggressive disease and a poor clinical outcome in several studies (reviewed by Pizer and Clifford, 2009). Our analysis revealed a marginally significant association between tumour pathological subtype and 17p LOH status (p= 0.075), where all cases with large cell/ anaplastic pathology subtype showed 17p RET. However, these data could not be validated in the larger PNET3 cohort, and was therefore not considered significant. In the PNET3 cohort, all 12 cases with the nodular/desmoplastic pathology subtype were 17p RET status (p= 0.011). This result is in concordance with the results of Scheurlen et al (1998), Lamont et al (2004) and MacManamy et al (2007). In a study by Scheurlen et al (1998) of 30 primary medulloblastoma cases reported that 17p loss was only detected in cases with non-nodular desmoplastic pathology. Lamont et al (2004), in a study of a cohort of 87 primary medulloblastoma samples described 13/87 cases (15%) with nodular/desmoplastic pathology, none had chromosome 17p loss, while it occurred at a higher frequency in tumours presenting with classic or large cell/ anaplastic

pathology. MacManamy et al (2007), in another study of 2 SIOP/UKCCSG trials (CNS 9102, patients aged 3-16 years and CNS 9204, patients aged < 3 years old at time of diagnosis), found that abnormalities of chromosome 17, including i(17q), were found exclusively in the non-desmoplastic nodular tumours. However, in the present study an equivalent relationship was not seen in the NMB cohort, where 6 cases with nodular/desmoplastic pathology subtype had 17p loss. These combined data strongly suggest that 17p LOH does not show a consistent association with any pathological tumour subtype. No significant association was observed between 17p LOH status and gender, metastatic stage, or extent of tumour resection in either cohort when tested.

3.5.4. Relationship between chromosome 17p LOH status and patients' outcome

Previous studies have shown conflicting relationships between chromosome 17p LOH status and patients' outcome in medulloblastoma (reviewed by Pizer and Clifford 2009). The power of the NMB cohort for the assessment of such relationship was limited by the small number of cases examined, the effect of age (cases above and below 3 years at diagnosis), the lack of uniform treatment protocol for all the patients, and the collection of material from different centres over a long period of time. Assessment of prognostic relationships using this cohort is therefore not appropriate. The analysis of wider, more extensive, and uniformly treated cohort is therefore required. Therefore, we used the PNET3 cohort, which is composed of more than 200 retrospectively collected medulloblastoma samples from a clinical trial, for whom full clinico-pathological data was available, to re-assess the relationship of chromosome

17p LOH and prognosis of medulloblastoma. 17p LOH showed no relationship to overall or event free survival (p= 0.31 and p= 0.21, respectively), suggesting that 17p status does not have prognostic utility in this disease. This is in accordance with the results of Emadian et al (1996), Biegel et al (1997) and Pan et al (2005), but contradicts the results of Batra et al (1995), Scheurlen et al (1998), Gilbertson et al (2001) and Lamont et al (2004). Pfister et al (2009) in a study of chromosome 17p aberrations in 2 independent primary medulloblastoma cohorts (n=340 collectively) found that 17q gain is overall more frequent than 17p deletion, and 17q gain and i(17q) arer better predictors for unfavourable survival than isolated 17p deletion. This supports the notion that the presence of oncogenes on 17q rather than TSGs genes on 17p may be the cause for unfavourable outcome.

A full investigation of the PNET3 cohort, including the analysis of other molecular markers, and assessment of the relationship between 17p LOH status and other molecular markers is reported in chapter 7.

3.6. Summary and conclusions

The major conclusions that can be drawn from the data reported in this chapter are:

1. HOMOD is a reliable method to test for genetic loss in FFPE samples lacking matched constitutional control DNA.

2. The overall incidence of chromosome 17p LOH in medulloblastoma is 26.3 % (70/266), based on our combined cohorts.

3. Chromosome 17p LOH is rare in infants, suggesting that these cases may be biologically distinct from medulloblastoma arising in older children.

4. Chromosome 17p LOH does not demonstrate any consistent relationship to patients' gender, metastatic stage, extent of tumour resection or histopathological subtype.

5. Chromosome 17p LOH was not associated with a poor clinical outcome, in a large cohort of medulloblastoma derived from the recent PNET3 clinical trial.

6. Microsatellite instability plays a minor role in the pathogenesis of medulloblastoma.

Chapter 4

Wnt/Wg pathway activation in medulloblastoma: detection of β-catenin nuclear localization by Immunohistochemistry

4.1. Introduction

The major aim of this thesis is to investigate the clinical significance of the different molecular correlates of Wnt/Wg pathway activation (i.e. β-catenin nuclear localization, *CTNNB1* mutation*s* and chromosome 6 loss) which have been identified in medulloblastoma. Previous research has demonstrated that Wnt/Wg pathway activation, determined by nuclear localization of β-catenin in medulloblastoma is associated with a favourable outcome (Ellison et al 2005, Gajjar et al 2006). Wnt/Wg pathway activation can not be distinguished on the basis of clinical or histopathological criteria and pathway activation is confirmed by molecular investigations, where nuclear expression of β-catenin, *CTNNB1* mutation or loss of heterozygosity (LOH) of chromosome 6 are present (Eberhart et al 2000, Dahmen et al 2001, Baeza et al 2003, Clifford et al 2006, Thompson et al 2006, Kool et al 2008, Fattet et al 2009). However, the prognostic significance of *CTNNB1* mutations and chromosome 6 loss have not been assessed to date. A goal of this study is therefore to assess whether the three alternative methods mentioned above identify Wnt/Wg activation, favourable risk disease, and their relative utilities for this.

This chapter focuses on the development of immuno-histochemical (IHC) methods for the detection of Wnt/Wg pathway activation, by assessment of the degree of β-catenin nuclear localization in individual cases, followed by its assessment in our large cohort of medulloblastomas derived from the PNET3 trial. The potential value of this molecular marker lies in the fact that it can be assessed alongside histological evaluation in large numbers of cases where FFPE material is available.

However, the interpretation of IHC staining results may well be subjective, and cut off criteria for the definition of positive cases can vary. Several studies have investigated β-catenin immuno-reactivity as a marker in medulloblastoma (Eberhart et al 2000, Ellison et al 2005, Clifford et al 2006, Thompson et al 2006, Fattet et al 2009).

Eberhart et al (2000) analysed 51 sporadic medulloblastomas including 1 medulloblastoma case from a patient with Turcot's syndrome. Positive cytoplasmic β-catenin staining was observed in all 51 sporadic medulloblastoma cases, with variation in their intensities, while positive nuclear localization was present in 9 cases (18%) and the staining was either equal or more intense than the surrounding cytoplasm. The percentage of positive nuclei in each case varied from 5-70% (Table 4.1). Positive cases showed broadly distributed nuclei throughout the tumour lesions. The rest of the non medulloblastoma tumours (n=48) were all negative for nuclear β-catenin staining while their cytoplasm were positive, serving as an internal control. Of interest, is that non-neoplastic cells also showed nuclear β-catenin staining.

Another study looked at 109 medulloblastoma samples from patients, which were entered in the SIOP/UKCCSG PNET3 trial (Ellison et al 2005). All cases were of the non-desmoplastic histopathological subtype. β-catenin nuclear localization was tested by immuno-histochemistery (IHC). Staining patterns were classified into 2 main groups, namely cytoplasmic and combined cytoplasmic and nuclear staining. The latter was characterized by sheets or groups of cells rather than scattered single cells and was divided into widespread /strong or moderate /patchy. 27/109 cases (25%) showed

nuclear β-catenin localization with 11/27 being widespread/strong (40.7%) and 16/27 (59.3%) being moderate/patchy.

In another study (Clifford et al 2006) of 19 cases of sporadic medulloblastoma analysed for β-catenin nuclear localization by IHC, 2/19 (10.5%) showed strong combined nuclear/cytoplasmic immuno-reactivity, using the same methods and criteria for categorizing β-catenin nuclear immuno-reactivity as Ellison (Ellison et al 2005). Gajjar et al (2006) studied 134 cases of sporadic medulloblastoma and analysed 69 cases (51%) using β-catenin IHC; 10 cases (14.5%) were reported as nucleopositive.

Finally, Fattet et al (2009) analysed 72 FFPE medulloblastoma samples and reported that 6 cases (8.2%) showed β-catenin nuclear staining in > 50% of cells, 3 cases (4%) had nuclear staining in <10% of cells and 63 (87.5%) with either cytoplasmic or negative staining.

The details of the methodologies used in these different studies and in the current study assessing β-catenin nuclear localization in medulloblastoma are summarised in Table 4.1.

Study	Sample no./ thickness of sections	Antibody to β-catenin dilution/ used	% of nuclear positivity	Patterns and criteria for assessing the results
Eberhart et al (2000)	n=51 /FFPE 5µm sections	Transduction laboratories (Lexington,KY) 1:500	Positive nuclear staining 9/51 +ve(18%) 1 case 5-10% of cases 3 cases 20-30% 2 cases 40-50% 1 cases 50-60% 2 cases 60-70% Cytoplasmic +ve 51 cases (100%)	Cases with positive nuclear staining were broadly distributed, limited regions only were lacking nuclear β-catenin staining
Ellison et al (2005)	n=109/ FFPE 5 µm sections	BD/ Transduction laboratories (San Jose, CA) 1:100	27/109 +ve (25%) Wide spread Strong 11/ 109(10%) Moderate 16/ 109 (14.7%) Negative nuclear staining 82/109 (75%)	Cytoplasmic and nuclear +ve staining presents as sheets or group of cells. Categorized as wide spread strong and moderate staining. Cytoplasmic staining appeared as scattered or focal labelling,
Clifford et al (2006)	n=19/ FFPE 5 µm sections	BD/ Transduction laboratories (San Jose, CA) 1:100	Positive nuclear staining 2/19 (10.5%) Negative nucleus and +ve cytoplasm 17/19 (89.5%)	As Ellison (2005). Widespread strong nuclear and cytoplasmic positive staining
Gajjar et al (2006)	n= 6 / FFPE section size undertaken (NA)	Cell Signalling Technology (Danvers, MA USA) dilution (NA)	Staining patterns not described 10/51 (14.5%)	NA
Fattet, et al (2009)	n=72 / FFPE 4 µm sections	Clone 14 Ventana (Tucson, USA)	Positive nuclear stainig 9/72 (12.5%) Extensive +ve nuclear 6/72 (8.3%) Focal +ve nuclear 3/72 (4.2%) Cytoplasm positive, nuclear negative 58/72 (80.5%) Nucleus + cytoplasm negative 5/72 (7%)	3 patterns observed: Extensive nuclear staining > 50% nucleus and cytoplasm Focal nuclear staining <10% nucleus and cytoplasm Negative nuclear staining
Present study	n= 207/ FFPE 5 µm sections	BD Transduction Laboratories (San Jose, CA,) 1/600	34/207 +ve (16.4%) Wide spread strong 21/207 (10.1%) Focal strong 11/207 (5.3%) Focal weak 2/207(0.96%) Negative nuclear staining 173/207 (83.6%)	4 patterns observed: Positive nuclear staining Wide spread and strong Focal and strong Focal and weak Negative nuclear staining

Table 4.1. Results of different studies and the current study of β-catenin nuclear localization by IHC in medulloblastoma, and methodologies used, (FFPE= formalin fixed paraffin embedded, NA= not available).

4.2. Aims

The aims of this chapter

1. To develop an immunohistochemical method for the detection of nuclear β-catenin staining.

2. To apply this method to assess the degree of Wnt/Wg activation in a large cohort of medulloblastomas from the PNET3 clinical trial.

3. To compare the incidence of pathway activation with previously published studies.

4. To investigate the correlation between the clinicopathological disease features and β-catenin nuclear localization in the PNET3 cohort.

4.3. Materials and Methods

4.3.1. The PNET3 cohort

This cohort represents a large series of retrospectively collected medulloblastoma samples in the form of FFPE material from patients aged 3 years and above at the time of diagnosis, who were treated in the PNET3 clinical trial (Taylor et al 2003) and have full clinicopathological data available. Full details of data for these samples are mentioned in chapter 2.

In the present study, 207 cases from this cohort were assessed for β-catenin nuclear immuno-reactivity using IHC, (see below).

4.3.2. Detection of β-catenin nuclear immuno-reactivity by IHC

β-catenin nuclear immuno-reactivity was assessed in 5µm FFPE tissue sections using methods described in chapter 2.

4.4. Results

4.4.1. β-catenin immuno-reactivity

A total of 207 cases were evaluated for β-catenin nuclear immuno-reactivity. In total, 34 cases showed evidence of positive nuclear staining (16.4%), while 173 were negative (83.6%). Staining patterns could be classified into 4 categories; (i) wide spread and strong, (ii) focal and strong, (iii) focal and weak and (iv) negative. 11/34 positive cases (32.4%), (11/207, 5.3% in total) showed focal and strong positive nuclear staining, 21/34 positive cases (61.8%), (21/207, 10% in total) showed widespread strong positive nuclear staining and 2/34 positive cases (5.9%)(2/207, 0.9% in total) showed focal weak positive nuclear staining (Table 4.2, Figure 4.1). No evidence of nuclear staining was observed in the remaining cases (n=173), (173/207, 83.6% in total). Sections taken from colorectal carcinoma were used as positive controls (Figure 4.1E). Positive β-catenin nuclear staining was observed in all controls tested indicating that the staining method worked as expected

4.4.2. Relationship to clinicopathological disease features

An initial assessment of the relationship between β-catenin nuclear immuno-positivity and clinical and pathological disease features (age, gender, metastatic stage at diagnosis and pathology) was undertaken (Table 4.3). For the purpose of these analyses, all cases displaying any evidence of nuclear staining were grouped together.

The mean age for cases with β-catenin positive nuclear staining was 8.79 years versus 8.72 for negative nuclear staining; no significant difference was observed

between these groups (t-test, p= 0.91). 19/131 males (14.5%) and 15/76 females (19.7%) were β-catenin positive (Fisher's exact test, p= 0.34). 31/175 (17.7%) of the classic medulloblastoma histopathology subtype and 3/19 cases with the large cell/ anaplastic subtype (15.8%), were positive while all 13 cases with nodular/ desmoplastic subtype (6.3%) showed negative β-catenin staining but this did not reach statistical significance (Fisher's exact test, p= 0.09). However, the 3 cases with large cell/anaplastic pathology had M0/1 stage at diagnosis and were alive disease free with OS of 5, 10.4 and 11.4 years. No significant association was observed with metastatic stage, where 30/169 (17.6%) of M0/1 cases were positive and 4/38 (10.5%) M2/3 cases were positive (Fisher's exact test, p= 0.34). The clinical profile of the 4 cases with positive β-catenin nuclear localization and M2/3 stage is shown in table 4.4. They had classic pathology and subtotal tumour resection achieved. Three cases survived disease free with an average follow up of 11 years. The fourth case (case, 50256), a male aged 4.2 years who had an early recurrence after treatment (0.3 year) and survived for 0.8 year post diagnosis. His molecular profile was, weak focal β-catenin nuclear localization, *CTNNB1* wild-type and chromosome 6 retention of heterozygosity (RET).

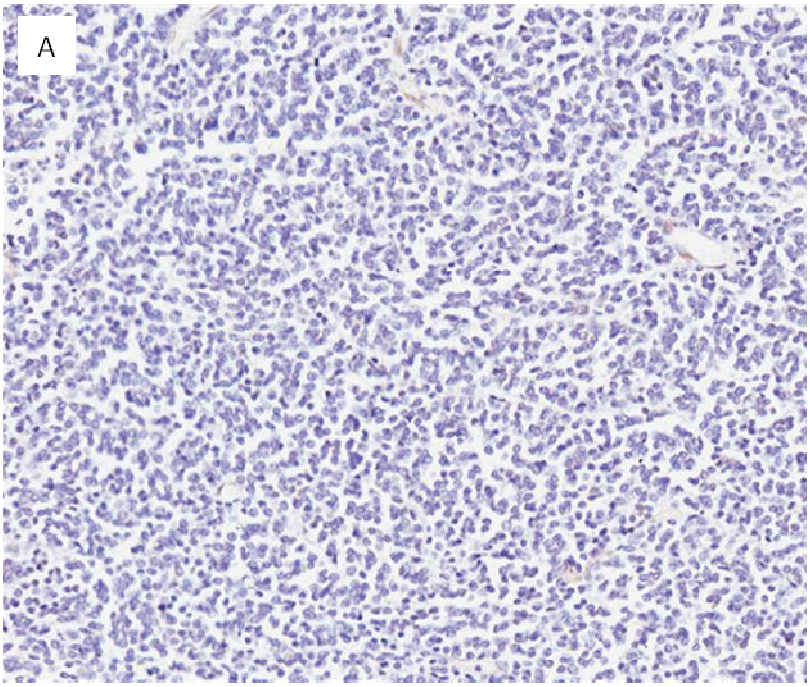
A

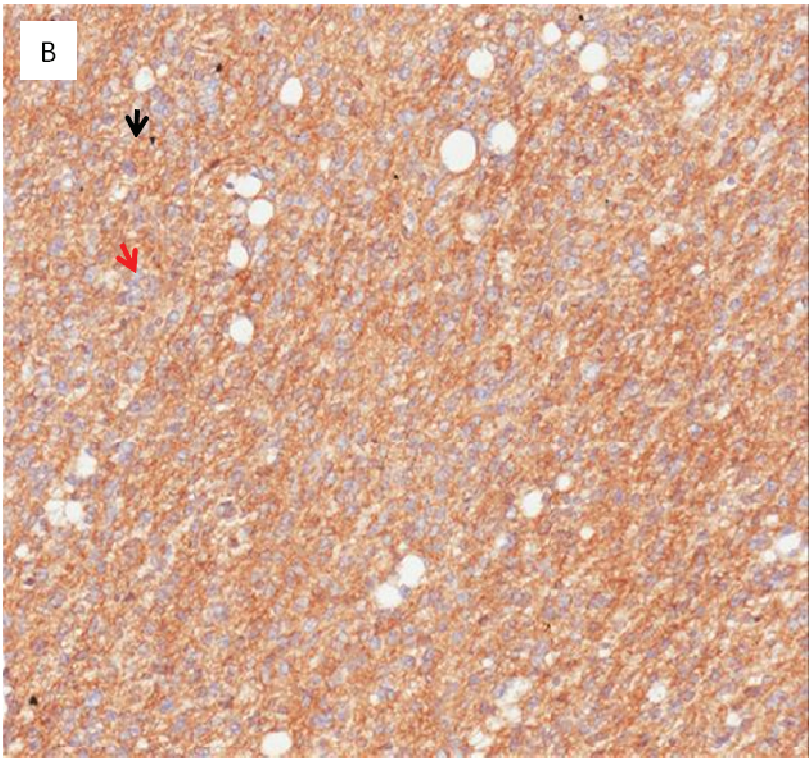
B

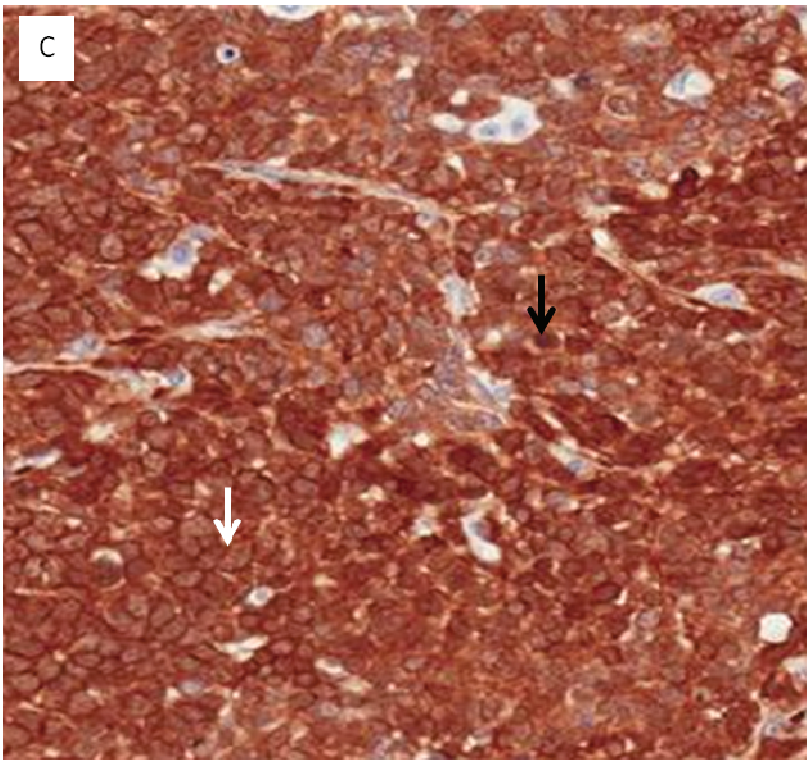
C

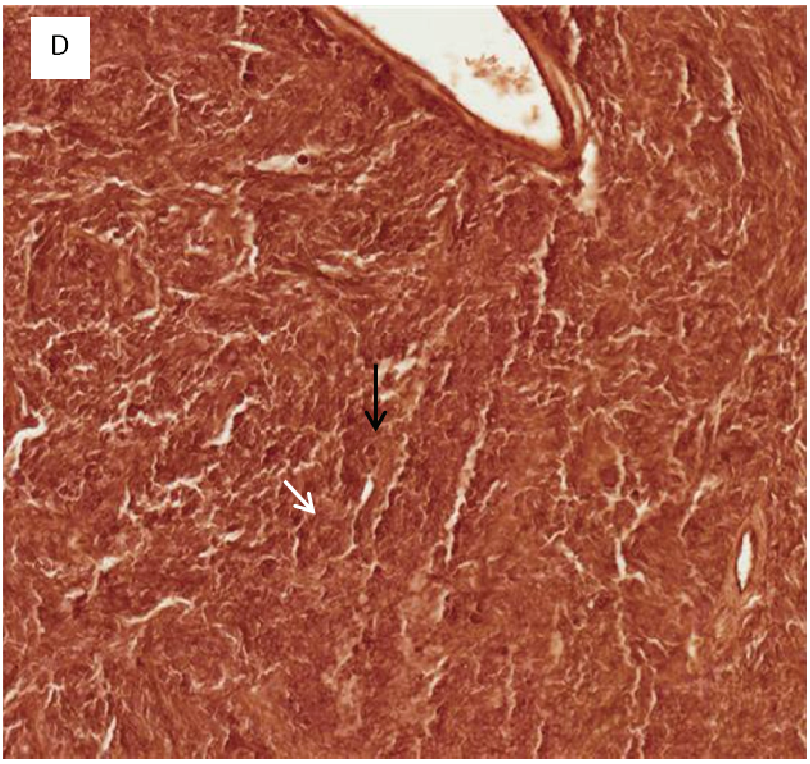
D

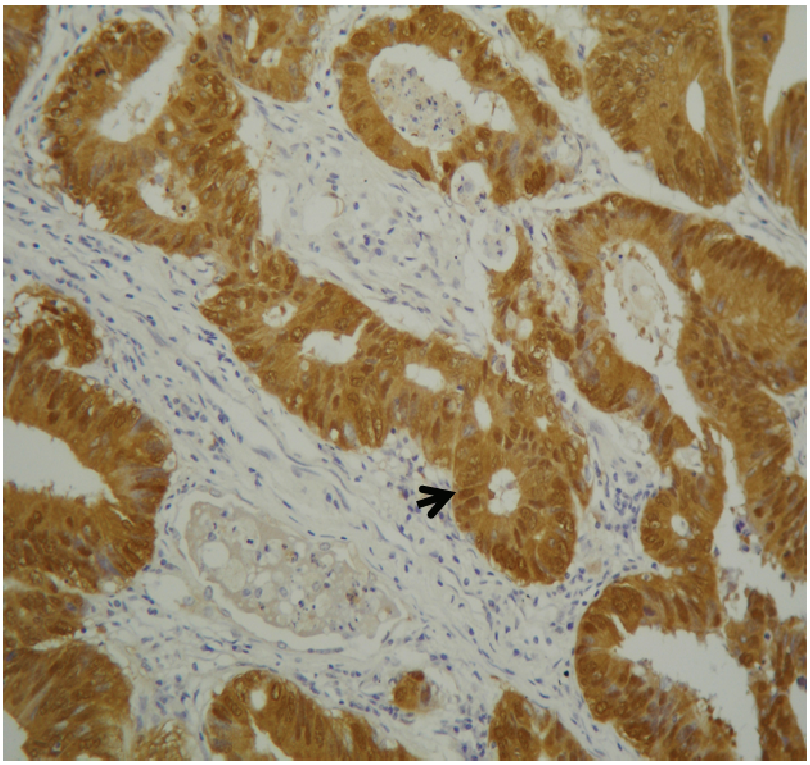

Figure 4.1. Immunohistochemical assessment of β-catenin in medulloblastoma . Illustrative cases are shown following counter staining with hematoxlin and eosin, representing:A. Medulloblastoma case showing negative β-catenin nuclear and cytoplasmic staining. B. Medulloblastoma case showing negative β-catenin nuclear staining (Red arrow) and positive cytoplasm staining (Black arrow). C. Medulloblastoma case showing strong focally positive β-catenin nuclear staining (White arrow) along side areas of cytoplasmic only staining (Black arrow). D. Medulloblastoma case showing widespread positive β-catenin nuclear staining (black arrow) associated with strong positive cytoplasmic staining (White arrow); E. Section of colorectal carcinoma showing positive nuclear and cytoplasmic staining (Arrow). Magnification is 40X in A, B, D; 100X E and 300X in E.

B-catenin immuno reactivity	Patterns of positivity	No of cases	% of positive cases	% of total (207) cases
Cases with positive β-catenin nuclear staining	Wide spread and strong Focal and strong Focal and weak Total	21 11 2 34	61.8% 32.4% 5.8% 100%	10.1% 5.3% 1.0% 16.4%
Cases with negative β-catenin nuclear staining		173		83.6%

Table 4.2. Degree of β-catenin immuno-reactivity in 207 cases assessed

Clinicopathological variables		β-catenin nuclear localization		Total	'p` value
		Negative	Positive		
Gender	Male Female	112 61	19 15	131 76	0.34
Pathology	Classic Nodular desmoplastic Large cell / Anaplastic	144 13 16	31 0 3	175 13 19	0.09
Metastatic stage	Metastatic stage 0/1 Metastatic stage 2/3	139 34	30 4	169 38	0.3

Table 4.3. Correlation between β-catenin nuclear localization and clinicopathological variables in 207 medulloblastomas

Case no.	Age In years	Path	Gender	Treat.	Extent of Tumour resection	Recur.	Time to recur. (y)	Current status	Time to Current status (y)
28	7.2	Classic	F	RTX+CTT	Subtotal	No	-	Alive	10.8
50021	14	Classic	M	RTX+CTT	Subtotal	No	-	Alive	11.00
50086	10.4	Classic	F	RTX+CTT	Subtotal	No	-	Alive	11.00
50256	4.2	Classic	M	RTX+CTT	Subtotal	yes	0.3	Dead	0.8

Table 4.4. The clinicopathological profile of the 4 cases with positive β-catenin IHC and M 2/3 metastatic stage. F= female, M= male; Path= pathology; Treat=treatment, RTX= radiotherapy, CTT= chemotherapy; Recur=recurrence

4.5. Discussion

In this chapter we have successfully undertaken IHC analysis of β-catenin nuclear localization in a cohort of 207 medulloblastomas, representing the largest cohort reported to date. In this study, three predominant staining patterns were observed and we classified cases with positive β-catenin nuclear staining according to the degree of nuclear positivity into; wide spread and strong (21 cases), focal and strong (11 cases) and focal and weak (2 cases). Overall, evidence of positive nuclear staining was observed in 16.4% (34/207) cases, indicating activation of the Wnt/Wg pathway.

There is variation in the percentage of nucleopositive β-catenin samples reported in different published studies, ranging from 10.5-25% (Table 4.1). There were also differences in the way different centres and studies defined the criteria upon which cases were categorized as nucleo-positive. Some studies relied on the percentage of cells observed as positive (e.g. Eberhart et al 2000 and Fattet et al 2009), while others relied on the visual interpretation of the stained sections. This may have impact on defining the criteria for the identification of cases with active Wnt/Wg pathway. Discrepancies in the results between studies may relate to a number of factors such as the number of cases analysed in the study, the clinicopathological profile of the cases (for instance Ellison et al (2005) only assessed non-desmoplastic pathological variants). Similarly different antibodies and dilutions were used, their antigen retrieval methods (e.g. steaming versus microwave) varied, and differences may also arise in the way tissue blocks were fixed, as well as the thickness of cut

sections (Table 4.1). None the less, the overall rates of nuclear positivity observed in published studies are broadly consistent, ranging from 10.5 to 25% of cases assessed.

Our initial examination of the clinico-pathological significance of Wnt/Wg pathway positivity, as evident by β-catenin nuclear localization, indicate that pathway positivity occur in older children (mean age 8 years), but does not show any relationship to gender or metastatic disease status. Comparable rates of positivity were observed in the classic and large cell/ anaplastic variants, but data suggest that positivity is less commonly observed in the nodular/ desmoplastic variant. This association did not reach statistical significance, and the total number of nodular/ desmoplastic cases examined was small (n=13), thus further cases must now be examined to further investigate this potential relationship. Together, these findings demonstrate that Wnt/Wg positive cases can not be recognized by clinical or pathological disease features, and must be assessed using molecular methods.

The clinical and biological significance of these findings are further investigated in the following chapters. In chapter 5 and 6, other Wnt/Wg pathway markers (*CTNNB1* mutation, chromosome 6 loss, respectively) are examined, while their relationship to β-catenin immunopositivity and prognostic relevance is reported in chapter 7.

4.6. Conclusions

1. Immuno-histochemistry can be reliably applied to FFPE tissue samples for the detection of β-catenin nuclear localization as a marker of Wnt/Wg pathway activation.

2. β-catenin nuclear localization was observed in 16.4% of medulloblastomas, based on the analysis of the cohort of 207 cases derived from the PNET3 trial.

3. These rates of positive activation are consistent with previous studies.

4. Variable patterns of immuno-staining were observed, and β-catenin nucleopositive cases could be classified as (i) wide spread and strong positive staining. (ii) focal and strong positive staining (iii) focal and weak positive staining.

5. No evidence of β-catenin immunopositivity was present in the nodular/ desmoplastic medulloblastoma subtype.

6. Wnt/Wg pathway activation, as assessed by β-catenin immunohistochemistry, was not associated with any other clinicopathological disease features, therefore must be assessed by laboratory methods.

Chapter 5

Mechanisms of Wnt/Wg pathway activation in medulloblastoma: Mutation analysis of the *CTNNB1* gene

5.1. Introduction

A major aim of this project was to assess the potential use of the Wnt/Wg pathway as a marker of favourable clinical outcome in medulloblastoma. As described in chapter 4, Wnt/Wg activation as determined by nuclear localization of β-catenin, can not be detected by clinicopathological correlates, so molecular assays are needed. The methodologies for identifying tumours with an active pathway, which we are investigating in this thesis, include β-catenin nuclear immunoreactivity (discussed in chapter 4), *CTNNB1* mutation analysis (which will be discussed in this chapter) and chromosome 6 loss (which will be discussed in chapter 6). Integrated assessment of the 3 methods in parallel will eventually allow assessment of the optimal and most sensitive methods for the detection of pathway activation and outcome prediction (chapters 7 and 8).

As previously described, Wnt/Wg activation results from nuclear accumulation and stabilization of β-catenin (see chapter 1). The *CTNNB1* gene located on chromosome 3p22-p21.3 (Figure 5.1) codes for the β-catenin protein. A number of mutational mechanisms have been reported to lead to stabilization and accumulation of β-catenin in medulloblastoma. Inactivating mutations in the *APC* TSG (~ 2.5% of cases), and activating mutations at the GSK-3β phosphorylation sites within exon 3 of the *CTNNB1* gene (~ 10%) have been documented (Ellison et al 2003). Other components of the Wnt/Wg pathway have shown to rarely play a role in pathway activation, including *AXIN1* and *AXIN2* (conductin) gene mutations (Koch et al 2001).

(A)

(B)

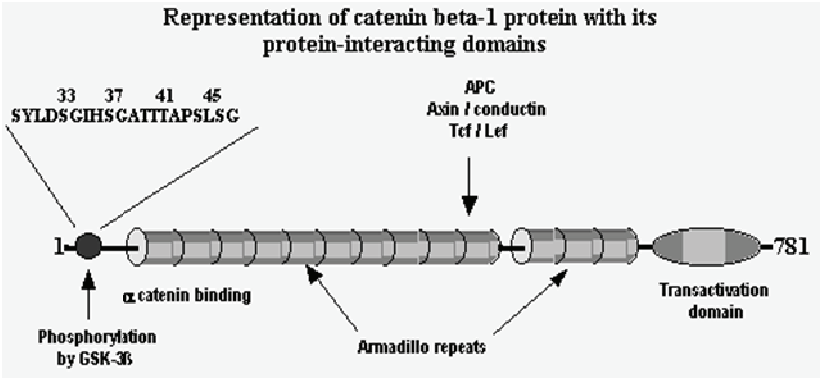

Figure 5.1. Chromosome 3 and corresponding *CTNNB1* gene
(A) an Idiogram of chromosome 3, demonstrating the bands numbered, starting from the centromere to the p and q arms respectively according to the International System for Cytogeneic Nomenclature (ISCN). (B) Schematic illustration of the beta catenin 1 gene, demonstrating the beta-1 protein with its protein-interacting domains (http://atlasgeneticsoncology.org/Genes/CTNNB1ID71.html).

One of the earliest studies which targeted *CTNNB1* mutation screening as a method to identify Wnt/Wg pathway activation was carried out by Zurawel et al (1998). They identified 3/67 cases (4.47%) of sporadic medulloblastoma with

mutations affecting the GSK-3β phosphorylation domain of exon 3 from the *CTNNB1* gene. The study did not examine the status of the *APC* gene. A subset of medulloblastoma samples tested showed LOH in th*e GSK-3*β gene however, none of these cases had mutations on the other allele. Subsequently, Eberhart et al (2000) identified 5/6 cases (83.3%) with *CTNNB1* mutations within 6 cases with positive nuclear localization of β-catenin, again occurring within its GSK-3β phosphorylation domain essential for β-catenin degradation. All mutations were amino acid substitutions predicted to act in a dominant manner. *APC* mutations were also not assessed in the 51 sporadic medulloblastoma cases analysed in this study. The cohort included one case with medulloblastoma associated with Turcot syndrome, due to germ line mutation in the *APC* gene and this case had positive β-catenin nuclear staining.

Ellison et al (2005) analysed 109 patients with sporadic medulloblastoma enrolled in the SIOP PNET3 clinical trial for *CTNNB1* mutations. The cohort comprised non-desmoplastic histopathological variant medulloblastoma samples only. *CTNNB1* missense mutations were found in 9/15 (60%) of cases with nucleopositive β-catenin staining. Notably, no evidence of *APC* gene mutation was observed in any case displaying evidence of Wnt/Wg pathway activation. In the following year, 3 major studies which focused on *CTNNB1* mutation analysis in medulloblastoma were reported (Giangaspero et al 2006, Clifford et al, 2006, Thompson et al, 2006). The first study looked at 364 medulloblastoma cases collected between 1984-1989 within the SIOP II clinical trial. Of these, 146 cases successfully amplified exon 3 of the *CTNNB1* gene from DNA extracted from archival sections. Mutations in *CTNNB1* were identified

in 10/146 cases (7%) analysed; 9/10 were females and 1/10 was male suggesting a possible gender bias. Clifford et al (2006) analysed 19 cases of sporadic medulloblastoma for *CTNNB1* where 3/19 cases (15.8%) showed mutation. Thompson et al (2006) reported gene expression profiles for 46 samples of medulloblastoma and 5 putative subgroup partitions were identified. A group characterized the expression of Wnt/Wg pathway genes was identified, which comprised 6 samples (13%), 5/6 of whom showed *CTNNB1* mutation (5/46 ,(10.9%) in total). All mutations again affected exon 3 (residues 32-34) of *CTNNB1.*

More recently, Kool et al (2008) assessed 62 medulloblastoma samples for mRNA expression profiles. Five molecular subgroups were identified. Group A comprised 9/62 cases (14.5%) and were found to have *CTNNB1* mutations resulting in amino acids changes at positions 32, 33, 34 or 37 of β-catenin. Finally, 72 medulloblastoma samples were assessed by Fattet et al (2009) in order to identify cases with Wnt/Wg activation, through assessing *CTNNB1* mutation, β-catenin protein expression and aCGH. A distinct subgroup of Wnt/Wg active cases was identified where 6/72 cases (8.35 %) showed mutations in exon 3 of the *CTNNB1* gene. All mutations were missense mutations affecting critical residues of the GSK-3β phosphorylation domains of *CTNNB1* gene. Table 5.1 summarizes the incidence of *CTNNB1* mutations in medulloblastoma reported in the literature.

Together, these studies indicate that *CTNNB1* mutations involving the GSK-3β phosphorylation domain within exon 3 are the predominant mechanism for Wnt/Wg activation in medulloblastoma and is strongly correlated with nuclear localization of β-

catenin. This marker may be used to identify this subset of medulloblastomas however, its relevance, clinical significance and relationship to other molecular makers of tumours subtype have not been tested in large cohorts from clinical trials.

***CTNNB1* mutation**			**Study**								
Residue	**Nucleotide change**	**Amino-acid substitute**	**Current study**	**Zurawel et al. 1998**	**Eberhart et al. 2000**	**Ellison et al. 2005**	**Clifford et al. 2006**	**Giangaspero et al. 2006**	**Thompson et al. 2006**	**Kool et al. 2008**	**Fattet et al. 2009**
32	GAC>CAC	ASP>HIS			1					Did not specify amino changes. Only affected residues described (32, 33, 34, 37)	1
32	GAC>AAC	ASP>ASN	2			1		1	1		
32	GAC>GTC	ASP>VAL	2			1		1			
32	GAC>TAC	ASP>TYR	3		1	3	1	1			1
32	GAC>TAC	ASP>VAL				1					
33	TCT>CCT	SER>PRO	1								
33	TCT>TAT	SER>TYR	2			1		1	1		
33	TCT>TGT	SER>CYS	1	2				2	1		
33	TCT>TTT	SER>PHE	2		2		1	3			3
34	GGA>AGA	GLY>ARG	3								
34	GGA>GAA	GLY>GLU	1			1	1	1	1		
34	GGA>GTA	GLY>VAL	2						1		
35		ILE>LYS									1
37	TCT>TAT	SER>TYR	1			1					
37	TCT>TGT	SER>CYS		1							
49	Single base pair deletion	NA			1						
Total no. of cases in the cohort			197	67	51	109	19	146	46	9	6
No. of mutations reported			20 (10.5%)	(4.5%)	* 9/51 IHC +ve (5/6 Mut.)	* 27/109 IHC +ve (9/15 Mut.)	(15.8%)	10 (7%)	5 (10.8%)	9 (14.5%)	6 (8.3%)
Total number of cases in all cohorts (with exception of Ellison et al. and Eberhart et al. cohorts).			490 cases								
Total % of cases with mutations in the above cohorts			56/490 (11.4%)								

Table 5.1. Frequencies of *CTNNB1* mutations reported in the literature and the current study
(Seq.= sequences, Mut.= mutation, IHC= immuno-histochemistry); * Not included in the final total as only a subset of the cohort was analysed for mutations.

5.2. Aims

1. To assess the incidence and nature of *CTNNB1* mutations in a large cohort of medulloblastomas.

2. To undertake initial investigations of the clinicopathological significance of *CTNNB1* mutations in this medulloblastoma cohort.

3. To compare the incidence and types of *CTNNB1* mutations found in our cohort with those reported in other studies.

5.3. Materials and methods

5.3.1. The PNET3 cohort

FFPE samples from the PNET3 cohort were analysed (Taylor et al 2003). In total, 208 samples from patients with medulloblastoma with ages at diagnosis ranging from 3 to 16 years were available for analysis. All samples had previously been investigated for β-catenin status by IHC in chapter 4. Full clinical data of the cohort is detailed in chapter 2, section (2.1.2).

5.3.2. DNA extraction and quality control

DNA was extracted from FFPE medulloblastoma samples as described in chapter 2, section (2.2.1).

5.3.3. Polymerase chain reaction (PCR)

Procedures used for amplification of exon 3 of the *CTNNB1* gene by PCR and the sequences of the specific primers used, are described in chapter 2, section (2.2.2.1). Successful amplification was confirmed by running the amplified PCR on agarose gel electrophoresis (Figure 5.2).

5.3.4. Mutation analysis of exon 3 of the *CTNNB1* gene

Direct DNA sequence analysis of PCR products generated for exon 3 of the *CTNNB1* gene, in both forward and reverse directions was performed according to the protocols detailed in chapter 2, section (2.2.5).

5.4. Results

5.4.1. Assessment of *CTNNB1* mutations

DNA was extracted from 208 FFPE medulloblastoma, and a total of 197 cases were successfully assessed for *CTNNB1* mutation by direct sequencing in forward and reverse directions. 177 (89.9%) cases were wild-type, while 20 (10.1%) showed evidence of mutation. All mutations were confirmed in both forward and reverse directions, and by repeat analysis. The mutations detected were all within codons 32, 33, 34, and 37 of the previously described mutation hot spot affecting the GSK-3β phosphorylation domain within exon 3 of the *CTNNB1* gene. All the mutations, and the corresponding amino acid changes associated, are summarized in Table 5.2 and examples of electopherograms are shown in figure 5.3. Ideally, confirming the mutations identified in *CTNNB1* gene is achieved by comparing tumour samples against constitutional DNA. However, since the PNET3 samples did not have matched DNA available, the 20 mutations identified in 197 PNET3 cases analyzed were confirmed using the SNPdatabase (*db SNP; http://www.ncbi.nlm.nih.gov./).*

5.4.2. Assessment of the clinicopathological significance of *CTNNB1* mutations

CTNNB1 mutations did not show a significant correlation with age; the mean age for cases with mutations versus cases with wild-type sequence was 9.4 years and 8.6 years respectively (t- test, p= 0.32). *CTNNB1* mutations occurred in 10/126 (8%) males and 10/71 (14%) females, there was no significant association with gender

(Fisher's exact test, p= 0.22). 18/167 (10.8%) of classic histopathology subtype tumours and 2/18 (11%) cases with the large cell / anaplastic subtype showed evidence of mutation, while all 12 cases with nodular / desmoplastic pathology were *CTNNB1* wild-type; no significant association was observed with pathology (Fisher's exact test, p= 0.28). No significant association was observed with metastatic stage (Fisher's exact test, p= 0.13), where 19/161 cases (12%) of M0/1 cases and 1/36 of M2/3 cases (3%) showed evidence of *CTNNB1* mutation (Table 5.3).

Codon / nucleotide alterations	Amino-acid alterations	Number of cases
32GAC>AAC	ASP>ASN	2
32GAC>GTC	ASP>VAL	2
32GAC>TAC	ASP>TYR	3
33TCT>CCT	SER>PRO	1
33TCT>TAT	SER>TYR	2
33TCT>TGT	SER>CYS	1
33TCT>TTT	SER>PHE	2
34GGA>AGA	GLY>ARG	3
34GGA>GAA	GLY>GLU	1
34GGA>GTA	GLY>VAL	2
37TCT>TAT	SER>TYR	1

Table 5.2. *CTNNB1* nucleotide mutations and corresponding amino acid alterations detected in the PNET3 cohort (n= 20).

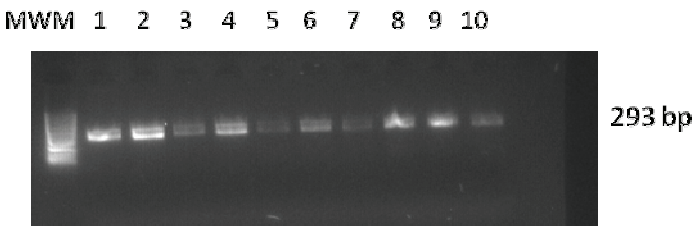

Figure 5.2. PCR amplification of *CTNNB1* gene exon 3. PCR products are shown following electrophoresis on 2% agarose gel. Bands were resolved and successfully amplified DNA of 10 samples of the expected molecular weight 293 bp.

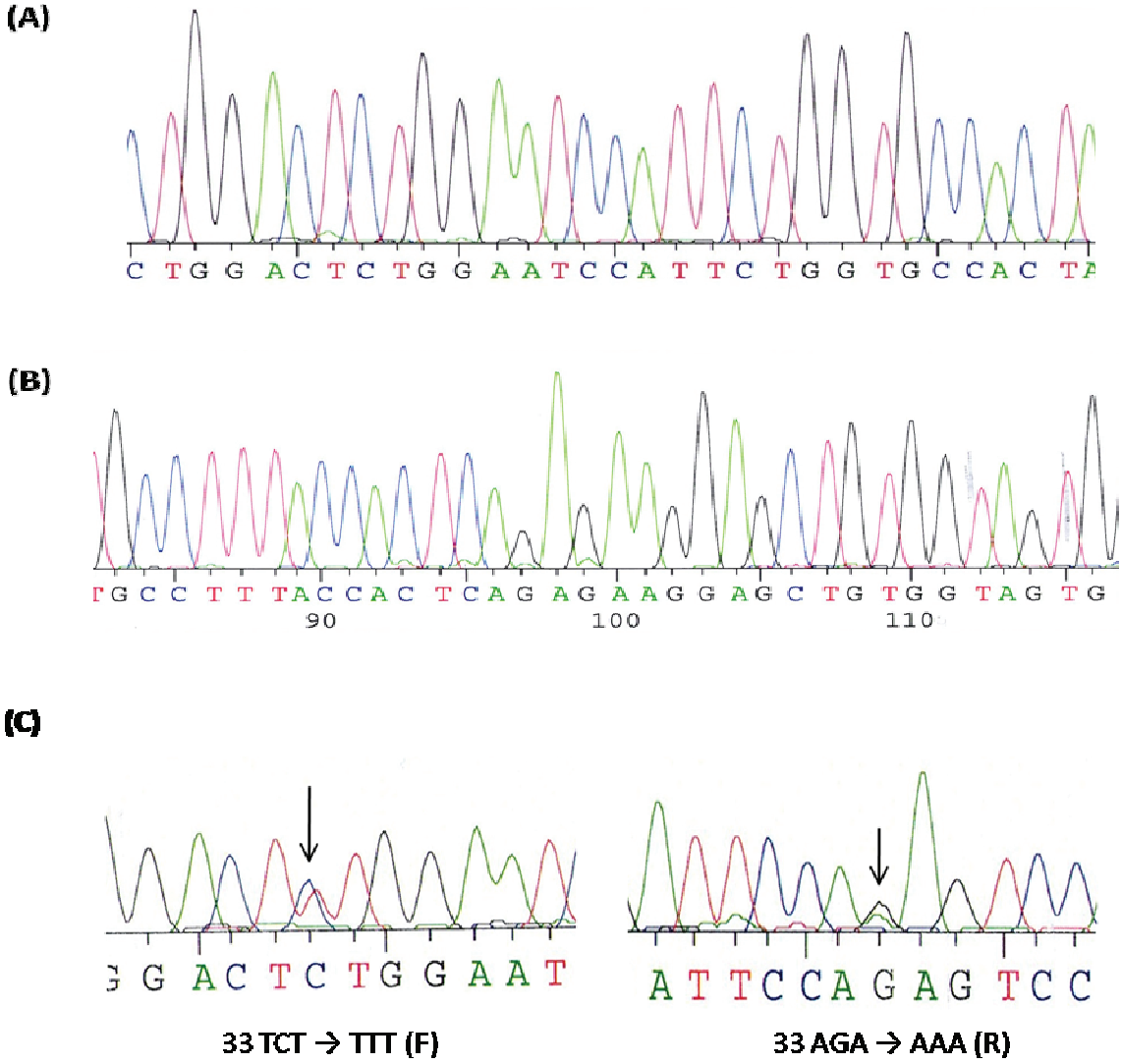

Figure 5.3. Direct sequencing of *CTNNB1* in medulloblastoma, demonstrating (A) *CTNNB1* sequence analysis showing wild-type sequence of exon 3 , residues 30-40 in forward direction. (B) *CTNNB1* sequence analysis showing wild-type sequence of exon 3, residues 50-40 in reverse direction. (C) Mutation at codon 33 (TCT>TTT) in forward direction and codon 33 (AGA>AAA) in reverse direction (arrows).

		CTNNB1		Total	'P` value
		Wild type	**Mutation**		
Sex	Male	116	10	126	0.22
	Female	61	10	71	
Pathology	Classic	149	18	167	0.28
	Nodular /desmoplastic	12	0	12	
	Large cell/anaplastic	16	2	18	
Metastatic stage	Metastatic stage 0/1	142	19	161	0.13
	Metastatic stage 2/3	35	1	36	

Table 5.3. Correlation between *CTNNB1* status and clinicopathological variables.

5.5. Discussion

In this study, a total of 197 PNET3 medulloblastoma samples were successfully analysed for *CTNNB1* mutations, the largest study carried out in this type of tumour to date. The results revealed an incidence of 10.2% (20/197) of cases harbouring *CTNNB1* mutations, which falls within the range of results previously reported in the literature, 4.5 - 16% (Table 5.1). The mutations identified in the PNET3 cohort were all point mutations within exon 3 of the *CTNNB1* gene, encompassing the critical residues 32, 33, 34 and 37. These mutations are predicted to interfere with phosphorylation of the GSK-3β-phosphorylation domain of β-catenin, leading to its accumulation and nuclear translocalization. Most studies, including this study, showed that all *CTNNB1* mutations resulting in Wnt/Wg activation in medulloblastoma are missense point mutations affecting the critical residues, 32-37, of the GSK-3β of exon 3 of the *CTNNB1* gene. Notably, in line within mutational studies of *CTNNB1* reported in other malignancies (e.g. colorectal and hepatocellular carcinoma, Legoix et al 1999; Nhieu et al 1999), mutational analysis has been restricted to this 'hot spot` within exon 3. The possibility exists that mutations affecting other region of the *CTNNB1* may exist, and screening of its full coding region may prove informative. The potential role of mutations within *CTNNB1* in medulloblastoma and of other pathway components, are further discussed in chapter 9.

The discrepancy in the incidence of *CTNNB1* mutations reported in the literature could be due to several factors, such as (i) the number of cases in the study and the clinicopathological profile of the patients (ii) the difference in the target

subgroup of the samples chosen to be analysed (e.g. analysing the whole cohort versus only analysing cases with β-catenin nuclear localization), (iii) the technique used to identify the mutations or (iv) the quality of DNA available for analysis.

Several studies have suggested correlations between *CTNNB1* mutations, age, histopathology and metastatic stage at diagnosis where mutations occur in cases of older age, classic histopathology and no metastasis at time of diagnosis (Thompson et al 2006, Kool et al 2008, Fattet et al 2009), while other studies did not find such significant correlations (Zurawel et al 1998, Eberhart et al 2000, Giangaspero et al 2006). In this study, no significant correlation was found between mutation and these 3 clinicopathological variables, further supporting the notion that Wnt/Wg pathway activation in medulloblastoma can not be detected by clinicopathological associations. However, there was an evident trend for *CTNNB1* mutations cases to be of older age, of classic variant (90% of cases in this study had classic pathology variant and no cases with *CTNNB1* mutations were of the desmoplastic variant), and one case with *CTNNB1* mutation had metastatic stage 2/3 at diagnosis. Analysis of larger cohorts may help to clarify these associations.

The main aim in this chapter was to evaluate the incidence of *CTNNB1* mutations, as an indicator of Wnt/Wg activation in the PNET3 cohort, as a prelude to investigations of its association with other Wnt/Wg pathway markers (e.g. β-catenin nuclear localization and chromosome 6 loss; chapter 7), and its potential as a marker of favourable disease risk in medulloblastoma (chapter 7, 8).

5.6. Conclusions

1. *CTNNB1* mutation analysis can be used as a method to identify Wnt/Wg active medulloblastomas.

2. *CTNNB1* mutations occurred at an incidence of 10.2% in the PNET3 cohort, in line with reports in the literature which range from 4.5 to 16% in cohort-wide studies.

3. *CTNNB1* mutations in medulloblastoma are mainly missense point mutations, affecting the critical residues 32-37, predicted to interfere with the phosphorylation and degradation of the encoded β-catenin protein.

4. *CTNNB1 m*utations do not show significant associations with pathological subtype, metastatic stage and patients' age at diagnosis or gender, but do show a trend towards presence in older children of classic or large cell/ anaplastic pathology without metastatic disease, which now requires further investigation in larger cohorts.

Chapter 6

Molecular correlates of Wnt/Wg pathway activation: analysis of chromosome 6 loss in medulloblastoma

6.1. Introduction

The third method used to identify Wnt/Wg active medulloblastoma tumours in this study is the identification of chromosome 6 loss. A number of studies have now reported that loss of chromosome 6 is strongly associated with medulloblastoma tumours displaying activation of the Wnt/Wg pathway (Clifford et al 2006, Thompson et al 2006, Kool et al 2008, Fattet et al 2009).

Thompson et al (2006) analysed 46 medulloblastoma cases and identified 5 subgroups, based on their transcriptional signatures. A Wnt/Wg pathway signature, associated with over-expression of pathway genes and *CTNNB1* mutations, was present in 6 cases and 4/5 of these showed chromosome 6 loss compared to chromosome 6 loss in 2/36 cases falling within the other 4 subgroups ($p< 0.01$). In a similar study done by Kool et al (2008), mRNA expression profiling was done for 62 medulloblastoma samples; 52 of them were also analysed by aCGH. 5 medulloblastoma subgroups were identified. Subgroup "A" showed a Wnt/Wg active pathway expression signature (n=9 cases) and correlation with *CTNNB1* mutation. Loss of one copy of chromosome 6 was found in all 9 cases (14.5%), as evidenced by a 50% reduction in expression of most genes across chromosome 6. Array CGH analysis was done for 4/9 cases and it was confirmed that 4/4 cases had deletion of an entire copy of chromosome 6. Evidence of chromosome 6 loss was not found in any of the other subgroups (n= 53 cases).

Clifford et al (2006) reported an incidence of chromosome 6 loss of 3/19 (15.8%) within one cohort, followed by testing another larger cohort (n=32) derived

from a previous study which contained known Wnt/Wg active tumours (n=13) and Wnt/Wg negative tumour samples (n=19); chromosome 6 loss was observed in 8/13 and 0/19 of the groups respectively (p= 0.0001). Finally, Fattet et al (2009) evaluated 72 cases for β-catenin protein expression by IHC and genomic defects by aCGH, 6/72 (8.3%) showed extensive nuclear staining (> 50% of the tumour cells), 6/6 cases had *CTNNB1* mutations and 5/6 showed chromosome 6 loss. Altogether, these data confirm that these cases represent a distinct molecular subgroup of Wnt/Wg active medulloblastomas. Notably, none of these cases displayed chromosome 17 abnormalities. All cases were of older age, classic histopathology variant and M0.

A series of further studies have investigated chromosome 6 loss in medulloblastoma without reference to Wnt/Wg pathway activation status. Pfister et al (2009) analysed chromosome 6 status in 2 independent retrospective cohorts of 80 and 260 medulloblastoma samples. The first cohort (n=80) was analysed using aCGH and the results were validated by the second cohort (n=260) using FISH methods. The results were correlated with the patients' clinicopathological features (age, histopathology and metastatic stage at diagnosis) and with patient survival. Hierarchical clustering analysis identified 5 subgroups of medulloblastoma based on their genomic defects. The incidence of chromosome 6q loss within the first cohort was 8/80 (10%) and these cases had a 100% survival. In the validation set, the incidence was similar 31/260 (12%). Tumours with 6q deletion showed excellent outcome (5 years OS, p= 0.002).

Additionally, studies by Michiels et al (2002) and Thomas & Raffel (1991) found loss of 6q in 33.3% and 22% of medulloblastomas respectively. Homozygous deletion of chromosome 6q23 was detected by Hui et al (2005) in the medulloblastoma cell line DAOY, and copy number loss was detected in 30% of primary tumours. This study succeeded to map the smallest region of homozygous deletion to a 0.887 Mb interval on 6q23.1. Three genes were mapped to this area: *BC060845* (L3MBTL3 protein), *AK091351* (hypothetical protein FLJ34032), and *KIAA1913*. Compared to normal cerebellum, the expression levels of these 3 genes were not detected in the cell line DAOY with homozygous deletion and their expression was reduced in medulloblastoma cell lines D283 and D384. The expression of these genes was also reduced in 10 analyzed primary tumours, with frequencies of 70% (*KIAA1913*), 50% (*AK091351*) and 10% (*BC060845*).Therefore, at least 2 of those genes may be candidate TSGs implicated in medulloblastoma development.

In summary, a series of studies have reported a significant association between chromosome 6 loss and Wnt/Wg pathway activation in medulloblastoma. Despite this, the prognostic value of chromosome 6 loss, its relationship to other features of Wnt/Wg pathway activation (*CTNNB1* mutation, β-catenin nuclear localization), and its clinicopathological significance, have not been comprehensively addressed in large cohort of cases derived from clinical trials. The incidence of chromosome 6 loss in published medulloblastoma studies is shown in Table 6.1.

	Number of cases	No. of cases Chromosome 6 loss	%	Method used
Clifford et al (2006)	19	3	15.8%	HOMOD
Thompson et al (2006)	46	4	8.7%	aCGH
Kool et al (2008)	62	9	14.5%	aCGH
Fattet et al (2009)	72	5	7%	aCGH
Pfister et al (2009) (2 independent cohorts)	80 260	8 31	10% 12%	aCGH
Current study	190	20	10.5%	HOMOD
Total	729	80	10.8%	All methods

Table 6.1. Incidence of chromosome 6 Loss in current and previously published studies.

6.2. Aims

1. To develop a HOMOD method for the detection of chromosome 6 loss in FFPE medulloblastoma samples

2. To use this method to investigate the incidence of chromosome 6 loss in a large cohort of medulloblastomas studied in the PNET3 clinical trial.

3. To compare the incidence of chromosome 6 loss detected with those reports from previous studies.

4. To undertake an initial assessment of any associations between chromosome 6 LOH and clinicopathological disease features.

6.3. Materials and methods

6.3.1. The PNET3 cohort

As previously described in chapters 3-5, the cohort analysed consisted of 208 samples from patients with medulloblastoma of ages ranging from 3 to 16 years. Full clinical data of the cohort is detailed in chapter 2, section 2.1.2.

6.3.2. DNA extraction and quality control

DNA was extracted from 208 FFPE medulloblastoma samples as detailed in chapter 2, section 2.2.1.

6.3.3. Polymerase chain reaction (PCR)

Amplification of DNA was performed as detailed in chapter 2, section 2.2.2.1. Agarose gel electrophoresis was performed as detailed in chapter 2,section 2.2.3, to confirm that successful amplification had occurred. Details of the polymorphic microsatellite primers used for chromosome 6 LOH analysis are shown in Table 6.2.

6.3.4. Loss of heterozygosity analysis, using the HOMOD method

Loss of heterozygosity of chromosome 6 was assessed in the PNET3 cohort using the HOMOD method as detailed in chapter 2, section 2.2.4. Each polymorphic marker was scored as; (i) Homozygous, if there was only one peak or where the second peak with intensity of less than ≤ 30% was seen. (ii) Heterozygous, if two peaks were seen with a difference of ≤ 50%. (iii) Heterozygous + MSI, if more than two peaks or the appearance of novel peaks were seen (Figure 6.1).

Primers	Forward primer (5′ medulloblastoma – 3′)	Reverse primer (5′ – 3′)	DNA product size (bp)	Position	Gene bank
D6S1017	**GGATGGATGGACATAATGGA**	**CACCTTTTCATCTGTCCACC**	151-171 bp	6p21	G08578
D6S1006	**ACCAACCCCACTAAGGTACC**	**AGGTTGATGGGTGTAGCAAA**	194-203 bp	6p24.1	G08516
D6S1056	**ACAAGAACAGCATGGGGTAA**	**CCTGGATCATGAATTGCTAT**	237-273 bp	6q16.1	G08558
D6S474	**TGTACAAAAGCCTATTTAGTCAGG**	**TCATGTGAGCCAATTCCTCT**	151-167 bp	6q22.1	GO8540
D6S1009	**AATAGTGACATTCTCTTCTTATGGC**	**AGGTATGGTGCCACACACTT**	237-273 bp	6q23.2	GO8542
D6S2436	**CAGGATTTTTCAGAAAGGCA**	**CTGTCACAGACTTTTTCAGCC**	121-149 bp	6q24.1	G27284

6.2. Polymorphic microsatellite markers used for the analysis of chromosome 6 LOH.

6.4. RESULTS

6.4.1. Assessment of chromosome 6 loss

190/208 DNA samples from the PNET 3 cohort were successfully assessed for chromosome 6 LOH status using the HOMOD method. Twenty cases (10.5%) showed LOH affecting the entire chromosome, while 170 cases (89.5%) did not (Figures 6.1 and 6.2, Table 6.3). All 20 cases showed homozygosity affecting, all polymorphic markers tested across chromosome 6. All results were reproducible on replicate analysis. Details of the primers used for chromosome 6 LOH are summarized in Table 6.2.

6.4.2. The correlation between chromosome 6 status and clinicopathological disease features

There was no significant correlation with age; the mean age for cases with chromosome 6 LOH versus those without LOH was 9 and 8.8 years respectively (t- test, p= 0.67). There was no significant relationship with gender (Fisher's exact test, p= 0.22). 10/121males (8.3%) had LOH status, while 10/69 (14.5%) females had LOH. Chromosome 6 LOH was detected at equivalent rates, in 18/161 (11%) Classic and 2/17 (11.8%) Large cell / anaplastic medulloblastoma samples but not in any nodular / desmoplastic cases (n=12), however this did not reach statistical significance (Fisher's exact test, p= 0.25). There was also a trend for metastasis to occur among cases without chromosome 6 loss. Two out of 20 patients with chromosome 6 LOH had metastatic stage M2/3 (10%) compared with 32 out of 138 cases with chromosome 6 RET (23.2%),

however, again, this trend did not reach statistical significance (Fisher's exact, p= 0.54) (Table 6.4).

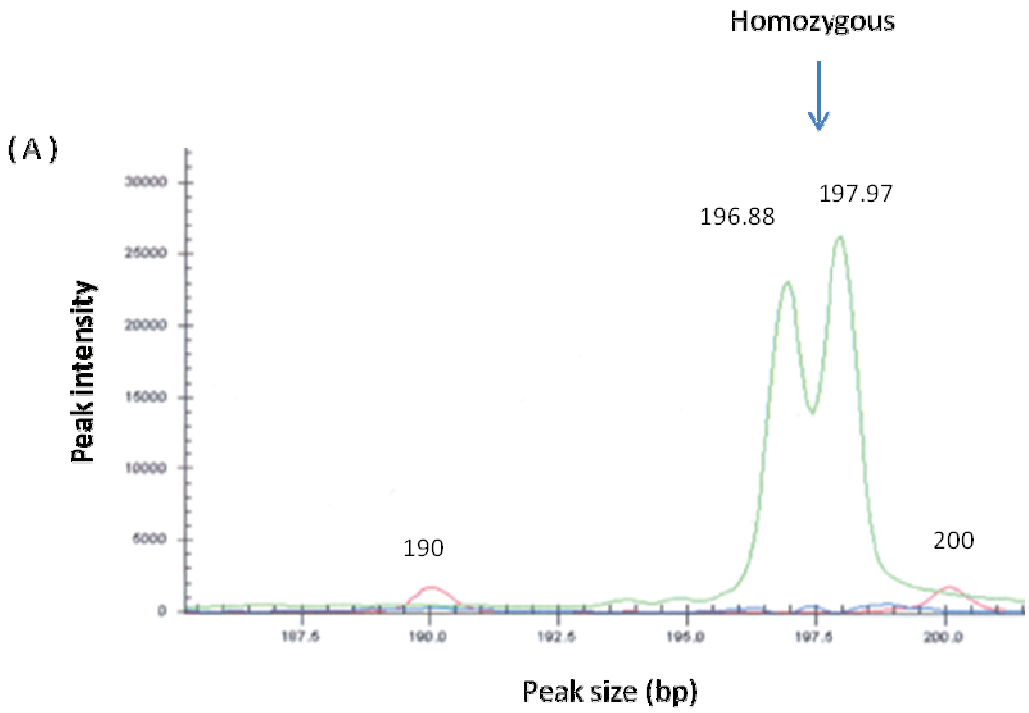

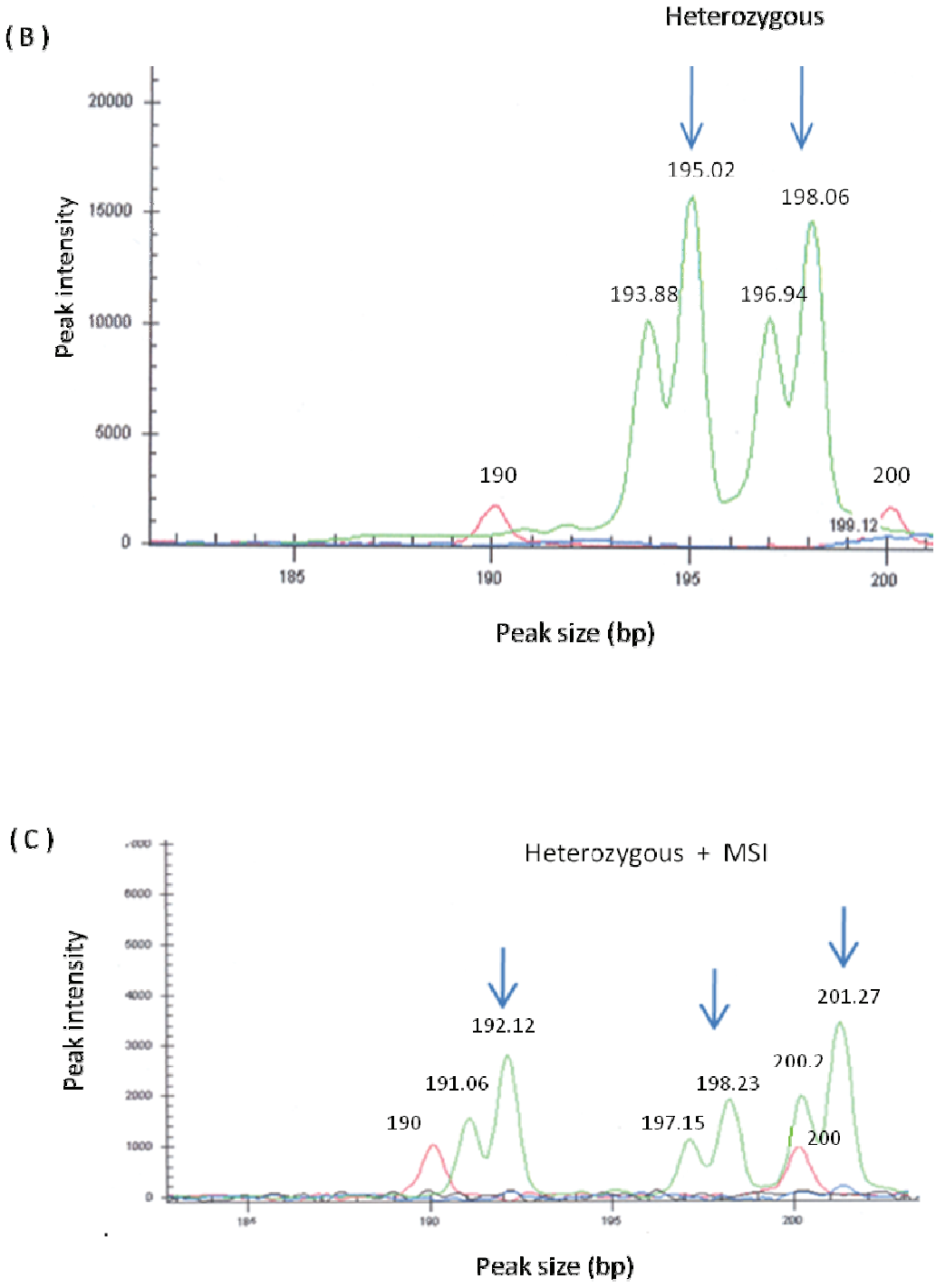

Figure 6.1. Assessment of chromosome 6 LOH by HOMOD using PCR-based polymorphic microsatellite markers, showing examples of electropherogram traces representing; (A) homozygosity (one peak); (B) heterozygosity (2 peaks), (C) heterozygosity and microsatellite instability (3 or more peaks). Illustrative results obtained using marker (D6S1009) are shown. Major peaks are marked with arrows. Red peaks represent exogenous size standard markers.

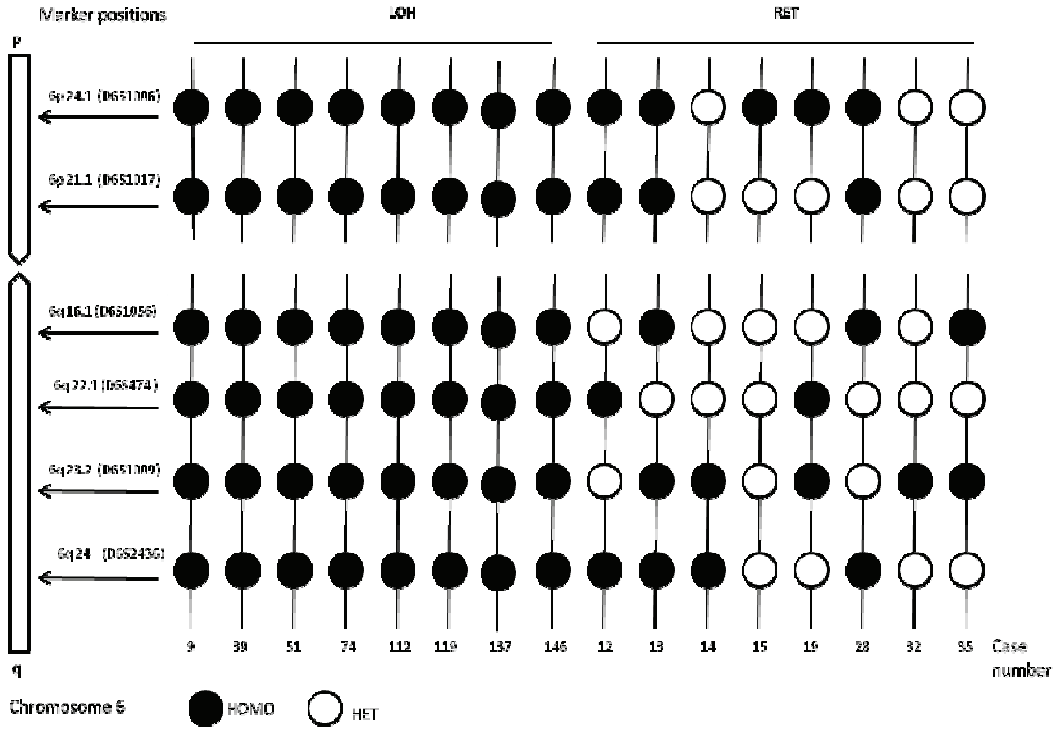

Figure 6.2. Illustrative analysis of chromosome 6 LOH status using HOMOD in PNET3 cases.
HOMO= homozygous, HET= heterozygous; cases with LOH of chromosome 6 display ≥ 5 consecutive homozygous markers.

Stud no.	PNET3 CASE.	Polymorphic microsatellite markers						Ch6 status
		D6S 1006	D6S 1017	D6S 1056	D6S 474	D6S 1009	D6S 2436	
1	2							
2	9							
3	12							
4	13							
5	15							
6	18							
7	19							
8	28							
9	30							
10	31							
11	32							
12	33							
13	35							
14	38							
15	39							
16	41							
17	43							
18	44							
19	47							
20	48							
21	51							
22	52							
23	54							
24	62							
25	65							
26	66							
27	69							
28	72							
29	75							
30	77							
31	78							
32	81							
33	82							
34	83							
35	90							
36	95							
37	101							
38	105							
39	106							
40	107							
41	112							
42	113							
43	116							
44	119							
45	120							
46	121							
47	124							
48	126							
49	129							
50	131							
51	132							
52	134							
53	137							
54	139							
55	141							
56	145							
57	146							
58	147							
59	148							
60	149							
61	150							
62	152							
63	157							
64	160							
65	161							
66	164							
67	165							
68	166							
69	169							
70	171							
71	172							
72	175							
73	178							
74	179							
75	180							
76	182							
77	185							
78	186							
79	191							

Table 6.3 continued

Study no.	PNET3 case.	Polymorphic markers						Ch6 status
		D6S 1006	D6S 1017	D6S 1056	D6S 474	D6S 1009	D6S 2436	
80	193							
81	195							
82	186							
83	199							
84	201							
85	202							
86	207							
87	209							
88	210							
89	214							
90	216							
91	217							
92	50001							
93	50010							
94	50011							
95	50012							
96	50014							
97	50015							
98	50016							
99	50017							
100	50019							
101	50021							
102	50034							
103	50035							
104	50040							
105	50041							
106	50044							
107	50045							
108	50047							
109	50049							
110	50056							
111	50057							
112	50058							
113	50060							
114	50063							
115	50068							
116	50072							
117	50075							
118	50079							
119	50080							
120	50086							
121	50088							
122	50090							
123	50091							
124	50092							
125	50099							
126	50100							
127	50104							
128	50111							
129	50113							
130	50116							
131	50117							
132	50120							
133	50124							
134	50128							
135	50129							
136	50132							
137	50133							
138	50137							
139	50142							
140	50145							
141	50147							
142	50150							
143	50153							
144	50154							
145	50159							
146	50161							
147	50163							
148	50165							
149	50166							
150	50167							
151	60167							
152	50169							
153	50170							
154	50172							
155	50174							
156	50176							

Table 6.3 continued

Study no.	PNET3 case.	Polymorphic markers						Ch6 status
		D6S 1006	D6S 1017	D6S 1056	D6S 474	D6S 1009	D6S 2436	
157	50184							
158	50189							
159	50193							
160	50197							
161	50198							
162	50204							
163	50206							
164	50208							
165	50209							
166	50212							
167	50217							
168	50218							
169	50224							
170	50233							
171	50236							
172	50241							
173	50244							
174	50245							
175	50248							
176	50249							
177	50250							
178	50251							
179	50253							
180	50254							
181	50256							
182	50259							
183	50263							
184	50268							
185	50274							
186	50276							
187	50284							
188	50290							
189	50291							
190	50292							

Table 6.3. Complete data of chromosome 6 LOH status analysis in the PNET3 cohort using 6 microsatellite markers. Yellow cell = heterozygous, sky blue cell = homozygous, white cell = PCR failed, dark blue cell = MSI. Status is shown in the final column (red cell = LOH; grey cell = no evidence of LOH). LOH= loss of heterozygosity. Failed PCRs were not repeated where evidence of ≥ 2 heterozygous markers had already been detected in an individual sample indicating heterozygosity on chromosome 6. All analyses were repeated for cases displaying evidence of chromosome 6 LOH, or with ≤ 1 marker demonstrating heterozygosity.

Clinicopathological variables		Chromosome 6		Total	'P` value
		RET	LOH		
Gender	Male	111	10	121	0.22
	Female	59	10	69	
Pathology	Classic	143	18	161	0.25
	Nodular / desmoplastic	12	0	12	
	Large cell / anaplastic	15	2	17	
Metastatic stage	Metastatic stage 0/1	138	18	156	0.53
	Metastatic stage 2/3	32	2	34	
Total		170	20	190	

Table 6.4. Correlation between chromosome 6 Loss and clinicopathological variables in the PNET3 cohort (n=190).

6.5. Discussion

In total, 190 samples were successfully evaluated for chromosome 6 LOH status using the HOMOD method, 20 cases showed clear and reproducible evidence of LOH affecting the entire chromosome (10.5%). These data are highly consistent with previously published studies (Table 6.1). The incidence of chromosome 6 loss in these studies varied between 7% and 15.8 %. These differences are small, and most likely due to factors including the number of cases studied in the different cohorts, or methods used to test for LOH (i.e. HOMOD, FISH and aCGH). Given the consistency of incidences observed in this and other studies using different methods for the detection of chromosome 6 loss, it was decided not to validate results obtained using the HOMOD method. This decision was also inferred by the close correlation obtained between whole arm chromosomal losses detected using HOMOD and aCGH for chromosome 17 in chapter 3. Consistent with these studies, where sufficiently sensitive methods were used, losses appeared to affect the entire chromosome. The significance of these patterns of loss, and strategies for the identification of candidates and in future investigation of the contribution of chromosome 6 loss are discussed in chapter 9.

No significant correlations were found in this study between chromosome 6 status and clinicopathological disease features, indicating that this molecular alteration can not be detected clinically and requires the use of molecular/ immuno methods, however, a number of interesting trends were seen, which now require further investigation in wider cohorts. First, studies by Thompson et al (2006), Kool et al (2008) and Fattet et al (2009) showed a correlation between chromosome 6 loss and clinical

features (histopathology, metastatic stage at diagnosis), where all cases with chromosome 6 loss presented with classic or large cell / anaplastic histopathology and metastatic stage 0. Although in this study no significant correlation was found between chromosome 6 LOH and these 2 variables, comparable trends were seen, but which did not reach statistical significance (Table 6.4).

In the next chapters, we proceed to examine any relationship between chromosome 6 loss and the other molecular markers of Wnt/Wg pathway activation in medulloblastoma, as well as its utility for prediction of therapeutic outcome.

6.6. Conclusions

1. The HOMOD method was successfully applied to examine chromosome 6 status in a large series of medulloblastoma.

2. The incidence of chromosome 6 loss in this cohort of 190 cases derived from the PNET3 clinical trial was 10.5% (20/190) Comparable to results using other methods in previous studies.

3. Chromosome 6 status was not significantly associated with clinicopathological disease features, but showed a trend towards an increased incidence in tumours of classic / large cell subtype tumours without metastasis.

4. Chromosome 6 LOH status can only be detected through molecular/immuno testing.

Chapter 7

Assessment of the prognostic significance of clinicopathological and molecular disease features of the PNET3 cohort in univariate survival analyses.

7.1. Introduction

Clinical disease features form the basis of current disease stratification in medulloblastoma. The presence of metastatic disease and the extent of tumour resection at initial surgery have been consistently associated with high-risk disease in patients aged ≥ 3 years at diagnosis. These features and their prognostic association have been extensively discussed in chapter 1, section (1.3.3.3). In addition to these features, molecular and histological disease features have also been reported to have prognostic value; and may be have utility to refine current risk stratification. The major aim of this chapter is to examine the prognostic significance of clinical and pathological disease markers in the PNET3 cohort we have investigated in this thesis, alongside the prognostic significance of molecular markers tested in the preceding chapters.

7.1.1. The prognostic significance of disease histopathology in medulloblastoma

Medulloblastoma is a heterogeneous disease at the histopathological and molecular levels. The WHO (Louis et al 2007) classified medulloblastoma into 4 categories based on their histopathological features (see chapter 1, section 1.3.2) however, these categories overlap, for example features of anaplasia can be found focally in classic medulloblastoma, and less frequently in desmoplastic medulloblastoma. Also, variations in the degree of anaplasia can be present in the same lesion. Two different approaches have been used in correlating tumour histopathology with patients' survival. The first approach followed the WHO classification and correlated each pathological subtype with survival (e.g. Ellison 2002,

Gajjar et al 2004, Lamont et al 2004, McManamy et al 2007 and others). The second approach based correlations on the degree of cell differentiation (anaplastic and non-anaplastic) and its distribution (widespread or focal) (Brown et al 2000, Eberhart et al 2002, Giangaspero et al 2006). The results of some of these studies are detailed below.

Rutkowski et al (2005) and McManamy et al (2007) reported that tumours with the nodular / desmoplastic pathology subtype had a better outcome in children < 3 years of age and that this significance appears to be less important in children over 3 years of age at diagnosis. Gajjar et al (2004) reported a cohort of 86 primary medulloblastoma samples, 18 cases (21%) were classified as large cell / anaplastic pathological variants; their 5 year EFS was 42% compared to 63% for classic and nodular / desmoplastic tumours, but this did not reach a statistical significance. Lamont et al (2004), in a study for 87 patients with primary medulloblastoma, reported that 74 samples (85%) were of the non-desmoplastic pathological variant, of which 59/74 cases (80%) were classic and 15/74 cases (20%) showed large cell / anaplastic pathology. 13/87 cases (15%) were of the nodular / desmoplastic pathology variant. Univariate survival analysis for the non-desmoplastic group showed that the classic pathology subtype showed an increased OS and EFS than cases with large cell / anaplastic variant (p= 0.0005 and p= 0.0007, respectively).

McManamy et al (2007) studied the clinicopathological features and biological behavior of medulloblastoma in 2 SIOP/UKCCSG trial cohorts; CNS 9102 PNET3 (n= 315, aged 3-16 years) and CNS 9204 (n= 35, aged < 3 years). In the 2 cohorts collectively, 66% were of classic histopathology variant, 17% large cell / anaplastic, 8%

nodular / desmoplastic and 6% biphasic medulloblastoma (nodular / non-desmoplastic) variants. 57% of cases with the nodular / desmoplastic variant presented in infancy, compared to only 5% in children aged 3-16 years. Across both cohorts (age range from 0-16 years), 8% were nodular / desmoplastic histopathological variant. Univariate survival analysis showed that age, gender and treatment regimen revealed no significant survival association. While both, OS and EFS for extent of tumour resection and metastatic stage at diagnosis showed a significant correlation with survival ($p= 0.04$, $p= 0.01$) and ($p< 0.001$) respectively, favouring total tumour excision and M0/1 stage. Nodular / desmoplastic tumours showed the best OS and EFS (83% and 77% respectively), followed by the classic variant (OS and EFS were 73% and 64%, respectively), while cases with the large cell / anaplastic pathology variant showed worse survival (OS and EFS were 57% and 51%, respectively), ($p= 0.01$).

Pfister et al (2009), studied the correlation of clinicopathological variables with survival in 2 independent primary medulloblastoma cohorts (n= 340 collectively). A significant correlation was found with presence of metastasis at time of diagnosis and pathology, (both had 5 years OS, $p< 0.001$). Cases with nodular / desmoplastic pathology had best outcome while cases with large cell / anaplastic pathology had worse outcome.

Eberhart et al (2002) analysed a cohort of 330 patients with primary medulloblastoma for the correlation between the degree and extent of anaplasia with patients' survival. 225 cases (68%) showed no anaplasia, 25 (8%) showed slight anaplasia, 46 (14%) showed moderate anaplasia and 34 (10%) had severe anaplasia.

Anaplasia was focally distributed in 49 cases and widespread distributed in 56 cases. A significant correlation with survival was found, where moderate and severe anaplasia as well as anaplasia with widespread distribution had the worst survival ($p< 0.0001$). Of the 330 tumours examined, 96 tumours (29%) displayed regions of nodularity. Extensive nodularity was associated with better clinical outcome but it did not reach a statistically significant value, however patients outcome was directly proportional to the degree of nodularity where widespread nodularity was associated with best OS and EFS, followed by moderate nodularity then slight nodularity.

Giangaspero et al (2006) correlated the degree of anaplasia with clinical outcome in a cohort of 364 medulloblastoma patients (which have been recruited in the SIOP II clinical trial, conducted by the International Society of Paediatric Oncology). A three-tiered grading system was used to assess the degree of anaplasia; mild, moderate, and severe anaplasia. Large cell / anaplastic medulloblastomas were all graded as severely anaplastic. For 257 cases, anaplasia data was available, where mild, moderate, and severe anaplasia were observed in 18 cases (7%), 152 cases (59%), and 87 cases (34%), respectively. The patients with severely anaplastic tumours had the poorest outcome, while patients with mild or moderate anaplasia had a better outcome. The 5 year OS and EFS of cases with severe anaplasia versus cases with moderate anaplasia was (50.6% versus 67.4%, $p= 0.003$) and (49.5% versus 65.4%, $p= 0.001$) respectively. Within 251 tumours where data on nodularity was available, 30 (12%) tumours displayed regions of nodularity, and no evidence of an association between nodularity and outcome was observed ($p= 0.11$). It could be concluded from

the above studies that there is significant association between poor outcome and the large cell / anaplastic phenotype.

7.1.2. The potential prognostic significance of patients' gender in medulloblastoma

Investigating the relationship between patients' gender and clinical outcome has yielded controversial results therefore, this clinical variable is not used in current risk classification systems. Two of the most cited studies that reported a significant association between gender and patients' prognosis were those conducted by Weil et al (1998) and Curran et al (2009). In the former study, 109 medulloblastoma cases were assessed (62 males and 47 females), where univariate survival analysis identified gender to be a statistically significant prognostic factor ($p= 0.01$). Cox regression analysis produced a final model for disease outcome prediction and estimation of hazard ratio where gender showed a hazard ratio of 0.52 ($p= 0.03$) favoring females. The author concluded that females did remarkably better than males and suggested that this may have been due to the fact that females were more sensitive to therapy, where treatment-induced precocious puberty may have a hormonal (estrogen, progesterone) influence or interaction on medulloblastoma. The latter study by Curran et al (2009) yielded similar results but on a larger data set of 1226 medulloblastomas. This cohort consisted of 763 males and 463 females, which increased the power of the study and minimized ascertainment bias. The cohort consisted of patients below and above 3 years at diagnosis. Within the <3 years group 95 were males and 82 were females, eliminating the male predominance in the under 3 years age group. Within the ≥3 years aged group, 668 were males and 381 were females (ratio 1.7:1). Overall,

there was no significant difference in survival between the males and females (p= 0.22) however, within the cases ≥3 years at diagnosis there was a significantly better survival for females (p= 0.02). While for patients <3 years at diagnosis there was a trend towards worse prognosis among females (p= 0.24), median survival time for females was 13 months compared to 27 months for males. Therefore, a significant interaction between age and gender was observed (p= 0.03). The authors' explanation for the inferior clinical outcome among male patients aged ≥3 years at diagnosis was a possible innate effect of gender on medulloblastoma biology, varying response to treatment or a hormonal effect.

In the present study, we used 3 molecular methods to identify and characterize medulloblastoma tumours with Wnt/Wg active pathway namely; β-catenin nuclear localization (chapter 4), *CTNNB1* mutation analysis (chapter 5) and chromosome 6 LOH (chapter 6) in the PNET3 cohort. Also, 17p LOH status was assessed in the same cohort (chapter 3), being the most common chromosomal abnormality in medulloblastoma which has been reported to be mutually exclusive of Wnt/Wg pathway activation. The previously reported prognostic associations of these markers have been described in chapters 4, 5, 6 and 3 respectively.

7.2. Aims

In the 4 previous chapters, the incidences of each of these 4 molecular abnormalities in the PNET3 cohort have been identified. In this chapter, the correlations of these factors with the clinicopathological features of the patients described in chapters 3 to 6 will be undertaken alongside survival analysis of all clinicopathological and molecular variables of the cohort to establish any relationship between the molecular variables, and their relative utilities for the prediction of Wnt/Wg pathway activation. This approach should allow identification of the most informative and practical markers to use in clinical trials to identify Wnt/Wg active medulloblastomas.

Together, these findings will then be used to form the basis of the development of the optimal models for the assessment of disease risk in medulloblastoma using clinical, pathological and molecular markers, which will be described in chapter 8.

The specific aims of this chapter are:

1. To estimate the overall incidence of Wnt/Wg pathway active tumours in the PNET3 cohort, as detected in chapters 4-6.

2. To undertake univariate survival analysis for the clinicopathological variables of the PNET3 cohort.

3. To undertake univariate survival analysis for the Wnt/Wg pathway molecular markers tested, (*CTNNB1* mutations, β- catenin nuclear localization, chromosome 6 LOH) and chromosome 17p LOH.

4. To examine the relationship between the 3 molecular markers of the Wnt/Wg medulloblastoma subtype, to identify the best predictor for Wnt/Wg activation in future studies.

7.3. Material and methods

7.3.1. PNET3 cohort, clinical, pathological and molecular variables

The PNET3 cohort was composed of 208 primary medulloblastoma samples. Clinicopathological feature data (age, gender, histopathology subtypes, metastatic stage at time of diagnosis, treatment given, recurrence and outcome) were available for all except 6 cases where extent of tumour resection data was not available. Clinical data are summarized in chapter 2, section (2.2.2). All cases were tested for β-catenin nuclear localization by immuno-histochemistry (chapter 4), *CTNNB1* mutations by direct sequencing (chapter 5), chromosome 6 loss (chapter 6) and chromosome 17p LOH (chapter 3) by the HOMOD method. Successful results were achieved in 207 cases for β-catenin nuclear localization, 197 samples for *CTNNB1* mutations and concomitant 190 samples for chromosome 6 LOH and chromosome 17p LOH. The results for these samples were used in the univariate analysis (see below). In 184 cases, a successful result for all 4 markers was achieved. The results for these 184 cases were used to analyse the correlation between the 4 molecular markers described here as well as the multivariate survival analysis described in chapter 8.

7.3.2. Statistical analysis

Correlation between the patients' clinicopathological variables (gender, histopathology subtype, metastatic stage at diagnosis, recurrence, treatment, extent of tumour resection) and molecular variables (β- catenin nuclear staining, *CTNNB1* mutation status, chromosome 6 and 17p LOH status) were performed using Fisher's

exact test and likelihood ratio tests (as appropriate to the data). Overall survival (OS) and event free survival (EFS) were analyzed. OS was calculated as the time from date of diagnosis to date of death of disease. Patients still alive were censored at date last seen. EFS was calculated as the time from date of diagnosis to date of first event or to the last follow-up date for patients who did not have an event. An event was defined as a recurrence or death. In those cases where death followed recurrence, the event was the recurrence.

OS and EFS for both biological and molecular variables were computed using Kaplan-Meier (Kaplan & Meier 1958) survival curves. For comparison of two or more survival curves, the log-rank test was used. The results were considered statistically significant if the 'p` value was ≤ 0.05. All the statistical analyses were done using the statistical package for the social science (SPSS), version 16.

7.4. Results

7.4.1. Assessment of correlations between clinical and histopathological variables

Correlations between the clinicopathological variables; pathology, gender and M-stage at diagnosis were found to be insignificant (Table 7.1). Correlation between M-stage and extent of tumour resection was highly significant, 95/167 cases (59.9%) with stage M 0/1 at time at diagnosis had total tumour excision compared to 10/35 cases (28.6%) with M 2/3 stage (p= 0.003). The relationship between pathology and extent of tumour resection was also significant; total tumour excision was achieved in 84/170 (49.4%) of cases with classic histopathology variant, 11/13 (84.6%) of cases with nodular/desmoplastic pathology variant and 10/19 (52.6%) of large cell / anaplastic cases, (p= 0.05) (Table 7.2).

	Pathology	**Gender**	**Metastatic stage**
Gender	0.64		
Metastatic stage	0.25	1.00	
Extent of tumour resection	0.05	0.24	0.003

Table 7.1. Inter-correlation matrix for clinicopathological variables within the PNET3 cohort. Analyses were performed using Fisher's exact test.

Clinico-pathological variables		Extent of tumour resection			Total	p value
		Total tumour excision		Subtotal tumour excision		
Pathology	Classic	84	(49.4%)	86	170	P=0.003
	N/D	11	(84.6%)	2	13	
	LC/A	10	(52.6%)	9	19	
Metastatic stage at diagnosis	M0/1	95	(60%)	72	167	P=0.05
	M2/3	10	(28.6%)	25	35	
Total		**105**		**97**	**202**	

Table 7.2. Correlation between extent of tumour resection, pathology and metastatic stage at time of diagnosis in the PNET3 cohort (Fisher's exact test)**;** N/D= nodular/ desmoplastic, LC/A= large cell/ anaplastic; M= metastatic stage.

7.4.2 Univariate survival analysis for the clinico-pathological features of the PNET3 cohort

7.4.2.1. OS and EFS characteristics of the PNET3 cohort

The median OS time for the cohort was 10.9 years (range from 10.2 to 11.8 years), 140 (67.3%) cases were censored and 68 (32.7%) died of disease; overall 5 year survival was 75.2% (Figure 7.1). The median EFS time was 10.8 years (range from 9.6 to 11 years); 136 cases (65.4%) had no events, 72 cases had events (34.6%). The 5 year EFS was 69.4% (Figure 7.2). The different treatment groups did not show a significant survival difference, 111/208 cases (53.4%) had combined radiotherapy and chemotherapy while 97/208 cases had radiotherapy only (OS and EFS, p= 0.23 and p= 0.29, respectively) (Figure 7.3).

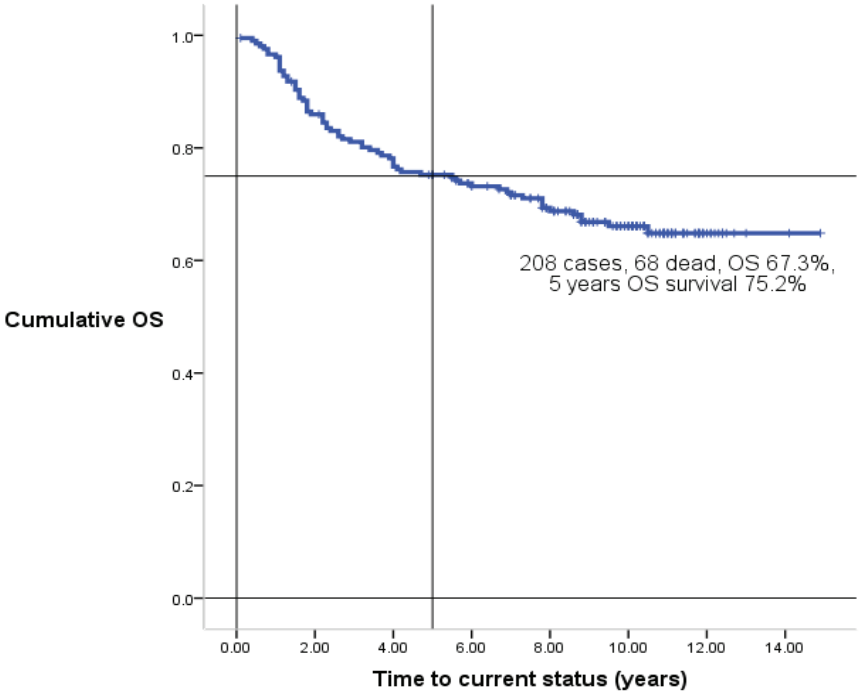

Figure 7.1. Kaplan-Meier survival analysis for overall survival (OS) of the PNET3 cohort (n=208)
The centre of the cross represents the 5 years survival.

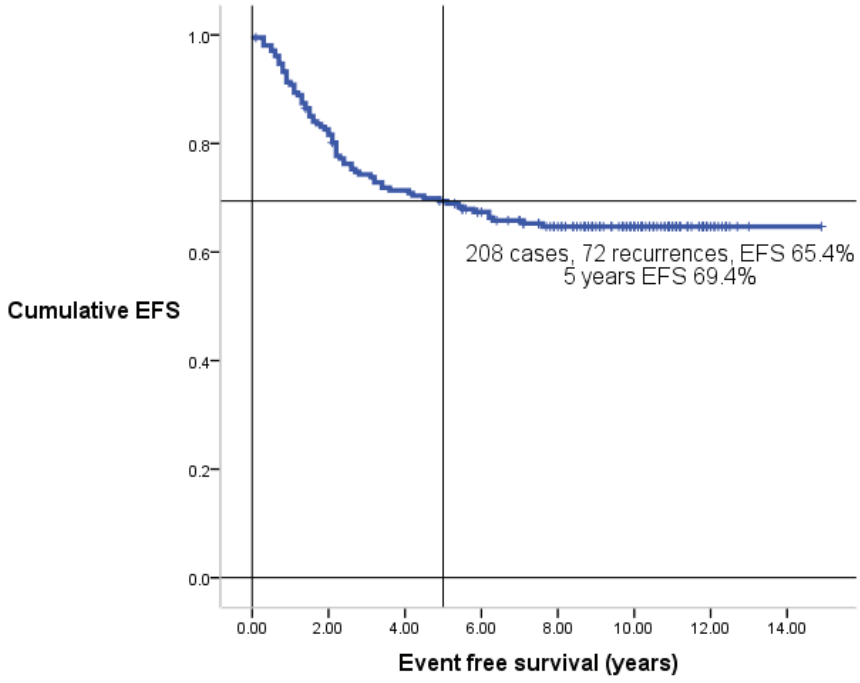

Figure 7.2. Kaplan-Meier analysis for event free survival (EFS) for the PNET3 cohort
The centre of the cross represents the 5 years EFS

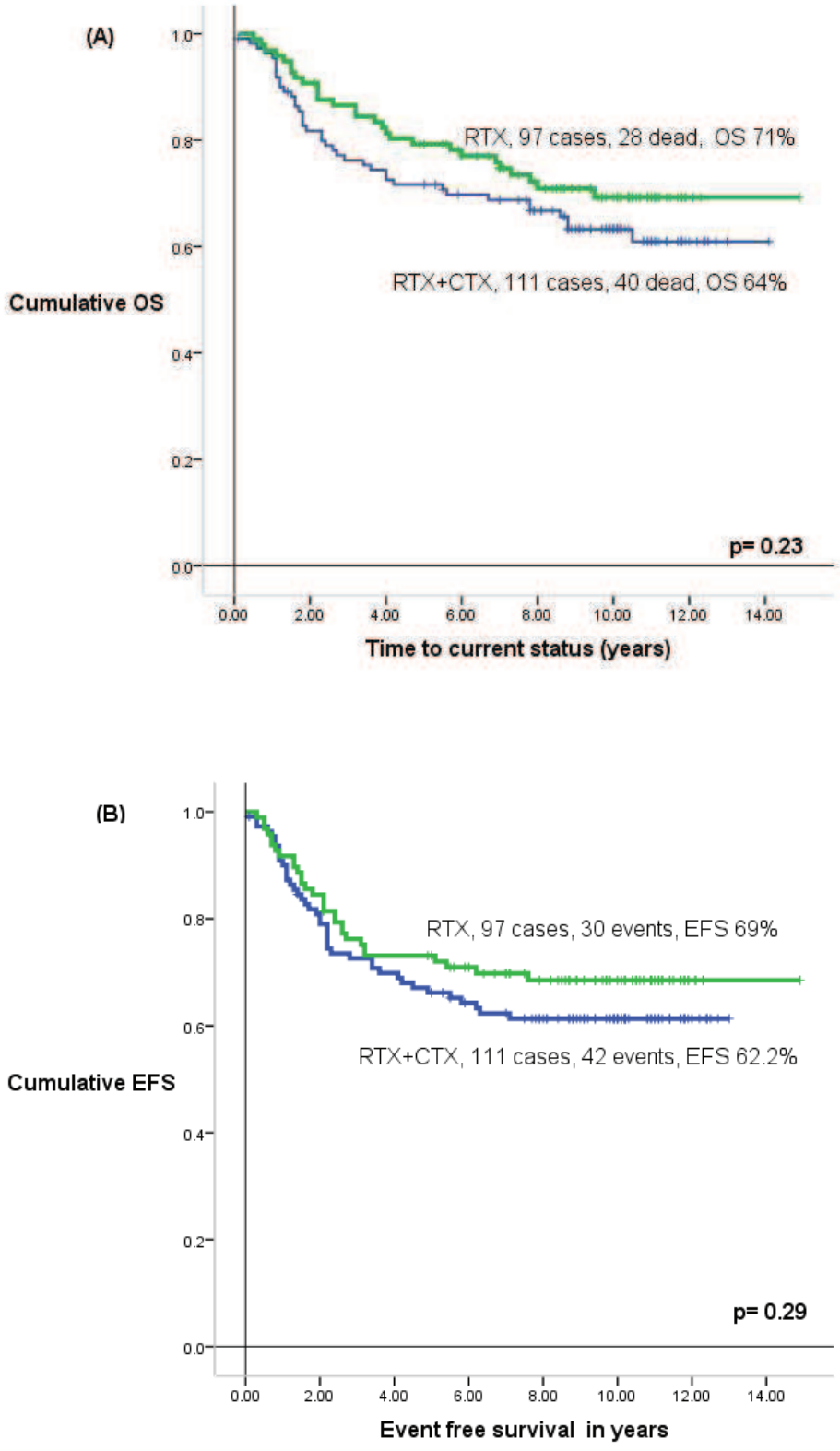

Figure 7.3. Overall survival analysis for treatment A. Overall survival (OS), B. Event free survival (EFS) (Kaplan Meier estimates and log-rank test) RTX= Radiotherapy, CTX= Chemotherapy.

7.4.2.2. Assessment of relationships between age and survival

To assess potential relationships between age and survival, the cases were grouped in 2 year intervals and data was analysed and plotted using Kaplan Meier estimates; the log-rank test was insignificant (p= 0.165). While the best survival was observed for cases aged 11-14 years (82.5%), and the worst survival was for cases aged 15-16 years (9 cases) (44.4%), the differences observed were not statistically significant (Figure 7.4, Table 7.3).

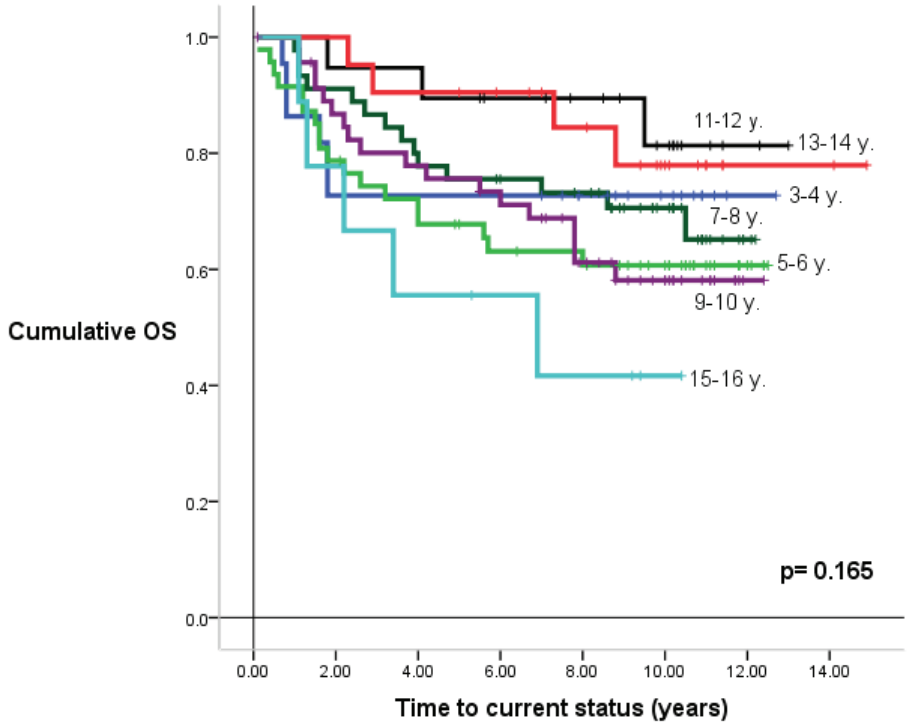

Figure 7.4. Kaplan-Meier survival curves for age grouped in 2 year intervals

2 years age interval	Total number	Number of Events	Censored	
			No.	%
≥ 3 to 4	22	6	16	72.7%
≥ 5 to 6	46	18	29	61.7%
≥ 7 to 8	44	14	31	68.9%
≥ 9 to 10	47	18	29	61.7%
≥ 11 to 12	19	3	16	84.2%
≥ 13 to 14	21	4	17	81.0%
≥ 15 to 16	9	5	4	44.4%
Total	208	68	142	67.6%

Table 7.3. Survival analysis for age grouped in 2 year intervals

7.4.2.3. Relationships between other clinicopathological disease features and survival

Gender showed a statistically significant correlation with survival, where OS and EFS 'p` values were 0.029 and 0.047, respectively favouring females. For histopathology, Large cell / anaplastic cases showed a significantly worse prognosis (p= 0.001). Metastatic stage at time of diagnosis also showed a significant correlation with OS and EFS. 121/169 (71.6%) M0/1 cases were alive compared with 19/39 (48.7%) M2/3 cases (p= 0.001). Finally, extent of tumour resection was significantly associated with a poor OS and EFS; in the total resection group, 79/105 (75.2%) cases were surviving compared with 59/97 (60.8%) for those with subtotal resection, (p= 0.027) (Tables 7.4, 7.5; Figures 7.5, 7.6).

	Variable	No.	Alive	Dead	Mean OS (Y)	95% CI (Y)	5 years OS	'p` value
Gender	Male Female	132 76	79 57	51 17	10.3 11.5	9.4-11.3 10.5-12.7	72% 81%	0.029
Pathology	Classic N/D LC/A	175 13 20	118 11 7	53 2 13	11.4 10.9 5.1	10.6-11.4 9.39-12,5 3.1-7.2	78% 92% 40%	0.001
Metastatic stage	M0/1 M2/3	169 39	21 19	48 20	11.6 6.9	10.8-12.4 5.3 – 8.5	79.6% 56.4%	0.001
Extent of tumour of resection	Total Subtotal	105 97	77 57	26 38	11.4 10.2	10.5-12.3 9-11.3	81.8% 69.6%	0.027

Table 7.4. Summary of Overall survival analyses for clinicopathological variables (Log-rank test)
(ND= Nodular/desmoplastic, LCA= Large cell/ Anaplastic; RTX= radiotherapy, CTX= Chemotherapy, Y= years).

	Variable	No.	Alive	Event	Mean OS (Y)	95% CI (Y)	5 years OS	'p` value
Gender	Male Female	132 76	79 57	53 19	9.8 10	8.7-10.9 9-11.2	65% 77%	0.047
Pathology	Classic N/D LC/A	175 13 20	118 11 7	57 2 13	10 10.6 4.8	10-11.6 8.9-12.4 2.6-7	71.7% 92% 35%	0.001
Metastatic stage	M0/1 M2/3	169 39	18 18	51 21	11 63	10-12 4.7-8	74.2% 48.7%	0.001
Extent of tumour resection	Total Subtotal	105 97	77 57	28 40	9.9 9.5	9-10.8 8-11	80% 60%	0.025

Table 7.5. Summary of event free survival analysis for clinicopathological variables (Log-rank test)
(ND= Nodular/desmoplastic, LCA= Large cell/ Anaplastic; RTX= radiotherapy, CTX= Chemotherapy, Y= years).

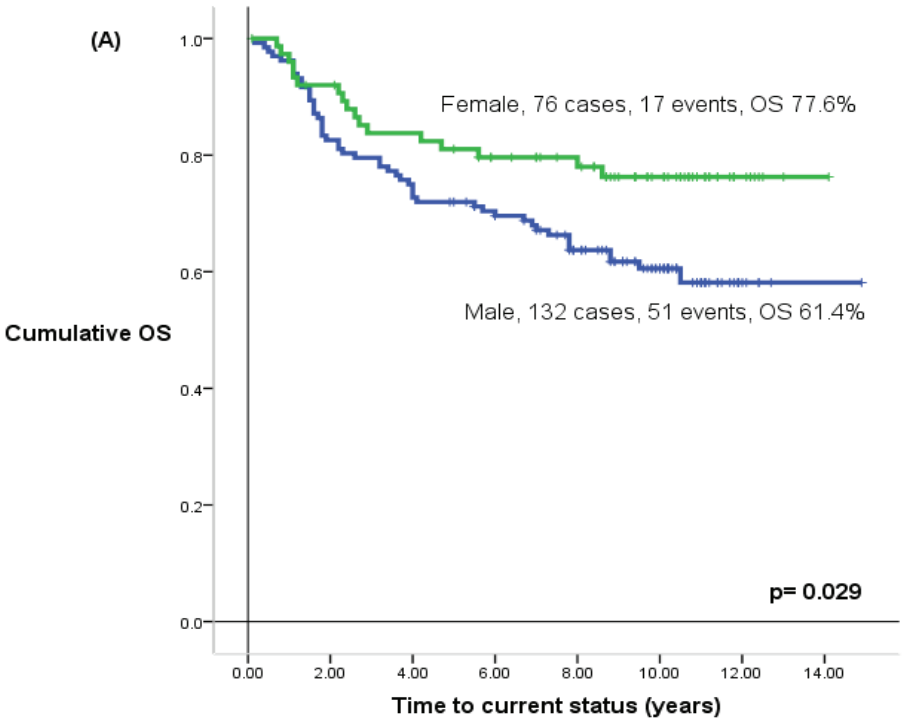
(A)
Female, 76 cases, 17 events, OS 77.6%
Male, 132 cases, 51 events, OS 61.4%
Cumulative OS
p= 0.029
Time to current status (years)

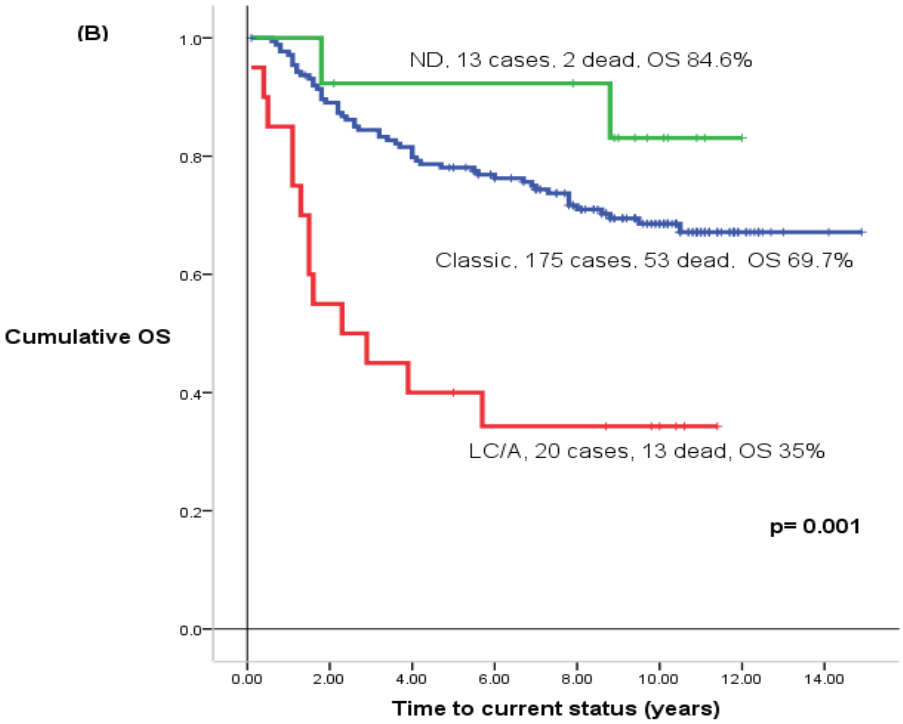
(B)
ND, 13 cases, 2 dead, OS 84.6%
Classic, 175 cases, 53 dead, OS 69.7%
LC/A, 20 cases, 13 dead, OS 35%
Cumulative OS
p= 0.001
Time to current status (years)

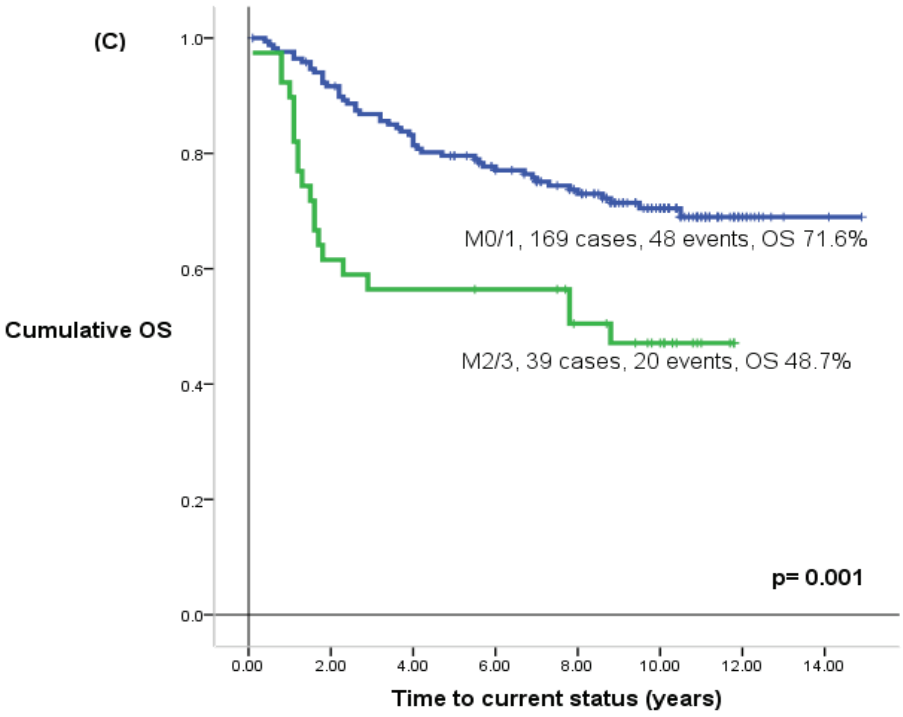

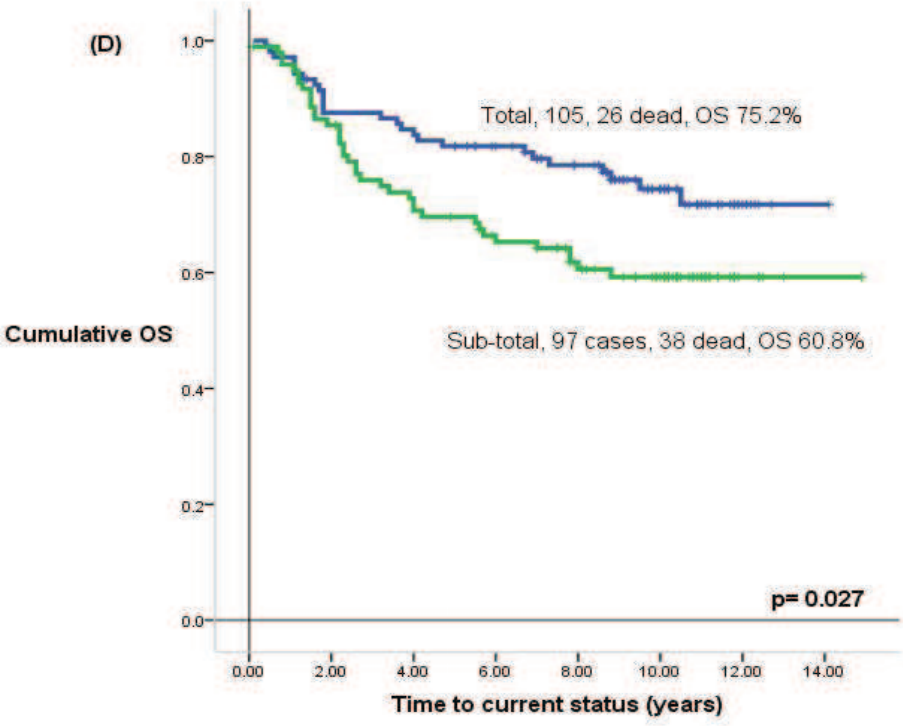

Figure 7.5. Overall survival analysis for clinicopathological variables. Kaplan Meier estimates and Log-rank tests are shown for gender (A) histopathology (B) M stage (C) extent of tumour resection (D) OS= Overall survival; F= Female, M= Male; C= Classic, ND= nodular/desmoplastic, LCA= Large cell/anaplastic; M0/1= Metastatic stage 0/1, M2/3= Metastatic stage M2/3; Total= total tumour resection, Subtotal= subtotal tumour resection).

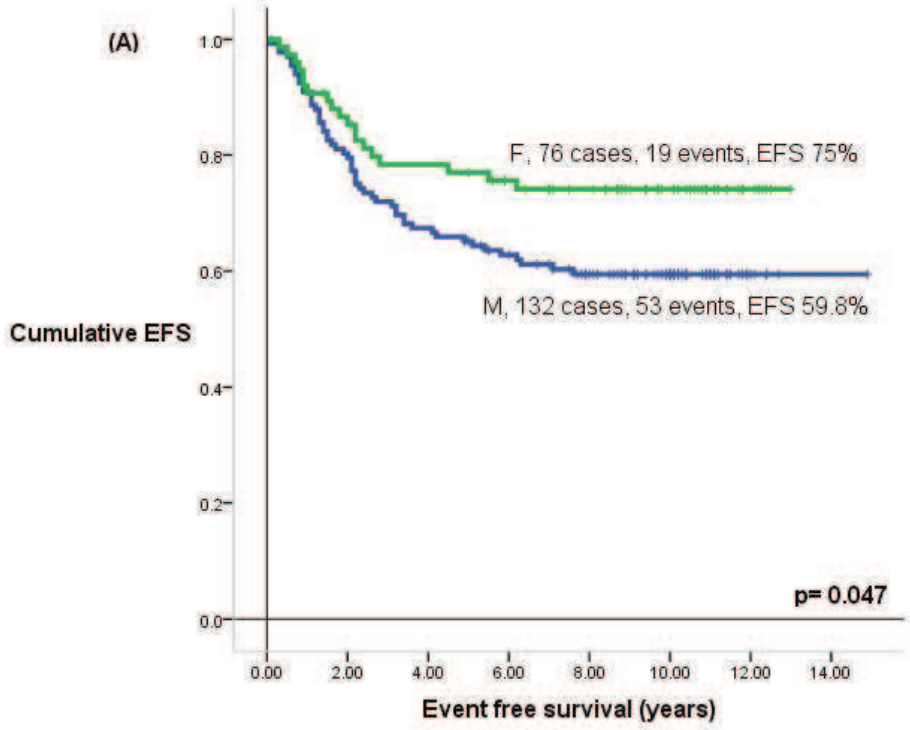
(A)
1.0
0.8
0.6
0.4
0.2
0.0
Cumulative EFS
F, 76 cases, 19 events, EFS 75%
M, 132 cases, 53 events, EFS 59.8%
p= 0.047
0.00
2.00
4.00
6.00
8.00
10.00
12.00
14.00
Event free survival (years)

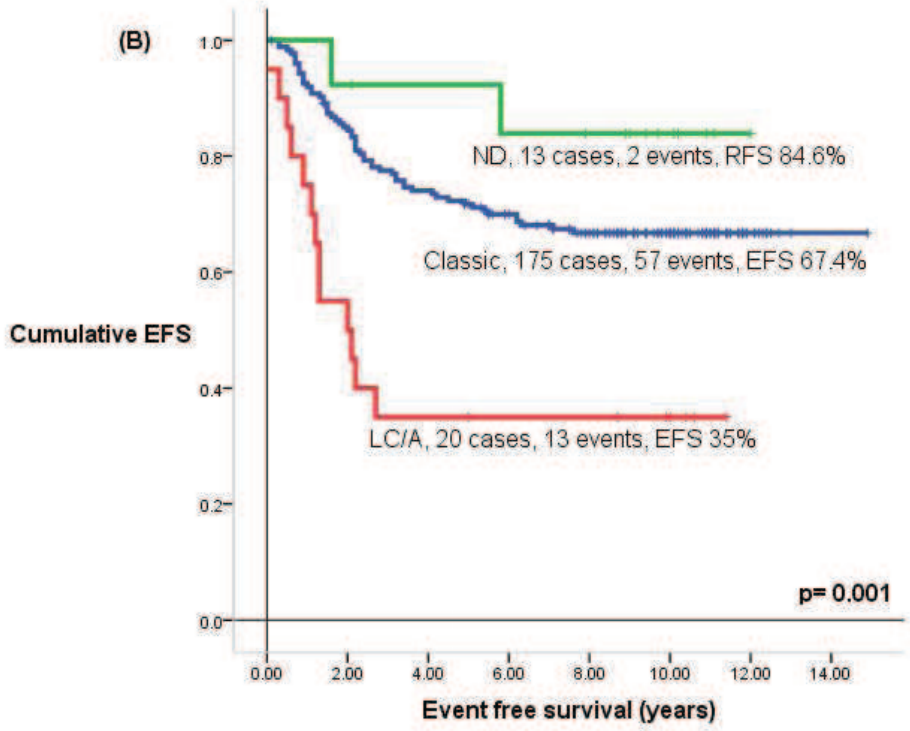
(B)
1.0
0.8
0.6
0.4
0.2
0.0
Cumulative EFS
ND, 13 cases, 2 events, RFS 84.6%
Classic, 175 cases, 57 events, EFS 67.4%
LC/A, 20 cases, 13 events, EFS 35%
p= 0.001
0.00
2.00
4.00
6.00
8.00
10.00
12.00
14.00
Event free survival (years)

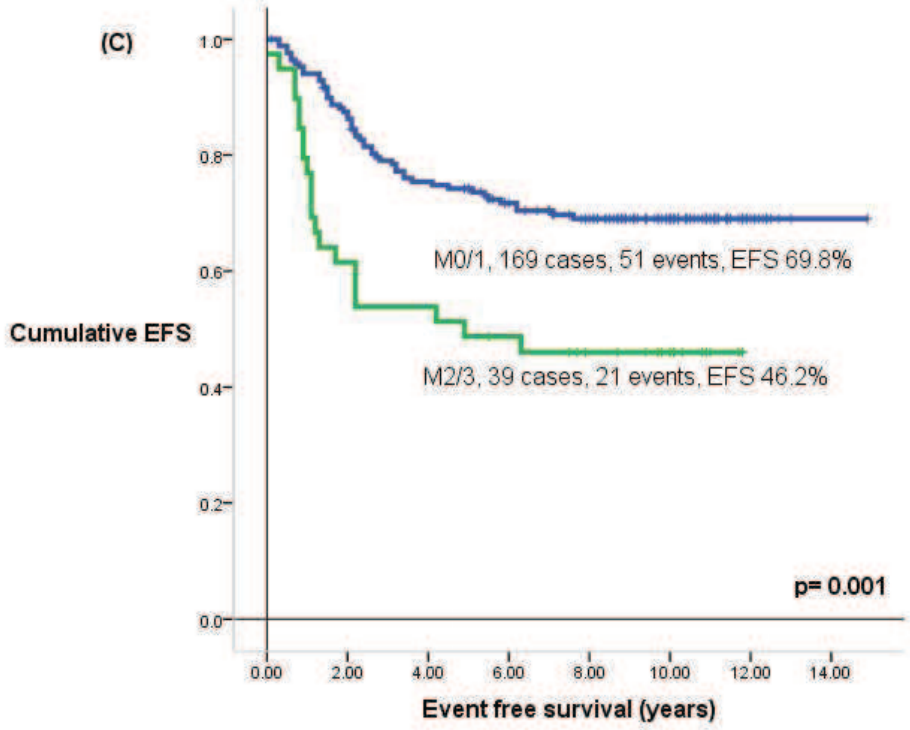

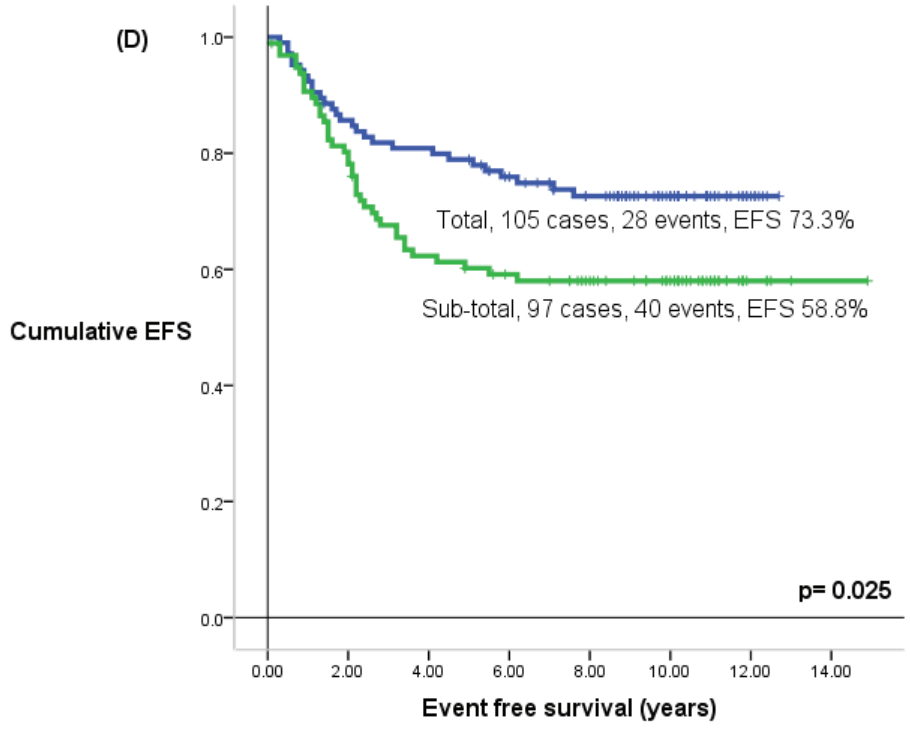

Figure 7.6. Event free survival analysis for clinicopathological variables. Kaplan Meier estimates and Log-rank tests are shown for gender (A) histopathology (B) M stage (C) extent of tumour resection (D) OS= Overall survival; F= Female, M= Male; C= Classic, ND= nodular/desmoplastic, LCA= Large cell/anaplastic; M0/1= Metastatic stage 0/1, M2/3= Metastatic stage M2/3; Total= total tumour resection, Subtotal= subtotal tumour resection).

7.4.3. Analysis of molecular variables

Univariate survival analysis of each molecular marker was computed using Kaplan-Meier survival estimates. Correlations of molecular markers with clinicopathological features and with one another were performed using Fisher's exact test.

7.4.3.1. *CTNNB1* mutations

7.4.3.1.1. Incidence in the PNET3 cohort and its clinicopathological association

A total of 197 cases were assessed for *CTNNB1* mutation by direct sequencing. 177 (89.9%) cases were wild-type, while 20 (10.1%) showed mutations. Clinicopathological associations for *CTNNB1* mutation have been described elsewhere (chapter 4).

7.4.3.1.2. Univariate survival analysis

There was a significant correlation between *CTNNB1* mutations and patients' OS and EFS (Log-rank test, p= 0.029, p= 0.022, respectively); 18/20 (90%) of cases with mutations were alive at last follow up in comparison to 111/177 cases (65%) with wild-type status. The 5 year OS for cases with *CTNNB1* mutations was 90% versus 73% for cases with wild-type *CTNNB1* (p= 0.029).The EFS at last follow-up and 5 year EFS, for cases with mutations versus wild-type cases were 90% versus 62.7% and 90% versus 66.8%, respectively (p= 0.022) (Figure 7.7). The mean EFS time for cases with mutation versus wild-type was 11.9 and 10 years, respectively.

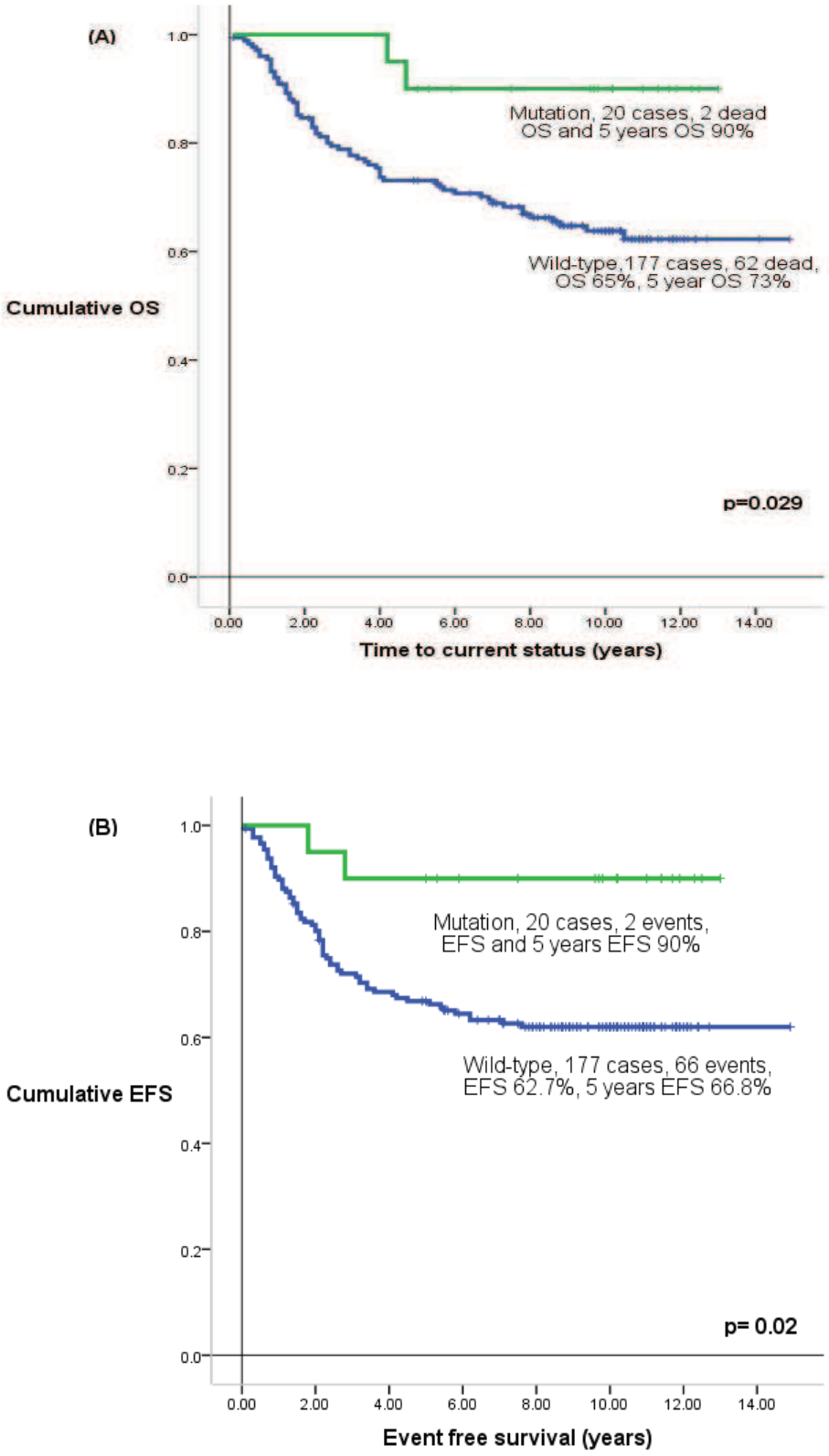

Figure 7.7. Kaplan Meier survival estimates for *CTNNB1* mutated and wild-type cases in the PNET3 cohort. (A) Overall survival (OS). (B) Event free survival (EFS)

7.4.3.2. β-catenin nuclear localization

7.4.3.2.1. Incidence in the PNET3 cohort and clinicopathological associations

A total of 207 cases were evaluated for β-catenin nuclear immuno-reactivity. 34 cases showed positive nuclear staining (16.4%), while 173 were negative (83.6%). 11/34 cases (32.4%) showed focal and strong positive staining, 21/34 cases (61.8%) showed widespread strong positive staining and 2/34 cases (5.9%) showed focal weak positive staining. These results and their associations with clinicopathological disease features are described in chapter 4.

7.4.3.2.2. Univariate survival analysis

β-catenin nuclear positive staining showed a significant correlation with OS and EFS (p= 0.004 and p= 0.002, respectively); 31/34 (91.2%) β-catenin nucleopositive cases were alive at last follow up in comparison to 109/173 (63%) negative nuclear staining cases. The EFS was 91.2% versus 60.7% for nucleopositive and nucleonegative respectively. The 5 year OS for β-catenin nucleopositive cases was 91.2% versus 72.8% for nucleonegative cases, and the 5 year EFS for the nucleopositive cases was 91.2% versus 65.8% for nucleonegative cases. Three β-catenin nuclear positive cases died of their disease during the first 5 years post-diagnosis (0.8, 4.2 and 4.8 years) (Figure 7.8). The mean overall and event free survival time was 12.1 years for β-catenin nucleopositive cases versus 10.5 years for nucleonegative cases; and 11.5 years for nucleopositive cases versus 9.9 years for nucleonegative cases respectively.

Analysis of the correlation between the degree of β-catenin nuclear staining and survival showed that cases with strong nuclear reactivity had best survival but no survival difference could be distinguished between cases with widespread or focal staining (Figure 7.9). However, the few (n=2) cases with focal and weak nuclear staining did worse, (p= 0.029) although this would require confirmation in larger cohort of samples.

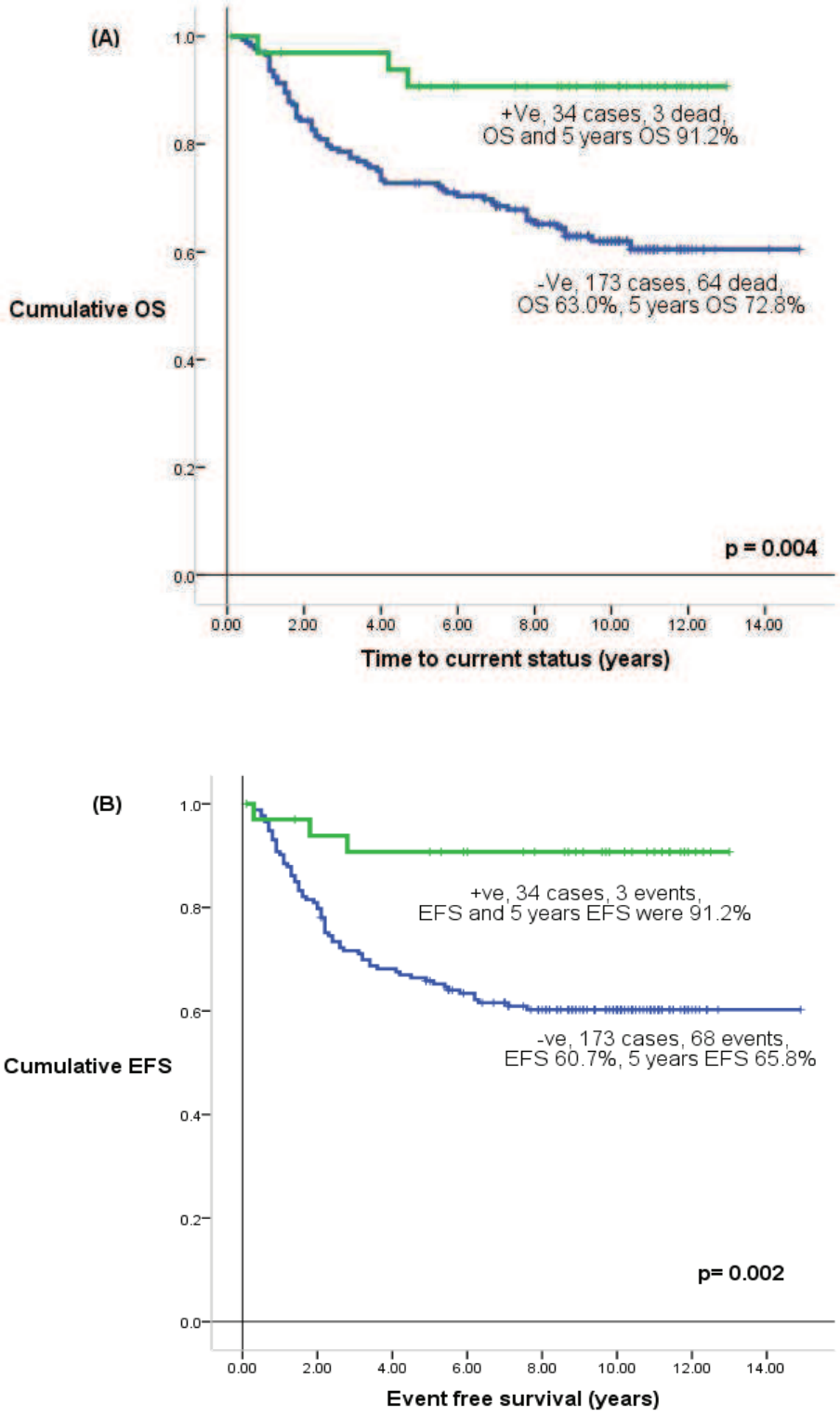

Figure 7.8. Overall survival (A) and event free survival (B) for β-catenin nuclear localization by immuno-histochemistry, positive cases versus negative cases. (Kaplan-Meier estimates and log-rank 'p` value). (+ve= positive β-catenin nuclear localization; -ve= negative β-catenin nuclear localization; OS= overall survival, EFS= Event free survival)

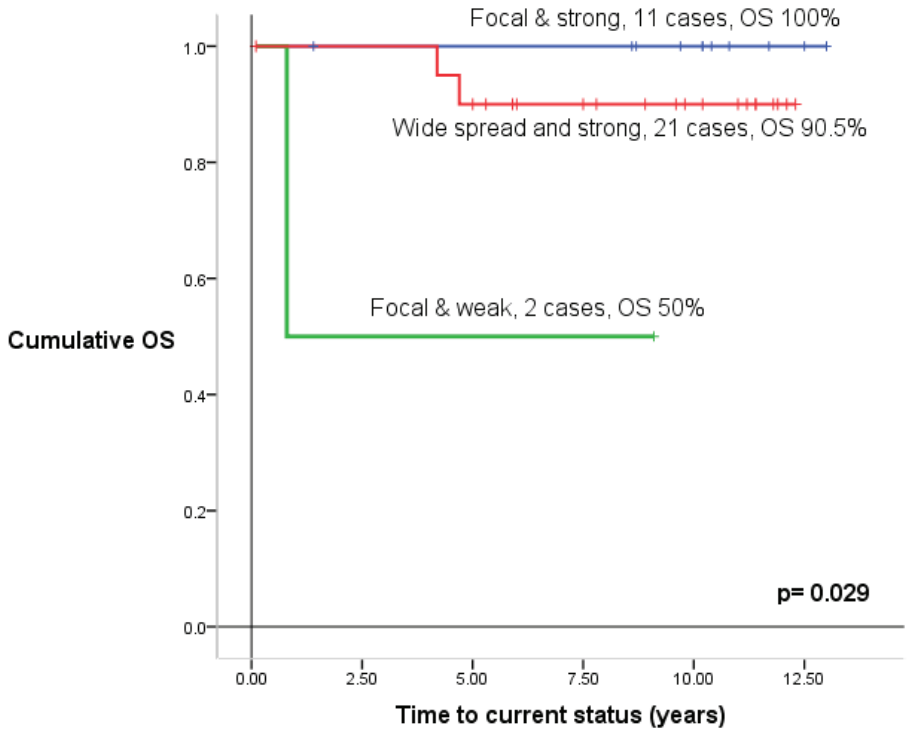

Figure 7.9. Kaplan Meier estimates of survival associations with the degree of β-catenin immuno-reactivity observed in cases with positive nuclear reactivity

7.4.3.3. Chromosome 6 LOH

7.4.3.3.1. Incidence in the PNET3 cohort and clinicopathological associations

The PNET3 cohort consists of 208 sporadic medulloblastoma samples; all were tested for chromosome 6 LOH status using the HOMOD method. A total of 190 cases successfully yielded results for chromosome 6 LOH status. Twenty cases (10.5%) showed LOH while 170 cases (89.5%) showed RET, and their clinicopathological associations have been described in chapter 6.

7.4.3.3.2. Univariate survival analysis

There was a trend for cases with chromosome 6 LOH to have a better OS and EFS but this did not reach statistical significance. OS for chromosome 6 LOH was 16/20 (80%), compared to 113/170 cases (66.5%), in the group with chromosome 6 retention (RET) (Log-rank test, p= 0.23). The 5 year OS for LOH cases compared to RET cases was 80% versus 75.6%. The EFS for chromosome 6 LOH was 80% (16/20) compared to 109/170 (64%) in cases with chromosome 6 RET (Log-rank p= 0.19). 5 year EFS for cases with chromosome 6 LOH compared to cases with RET are 80% and 68%, respectively (Figure 7.10).

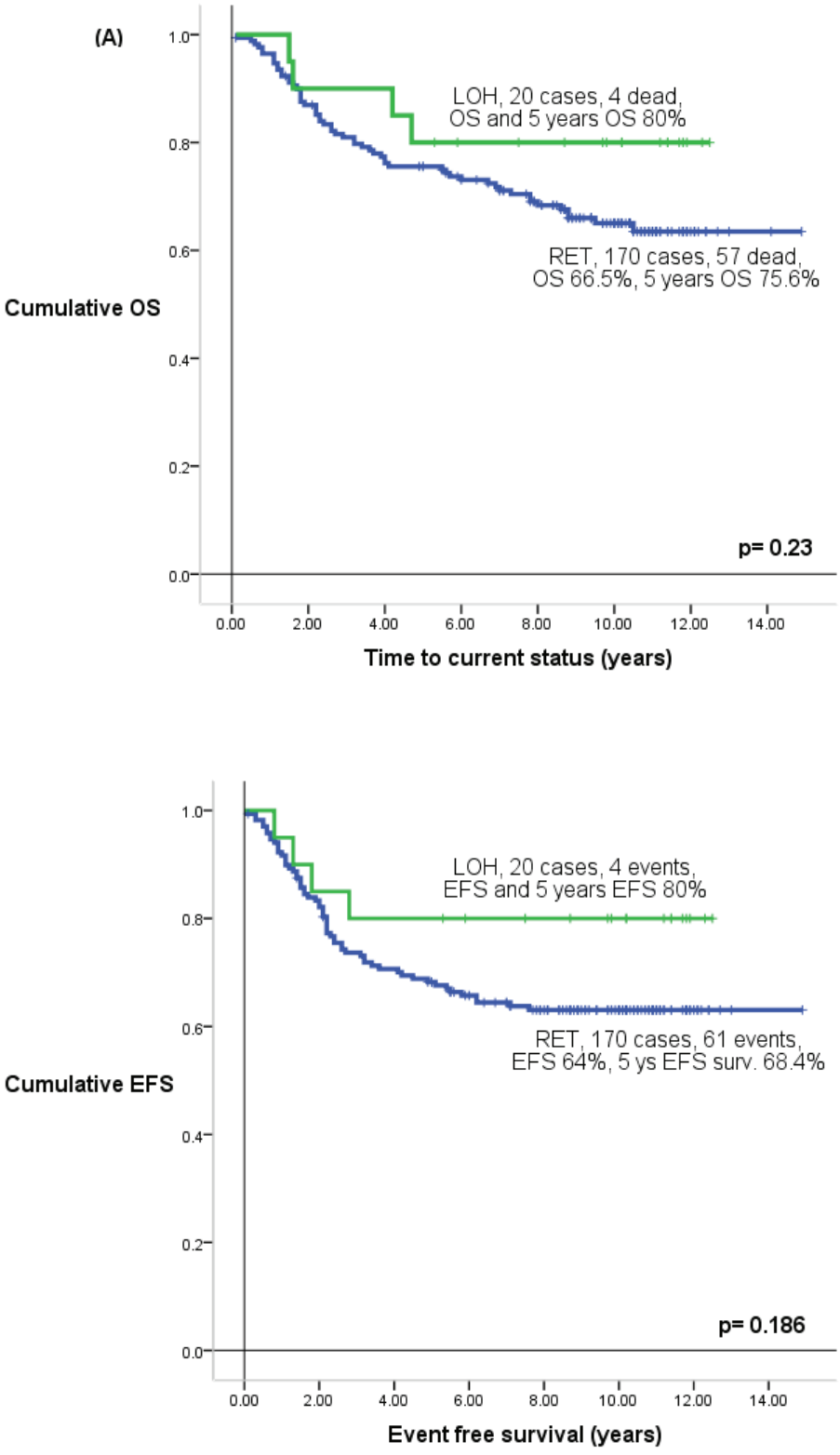

Figure 7.10. Relationship between chromosome 6 status and overall survival (OS) (A) and event free survival (B). Kaplan-Meier survival estimate, log rank test, LOH= loss of heterozygosity, RET= loss of heterozygosity.

7.4.3.4. Correlations between molecular variables

A significant relationship was found between β-catenin nuclear localization, *CTNNB1* mutation and chromosome 6 LOH. All cases with *CTNNB1* mutation (n=20) showed β-catenin nuclear localization, 6 with focal strong staining and 14 with widespread strong staining (Fisher's exact test, p= 0.001). The remaining 12/32 cases of β-catenin nuclear localization were *CTNNB1* wild-type. A marginally significant relationship was observed between extent of β-catenin nuclear positivity and *CTNNB1* mutation (Fisher's exact test, p= 0.07) and notably the 2 cases with weak focal β-catenin nuclear staining were *CTNNB1* wild-type (Table 7.6).

15/18 cases (83.3%) with chromosome 6 LOH showed *CTNNB1* mutation compared to 4/167 (2.4%) of cases within the chromosome 6 RET group (p= 0.001). 17/20 (85%) cases with chromosome 6 loss showed β-catenin nuclear localization compared to 16/169 (9.5%) cases with chromosome 6 RET (Fisher's exact test, p= 0.001) (Tables 7.7 and 7.8).

No significant correlation was observed between chromosome 17p status and β-catenin nuclear localization or *CTNNB1* mutation. 5/48 (10.4%) cases with chromosome 17p loss showed β-catenin nuclear localization compared to 28/141 (85%) cases with chromosome 17p retention (Fisher's exact test, p= 0.19). 2/48 cases (4%) with chromosome 17p loss showed *CTNNB1* mutation compared to 17/137 (12.4%) cases with chromosome 17p retention (Fisher's exact test, p= 0.165). There was a statistically significant inverse relationship between chromosome 6 LOH and chromosome 17p LOH, suggesting that the 2 events may be mutually exclusive. Only

one case had both chromosome 6 LOH and chromosome 17p LOH, while 19/20 cases with chromosome 6 LOH had chromosome 17p RET and 46/169 cases with chromosome 6 RET had chromosome 17p LOH (Fisher's exact test, p= 0.029) (Tables 7.7, 7.8, 7.9).

β-catenin positive nuclear reactivity	***CTNNB1***		**Total**
	Wild type	**mutation**	
Focal and strong	5	6	11
Wide spread and strong	5	14	19
Focal and weak	2	0	2
Total	12	20	32
Likelihood ratio, p= 0.071			

Table 7.6. Correlations between β-catenin immuno-nuclear reactivity patterns and *CTNNB1* mutation status

Molecular markers		***CTNNB1* status**			**'p' value**
		Wild-type	**Mutation**	**Total**	
		No. of cases	No. of cases	No. of cases	
β-catenin nuclear localization	**Negative**	164	0	164	p= 0.001
	Positive	12	20	32	
	Total	176	20	196	
Chromosome 6 status	**RET**	163	4	167	p=0.001
	LOH	3	15	18	
	Total	166	19	185	
Chromosome 17p status	**RET**	120	17	137	p= 0.165
	LOH	46	2	48	
	Total	166	19	185	

Table 7.7. Assessment of associations between *CTNNB1* mutations, β-catenin nuclear staining, chromosome 6 LOH and Chromosome 17p LOH status. RET = retention of heterozygosity, LOH = loss of heterozygosity.

Molecular markers		β-catenin nuclear localization status			´p` value
		Negative	Positive	Total	
		No. of cases	No. of cases	No. of cases	
***CTNNB1* status**	**Wild type**	164	12	176	p= 0.001
	Mutation	0	20	20	
	Total	164	32	196	
Chromosome 6 status	**RET**	153	16	169	p=0.001
	LOH	3	17	20	
	Total	156	33	189	
Chromosome 17p status	**RET**	113	28	141	p= 0.187
	LOH	43	5	48(	
	Total	156	33	189	

Table 7.8. Correlations between β-catenin nuclear localization, *CTNNB1* mutations, Chromosome 6 status and chromosome 17p status. RET = retention of heterozygosity, LOH = loss of heterozygosity.

Molecular markers		Chromosome 6 status			`p` value
		RET	LOH	Total	
		No. of cases	No. of	No. of cases	
Chromosome 17p status	**RET**	123	19	142	p= 0.029
	LOH	46	1	47	
	Total	169	20	189	
β-catenin nuclear localization	**Negative**	153	3	156	p=0.001
	Positive	16	17	33	
	Total	169	20	189	
***CTNNB1* status**	**Wild**	163	3	166	p= 0.001
		4	15	19	
	Mutatio	167	18	185	
	Total				

Table 7.9. Correlations between chromosome 6 status, chromosome 17p status, β-catenin nuclear localization and *CTNNB1* mutation status. RET = retention of heterozygosity, LOH = loss of heterozygosity.

7.4.3.5. Correlations between β-catenin nuclear localization, *CTNNB1* mutation and chromosome 6 LOH: Impact on patient survival

The positive correlations between *CTNNB1* mutations, β-catenin nuclear localization and chromosome 6 LOH have been described in the preceding section. Their impact as combinations in univariate survival analysis were further studied in the 184 cases which had results available for all 3 molecular markers. The 184 cases were grouped into all possible combinations and this yielded six combinations: Group A, β-catenin nuclear localization in isolation (11 cases); Group B, β-catenin nuclear localization and *CTNNB1* mutation (4 cases); Group C, β-catenin nuclear localization and chromosome 6 LOH (one case); Group D, β- catenin nuclear localization and *CTNNB1* mutations and chromosome 6 LOH (15 cases) ; Group E, chromosome 6 LOH in isolation (2 cases); Group F, negative β-catenin nuclear localization and *CTNNB*1 wild-type and chromosome 6 RET (151 cases). Their associations are summarized diagrammatically in (Figure 7.11) and shown in (Table 7.10). Kaplan-Meier survival curves for the groups are shown in Figure 7.12. Differences in survival between groups were significant. The groups negative for all Wnt/Wg pathway markers (F) and chromosome 6 loss in isolation (E) did worse. No significant differences were found between the remaining groups, which displayed β-catenin nuclear localization, either in isolation (A) or in combination with chromosome 6 loss and/ or *CTNNB1* mutations (B-D). All data shown represent OS analysis; identical associations were observed in EFS analysis (data not shown).

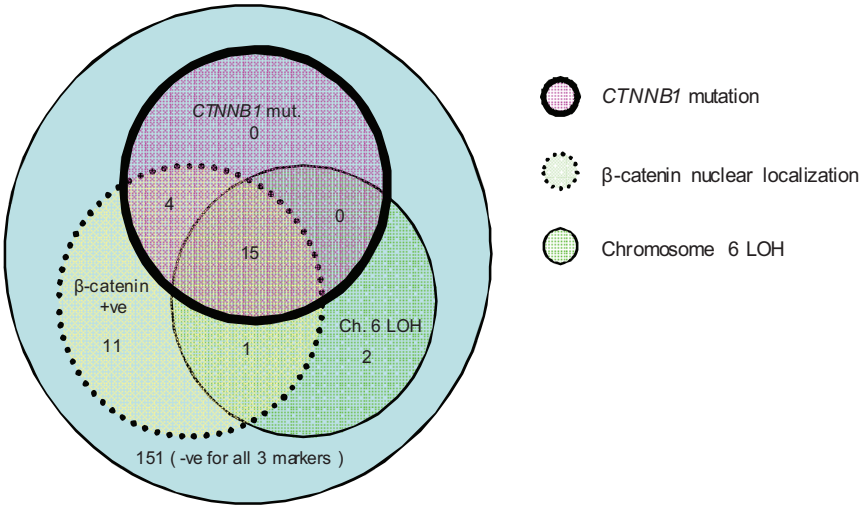

Figure 7.11. Venn diagram showing the correlation between *CTNNB1* mutations, β-catenin nuclear localization and chromosome 6 LOH in 184 cases from the PNET3 cohort

Combination groups	Possible combinations of molecular markers	No. of cases
Group A	β-catenin nuclear localization	11
Group B	β-catenin nuclear localization + *CTNNB1* mutation	4
Group C	B-catenin nuclear localization + chromosome 6 LOH	1
Group D	β-catenin nuclear localization + *CTNNB1* mutation + chromosome 6 LOH	15
Group E	Chromosome 6 LOH	2
Group F	Negative β-catenin nuclear localization + *CTNNB1* wild-type + chromosome 6 RET	151
Total number of cases		184

Table 7.10. Summary of cases displaying combinations of Wnt/Wg associated molecular markers.

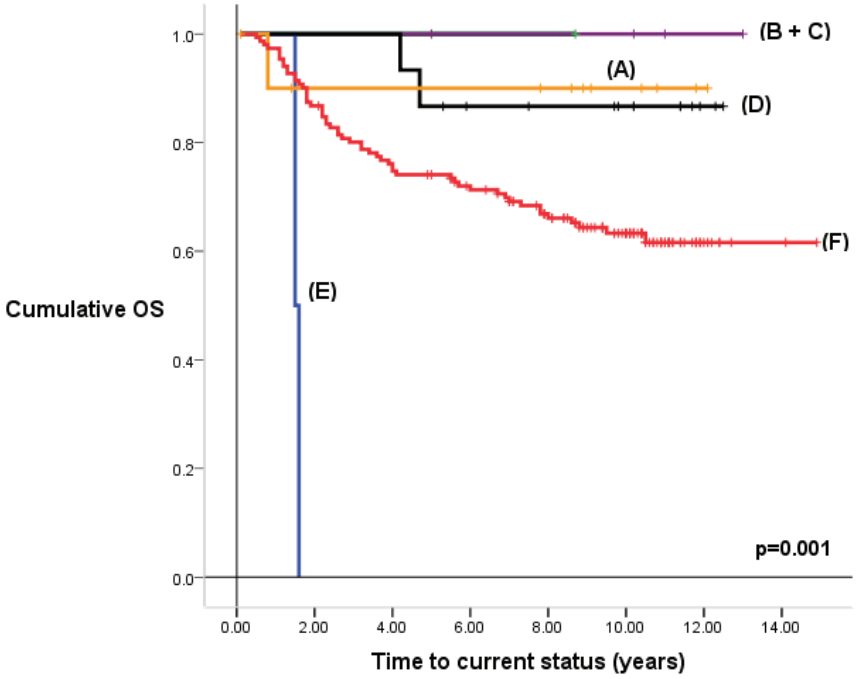

Figure 7.12. Survival analysis for Wnt/Wg associated marker groupings shown in Table 7.10.

7.5. Discussion

7.5.1. Correlations between clinicopathological disease features

The PNET3 cohort composed of 208 primary medulloblastoma samples and relationship between its clinicopathological features were analysed. A significant association was observed between extent of tumour resection and histopathology subtype (Fisher's exact test, p= 0.05) and metastatic stage at diagnosis (Fisher's exact test, p= 0.003). Total tumour excision was more successfully achieved in cases with nodular/desmoplastic histopathology and in cases which presented with M0/1 at time of diagnosis, than in cases with non-desmoplastic pathology or had M2/3 disease at time of diagnosis. The implications of these findings on the outcome of patients are discussed below.

7.5.2. Correlations between molecular markers and clinicopathological disease features

The correlation between molecular markers of Wnt/Wg pathway activation (β-catenin nuclear localization, *CTNNB1* mutation and chromosome 6 LOH) and clinicopathological disease features (age, gender, metastatic stage at diagnosis, extent of tumour resection and treatment) were all insignificant. This indicates that tumours with Wnt/Wg activation can only be detected using molecular/immuno methods (see also chapters 4-6). For 17p LOH, the only significant association was with histopathological subtype, where its relationship with chromosome 17p LOH was significant (p= 0.01); all nodular/desmoplastic cases were chromosome 17p RET (see

chapter 3). This contradicts the findings of Lamont et al (2004) and McManamy et al (2007) where they found that 17p defects occurred across all pathological variants.

7.5.3. Correlation between the molecular markers

There was a significant correlation between β-catenin nuclear localization and *CTNNB1* mutations. 32 cases showed β-catenin nuclear localization and 20/32 (62.5%) showed *CTNNB1* mutations. The 12 wild-type samples may represent cases with mutations in exons other than exon 3 of *CTNNB1*, or with mutations affecting other components of the Wnt/Wg pathway, and this will be of interest for further analysis. Cases with β-catenin nuclear localization lacking *CTNNB1* mutations were previously reported in other studies (Eberhart et al 2000, Ellison et al 2005, Clifford et al 2006, Thompson et al 2006). However, all found that mutations were exclusively found in tumours with β-catenin nuclear localization, consistent with our findings.

Correlations between chromosome 6 LOH, *CTNNB1* mutations and β-catenin nuclear localization were also significant, in concordance with other studies (Clifford et al 2006, Thompson et al 2006, Kool et al 2008, Fattet et al 2009, Pfister et al 2009), while a significant inverse correlation was found between chromosome 6 LOH and chromosome 17p LOH suggesting that the 2 events may be mutually exclusive.

The relationship between β-catenin nuclear accumulation and chromosome 6 LOH or *CTNNB1* mutations was independent of the degree of nuclear immunopositivity observed for β-catenin; equivalent associations were observed in both focal and widespread nuclear staining cases. Notably the two cases with weak nuclear positive

immunostaining were not associated with either chromosome 6 loss or *CTNNB1* mutations, suggesting they do not display Wnt/Wg pathway activation.

7.5.4. Univariate survival analysis

The 5 years OS and EFS for the entire cohort were 75.2% and 69.4% respectively, consistent with survival rates for standard-risk medulloblastoma in studies reported in the literature (Ellison 2002). All cases reported in the trial were ≥ 3 years of age at diagnosis. In this chapter, all cases were assessed for univariate survival associations based on each of the 3 molecular markers of Wnt/Wg activation (β-catenin nuclear localization, *CTNNB1* mutations and chromosome 6 LOH) tested, and with clinical and pathological disease features. Chromosome 17p survival association in this cohort has already been described in chapter 3.

7.5.4.1. Correlation between clinicopathological features and survival

For clinical features, age at diagnosis showed no significant correlation with survival (t-test, 0.67). The OS and EFS univariate analysis revealed that clinicopathological variables (gender, histopathology, metastatic stage at diagnosis and extent of tumour resection) showed significant correlation with both EFS and OS; male gender, large cell / anaplastic pathology, M2/3 stage and subtotal tumour resection were each associated with a poor prognosis, consistent with previous findings (reviewed by Pizer and Clifford 2009). While the association between metastatic disease and the extent of tumour resection have been widely reported (Gilbertson et al 2001, Pfister et al 2009), and currently influence clinical disease stratification, the

poor prognostic association with male gender and large cell / anaplastic pathology in not currently used in the assessment of disease risk.

7.5.4.2. Correlations between molecular markers and survival

The overall and event free survival analysis showed significant association between favourable prognosis and β-catenin nuclear localization, consistent with previous studies (Ray et al 2004, Ellison et al 2005, Clifford et al 2006, Fattet et al 2009). Notably, a similar relationship was also obtained for *CTNNB1* mutation, which has not been reported previously. Despite its significant correlation with *CTNNB1* mutations and β-catenin nuclear localization, chromosome 6 loss was not associated with a better prognosis. As reported and discussed in chapter 3, chromosome 17p LOH was not significantly associated with a poor survival.

To assess the relative prognostic impact of the 3 molecular markers of Wnt/Wg activation *(CTNNB1* mutation, β-catenin nuclear localization and chromosome 6 LOH), the 184 samples which successfully yielded results for all 3 markers were clustered into all possible combinations; this yielded six groups (Table 7.10 ,Figure 7.11 and 7.12). Kaplan-Meier estimates showed equivalent good survival in cases with β-catenin nuclear localization alone or in combination with other pathway markers (chromosome 6 LOH, *CTNNB1* mutations), while a worse survival was seen in cases with chromosome 6 RET, *CTNNB1* wild-type and negative β- catenin nuclear localization, or chromosome 6 loss in isolation and this yielded a highly significant result between the 6 curves (Figure 7.12, P=0.001). Thus, cases with β-catenin nuclear localization alone did not appear to behave differently to cases with nuclear localization combined with another marker of the Wnt/Wg disease subgroup,

suggesting that examination of β-catenin status is sufficient for the identification of this favourable prognosis group in future studies. Nonetheless, *CTNNB1* mutation and/ or chromosome 6 loss, when found in conjunction with nuclear β-catenin accumulation, do offer useful confirmative markers of the Wnt/Wg disease group.

Notably, the 2 cases with weak positive β-catenin nuclear staining both showed *CTNNB1* wild-type and had a poor survival, further indicating that these cases are not associated with Wnt/Wg activation or a good prognosis. In the study by Fattet et al (2009) three cases which showed positive β-catenin nuclear staining in < 10% of the cells were *CTNNB1* wild-type, and all had poor survival. It may be postulated that this subgroup is comparable to our subgroup presenting with positive weak nuclear staining.

The interplay between Wnt/Wg pathway activation and other prognostically significant clinicopathological features, and their multivariate survival analysis, will be undertaken in the next chapter. This will help in assessing risk factors and defining optimal disease risk stratification schemes based on clinicopathological and molecular variables.

7.6. Conclusions

1. The overall survival and event free survival of the PNET3 cohort was 67.3% and 65.4% respectively, which is similar to survival rates for equivalent cases reported in the literature.

2. Univariate survival analysis showed significant associations between OS and EFS for gender favouring females; histopathology favouring classic and nodular/ desmoplastic; metastatic stage at diagnosis favouring M0/1 and extent of tumour resection favouring total excision.

3. There is a strong correlation between the 3 molecular markers (*CTNNB1* mutations, β-catenin nuclear localization and chromosome 6 LOH) of Wnt/Wg pathway activation in individual samples.

4. A significant inverse correlation between chromosome 6 LOH and chromosome 17p LOH was observed, suggesting they are mutually exclusive.

5. *CTNNB1* mutation and β-catenin nuclear localization showed a highly significant correlation with an improved survival.

6. Chromosome 6 LOH was not associated with improved survival.

7. Cases with strong, focal or widespread, nuclear accumulation of β-catenin display equivalent relationships to survival, *CTNNB1* mutation and chromosome 6 loss.

Weakly staining cases are not associated with a good prognosis, *CTNNB1* mutation or chromosome 6 loss, indicating they do not represent Wnt/Wg subtype cases.

Chapter 8

Combination of clinical, histopathological and molecular markers for disease risk stratification in medulloblastoma

8.1. Introduction

Vast improvements have been made in the diagnosis and treatment of patients with medulloblastoma; survival rates can reach 60-80% for clinical standard-risk patients, but can still be as low as 40% for high-risk patients. However, clinical indices for the prediction of outcome are imprecise. Currently, patients are classified according to clinical risk stratification markers (e.g. metastatic stage at diagnosis, extent of tumour resection; see Introduction). 20-40% of standard-risk patients will experience disease relapse, while a subset of low-risk patients could potentially be cured with less invasive therapeutic protocols, sparing them the devastating side effects of treatment (Rutkowski et al 2007). Also, a subset of high-risk patients are cured using conventional therapeutic protocols. Subsets of patients may therefore be placed in the wrong risk category, as their disease risk can not be identified by clinical factors alone. Adding molecular markers of known prognostic significance may allow improvement of the current classification and accordingly more accurate tailoring of treatment, and has been the focus of many research studies in recent years.

Several studies have assessed the utility of combinations of clinicopathological and molecular markers to improve the current disease risk stratification system for medulloblastoma. In 2004, Gajjar et al investigated 97 medulloblastoma samples for several molecular markers (*ERBB2, MYCC*, *MYCN* and TrkC mRNA) alongside clinical and histopathological review of these samples. Statistical analysis revealed that ERBB2 expression was associated with poor survival and large cell/anaplastic pathology ($p= 0.031$ and $p= 0.005$, respectively). All ERBB2 negative patients were alive at 5 years

versus 54% of standard-risk, ERBB2 positive patients (p= 0.0001). Therefore, these data suggest the use of ERBB2 expression could be added to clinicopathological risk factors to provide more accurate disease risk stratification.

Ray et al (2004) assessed combining clinical and biological markers in order to quantify the risk for medulloblastoma patients in order to provide a more informative stratification system. The molecular variables they used included expression of MYC, P53, PDGFA, ERBB2, MIBI and TrkC detected by IHC as well as assessing markers of apoptosis. Univariate and multivariate analysis were used to characterize the association between survival, clinical and biological markers. This showed that the 4 strongest predictors of survival were metastatic disease at presentation (H.R. 2.02; p= 0.01), *P53* (H.R. 2.29; p= 0.02), *ERRB2* (H.R. 1.51; p= 0.21) and TrkC (H.R. 0.65, p= 0.14). The group proposed combining clinical and biological markers to quantify risk in medulloblastoma patients and to shy away from the rigid framework of dividing all patients into groups of high-risk and low-risk since a substantial number of patients do not meet the outcome prediction of one of the above mentioned groups.

In 2009, Pfister et al investigated the introduction of novel tumour-derived biomarkers aiming to improve the current clinical classification and its dependent treatment decision. They used aCGH and FISH techniques on 2 independent cohorts of 80 and 260 medulloblastoma samples, respectively. The latter technique, which served as a validation set, analysed chromosome 6q, 17p, 17q, *MYCC* and *MYCN.* Copy number aberrations were correlated with the clinicopathological disease features and patients' outcome.

Accordingly, they proposed and defined a hierarchical molecular staging system composed of 5 groups; (1) *MYC*/*MYCN* amplification, (2) 6q gain, (3) 17q gain, (4) 6q and 17q balanced, and (5) 6q deletion. Group (1) showed the worst prognosis while group (5) was the most favourable. This staging system was tested and validated in the validation set (n=260) using FISH. They compared the Cox proportional hazards model including only clinicopathological variables with the Cox model that additionally included the above molecular staging system. A highly significant additional effect of the molecular staging system on the prediction of EFS and OS was found (each $p < 0.001$). These results led to the conclusion that genomic aberrations represent powerful independent prognostic markers and their addition to established clinicopathological variables could substantially improve the established clinical disease classification.

Another study by Lamont et al (2004) demonstrated that combining histopathological indices and molecular cytogenetics may refine patients' disease classification, offering a reduction in the therapeutic late effects among patients with predicted good outcome. 87 medulloblastoma cases were assessed for their histopathological subtype, as well as investigating chromosome 17 aberrations, losses of 9q22, 10q24 and amplification of the *MYCC* and *MYCN* oncogenes. Medulloblastomas of large cell / anaplastic pathology represented 20% of the cases and are significantly associated *MYCC* or *MYCN* amplifications; both of these events appeared to be independent prognostic markers. Collectively, patients with large cell / anaplastic pathology, 17p13.3 loss or high-frequency *MYC* amplification represented a

subgroup with a significantly poor outcome compared to patients not displaying any of these characteristics.

Previous studies have shown that Wnt/Wg active tumours are a distinct subgroup of medulloblastoma that can be identified using molecular methods (Clifford et al 2006). In the previous chapter, we assessed the prognostic significance of 3 molecular markers of Wnt/Wg activation (*CTNNB1* mutations, β-catenin nuclear localization and chromosome 6 LOH) and chromosome 17p LOH in a large set of cases from the PNET3 cohort. Correlations between these markers and clinicopathological features of the disease with survival showed that gender, metastatic stage at diagnosis, pathological subtypes, extent of tumour resection, *CTNNB1* mutations, and β-catenin nuclear localization were all significant markers of prognosis in univariate analysis.

This final chapter reports the development of combined schemes in which these markers may be used for the improved prediction of disease risk in medulloblastoma.

8.2. Aims

The aims of this chapter are:

1. To assess the incorporation of all the clinical, pathological and molecular variables which proved independently statistically significant in chapter 7 by univariate survival analysis, into a multivariate Cox regression analysis in order to produce a weighted predictive score based on their hazard ratios.

2. To use this scoring system to construct models which could be applied to individual patients in order to predict their prognosis more accurately.

8.3. Materials and Methods

8.3.1. The PNET3 cohort

The PNET3 cohort assessed was composed of 208 primary medulloblastoma samples. The full characteristics of the cohort are described in chapter 2, section 2.1.2.

8.3.2. Statistical analysis

Survival analysis for the clinicopathological variables (gender, metastatic stage at diagnosis, extent of tumour resection, pathology) and the molecular variables (β-catenin nuclear localization and *CTNNB1* mutation) were computed using Kaplan-Meier survival curves. For comparing 2 or more survival curves the log-rank test was used. Multivariate survival analysis was computed for the significant clinicopathological and molecular variables using Kaplan-Meier estimates and log-rank tests.

Prognostic variables observed and associated hazard ratios were tested individually in Cox proportional regression models. Those significant ($p< 0.05$) variables were entered into multiple multivariate Cox proportional regression hazard ratio analyses taking the value of $p< 0.05$ to enter and $p> 0.05$ to be removed.

8.3.3. Variables used in multivariate survival analysis and their categorization

The variables which were significant using univariate survival analysis in chapter 7 were incorporated in multivariate survival analysis. These factors were;

metastatic stage at diagnosis, extent of tumour resection, gender, pathology, and β-catenin nuclear localization. Although significantly associated, *CTNNB1* mutation was not assessed since it represented a subset of cases sharing β-catenin nuclear localization, which did not have a significantly different prognosis from the wider group (Chapter 7).

Metastatic stage at diagnosis was categorized M0/1 for standard-risk and M2/3 for high-risk, extent of tumour resection was categorized into total and sub-total for standard-risk and high-risk respectively, β-catenin nuclear localization was classified as positive nuclear localization for cases showing strong wide spread or focal staining and negative nuclear localization for cases showing cytoplasmic or negative staining. Pathologically, cases were grouped into a classic and/or nodular / desmoplastic category and large cell / anaplastic category. Finally, samples were categorized according to patients' gender into groups of males and females.

8.4. Results

8.4.1. Classification of cases using current clinical criteria

Risk assessment for medulloblastoma patients is currently based on clinical parameters; where high and standard-risk groups are classified using the three clinical variables of age, metastatic stage at time of diagnosis and extent of tumour resection. Cases at time of diagnosis aged ≥ 3 years, with M0/1 stage, and a total tumour resection are considered to be standard-risk, while cases aged less than 3 years at diagnosis and/or M2/3 disease and/or with subtotal tumour excision are considered to be high-risk (reviewed in Pizer and Clifford 2009).

The PNET3 cohort were all aged ≥ 3 years, so only 2 clinical variables were used to assign disease risk; metastatic stage and extent of tumour resection. The cases were therefore classified into a standard-risk group (M0/1 and gross tumour resection; 95 cases) and a high-risk group (M2/3 and/or subtotal tumour resection; 107 cases) (Table 8.1, Figure 8.1). Survival analysis of these groups showed a statistically significant result (p= 0.011).

Risk variables	Total no.	Event	Censored	% OS
M0/1 + gross tumour resection (standard-risk)	95	22	73	76.8%
M2/3 or subtotal tumour resection (high-risk)	107	42	65	60.8%
Total	202	64	138	
Log-rank test, p= 0.011				

Table 8.1. Survival analysis using current clinical stratification schemes based on metastatic stage and extent of tumour resection. M = metastatic stage, OS = overall survival.

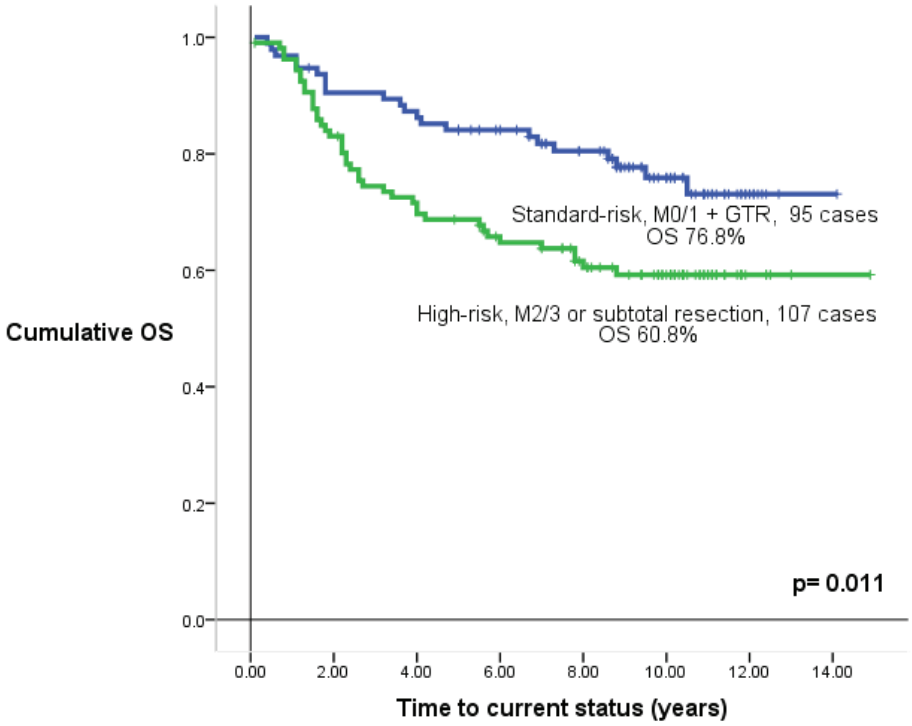

Figure 8.1. Survival analysis based on clinical stratification variables, (metastatic stage and extent of tumour resection). GTR = gross tumour resection.

Although the current clinical classification mentioned above successfully classifies patients, still it lacks precision and some standard-risk patients develop tumour relapse while some high-risk patients are cured.

8.4.2. Investigation of statistical models based on combined clinical, pathological and molecular markers

Supplementing the established clinical variables with additional clinical, pathological or molecular variables may refine the current risk classification. Models could be developed which help predict the hazard ratio for specific disease features.

The data was therefore next analysed using univariate and multivariate multiple Cox proportional regression hazard ratio models.

Univariate Cox proportional hazard ratio regression analyses were first applied for all the biological and molecular variables. These were tested independently to see which were significant and could be used in multivariate multiple Cox regression analyses. Gender (p= 0.032, hazard ratio 0.55 favouring females), pathology (p= 0.001, hazard ratio 3.57, favouring the classic and nodular/desmoplastic group), metastatic stage at time of diagnosis (p= 0.001, hazard ratio 2.36, favouring M0/1), extent of tumour resection (p= 0.03, hazard ratio 1.74, favouring total resection), and β-catenin nuclear localization (p= 0.009, hazard ratio 0.21 favouring positive nuclear staining) were all significantly associated with overall survival. Chromosome 6 status and chromosome 17p status, age at diagnosis and treatment allocated all showed no significant relationship to survival (Table 8.2).

	`B'	**`p' value**	**Hazard ratio**
Gender (male vs. female)	-.602	0.032	0.55
Pathology (CLA/ND vs LC/A)	1.272	0.000	3.57
M-stage (MO/1 vs M2/3)	.858	0.001	2.36
Treatment	.292	0.236	0.75
Extent of tumour resection Total vs subtotal excision	.554	0.030	1.74
Age	.023	0.544	0.977
β-catenin nuclear localization	-1.54	0.009	0.21

Table 8.2. Summary of Cox regression univariate survival analyses for clinical and molecular variables
CLA= classic, ND= nodular/desmoplastic, LC/A = large cell/anaplastic; `B' = regression coefficient of the variable.

8.4.2.1. A combination model for the prediction of disease risk based on 5 variables

Initially, a model incorporating all variables which had a statistically significant ‘p` values in the univariate Cox proportional regression analysis was constructed. The variables used in this model were gender, pathology, metastatic stage at time of diagnosis, extent of tumour resection and β-catenin status. In this model, variables tested showed a significant ‘p` value, with the exception of metastatic stage at diagnosis and extent of tumour resection (p= 0.233 and p= 0.098, respectively, Table 8.3). Although these last 2 variables showed a significant ‘p` value in their univariate survival analysis (Log-rank test, OS p= 0.001 and p= 0.027, respectively, Table 7.4) and in their univariate Cox proportional regression analysis (see above), when they were incorporated in the 5 variables model they showed insignificant ’p` values because of their multicolinear relationship (Fisher’s exact test, p= 0.003, Table 7.1). The extent of tumour resection variable was therefore preferentially excluded since it may depend on the surgical technique and resources as well as surgeons’ experience and not on the clinicopathological patients’ profile. This led to the construction of a 4 variable model (see next section).

Variables in the equation.	b	'p`	HR	95% CI	
				Lower	Upper
Gender (female vs. male)	-0.617	0.038	0.54	0.301	0.967
Pathology (CLA or N/D vs. LC/A)	1.217	0.001	3.376	1.733	6.577
Metastatic stage (M0/1 vs. M2/3)	0.37	0.233	1.448	0.788	2.661
Ext. of tumour resection (total vs. subtotal)	0.438	0.098	1.55	0.922	2.607
β-catenin nuclear staining (+ve vs. –ve)	-1.537	0.010	0.215	0.067	0.690

Table 8.3. Cox proportional regression hazard model incorporating 5 variables. CLA = classic, N/D = nodular/desmoplastic, b= coefficient of the independent explanatory variable, HR = hazard ratio CI= confident interval of the hazard ratio.

8.4.2.2. A combination model for the prediction of disease risk based on 4 significant variables

A model was constructed based on 4 significant variables (β-catenin status, metastatic stage at time of diagnosis, pathology and gender). Multiple Cox forward step-wise proportional regression hazard ratio analysis was applied to the above named variables. All variables were independently prognostic, and yielded statistically significant 'p` values; β-catenin status (p =0.009 and hazard ratio 0.212, favouring positive nuclear staining); metastatic stage at time of diagnosis (p= 0.017 and hazard ratio 1.933, favouring M0/1); pathology (p= 0.001 and hazard ratio 3.354, favouring classic or nodular/desmoplastic cases) and gender (p= 0.039 and hazard ratio 0.56, favouring females) (Table 8.4).

Independent risk variable	b	'p`	H.R.	95% CI for H.R.
β-catenin status	-1.539	0.009	0.215	0.067-0.69
Pathology	1.205	0.000	3.338	1.76-6.32
Gender	- 0.562	0.046	0.57	0.33-0.99
Metastatic stage	0.654	0.017	1.924	1.12-3.31

Table 8.4. Multiple multivariate Cox proportional hazard regression model incorporating β-catenin status, pathology, gender and metastatic stage at time of diagnosis. b = regression variable coefficient, H.R.= hazard ratio, CI = confident interval for the hazard ratio**.**

Based on these 4 variables, patients may present with a variety of clinicopathological and molecular disease features. These individualized criteria lead to 16 different combinations by which a patient can present; each has a different hazard ratio for death to occur. The linear Cox proportional hazard ratio regression equation was applied to each possible combination (Table 8.5). The Cox proportional hazard ratio regression equation is ($Y = b_0 + b_1X_1 + b_2 X_2 + b_3 X_3 + b_k X_k$) (Cox 1972, Clark et al 2003, Bradburn et al 2003) ('Y` is the log of the hazard ratio to occur, 'b` is the regression coefficient of the variable and 'X` is the independent explanatory variable). From this table, the combination with least hazard of death to occur was number 1 (tumours with β-catenin IHC positive, classic or nodular/desmoplastic pathology, M0/1 metastatic stage at time of diagnosis and females (hazard ratio 0.12)). The combination with the highest hazard of death was model 16 (β-catenin IHC negative, large cell/anaplastic pathology subtype, metastatic stage M2/3 and male (Hazard ratio 6.5)). Generally, models with a positive β-catenin nuclear localization had a lower hazard ratio than those with a negative β-catenin nuclear localization. In order to simplify clinical application of these combinations, hazard ratios were grouped into favourable-risk group (cases with H.R. <1), a standard-risk group (H.R. = 1) and a high-risk group (H.R. >1). Notably, none of the cases in the PNET3 cohort presented with

combination number 11 (tumours with β-catenin nucleopositive staining, M2/3 stage at time of diagnosis, large cell / anaplastic histopathology and male).

	β-Catenin status	Pathology	Metastatic stage	Gender	Y = log of H.R.	Hazard ratio	No. of cases observed in the PNET3 cohort	Risk
1	Positive(1) $b_1 \times 1 = b_1$	Classic N/D (0) $b_2 \times 0 = 0$	M0/1 (0) $b_3 \times 0 = 0$	Female(1) $b_4 \times 1 = b_4$	$b_1 + b_4 = -2.101$	0.122	29	F.R.
2	Positive(1) $b_1 \times 1 = b_1$	Classic N/D (0) $b_2 \times 0 = 0$	M0/1 (0) $b_3 \times 0 = 0$	Male(0) $b_4 \times 0 = 0$	$b_1 = -1.539$	0.214	15	F.R.
3	Positive(1) $b_1 \times 1 = b_1$	Classic N/D (0) $b_2 \times 0 = 0$	M2/3(1) $b_3 \times 1 = B_3$	Female(1) $b_4 \times 1 = b_4$	$b_1 + b_3 + b_4 = -1.447$	0.235	2	F.R.
4	Positive(1) $b_1 \times 1 = b_1$	LC/A(1)) $b_2 \times 1 = b_2$	M0/1 (0) $b_3 \times 0 = 0$	Female(1) $b_4 \times 1 = b_4$	$b_1 + b_2 + b_4 = -0.896$	0.408	2	F.R.
5	Positive(1) $b_1 \times 1 = b_1$	Classic N/D (0) $b_2 \times 0 = 0$	M2/3 (1) $b_3 \times 1 = b_3$	Male(0) $b_4 \times 0 = 0$	$b_1 + b_3 = -0.885$	0.412	2	F.R.
6	Negative(0) $b_1 \times 0 = 0$	Classic N/D (0) $b_2 \times 0 = 0$	M0/1 (0) $b_3 \times 0 = 0$	Female(1) $b_4 \times 1 = b_4$	$b_4 = -0.562$	0.570	45	F.R.
7	Positive(1) $b_1 \times 1 = b_1$	LC/A(1)) $b_2 \times 1 = b_2$	M0/1 (0) $b_3 \times 0 = 0$	Male(0) $b_4 \times 0 = 0$	$b_1 + b_2 = -0.334$	0.716	2	F.R.
8	Positive(1) $b_1 \times 1 = b_1$	LC/A(1) $b_2 \times 1 = b_2$	M2/3(1) $b_3 \times 1 = b_3$	Female(1) $b_4 \times 1 = b_4$	$b_1 + B_2 + b_3 + b_4 = -0.242$	0.785	1	F.R.
9	Negative(0) $b_1 \times 0 = 0$	Classic N/D (0) $b_2 \times 0 = 0$	M0/1 (0) $b_3 \times 0 = 0$	Male(0) $b_4 \times 0 = 0$	0	1.00	83	S.R
10	Negative(0) $b_1 \times 0 = 0$	Classic N/D (0) $b_2 \times 0 = 0$	M2/3 (1) $b_3 \times 1 = b_3$	Female(1) $b_4 \times 1 = b_4$	$b_3 + b_4 = 0.092$	1.096	11	H.R
11	Positive(1) $b_1 \times 1 = b_1$	LC/A(1) $b_2 \times 1 = b_2$	M2/3(1) $b_3 \times 1 = b_3$	Male(0) $b_4 \times 0 = 0$	$b_1 + B_2 + b_3 = .32$	1.377	0	H.R.*
12	Negative(0) $b_1 \times 0 = 0$	LC/A(1)) $b_2 \times 1 = b_2$	M0/1 (0) $b_3 \times 0 = 0$	Female(1) $b_4 \times 1 = b_4$	$b_2 + b_4 = 0.64$	1.929	4	H.R.
13	Negative(0) $b_1 \times 0 = 0$	Classic N/D (0) $b_2 \times 0 = 0$	M2/3 (1) $b_3 \times 1 = B_3$	Male(0) $b_4 \times 0 = 0$	$b_3 = 0.654$	1.924	18	H.R.
14	Negative(0) $b_1 \times 0 = 0$	LC/A(1)) $b_2 \times 1 = b_2$	M0/1 (0) $b_3 \times 0 = 0$	Male(0) $b_4 \times 0 = 0$	$b_2 = 1.205$	3.33	7	H.R.
15	Negative(0) $b_1 \times 0 = 0$	LC/A(1) $b_2 \times 1 = B_2$	M2/3(1) $b_3 \times 1 = B_3$	Female(1) $b_4 \times 1 = b_4$	$b_2 + b_3 + b_4 = 1.297$	3.65	1	H.R.
16	Negative(0) $b_1 \times 0 = 0$	LC/A(1) $b_2 \times 1 = b_2$	M2/3(1) $b_3 \times 1 = b_3$	Male(0) $B_4 \times 0 = 0$	$b_2 + b_3 = 1.859$	6.42	4	H.R.

Table 8.5. Multiple multivariate Cox proportional regression hazard model based on 4 variables: β-catenin, pathology, metastatic stage and gender applied on the PNET3 cohort Pathology, Classic or N/D = Classic or nodular/desmoplastic; LC/A= large cell /anaplastic; R.S. = risk stratification; F.R= Favourable risk, S.R. = Standard risk, H.R= High risk. The Cox multivariate proportional regression equation is: $Y = b_0 + (b_1X_1 + b_2X_2 + b_3X_3)$Y = log of the hazard ratio; b = regression coefficient variable; X = independent variable. X_1 = M stage variable, $b_1 = 0.654$; X_2 = Pathology variable; $b_2 = 1.205$; X_3 = β-catenin status variable, $b_3 = -1.539$; X_4 = gender, $b_4 = -0.562$. Y is log Hazard ratio of the event happening.Code for (X) Independent variables: β-catenin status: positive = 1, negative = 0; Pathology: Classic or N/D = 0, LC/A=1; Metastatic stage: M0/1 = 0, M2/3 = 1. Dependant variable (status or event): Alive = 0 and Dead = 1. R.S = risk stratification, F.R.= favourable risk result, S.R. = standard risk result; H.R. = high risk result . H.R.* = no cases in this category in this cohort.

8.4.2.3. A combined model for predicting disease risk based on 3 significant variables

Although gender was a significant independent prognostic factor, it has produced an inconsistent association with survival in different previous studies. Weil et al (1998) reported a significant association between females and better outcome compared to males, while Curran et al (2009) identified a similar correlation only among patients aged >3 years at diagnosis but not among patients <3 years at diagnosis. Also, gender has not been fully investigated in large clinically controlled trials. On the other hand, the other 3 variables used in the above model (metastatic stage at diagnosis, pathology and β-catenin nuclear staining) have all now been tested and validated in multiple trials-based cohorts (reviewed by Pizer and Clifford 2009).Therefore, a 3 variable model was constructed, which could be confidently clinically applied at the present time.

A model based on these 3 significant variables (β-catenin status, M-stage at diagnosis and pathology) may therefore help in calculating the hazard ratio for death and would be used to predict patients' outcome (Table 8.6). Based on these 3 variables, patients can present with 8 different possible combinations; each carried a different hazard ratio for death to occur. The multiple Cox proportional hazard regression equation was applied to each possible combination (Table 8.7). It could be concluded that the least hazard for death to occur was combination number 1 (nuclear positive β-catenin, classic or nodular/desmoplastic pathology and metastatic stage M0/1 (H.R. = 0.21)). The combination with the worst outcome was number 8 (negative

nuclear β-catenin, large cell / anaplastic pathology and M2/3 (H.R. = 6.51)). Not a single case in the 208 cases of the PNET3 cohort presented with combination number 5 (positive β-catenin nuclear staining and metastatic stage at diagnosis M2/3 and large cell / anaplastic histopathology).

Independent risk variable	b	'p`	H.R.	95% CI for H.R.
β-catenin status	-1.551	0.009	0.212	0.066-0.677
Pathology	1.206	<0. 00001	3.34	1.768-6.308
Metastatic stage	0.668	0.015	1.95	1.138-3.344

Table 8.6. Multiple multivariate Cox proportional hazard regression model incorporating β-catenin status, pathology and metastatic stage at time of diagnosis. b = regression variable coefficient, H.R.= hazard ratio, CI = confident interval for the hazard ratio.

	β-catenin status (1)	Pathology (2)	Metastatic stage (3)	Y = log of HR	Hazard ratio	No. of cases observed in the PNET3 cohort	Overall risk status
1	Positive (1) $b_1 X 1 = b_1$	Classic-N/D (0) $b_2 X 0 = 0$	M0/1(0) $b_3 X 0 = 0$	$b_1 = -1.551$	0.21	27	F.R.
2	Positive (1) $b_1 X 1 = b_1$	Classic-N/D (0) $b_2 X 0 = 0$	M2/3(1) $b_3 X 1 = b_3$	$b_1 + b_3 = 0.883$	0.41	4	F.R.
3	Positive (1) $b_1 X 1 = b_1$	LC/A(1) $b_2 X 1 = b_2$	M0/1(0) $b_3 X 0 = 0$	$b_1 + b_2 = 0.345$	0.71	3	F.R.
4	Negative (0) $b_1 X 0 = 0$	Classic-N/D (0) $b_2 X 0 = 0$	M0/1(0) $b_3 X 0 = 0$	0	1	128	S.R.
5	Positive (1) $b_1 X 1 = b_1$	LC/A(1) $b_2 X 1 = b_2$	M2/3(1) $b_3 X 1 = b_3$	$b_1 + b_2 + b_3 = 0.323$	1.4	0	H.R.*
6	Negative (0) $b_1 X 0 = 0$	Classic-N/D (0) $b_2 X 0 = 0$	M2/3(1) $b_3 X 1 = b_3$	$b_3 = 0.668$	1.95	29	H.R.
7	Negative (0) $b_1 X 0 = 0$	LC/A (1) $b_2 X 1 = b_2$	M0/1(0) $b_3 X 0 = 0$	$b_2 = 1.206$	3.34	11	H.R.
8	Negative (0) $b_1 X 0 = 0$	LC/A (1) $b_2 X 1 = b_2$	M2/3(1) $b_3 X 1 = b_3$	$b_2 + b_3 = 1.874$	6.51	5	H.R.

Table 8.7. Multiple Cox proportional regression model based on β-catenin status, M-stage and pathology groupings applied on the PNET3 cohort. Classic or N/D = Classic or nodular/desmoplastic pathology; LC/A= large cell /anaplastic pathology; R.S. = risk stratification; F.R= Favourable risk, S.R. = Standard risk, H.R= High risk, H.R.* no cases with this combination presented in PNET3 cohort.The Cox multivariate proportional regression equation is: $Y = b_0 + (b_1X_1 + b_2X_2 + b_3X_3)$. Y = log of the hazard ratio; b = regression coefficient variable; X = independent variable. X_1 = M stage variable, $b_1 = 0.668$; X_2 = Pathology variable; $b_2 = 1.206$; X_3 = β-catenin status variable, $b_3 = -1.551$, Y is log Hazard ratio of the event happening. Code for the (X) independent variables: β-catenin status: positive = 1, negative = 0; Pathology: Classic or N/D = 0, LC/A=1; Metastatic stage: M0/1 = 0, M2/3 = 1; Dependant variable (status or event): Alive = 0 and Dead = 1

8.4.2.4. Kaplan-Meier survival estimates applied to a model based on 3 variables

Based on the factors showing prognostic significance in univariate survival analysis, multivariate survival analysis was undertaken for the 3 variables (β-catenin status, pathology and metastatic stage at diagnosis). The PNET3 cohort was divided into 3 groups and compared using Kaplan Meier estimates and log-rank tests. Group 1 comprised cases with metastatic at diagnosis M0/1, classic or nodular/ desmoplastic pathology, and positive β-catenin nuclear localization. Group 2 were as group 1 but with negative β-catenin nuclear localization. Group 3 comprised cases with metastatic stage M2/3 or large / cell anaplastic pathology subtype irrespective of β-catenin status. Group 1 had the best survival and hence was termed favourable-risk group (F). The third group had the worst survival and was termed the high-risk group (H). Group 2 survival was termed the standard-risk group (S) (Table 8.8, Figure 8.2). Despite the significant association between positive β-catenin nuclear staining and favourable prognosis, Insufficient data currently exists to alter the risk status for patients which also display any of the clinical high-risk criteria, which have been strongly associated with aggressive medulloblastoma phenotype indicating intensive therapeutic protocols, and it may be risky to propose any reduction in therapy based on current evidence. Therefore, the high-risk group did not take in consideration the β-catenin nuclear status in this analysis.

Risk variables	No. of cases	Events	Censored	% OS
Favourable-risk group M0/1 + classic N/D + positive β-catenin IHC	27 (13%)	2	25	92.6%
Standard-risk group M0/1 + classic N/D + negative β-catenin IHC	128 (61.5%)	38	90	70.3%
High-risk group M2/3 or LCA (β-catenin positive or negative)	53 (25.5%)	28	25	47.2%
Total	208	68	140	
Log-rank test, p = 0.001				

Table 8.8. Survival analysis for risk groups defined by β-catenin nuclear localization, metastatic stage and pathology variables. ND = nodular/desmoplastic, LCA = large cell/anaplastic, OS= overall survival.

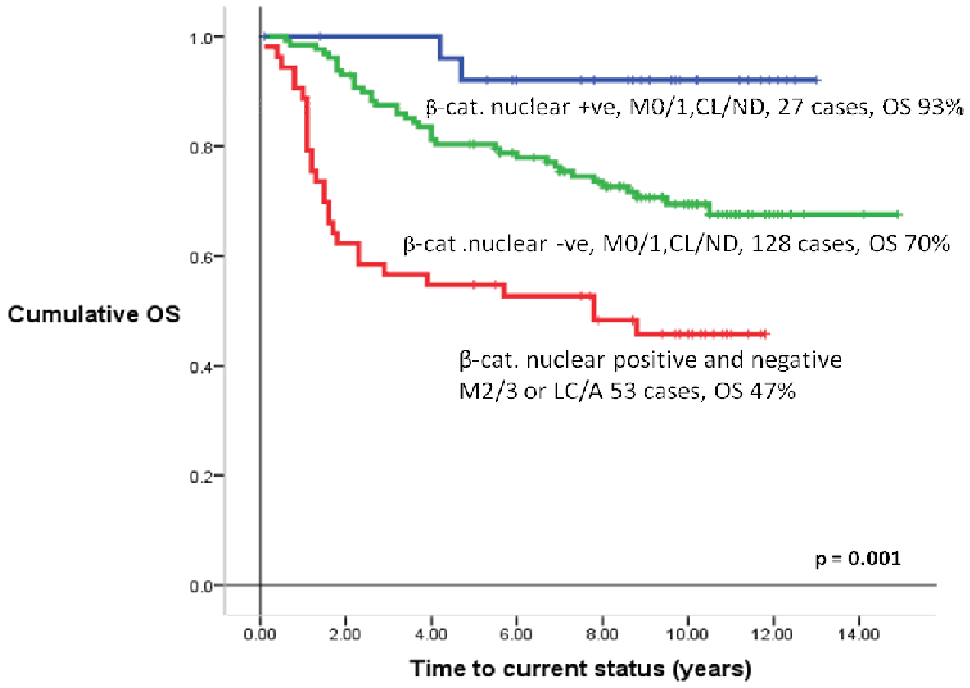

Figure 8.2. Survival analysis for favourable (blue), standard (green) and high (red) risk groups defined by β-catenin nuclear localization, metastatic stage and pathology variables (CL= classic, ND= nodular/ desmoplastic, LC/A= large cell/anaplastic)

8.4.2.5. Interaction between Wnt/Wg subtype tumours and high-risk disease markers

Relationships of high-risk disease features (metastatic stage at time of diagnosis and pathological subtypes) to the positive β-catenin IHC cases were next compared. Group 1 cases consisted of cases with β-catenin positive nuclear staining, M0/1 and classic or nodular/desmoplastic pathology (i.e. with no high-risk features); and group 2 cases had positive β-catenin nuclear staining and M2/3 disease and/or large cell / anaplastic pathology. Although Group 1 had a trend toward a better outcome, this did not reach significance (log-rank test, p= 0.57) in multivariate survival analysis (Table 8.9, Figure 8.3). These data indicate that clinical and pathological high-risk markers are not associated with an adverse prognosis when observed in the context of Wnt/Wg subgroup cases. Of particular note, this approach further supports the observation that β-catenin nuclear-positive cases which also display high-risk features (large cell / anaplastic pathology or M2/3 disease), are associated with a favourable disease risk.

Risk variables	No. of cases	Events	Censored	% OS
Group1 Positive nuclear β-catenin + M0/1 + classic or N/D pathology	27	2	25	92.6%
Group 2 Positive nuclear β-catenin + M2/3 or LC/A pathology	7	1	6	85.7%
Total	34	3	31	
Log-rank test, p = 0.57				

Table 8.9. Survival analysis for metastatic stage and pathology variables in cases with β-catenin nuclear positivity. M= metastatic stage, N/D = nodular/desmoplastic, LCA = large cell/anaplastic.

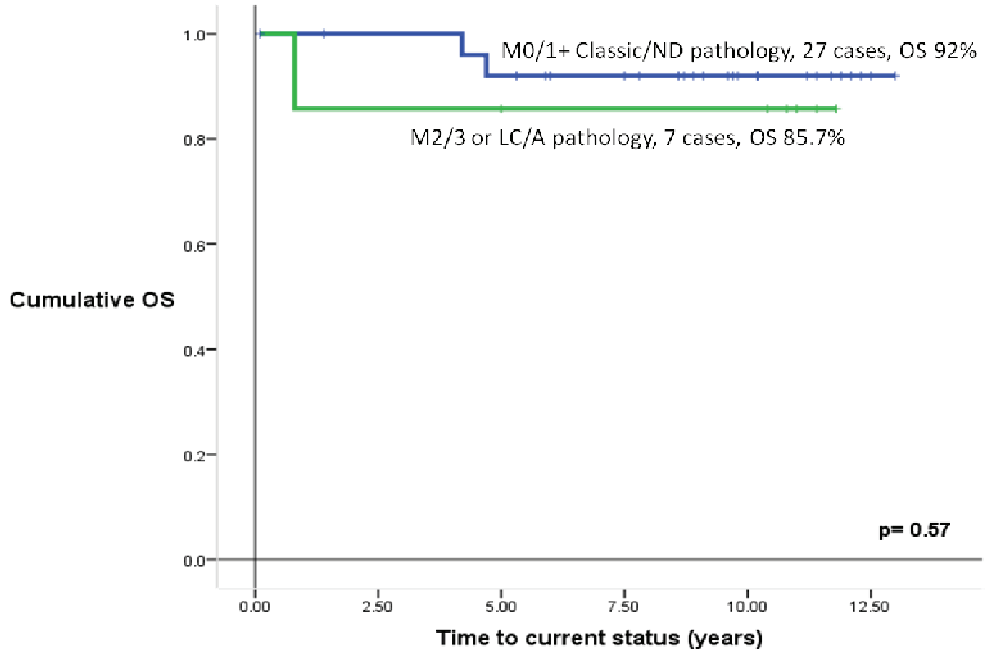

Figure 8.3. Kaplan-Meier survival curves for M-stage and pathology variables in cases with positive β-Catenin nuclear positivity. OS= overall survival; CL= classic; LC/A= large cell anaplastic; N/D= nodular desmoplastic.

8.4.2.6. Effect of gender and extent of tumour resection on survival in β-catenin positive cases

Survival analysis estimates were generated to compare cases with positive β-catenin nuclear staining and gender (males versus females). An insignificant association was observed (Log-rank test, p= 0.37) (Figure 8.4). A similar concept was applied for the extent of tumour resection, where survival analysis was produced comparing cases with positive β-catenin nuclear staining and extent of tumour resection (total tumour resection versus cases with subtotal tumour resection). There was no difference in survival between the 2 groups (figure 8.5; Log-rank test, p= 0.44), denoting that extent of tumour resection did not provide additional information for disease risk stratification among cases with positive β-catenin nuclear localization.

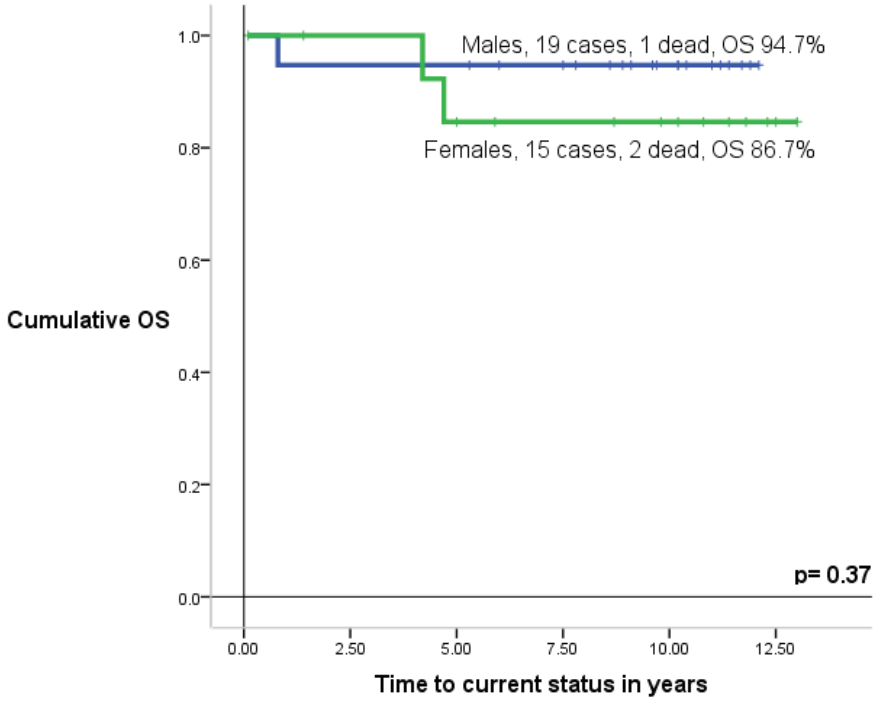

Figure 8.4. Kaplan-Meier survival curves for genders in cases with β-catenin nuclear positivity.
OS= overall survival.

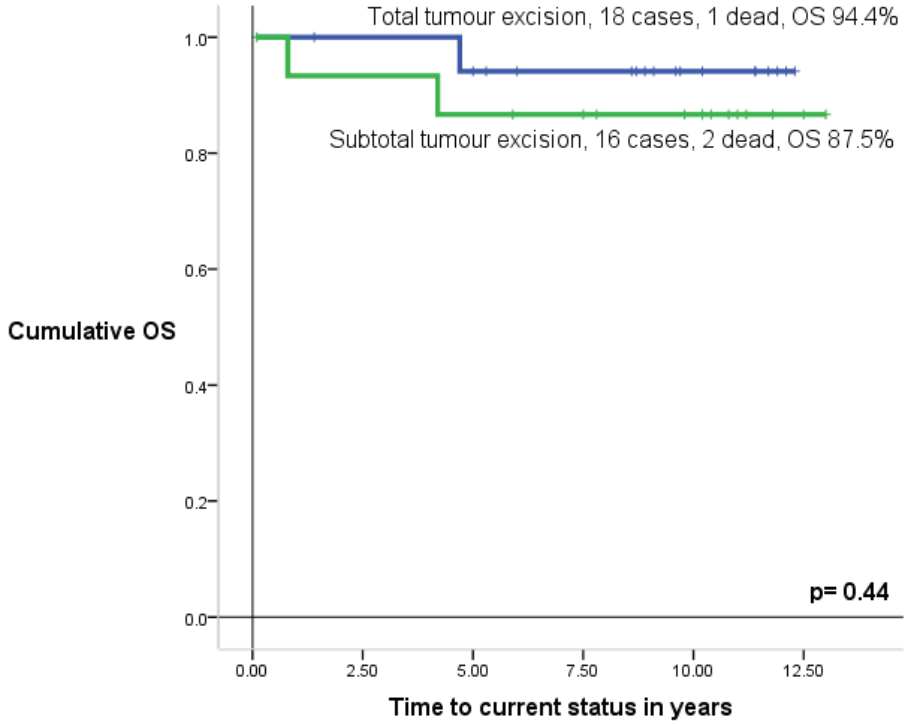

Figure 8.5. Survival analysis for extent of tumour resection in cases with positive nuclear β-catenin,
OS= overall survival.

8.4.2.7. Interesting cases

Seven cases with positive β-catenin nuclear localization also diagnosed high risk disease features; 4 had metastatic 2/3 stage at diagnosis and the other three had large cell / anaplastic pathology subtype. 6/7 had no recurrence and were alive disease free with a OS of 5-11.4 years. On the other hand, 3 cases showing positive β-catenin nuclear localization had recurrence and died, 2/3 of them had strong nuclear expression of β-catenin (case 139 and 146), the third case (case 50256) had focal weak positive β-catenin nuclear localization and was *CTNNB1* wild-type (Table 8.10).

	M stage	Age (Y)	Path	Sex	T.T	Surg.	Rec.	Time to Rec.(Y)	Current status	Time to C.S.(Y)	B-cat IHC	*CTNNB1* status	Ch 6 loss	Ch 17p loss
28	2/3	7.2	Class	F	R+C	S.T.	No	-	Alive	10.8	F.S	W.T.	No	Yes
50021	2/3	14	Class	M	R+C	S.T.	No	-	Alive	11	W.S	Mut.	No	No
50068	2/3	10.4	Class	F	R+C	S.T.	No	-	Alive	11	W.S.	W.T.	No	No
50256	2/3	4.2	Class	M	R+C	S.T.	Yes	0.3	Dead	0.8	F.W.	W.T.	No	No
78	0/1	3	LC/A	M	R	S.T.	No	-	Alive	10.4	F.S.	W.T.	No	Yes
131	0/1	5.4	LC/A	F	R+C	GTR	No	-	Alive	5	W.S	Mut.	No	Yes
137	0/1	13.4	LC/A	M	R+C	GTR	No	-	Alive	11.4	W.S	Mut.	Yes	yes
139	0/1	7.7	Class	F	R	GTR	Yes	1.8	Dead	4.7	W.S.	Mut.	Yes	No
146	0/1	9	class	F	R+C	GTR	Yes	2.8	Dead	4.2	W.S.	Mut.	Yes	No

Table 8.10. The clinicopathological profile of cases with β-catenin nuclear localization and had interesting outcome. M= metastatic stage; Path= pathology, Class= classic, LC/A= large cell / anaplastic ;T.T.= treatment, R.= radiotherapy, C.= chemotherapy, Surg.= surgery, S.T.= subtotal resection, GTR= gross tumour resection; Rec.= recurrence: C.S.= current status; β-cat IHC= β-catenin immunohistochemistery, F.S.= focal and strong, W.S. = wide spread and strong, F.W.= focal and weak; Mut. = mutation, W.T. = wild type; Ch= chromosome; Y= years.

8.5. Discussion

The integration of clinical, molecular and histopathological criteria into future disease risk classifications is a clear goal in medulloblastoma, and will be tested in international clinical trials which are currently being planned (Pizer and Clifford 2009). Wnt/Wg pathway activation is associated with good prognosis and has clear potential as a favourable prognostic marker. Detection of Wnt/Wg active tumours has been reported using sophisticated molecular methods, which are available only in highly equipped labs and advanced centres (e.g. expression profile analyses and aCGH). Here, we used methods to detect Wnt/Wg active tumours using PCR, sequencing and immunohistochemistry, which we have validated in chapters 4-6, and all of which can be applied on FFPE material. The current study recruited cases from the PNET3 cohort and assessed the prognostic significance of clinicopathological and molecular variables using univariate survival analysis (Chapter 7), followed by introducing those that were significant into multiple Cox proportional regression hazard analysis to identify those variables with independent prognostic significance. This enabled us to construct models for disease outcome prediction, taking in consideration the significant clinicopathological and molecular factors.

Despite the fact that histopathological subtypes have been previously associated with disease prognosis (i.e. MBEN or nodular/desmoplastic pathology with good prognosis; large cell / anaplastic pathology with poor outcome) (reviewed by Pizer and Clifford 2009), so far it is not an established factor in disease classification. Our study demonstrated that longer survival was significantly associated with the

classic and nodular/desmoplastic subtypes therefore, supporting the inclusion of pathology in our models. Most previous studies have been limited to identifying Wnt/Wg active tumours and their associated survival relationships in isolation, while here we incorporated β-catenin nuclear localization (which we found to be the best predictor of Wnt/Wg activation (Chapter 7)) into models including other clinicopathological variables and constructed combination models to predict prognosis and estimate the disease hazard ratios for individual patients. Three combination models were generated depending on the number of variables incorporated in each. Combination models 1, 2 and 3 included 5, 4 and 3 variables respectively. A model incorporating all variables which had statistically significant 'p` values in their univariate Cox proportional regression analysis was used. These were gender, pathology, metastatic stage at time of diagnosis, extent of tumour resection and β-catenin nuclear staining. Multiple Cox forward stepwise proportional regression hazard ratio analysis was performed. Although metastatic stage and extent of tumour resection yielded significant 'p` values in their univariate analysis (p= 0.001 and p= 0.03 respectively), when they were incorporated in one model they both turned to be insignificant (p= 0.233 and p= 0.098 respectively). This was due to the multicolinear relationship they had because of their very significant inter-correlation (Fisher's exact test, p= 0.003), indicating that both variables cannot be used together in models for the prediction of disease outcome. The impact of gender on survival in medulloblastoma is controversial, some research has associated females with better prognosis, but only among patients >3 years at diagnosis (Curran et al 2009), while other studies did not take gender in consideration when assessing patients' prognosis.

Importantly, gender has not been validated as an independent prognostic marker in large studies conducted on clinical trials cohorts. Gender was found to be a statistically significant variable in its univariate overall and event free survival analysis in the PNET3 cohort (Log-rank test, p= 0.021 and p= 0.047 respectively). Therefore, a model was constructed which included 4 variables (β-catenin nuclear localization, metastatic stage at diagnosis, pathology and gender).

Multiple Cox proportional regression hazard ratio analysis was applied for the above mentioned variables, which yielded a model with statistically significant 'p` values for all the variables; β-catenin positive nuclear staining (p= 0.009 and hazard ratio 0.212 favouring cases with positive staining); metastatic stage at time of diagnosis (p= 0.017 and hazard ratio 1.933 favouring M0/1); pathology (p= 0.001 and hazard ratio 3.354 favouring classic and nodular/desmoplastic subtype) and gender (p= 0.039 and hazard ratio 0.56 favouring females) (Table 8.4). These data demonstrate the independent prognostic significance of each marker and their potential utility in models for disease stratification.

Based on these 4 variables, patients can present with 16 different combinations of risk markers and by applying the linear Cox proportional hazard regression equation, each combination produced a different hazard ratio for death to occur (Table 8.5). This table showed that the combination with least hazard for death to occur was number 1 (tumours with positive β-catenin nuclear staining, classic and nodular/desmoplastic pathology, metastatic stage at time of diagnosis M0/1 stage and female gender, hazard ratio 0.12). The combination with the maximum hazard for death was model 16 (β-

catenin negative nuclear staining cases, large cell / anaplastic pathology, metastatic stage M2/3 and male gender, hazard ratio 6.48). Generally, models with a positive β-catenin nuclear localization had fewer hazards to occur than those with a negative β-catenin nuclear staining.

However, gender has not been consistently significantly associated with survival in previous studies, and the current study is therefore the first to show significant association with survival in a trial-based cohort. Analysis of the association between gender (males vs females) in the group of patients with positive β-catenin nuclear localization was not significant (log-rank test, p= 0.37), indicating that within the β-catenin nuclear positive group, gender does not provide extra prognostic significance.

A model based on 3 variables (metastatic stage at diagnosis, tumour pathology and β-catenin nuclear localization) was constructed. In this model, patients could present with different combinations of these 3 variables. A table for the possible different combinations was made and the multiple Cox proportional hazard regression equation was applied to each possible combination to identify their overall hazard ratios. This yielded 8 different possible combinations, each with a different hazard ratio for death to occur (Table 8.6). It could be concluded from the table that the least hazard for death to occur was combination number 1 (positive β-catenin nuclear localization, classic and nodular / desmoplastic pathology and metastatic stage M0/1) (hazard ratio was 0.21), while the combination with the worst outcome was number 8

(negative β-catenin nuclear staining, large cell / anaplastic pathology and M2/3) (hazard ratio 6.51).

These modified disease risk classifications allow a better prediction of patients' prognosis and are more informative than the current clinical disease classification. Analysing β-catenin status in 7 cases which were considered to be high-risk category according to the current clinical classification (Table 8.10) showed that 6/7 had positive strong nuclear localization and they were alive disease free when last seen, with OS of 5-11.4 years. One case died who had focal weak β-catenin nuclear localization and *CTNNB1* wild type. This further demonstrates that adding β-catenin nuclear localization to clinical stratification schemes has a significant implicate on the prediction of patients' outcome.

In summary, the 5 variables model was disregarded due to the multicolinear relationship between metastatic stage at diagnosis and extent of tumour resection favouring using the former variable. The 4 variables model seemed to be the most informative and individualized model but, as gender has not previously been validated in large clinical trials and has shown inconsistent correlations with survival in previous studies, the 3 variables model based on β-catenin nuclear localization, metastatic stage at diagnosis and pathology is currently the best validated model to take to practice at the mean time, since all 3 variables included in this model have been extensively validated (Pizer and Clifford 2009).

8.6. Conclusions

1. Survival analysis based on current clinical classification is statistically significant but lacks precision and could benefit from the addition of molecular and histopathological variables.

2. Pathological subtype, β-catenin nuclear localization, metastatic stage at diagnosis, extent of tumour resection and gender were all significant prognostic factors in univariate analysis, while chromosome 6 and chromosome 17p status were not significant.

3. Multivariate Cox regression proportional hazard analysis using 3 and 4 of the significant variables (β-catenin nuclear localization, metastatic stage at diagnosis, pathology ± gender) produced 2 models which could be valuable in predicting patients' outcome.

4. Patients with positive β-catenin nuclear localization have a lower hazard ratio than patients with negative β-catenin nuclear localization.

5. Patients with positive β-catenin nuclear localization usually are typically accompanied by low-risk clinicopathological features and have a favourable outcome. Also, when observed in association with high clinical risk features, a favourable prognosis is still associated.

6. Patients may be classified based on clinicopathological and molecular variables using the proposed models, which could provide bases for a more specific and tailored therapeutic decisions.

7. Modifying therapeutic decisions based on these modified classification may allow de-escalating treatment for favourable-risk patients while intensifying treatment for high-risk patients. This will first require validating our findings in further prospective clinically controlled cohorts.

Chapter 9

Discussion

9.1. Introduction

Medulloblastoma is the most common malignant brain tumour among the paediatric population accounting for approximately 10% of all cancer related deaths in children and around 30% of all paediatric brain tumours. Despite vast advancement in diagnostic and therapeutic techniques, survival rates of around 60 and 80% are reported for high-risk and standard-risk patients, respectively. However, 20% of standard-risk patients will experience tumour relapse, while 60% of high-risk cases are cured using conventional treatment. Patients are currently risk-stratified according to clinical criteria; age, metastatic stage at diagnosis and extent of tumour resection. High-risk patients are those aged < 3 years or have metastatic stage of M2/3 at diagnosis or achieved subtotal tumour resection, while standard-risk patients are those aged ≥ 3 years with metastatic stage M0/1 at diagnosis and achieved total tumour resection (reviewed in Pizer and Clifford, 2009).

Another obstacle hampering the research in the field of medulloblastoma is the frequent lack of high quality tumour material (i.e. fresh frozen samples) frequently required for high-throughput molecular analysis of DNA, RNA and protein expression. Huge numbers of tumour samples are stored in different centres world wide, as FFPE material, and could potentially provide a valuable resource of material for research, if methodologies can be established to successfully interrogate this material.

9.2. Limitations of the current clinical classification in medulloblastoma

Although the current medulloblastoma disease classification system is widely accepted and used for deciding treatment regimens, it still lacks precision, leading to potentially preventable neuro-cognitive and neuro-endocrine late side effects in a subset of favourable-risk patients. On the other hand, another subset of poorer-risk patients may need intensification of their therapeutic protocols to achieve a better cure rate.

A number of molecular and histopathological biomarkers have been identified, which can potentially allow a more accurate prediction of patients' prognosis, with the potential to form the basis of stratification to more individualized therapies based on disease risk, leading to improved patient management and disease outcome. Recently, significant advancements in understanding the molecular mechanisms that underlie the pathogenesis of medulloblastoma have opened a new horizon for the development of novel therapies targeted against specific molecular defects, aiming to maximize survival whilst minimizing late effects (so called genomic medicine).

9.3. The initial aims of this study

The first part of this project started by developing and validating a method to test FFPE medulloblastoma samples, that do not have matched controlled DNA available, for regions of genetic loss which may potentially harbour TSGs and subsequently play a role in the development of medulloblastoma. The most common

chromosomal aberrations in medulloblastoma affect chromosome 17, where isolated 17p loss is seen in 20% of cases and i(17q) is observed in another 30%, which in total indicates abnormalities of chromosome 17 to involve 30-50% of all medulloblastomas. These data persuaded researchers that potential TSGs or oncogenes could reside on 17p and 17q, respectively. Further evidence for the potential involvement of this chromosome in medulloblastoma tumourigenesis lies in the fact that *TP53*, one of the most mutated TSGs in cancer, is located on 17p13.1 medulloblastoma, suggesting that gene mutation may not be the main mechanism for inactivation of *TP53* in medulloblastoma and other mechanisms play a role in the disruption of the *TP53* pathway. Alternatively, other TSGs may be present on 17p which have yet to be identified. 17p deletions and i(17q) have been correlated with patients' survival, however the results of different studies are not consistent. Emadian et al (1996), Beigel et al (1997), Pan et al (2005) and Pfister et al (2009) reported no association between 17p deletion and survival, while Cogen et al (1990) report a trend for 17p loss with unfavourable outcome. Batra et al (1995), Gilbertson et al (2001) and Lamont et al (2004) similarly reported poor clinical outcome in cases with 17p deletions. However, Lamont et al (2004) and Pan et al (2005) and Pfister et al (2009), in the same studies, reported that cases with i(17q) had a poor prognosis.

9.4. Using an initial cohort to develop and validate the HOMOD method

In the current study an initial cohort of 76 primary medulloblastoma samples was used to form a pilot study aimed at developing methods to test chromosome 17p

LOH by the HOMOD method (Goldberg et al 2000), followed by identifying the incidence of chromosome 17p LOH in this cohort, as well as investigating clinicopathological relationships associated with chromosome 17p LOH. This development and validation of the HOMOD method would support further investigations in this project.

Chromosome 17p LOH was detected in 30.3% (23/76) of the cases examined, which is in concordance with the incidence reported in the literature. Clinicopathological correlations identified only pathology and age to show significant results, where chromosome 17p LOH was significantly associated with desmoplastic pathology and patients aged ≥3 years at diagnosis.

In order to validate the HOMOD method, 26 cases were tested in parallel for chromosome 17p LOH using the conventional LOH (cLOH) method which compares tumour DNA with matched constitutional DNA for regions of genetic losses; 84.6% (22/26) of the cases showed equivalent results using both methods. The second method of validation involved comparing 17p LOH results generated by the HOMOD method with results for chromosome 17p status produced by aCGH in a subset of 29 medulloblastoma cases. Equivalent results were achieved by the 2 methods (HOMOD and aCGH) in 27/29 cases. One case was identified as 17p LOH by HOMOD but as chromosome 17 neutral by aCGH, suggesting a copy number-neutral genetic allelic loss. A further case was identified as having 17p retention by HOMOD but showed isolated 17p loss by aCGH (96.2% concordance overall).

In summary, the previous part of this project confirmed that the HOMOD method was a reliable and successful method to test for tumour samples for regions of genetic losses without the need for matched constitutional DNA in FFPE material.

9.5. Assessment of microsatellite instability in medulloblastoma

Of the 26 cases which were tested by cLOH, 5 showed evidence of microsatellite instability, which led to further investigation of this phenomenon using specific microsatellite markers chosen from a panel of markers chosen by the Betheseda committee (Umar et al 2004). These were the mono-nucleotide markers BAT25, BAT26, and the di-nucleotide markers D2S123, D5S346 and D17S250. This analysis revealed that only one case (NMB 49) (1/26; 3.8%) showed evidence of MSI-H (defined as showing MSI in ≥ 2 markers) identified at markers D17S 974 and D17S250. Few previous studies have looked at the role of MSI in medulloblastoma development, however most of them agree that this mechanism is rarely observed in sporadic medulloblastoma and probably plays as insignificant role in tumourigenesis (Lee et al 1998).

Recently, a study by Viana-Pereira et al (2009) investigated MSI in medulloblastoma development and identified one case (11%) to involve MSI-H, comparable to our results. This group used a slightly different technique to test for MSIs (quasimonomorphic microsatellite markers) which they reported to be more sensitive in identifying MSIs than other reported methods, although this method used microsatellite markers without testing matched constitutional DNA. These data show that there is evidence of MSI in a small subset of medulloblastoma, which will require

the collection of bigger cohorts to investigate if this mechanism, which affects MMR genes leading to defective DNA repair, does play a role in medulloblastoma and to establish any utility as a biomarker or therapeutic targets.

9.6. Age at diagnosis may define a distinct molecular subgroup of medulloblastomas

The pilot study of chromosome 17 loss in medulloblastoma results showed a significant correlation between age and 17p LOH, where only 1/21 (5%) case below the age of 3 years at diagnosis showed 17p LOH, while 20/21 (95%) showed 17p RET (p= 0.009). Previous studies have produced some evidence that medulloblastoma arising in infants may represent a distinct subset of this tumour with different biological background (Rutkowski et al 2007; Anderton et al 2008; Kool et al 2008). Gilbertson and Ellison (2008) proposed that medulloblastoma arising in infants may be a result of mutations in the granule neurone precursor (GNP) during late gestation and / or early childhood and subsequently activation of SHH signalling pathway which leads to medulloblastoma formation of the desmoplastic subtype. Also, infantile medulloblastoma include the MBEN subtype which is associated with an excellent prognosis (McManamy et al 2007, Ellison et al 2003).

COL1A2 methylation affects non-desmoplastic medulloblastoma in patients of all ages at diagnosis (86% and 83% for patients ≥ 3 and < 3 respectively), while a significant discrepancy was observed within the desmoplastic medulloblastomas where *COL1A2* methylation mainly affects patients ≥3 years compared to <3 years at

diagnosis (90% vs. 13%, respectively) suggesting that infantile desmoplastic medulloblastoma is a distinct molecular and histological group. Furthermore, gene expression studies identified that medulloblastoma with Wnt/Wg pathway activation were significantly associated with patients aged ≥ 3 years at diagnosis (Clifford et al 2006, Thompson et al 2006, Kool et al 2008, Fattet et al 2009). The current study did not involve such methodologies of analysis, but comparable associations could be seen, together supporting the notion that infantile medulloblastoma demonstrate unique histopathological and molecular features which may influence patients' clinical outcome.

9.7. Assessment of the Wnt/Wg pathway in medulloblastoma

The consistent evidence associating Wnt/Wg pathway active medulloblastomas with favourable prognosis (Clifford et al 2006) laid the foundation for deciding to investigate further the potential use of associated molecular markers to modify the current clinical disease stratification, better predict patients' prognosis and subsequently influence and tailor therapeutic decisions leading to the ultimate goal of reducing late effects and improving survival rates within different risk groups.

9.8. Molecular indices associated with Wnt/Wg pathway activation

The retrospective, clinically controlled, PNET3 cohort (Taylor et al 2003) provided a valuable resource upon which further analyses were undertaken in this project. Assessment of the PNET3 cohort confirmed that overall OS and EFS rates for

the cohort are in agreement to those reported in the literature. As predicted and in accordance with previous studies (reviewed by Pizer and Clifford, 2009) a significant association was observed between (i) the extent of tumour resection (ii) pathology and (iii) metastatic stage at diagnosis with an adverse outcome. Together, these data show that the cohort reflects an unbiased collection of medulloblastoma which allows it to be confidently used for further analyses and correlates.

Wnt/Wg pathway activation in medulloblastoma could not be identified using clinical parameters and requires testing using molecular indices. Three molecular correlations of Wnt/Wg activation (β-catenin nuclear localization, *CTNNB1* mutation and chromosome 6 loss) have been identified (Clifford et al 2006; Thompson et al 2006; Fattet et al, 2009), but the clinical utility of only β-catenin nuclear localization has been tested to date. Therefore, we assessed these 3 molecular markers in the PNET3 cohort and concluded that β-catenin nuclear localization is the most sensitive marker of pathway activation, since it identified the largest number of tumours with active pathway and other markers always occurred as a subset of these. A strong significant association was observed between β-catenin nuclear localization and each of *CTNNB1* mutation and chromosome 6 loss, which both serve as good confirmatory markers (secondary to nuclear β-catenin localization). The incidence of β-catenin nuclear localization and subsequently Wnt/Wg pathway activation was (16.4%) (34/207 cases) in the PNET3 cohort, which is consistent to rates reported in the literature (10-25%) (Clifford et al 2006). It is also worth noting that IHC technique could be applied successfully and reliably to FFPE material and was less labour extensive than direct sequencing (*CTNNB1* mutation) and chromosome 6 LOH analysis.

Since all cases with *CTNNB1* mutation were inclusive in the β-catenin nucleopositive group, the latter marker may confidently be used alone, however cases with chromosome 6 LOH were not exclusively associated with positive β-catenin nuclear localization which, justifies using both markers concomitantly to identify any cases with evidence of Wnt/Wg activation. The observation of cases showing β-catenin nuclear localization without evidence of *CTNNB1* mutation suggests that other genes (e.g. *AXIN1*, *APC*) or mechanisms may be responsible for pathway activation in the remaining β-catenin nucleopositive cases (Eberhart et al 2000). In concordance with other studies (Clifford et al 2006, Thompson et al 2006, kool et al 2008 and Fattet et al 2009), aberrations of chromosome 17 (17p LOH in the current study) were mutually exclusive from cases with chromosome 6 LOH, supporting the finding that Wnt/Wg active tumours do not display chromosome 17 defects and possess different molecular abnormalities driving these tumours. The significant association of chromosome 6 loss with Wnt/Wg active medulloblastomas is of particular interest and will be addressed later.

9.9. The role of Wnt/Wg activation in disease risk stratification

Establishing improved disease risk stratification systems, which was the main aim of this study, includes adding other clinicopathological and molecular criteria to the current clinical classification. Therefore, analysis of OS and EFS for clinicopathological and molecular variables was undertaken using the PNET3 cohort in order to identify those with prognostic significance using univariate survival analysis. Clinicopathological variables tested were all statistically significantly ($p< 0.05$)

associated with survival and included gender, pathology, metastatic stage at diagnosis and extent of tumour resection, while molecular variables tested which showed significant associations with survival were β-catenin nuclear localization and *CTNNB1* mutation. Although chromosome 6 loss showed a trend towards better survival, the result did not reach statistical significance. The prognostic significance of *CTNNB1* has not been previously been established, and these data represent the largest clinical trials cohort assessed for these molecular markers to date.

Cases with β-catenin nuclear localization displayed 3 patterns of immunostaining; wide spread strong, focal strong and focal weak nuclear staining. A study by Fattet et al (2009) only associated the strong wide spread pattern (>50% of cells showing β-catenin nuclear staining) with *CTNNB1* mutation, while we noticed this association in both focal and widespread nucleopositive cases. Additionally, both patterns showed equivalent associations with chromosome 6 loss and favourable survival, associated with activation of the Wnt/Wg pathway. Cases with focal weak nuclear β-catenin accumulation did not demonstrate any of these associations. In summary, wide spread or focal nuclear staining patterns show equivalent associations and can be combined for prognostic use.

9.10. The molecular bases of favourable prognosis in the Wnt/Wg subgroup medulloblastomas

Wnt/Wg pathway activation has been associated with the development of several cancers and their poor outcome and progression including colon,

hepatocellular and breast carcinoma, however a paradoxical effect of Wnt/Wg activation has been seen in some tumours including medulloblastoma, non-small cell lung carcinoma and ovarian cancer (reviewed in Rogers et al 2009). Such a surprising phenomenon in medulloblastomas could be linked to the fact that pathway activation may represent a subset of tumours with a less aggressive phenotype than other subgroups. Wnt/Wg activation may also have different effects on the cells including an influence on cell proliferation, apoptosis and differentiation. Thus, Wnt/Wg activation could disrupt the balance between proliferation and apoptosis in favour of the latter. Alternatively, Wnt/Wg pathway activation may influence the cells' response to treatment (Salaroli et al 2008). This finding may play an important role to develop innovative target therapies. However, further investigations for reasons behind the association of favourable prognosis among Wnt/Wg active medulloblastomas must be undertaken before strategies for targeting the pathway are developed.

9.11. The significance of chromosome 6 loss in medulloblastoma

Chromosome 6 loss was significantly associated with both *CTNNB1* mutation and β-catenin nuclear localization, however in isolation, it was not significantly associated with favourable survival and only showed a trend towards this. The relationship between chromosome 6 loss and the development of Wnt/Wg active medulloblastomas suggests that these two molecular events contribute to the development of a subgroup of tumours with a favourable clinical outcome, however, the exact mechanism underlying this correlation is still under investigation. Possible explanations could be due to chromosome-wide reduction in gene-dosage or specific

critical genes, which are targeted for inactivation by smaller genetic or epigenetic events. Alternatively, Wnt/Wg pathway activation may lead to imbalances on chromosome 6 which co-operate directly in promoting a subset of medulloblastoma (Clifford et al 2006, Fattet et al 2009). Further detailed analysis of chromosome 6 defects in medulloblastoma is now required in order to shed more light on this issue.

Chromosome 6 is one of the 23 pairs of the human chromosomes. It is a metacentric chromosome spanning over 170 million base pairs and represents between 5.5 and 6% of the human genome. The finished sequence comprises 166,880,988 base pairs, representing one of the largest chromosomes sequenced to date. Chromosome 6 is estimated to harbour between 1,100 and 1,600 genes among these genes are ones which are directly implicated in cancer, schizophrenia, autoimmunity and many other diseases.

A lot of research in other cancers has focused on the long arm of chromosome 6 since it harbours genes of importance in tumour progression in a wide range of solid and haematological malignancies. Therefore, vital TSGs are predicted to exist on chromosome 6q. Usually tumour specific mutations that inactivate TSGs affect large sale aberrations such as loss of the whole chromosome 6 or large fragments of it. Deletions of chromosome 6q commonly occur in diverse tumour types (such as pancreatic cancer, hepatocellular carcinoma, gastric cancer, ovarian cancer, leukaemia, etc.). The 6q23 locus seems to be a fragile site and a common break point which supports the fact that 6q23 is a potential critical locus harbouring tumour suppressor

genes involved in the development of human cancers (Jackson et al 1998, Koyama et al 1999, Shridhar et al 1999, Makino et al 2001).

Previous studies by Thomas et al (1991) and Michiels et al (2002) found loss of 6q in 33.3% and 26.1% of medulloblastomas respectively. Homozygous deletion on chromosome 6q23 was also detected by Hui et al (2005) in the medulloblastoma cell line, DAOY, and whole chromosome copy loss was also detected in 30% of primary tumours. This study mapped the smallest region of homozygous deletion to a 0.887 Mb on 6q23.1 where three genes were mapped to this area on chromosome 6q23.1: namely *BC060845* (L3MBTL3 protein), *AK091351* (hypothetical protein FLJ34032), and *KIAA1913*. Compared to normal cerebellum the expression levels of these 3 genes were not detected in the cell line DAOY showing homozygous deletion, while their expression was reduced in cell lines D283 and D384. It is worth mentioning that DAOY cell line has been repetitively questioned for being a true medulloblastoma since it lacks the biological features of medulloblastoma. The expressions of these genes were also reduced in 10 analyzed primary tumours with the frequencies of 70% in *KIAA1913,* 50% in *AK091351* and 10% in *BC060845.* Therefore, at least 2 of those genes may be candidate TSGs implicated in medulloblastoma development (Hui et al 2005).

One of the most recognized and important genomic features of chromosome 6 is the Major Histocompatability Complex cluster (MHC), encompassing a region of 3.6 mega bases (Mb) on band 6p21.3. The MHC plays an essential role in the innate and acquired immune system, which allows specific antigen recognition by the immune system and protection of the host (Sadasivan et al 1996, Seliger et al 1997, 2000). It is

believed that tumour formation may be associated with defects in the expression and/or function of HLA class 1 APM components, rendering recognition of tumour cells by CTL (cytotoxic T lymphocytes) and eventually a poor clinical outcome.

Usually, medulloblastoma seem to express low or even undetectable levels of some of the essential components of the MHC class 1, however, subsets of medulloblastoma seem to express levels of components of MHC class 1 along-side expressing other markers of poor prognosis (e.g. anaplasia, and *c-myc*) (Smith et al 2009). Therefore, medulloblastoma cases which express MHC class 1 associated with other markers of poor prognosis seem to behave more aggressively and have a poor clinical outcome. On the other hand, a paradoxical effect was observed, where lack of MHC class 1 expression has been associated with a favourable clinical outcome and increased survival among some medulloblastomas. This could be a logic explanation for the association between chromosome 6 loss and the favourable clinical outcome among medulloblastomas. This paradoxical response may be a result of an increased in the activity of NK cells, which generally function more effectively when target cells lack MHC class 1 (Chang and Ferrone 2007).

Another alternative explanation for the better clinical outcome for cases showing loss of chromosome 6 and potentially lacking MHC class 1 could be through the implication of β2m and heavy chain devoid of peptide and β2m, which modify signal transduction of several cell surface receptors, and enhancing the activation of ERK 1/2 (extracellular signal-regulated kinases), which increases the invasive capability of medulloblastoma cells. Deregulation of ERK 1/2 is implicated in tumorigenesis of

various tumours due to its role in phosphorylation of nuclear and cytoplasmic targets, regulation of cell proliferation, differentiation, survival, angiogenesis, migration and chromatin remodelling (Dunn et al 2006, Yoon and Sege, 2006). This may suggest an immune system-independent role of MHC class 1 in tumour progression (reviewed by Smith et al 2009). Therefore, the link between the expression of the MHC components and prognosis among medulloblastoma patients need to be investigated further.

9.12. The role of chromosome 17p LOH in medulloblastoma risk stratification

In this study, chromosome 17p LOH was also assessed in the PNET3 cohort, and was not significantly associated with any of the molecular markers of Wnt/Wg pathway activation (β-catenin nuclear localization, *CTNNB1* mutation, chromosome 6 loss) or patients survival, indicating it is not associated with active Wnt/Wg medulloblastoma tumours and not a marker for adverse prognosis. In this study, only 17p status was assessed but not 17q, which may explain the inconsistency between our results compared to studies which assessed the whole of chromosome 17 and identified cases with i(17q) and 17q gain (suggesting the presence of oncogenes on 17q) and correlation with unfavourable outcome among those cases (Lamont et al 2004, Pan et al 2005, Pfister et al 2009).

9.13. Further molecular markers in medulloblastoma

The concept of identifying novel prognostic markers to augment and modify the current clinical classification has been addressed by many researchers, aimed at

identifying the different pathways which drive medulloblastoma and their clinicopathological association. Genome-wide analysis and studies involving gene expression have identified distinct biological pathways associated with different subgroups of medulloblastoma displaying distinct clinicopathological features (Clifford et al 2006, Thompson et al 2006, Kool et al 2008). SHH and Wnt/Wg represent two of the most investigated and understood pathways, which appear to involve mutually exclusive tumour subsets despite the fact that the 2 pathways are inter-related, containing 3 common negative regulators; *SUFU, BTRC* and *GSK-3*β. SHH pathway activation does not seem to drive activation of Wnt/Wg pathway, despite mutations being observed in *SUFU*, a component of both the SHH and the Wnt/Wg pathways (Thompson et al 2006). This mutually exclusive association demonstrates that the two pathways may together be responsible for approximately 30-40 % of medulloblastomas in total. Although the Wnt/Wg pathway displays a consistent association with a favourable outcome, the SHH pathway does not seem to influence prognosis (Pizer and Clifford 2009).

Other molecular markers tested for their potential prognostic value in medulloblastoma include *MYC, TP53, PDGFRA, ERBB2, MIB, TrkC* detected by IHC and other markers associated with apoptosis (Ray et al 2004). Those which were strongly associated with prognosis included *ERBB2* (HR. 1.51*,* p= 0.21), *TP53* (HR. 2.2.29, p= 0.02) *and TrkC* (HR. 0.65, p= 0.14). These results led the group to encourage the addition of those significant markers to the current clinical classification in order to achieve a better disease-risk prediction.

The *ERBB2* is a member of the epidermal growth factor receptor family, which is expressed in up to 86% of medulloblastoma (Ray et al 2004). Similarly, in a study by Gilbertson and Clifford (2003) the platelet-derived growth factor receptor β (PDGFRβ) was differentially expressed in metastatic medulloblastoma, however a subsequent study by Gilbertson et al (2006) showed that activating mutations in hotspots within the PDGFR-RAS/MAPK pathway was rare in medulloblastoma development.

MYCC and *MYCN* amplification have been identified in 15-20% of medulloblastoma and have been associated with a poor prognosis and large cell anaplastic pathology in multiple studies, however this association is not absolute, and no relationship to prognosis or pathological features has been observed in other studies (Rutkowski et al 2007, Pfister et al 2009). *MYCL* amplification in medulloblastoma has been observed in 5% but its clinicoplathological significance was not fully assessed and less clear (Lo et al 2007). Although *MYC* amplification appears to be a potentially significant poor prognostic marker, only two studies have assessed its prognostic significance across clinical-trials based cohorts of medulloblastoma (Lamont et al 2004, Rutkowski et al 2007), and the number of *MYCC* and *MYCN* cases which showed amplification in these studies were small. Similarly, most studies assessed the significant prognostic value for *MYCC* and *MYCN* amplification in combination and did not assess each oncogene independently, probably due to small number of cases in each group. Therefore, prospective clinical trials are now required to validate the utility of *MYCC* and *MYCN* amplification as markers for poor prognosis in medulloblastoma.

The *TP53* oncogene is involved in the pathogenesis of many cancers and p53 immuno reactivity has been associated with adverse clinical outcome in medulloblastoma, alongside early recurrence and resistance to both chemotherapy and radiotherapy (reviewed in Tabori et al 2010). Immuno reactivity may occur as a result of both *TP53* mutation and other aberrations in its pathway. *TP53* mutations have been identified in <10% of sporadic medulloblastoma. In a study by Tabori et al (2010), 108 medulloblastoma cases were assessed for p53 immuno-reactivity of which 49 cases were also sequenced for *TP53* mutation, where 16% showed mutations. All cases with mutations had early recurrence and were associated with a worse outcome. 5 year survival among standard-risk patients with *TP53* mutation versus wild type was 0% versus 74% ($p< 0.0001$). In this study, *TP53* stabilization due to other mechanisms other than mutations did not seem to be responsible for treatment resistance.

Pfister et al (2009) identified 5 distinct cytogenetic subgroups using array-CGH analysis in 80 comparably treated medulloblastoma cases allowing them to postulate the following hierarchical molecular staging system; (1) Tumours with amplified *MYC* or *MYCN*; (2) tumours with 6q gain, showing adverse outcome; (3) 17q gain; (4) cases with 6q and 17q balanced; (5) Finally tumours with 6q gain, which showed the best prognosis. Combining these molecular markers to the current clinical classification repositioned some patients form the high-risk category into the average-risk allowing de-escalation of their treatment. These findings further emphasise that chromosome 6q is a critical region which may help in classifying medulloblastoma patients into high-risk or average-risk, depending whether there is 6q gain or 6q loss respectively.

9.14. Development of clinico-biological models for medulloblastoma risk prediction

The major goal of this project was to identify additional clinicopathological and molecular prognostic markers that can refine and improve the current clinical disease risk stratification. The investigation of the Wnt/Wg pathway in medulloblastoma as a favourable-risk marker formed the focus of this study, and its prognostic significance was demonstrated on a large clinically-controlled cohort.

The next stage of this project, therefore involved introducing all clinicopathological (gender, metastatic stage at diagnosis, extent of tumour resection and histopathology) and molecular markers (β-catenin nuclear localization, *CTNNB1* mutation) which have a significant prognostic association with survival (from their univariate survival analyses), into a multiple multivariate Cox proportional regression hazard ratio analysis in order to construct a model for disease risk stratification, prediction and estimation of hazard ratio. While β-catenin has been investigated in isolation, its value in prediction models alongside other markers has not previously been assessed.

β-catenin nuclear localization and *CTNNB1* mutation both showed highly significant association and all cases with mutations were β-catenin nucleopositive (Fisher's exact test, p= 0.001) hence only β-catenin nuclear localization was chosen to enter in the multivariate survival analysis. Initially, all significant variables described above were concomitantly entered into multiple multivariate Cox proportional

regression hazard ratio analysis in order to produce a weighted predictive score based on their hazard ratios and ultimately to use this scoring system to construct models which could be applied to individual patients to predict their prognosis more accurately and accordingly modify their treatment protocol. Practically, patients could present with a variety of disease features (combinations) which when entered into the constructed proposed models, would produce an overall hazard ratio which could be used to stratify the patients' disease risk. Both metastatic stage at diagnosis and extent of tumour resection had highly significant 'p` values (Fisher's exact test, p= 0.003) (Table 7.1).

Their multicolinear relationship reduced their independent significance when they were simultaneously incorporated in one model, and therefore only metastatic stage at diagnosis was included, since the extent of tumour resection may be influenced by factors other than the tumour phenotype such as surgical technique and surgeons' experience. These data convincingly led to the construction of a four variable based model using the same variables without inclusion of the extent of tumour resection as a variable. All 4 variables have been tested and validated in previous studies except for gender which has previously displayed inconsistent association with survival (discussed in chapter 7), with the current study being the first to demonstrate this association in a clinical trial cohort, associating females with a better prognosis. Despite this evidence of the prognostic value of gender, a 3 variable model was constructed, incorporating the highly significant which have now been validated in multiple studies and, in the meanwhile, can be confidently applied to patients. While the 4 variables model potentially offers more tailored disease risk

stratification, it still requires further evaluation and validation in wider clinically controlled cohorts.

Applying these models to the PNET3 cohort revealed some interesting results. Cases displaying positive β-catenin nuclear reactivity and clinical high-risk features (M2/3 or large cell/anaplastic pathology) or average-risk features (M0/1, classic or nodular/desmoplastic pathology) showed no difference in prognosis, which supports further the value of β-catenin nuclear localization as a favourable-risk prognostic marker. However, the favourable disease outcome associated with Wnt/Wg activation is not an absolute relationship. This was reflected through the observation of 2 cases which displayed full features of Wnt/Wg pathway activation (strong wide β-catenin localization, *CTNNB1* mutation and chromosome 6 loss) but had early recurrence and died of disease, which suggests that other factors can influence disease outcome within the Wnt/Wg active group. In order to confirm the influence and significance of Wnt/Wg activation on disease outcome in each of the above categories, larger numbers of cases displaying similar disease features and prognosis need to be collected and investigated.

9.15. Constructing disease risk combination models for the prediction of hazard ratios in medulloblastoma

Depending whether 3 or 4 disease risk variables are used, patients may present with 8 or 16 different combinations respectively, which are referred to as the 8 and 16 disease risk combination models. Each combination generates a unique hazard ratio. In

order to facilitate the clinical application of those models, an overall risk status was assigned to each combination where hazard ratio values ranging from 0.1-0.9 were termed as favourable-risk (F.R.), hazard ratio values of 1 were termed as standard-risk (S.R.), while hazard ratio values > 1 were termed high-risk (H.R.). The disease-risk classifications schemes constructed in the current study themes combine clinical, pathological and molecular criteria and statistical calculations to provide a more accurate evaluation of patients' prognosis compared to the current clinically based classification scheme. By adding other clinical (e.g. gender) and molecular markers indicating Wnt/Wg activation (β-catenin nuclear localization), a subset of patients clinically classified as a high-risk showing evidence of Wnt/Wg activation (i.e. positive β-catenin nuclear staining), appeared to have a favourable outcome and hazard ratio graded as standard-risk. These additional data may allow changing the patients' risk and consequently reduce the stringency of their treatment alleviating some of the late effects associated with such extensive treatment.

The disease-risk prognostic combination models proposed here offer advantages over previous studies, which were limited to identifying Wnt/Wg active tumours and their prognostic significance in isolation. This is due to several reasons; first, we have proven that the best marker to identify Wnt/Wg active tumours was testing β-catenin nuclear staining using IHC techniques, which is a robust and straightforward method applicable to use on FFPE material. Secondly, we incorporated the aforementioned molecular marker with other clinical and pathological significant prognostic variables and constructed combination models for the prediction of prognosis and accurate estimation of the disease hazard ratios for individual patients.

All the significant markers and variables used in our models were generated using routine methods and techniques achievable on FFPE tumour material (IHC, PCR and direct sequencing). The collection of fresh frozen tumour samples remains a major challenge in large clinical trials therefore it is of practical relevance that the analysis of the present study were all made from routinely processed FFPE medulloblastoma material.

9.16. Incorporation of other prognostic biological markers in future disease risk stratification and practical challenges

Modifying the current clinical risk stratification schemes by adding additional significant prognostic biological markers may be expanded to incorporate other markers after testing them in wide clinical-based cohorts and validating their independent prognostic significance. Therefore, as previously described, *MYCC, MYCN* amplification and *TP53* mutation appear to show evidence for their potential value as adverse prognostic markers in medulloblastoma, independent from Wnt/Wg pathway activation and could subsequently incorporated in the disease risk prediction models developed in this project following their validation as described.

Although a number of potential prognostic molecular markers have been under investigation for the last decade, only have few reached a point of potential practical application, due to reasons including their investigation in small, heterogeneously treated cohorts, and the variety of methods and techniques used to define and quantitate each marker tested. It is difficult to accumulate sufficient quantities of

uniformly treated medulloblastoma cases form a single institute, probably due to the relative infrequent occurrence of medulloblastoma within the general population. Therefore, multi-centre clinical trials provide the opportunity to assess different potential prognostic markers in uniformly treated medulloblastoma cohorts. This should take in consideration standardization of methods for collection, storage and shipping of samples within a defined period of time to referral centres, where uniform methodologies for genetic testing and interpretation can take place.

Attempts will be implemented in the near future (Pizer and Clifford 2009) to introduce molecular and histopathological markers to the current clinical indices to test whether more accurate prediction of disease outcome can be made in clinical trials. Proposed markers include β-catenin nuclear localization as a favourable-risk marker while *MYC* gene amplification and large cell/anaplastic pathology are being considered as high-risk markers. It is proposed that these markers will allow the stratification of patients into favourable, standard and high-risk treatment groups, where 2 concurrent trials will test whether treatment can be reduced for favourable-disease risk subgroup, aiming to maintain survival rates while reducing late side effects (PNET5). The second trial (PNET6) will aim to improve survival in the standard-risk groups.

The work reviewed by Pizer and Clifford (2009) represents one of the latest projects focused on introducing molecular and histopathological markers to the current clinical indices in order to allow a more accurate prediction of disease outcome. This includes collection, storage and shipping followed by centralized

molecular genetic and pathological assessments. For prognostic use, ideally this whole process should be fulfilled within a 30 days window following the initial excision of the tumour and before commencing adjuvant treatment, which usually takes place 1 month after the initial surgery. Such a meticulous and disciplined scheme is currently under construction through the collaboration of several European centres to support further clinical trials involving the stratification of therapy using molecular markers.

9.17. The current study provides a better disease risk prediction model compared to the models reviewed in the literature

Although several studies have identified biological markers and used them to construct models for disease risk stratification in medulloblastoma (Ray et al 2004, Pfister et al 2008, etc. discussed in chapter 8), most of them have involved investigation of small, heterogeneously treated cohorts, or cohorts derived from non clinical-based clinical trials. Moreover, the markers tested (e.g. *MYC* amplification and 17p deletion) have not yielded consistent results across the studies. In comparison, the current study was based on the PNET3 cohort, which allowed the validation of potential prognostic (β-catenin nuclear localization, *CTNNB1* mutation and chromosome 6 loss) markers, which have also previously shown equivalent associations with survival in other studies (Clifford et al 2006, Pfister et al 2008 and Fattet et al 2009).

Two clinicopathological factors (gender and histopathology) have been identified in this project which showed significant association with survival in medulloblastoma and have not been previously extensively tested nor validated in

wider clinical trials. Therefore, these two factors also represent novel significant prognostic markers for disease risk stratification. The influence of gender on prognosis has previously been addressed (Curran et al 2009) but showed controversial results (discussed in chapter 8, section 8.5), while the current study showed significant association between females and better survival across wide clinical-based trial. Similarly, histopathology has been repeatedly assessed for its prognostic value, where large cell anaplastic pathology is usually associated with poor prognosis, metastasis and other adverse molecular markers (e.g. *MYC* amplification) however, it is still not included in the established current disease risk stratification. Analysis of the PNET3 cohort in this study identified pathology as a significant independent prognostic factor in medulloblastoma. This data indicates incorporation of both gender and pathology in future disease risk stratification.

9.18. Applying similar disease risk assessment in medulloblastoma patients aged <3 years at diagnosis

The current study utilized the PNET3 cohort to successfully test and validate prognostic molecular markers in medulloblastoma patients aged >3 years at diagnosis. Patients <3 years at diagnosis form a vulnerable subgroup of this disease since they are classified as high-risk patients with overall survival of about 40%. Therefore, similar strategies for identifying significant prognostic clinicopathological and molecular markers (e.g. *COL1A2* methylation and MBEN pathology) may allow stratifying infantile medulloblastomas according to their predicted clinical outcome and subsequently therapeutic protocols.

9.19. Summary of the project

In summary, the cure rate of medulloblastoma is still compromised partially due to the imprecise current clinically based disease-risk classification. Therefore, modification of such classification to provide a more accurate and individualized disease-risk stratification, incorporating other clinical, pathological and molecular criteria formed the corner stone of this project. One of the initial issues addressed was developing and validating a method which allows testing of chromosomal losses in archival FFPE tumour samples lacking matched constitutional DNA. The HOMOD method proved to fulfil this requirement.

Activation of the Wnt/Wg pathway in medulloblastoma appears to be associated with favourable prognosis. This association has been observed across multiple studies however, it has not been assessed in large scale clinically controlled cohorts which is an essential step before taking this marker to practice. Such analysis and validation in an extensive clinically based trial (PNET3) has been fulfilled in this project.

Different clinicopathological and molecular potential markers of prognosis were independently tested and the significant ones were combined and used to produce disease-risk prediction models using Cox proportional regression hazard ratio analysis. Four and three variable based models were constructed incorporating gender, metastatic stage at diagnosis, histopathology and β-catenin nuclear localization, just the three variables, respectively. These models were applied to the 16 or 8 risk factor combinations, respectively, by which patient can present and each

combination showed a unique hazard ratio and equivalent disease-risk category (favourable, standard or high-risk). At the present time a three variable model may be the most practical model to take forward in practice since it incorporates variables which have been validated in multiple independent clinical trials.

Chapter 10

References

Alberts, B. & Johnson, A. (2002). Molecular biology of the cell. Garland Science.

Anderton, J., Lindsey, J., Lusher, M., Gilbertson, R., Bailey, S., Ellison, D. & Clifford, S. (2008). Global analysis of the medulloblastoma epigenome identifies disease-subgroup-specific inactivation of COL1A2. *Neuro Oncol.*, **10,** 981-94.

Bacha, D., Caparros-Sison, B., Allen, J., Walker, R. & Tan, C. (1986). Phase I study of carboplatin (CBDCA) in children with cancer. *Cancer Treat Rep.*, **70,** 865-9.

Baeza, N., Masuoka, J., Kleihues, P. & Ohgaki, H. (2003). *Axin*1 mutations but not deletions in cerebellar medulloblastomas. *Oncogene*, **22,** 632-6.

Bailey, P. & Cushing, H. (1925). Microchemical Color Reactions as an Aid to the Identification and Classification of Brain Tumors. *Proc Natl Acad Sci U S A.*, **11,** 82-4.

Barr, R. (2010). Imatinib mesylate in children and adolescents with cancer. *Pediatr Blood Cancer*, **55,** 18-25.

Batra, S., McLendon, R., Koo, J., Castelino-Prabhu, S., Fuchs, H., Krischer, J., Friedman, H., Bigner, D. & Bigner, S. (1995). Prognostic implications of chromosome 17p deletions in human medulloblastomas. *J Neurooncol.* , **24,** 39-45.

Biegel, J., Janss, A., Raffel, C., Sutton, L., Rorke, L., Harper, J. & Phillips, P. (1997). Prognostic significance of chromosome 17p deletions in childhood primitive neuroectodermal tumors (medulloblastomas) of the central nervous system. *Clin Cancer Res.*, **3,** 473-8.

Boland, C., Thibodeau, S., Hamilton, S., Sidransky, D., Eshleman, J., RW, B., Meltzer, S., Rodriguez-Bigas, M., Fodde, R., Ranzani, G. & Srivastava, S. (1998). A National Cancer Institute Workshop on Microsatellite Instability for cancer detection and familial predisposition: development of international criteria for the determination of microsatellite instability in colorectal cancer. *Cancer Res.*, **58,** 5248-57.

Boon, K., Eberhart, C. & Riggins, G. (2005). Genomic amplification of orthodenticle homologue 2 in medulloblastomas. *Cancer Res.*, **65,** 703-7.

Bowers, D., Liu, Y., Leisenring, W., McNeil, E., Stovall, M., Gurney, J., Robison, L., Packer, R. & Oeffinger, K. (2006). Late-occurring stroke among long-term survivors of childhood leukemia and brain tumors: a report from the Childhood Cancer Survivor Study. *J Clin Oncol.*, **24,** 5277-82.

Bradburn, M., Clark, G., Love, S. & Altman, D. (2003). survival analysis part II: Multivariate data analysis - an introduction to concepts and methods. *Br J Cancer*, **89,** 431-436.

Broderic, D.K., Parrett, T.J. & al, e. (2004). Mutations of PIK3CA in anaplastic oligodendrogliomas, high grade astrocytomas and medulloblastomas. *Cancer research*, **64,** 5048-5050.

Brown, H., Kepner, J., Perlman, E., Friedman, H., Strother, D., Duffner, P., Kun, L., Goldthwaite, P. & Burger, P. (2000). "Large cell/anaplastic" medulloblastomas: a Pediatric Oncology Group Study. *J Neuropathol Exp Neurol.* , **59,** 857-65.

Bühring, U., Strayle-Batra, M., Freudenstein, D., Scheel-Walter, H. & Küker, W. (2002). MRI features of primary, secondary and metastatic medulloblastoma. *Eur Radiol.*, **6,** 1342-8.

Chang, C. & Ferrone, S. (2007). Immune selective pressure and HLA class I antigen defects in malignant lesions. *Cancer Immunol Immunother.*, **56,** 227-36.

Chang, C., Housepian, E. & Herbert, C.J. (1969). An operative staging system and a megavoltage radiotherapeutic technic for cerebellar medulloblastomas. *Radiology*, **93,** 1351-9.

Clark, T.G., Bradburn, M., Love, S. & Altman, D. (2003). Survival analysis. Part 1: basic concepts and firs analyses. *Br J Cancer*, **89,** 232-238.

Clifford, S., Lusher, M., Lindsey, J., Langdon, J., Gilbertson, R., Straughton, D. & Ellison, D. (2006). Wnt/Wingless pathway activation and chromosome 6 loss characterize a distinct molecular sub-group of medulloblastomas associated with a favorable prognosis.*Cell Cycle*, **5,** 2666-70.

Cogen, P., Daneshvar, L., Metzger, A., Duyk, G., Edwards, M. & Sheffield, V. (1992). Involvement of multiple chromosome 17p loci in medulloblastoma tumorigenesis. *Am J Hum Genet.* , **50,** 584-9.

Cogen, P., Daneshvar, L., Metzger, A. & Edwards, M. (1990). Deletion mapping of the medulloblastoma locus on chromosome 17p. *Genomics*, **8,** 279-85.

Cox, D.R. (1972). Regression models and life tables. *J R Statist Soc*, **B 34,** 187-220.

Crawford, J., MacDonald, T. & Packer, R. (2007). Medulloblastoma in childhood: new biological advances. *Lancet Neurol.*, **6,** 1073-85.

Curran, E.K., Sainani, K.L., Le, G.M., Propp, J.M. & Fisher, P.G. (2009). Gender affects survival for medulloblastoma only in older children and adults: A study from the surveillance epidemiology and end results registry. *Pediatric blood cancer*, **52,** 60-64.

Dahmen, R.P., Koch, A. & Denkhaus, D. (2001). Deletions of *AXIN1*, a component of the Wnt/wingless pathway, in sporadic medulloblastomas. *Cancer Res*, **61,** 7039-43.

Di Marcotullio, L., Ferretti, E., De Smaele, E., Argenti, B., Mincione, C., Zazzeroni, F., Gallo, R., Masuelli, L., Napolitano, M., Maroder, M., Modesti, A., Giangaspero, F., Screpanti, I., Alesse, E. & Gulino, A. (2004). REN(KCTD11) is a suppressor of Hedgehog signaling and is deleted in human medulloblastoma. *Proc Natl Acad Sci U S A.*, **101,** 10833-8.

Dunn, K., Espino, P., Drobic, B., He, S. & Davie, J. (2006). The Ras-MAPK signal transduction pathway, cancer and chromatin remodeling. *Biochem Cell Biol.*, **83,** 1-14.

Eberhart, C., Tihan, T. & Burger, P. (2000). Nuclear localization and mutation of beta-catenin in medulloblastomas. *J Neuropathol Exp Neurol*, **59,** 333-7.

Eberhart, C.G., Schuster, A., Goldthwait, P., Cohen, K.J., Perlman, E.J. & Burger, P.C. (2002). Comparative genomic hybridization detects an increased number of chromosomal alterations in large cell/anaplastic medulloblastoma. *Brain Pathol*, **12,** 36-44.

Egger, G., Liang, G., Aparicio, A. & A, J.P. (2004). Epigenetics in human disease and prospects for epigenetic therapy. *Nature*, **429,** 457-63.

Ellison, D. (2002). Classifying the medulloblastoma: insights from morphology and molecular genetics. *Neuropathol Appl Neurobiol.* , **28,** 257-82.

Ellison, D., Clifford, S., Gajjar, A. & Gilbertson, R. (2003). What's new in neuro-oncology? Recent advances in medulloblastoma. *Eur J Paediatr Neurol.*, **7,** 53-66.

Ellison, D., Onilude, O., Lindsey, J., Lusher, M., Weston, C., Taylor, R., Pearson, A. & Clifford, S. (2005). beta-Catenin status predicts a favorable outcome in childhood medulloblastoma: the United Kingdom Children's Cancer Study Group Brain Tumour Committee. *J Clin Oncol.*, **23,** 7951-7.

Ellison, D.W., Clifford, S.C. & Giangaspero, F. (2006). Medulloblastoma; Russel and Rubinstein's pathology of tumours of the nervous system, Roger, E.M., Marc, K.R. & Darell, D.B. (eds) pp. 247-264. Oxford University Press Inc.

Emadian, S., McDonald, J., Gerken, S. & Fults, D. (1996). Correlation of chromosome 17p loss with clinical outcome in medulloblastoma. *Clin Cancer Res.*, **9,** 1559-64.

Evans, D., Farndon, P., Burnell, L., Gattamaneni, H. & Birch, J. (1991). The incidence of Gorlin syndrome in 173 consecutive cases of medulloblastoma. *Br J Cancer*, **64,** 959-61.

Fan, X. & Eberhart, C.G. (2008). Medulloblastoma Stem Cells. *J Clin Oncol.*, **26,** 2821-2827.

Fan, X., Mikolaenko, I., Elhassan, I., N, i.X., Wang, Y., Ball, D., Brat, D., Perry, A. & Eberhart, C. (2004). Notch1 and notch2 have opposite effects on embryonal brain tumor growth. *Cancer Res.*, **64,** 7767-93.

Fan, X., Wang, Y., Kratz, J., Brat, D., Robitaille, Y., Moghrabi, A., Perlman, E., Dang, C., Burger, P. & Eberhart, C. (2003). hTERT gene amplification and increased mRNA expression in central nervous system embryonal tumors. *Am J Pathol.*, **162,** 1763-9.

Fattet, S., Haberier, C., Legoix, P., Varlet, P., Tubiana, A., Lellouch, Lair, S., Manie, E., Raquin, M.A., Bours, D., Carpentier, S., Barillot, E., Grill, J., Doz, F., Puget, S., Janoueix-Lerosey, I. & Delattre, O. (2009). Beta-catenin status in paediatric medullblastomas: correlation of immunohistochemical expression with mutational status, genetic profiles, and clinical characteristics. *J Pathol*, **218,** 86-94.

Fossati, P., Ricardi, U. & Orecchia, R. (2009). Pediatric medulloblastoma: toxicity of current treatment and potential role of protontherapy. *Cancer Treat Rev.*, **35,** 79-96.

Frank, L.M. & Teich, N.M. (1997). *Introduction to the cellular and molecular biology of cancer*. Oxford University Press.

Friedman, H., Mahaley, M.J., Schold, S.J., Vick, N., Falletta, J., Bullard, D., D'Souza, B., Khandekar, J., Lew, S. & Oakes, W. (1986). Efficacy of vincristine and cyclophosphamide in the therapy of recurrent medulloblastoma. Neurosurgery. *Neurosurgery*, **18,** 335-40.

Gajjar, A., Chintagumpala, M., Ashley, D., Kellie, S., Kun, L., Merchant, T., Woo, S., Wheeler, G., Ahern, V., Krasin, M., Fouladi, M., Broniscer, A., Krance, R., Hale, G., Stewart, C., Dauser, R., Sanford, R., Fuller, C., Lau, C., Boyett, J., Wallace, D. & RJ., G. (2006). Risk-adapted craniospinal radiotherapy followed by high-dose chemotherapy and stem-cell rescue in children with newly diagnosed medulloblastoma (St Jude Medulloblastoma-96): long-term results from a prospective, multicentre trial. *Lancet Oncol*, **7,** 813-20.

Gajjar, A., Hernan, R., Kocak, M., Fuller, C., Lee, Y., McKinnon, P., Wallace, D., Lau, C., Chintagumpala, M., Ashley, D., Kellie, S., Kun, L. & Gilbertson, R. (2004). Clinical, histopathologic, and molecular markers of prognosis: toward a new disease risk stratification system for medulloblastoma. *J Clin Oncol.*, **22,** 9893.

Gajjar, A., RK, M., Heideman, R., Sanford, R., Douglass, E., Kovnar, E., Langston, J., Jenkins, J. & Kun, L. (1994). Medulloblastoma in very young children: outcome of definitive craniospinal irradiation following incomplete response to chemotherapy. *J Clin Oncol.*, **12,** 1212-6.

Gandola, L., Massimino, M., Cefalo, G., Solero, C., Spreafico, F., Pecori, E., Riva, D., Collini, P., Pignoli, E., Giangaspero, F., Luksch, R., Berretta, S., Poggi, G., Biassoni, V., Ferrari, A., Pollo, B., Favre, C., Sardi, I., Terenziani, M. & Fossati-Bellani, F. (2009). Hyperfractionated accelerated radiotherapy in the Milan strategy for metastatic medulloblastoma. *J Clin Oncol.*, **27,** 566-71.

Giangaspero, F., Perilongo, G., Fondell, i.M., Brisigotti, M., Carollo, C., Burnelli, R., Burger, P. & Garrè, M. (1999). Medulloblastoma with extensive nodularity: a variant with favorable prognosis. *J Neurosurg.* , **91,** 971-7.

Giangaspero, F., Wellek, S., Masuoka, J., Gess, i.M., Kleihues, P. & Ohgaki, H. (2006). Stratification of medulloblastoma on the basis of histopathological grading. *Acta Neuropathol.* , **112,** 5-12.

Gilbertson, R. (2004). Medulloblastoma: signalling a change in treatment. *Lancet Oncol.*, **5,** 209-18.

Gilbertson, R. & Clifford, S. (2003). PDGFRB is overexpressed in metastatic medulloblastoma. *Nat Genet.*, **35,** 197-8.

Gilbertson, R., Langdon, J., Hollander, A., Hernan, R., Hogg, T., Gajjar, A., Fuller, C. & Clifford, S. (2006). Mutational analysis of PDGFR-RAS/MAPK pathway activation in childhood medulloblastoma. *Eur J Cancer.*, **42,** 646-9.

Gilbertson, R., Wickramasinghe, C., Hernan, R., Balaji, Hunt, D., D, J.-W., Crolla, J., Perry, R., Lunec, J., Pearson, A. & Ellison, D. (2001). Clinical and molecular stratification of disease risk in medulloblastoma. *Br J Cancer*, **85,** 705-12.

Gilbertson, R.J. (2002). Paediatric embryonic brain tumours: biological and clinical relevance of molecular genetic abnormalities. *European Journal of cancer*, **38,** 675-685.

Gilbertson, R.J. & Ellison, D. (2008). The origins of medulloblastoma subtypes. *Annu. Rev. Pathol. Dis.*, **3,** 341-365.

Goldberg, E., Glendening, J., Karanjawala, Z., Sridhar, A., Walker, G., Hayward, N., Rice, A., Kurera, D., Tebha, Y. & Fountain, J. (2000). Localization of multiple melanoma tumor-suppressor genes on chromosome 11 by use of homozygosity mapping-of-deletions analysis. *Am J Hum Genet.* , **67,** 417-31.

Gorlin, R.J. (1987). A first description of dysegmental dysplasia. *Am J Med Genet*, **28,** 1915-6.

Griffin, C., Hawkins, A., Packer, R., Rorke, L. & Emanuel, B. (1988). Chromosome abnormalities in pediatric brain tumors. *Cancer Res.* , **48,** 175-80.

Guessous, F., Yunqing, L. & Roger, A. (2008). Signaling pathways in medulloblastoma *J of Cell Physiol*, **217,** 577-583.

Hamilton, S., Liu, B., Pearson, r.F., Papadopoulos, n., Powell, S., Krush, A., Berk, T., Cohen, Z., Tetu, B., Burger, P.C., Peter, C., Wood, P., Taqi, F., Booker, B., Petersen, G., Offerhaus, G., Tersmette, A., giandiello, F., Vogelstein, B. & Kinzler, K. (1995). The molecular basis of Turcot's syndrome. *N. Engl J. Med* **332,** 839-47.

Hanahan, D. & Weinberg, R. (2000). The hallmarks of cancer. *Cell*, **100,** 57-70.

Hoff, K., Hartmann, W., Bueren, A.V., Gerber, N.U., Grotzer, M., Pietsch, T. & Rutkowski, S. (2010). Large cell/ anaplastic medulloblastoma: outcome according to *Myc* status, histopathological, and clinical risk factors. *Pediatr Blood Cancer*, **54,** 369-376.

Hui, A., Takano, H., Lo, K., Kuo, W., Lam, C., Tong, C., Chang, Q., Gray, J. & Ng, H. (2005). Identification of a novel homozygous deletion region at 6q23.1 in medulloblastomas using high-resolution array comparative genomic hybridization analysis. *Clin Cancer Res.*, **11,** 4707-16.

Jackson, A., Panayiotidis, P. & Foroni, L. (1998). The human homologue of the *Drosophila* tailless gene (*TXL*): characterization and mapping to a region of comon deletion in human lymphoid leukemia on chromosome 6q21. *Genomics*, **50,** 34-43.

Jung, H.L., Wang, K.-C., Kim, S.-K., Sung, K.W., Koo, H.H., Shin, H.y., Ahn, H.S., Shin, H.J. & Cho, B.-K. (2004). Loss of heterozygosity analysis of chromosome 17p13.1-13.3 and its correlation with clinical outcome in medulloblastoma. *J Neuro-Oncol*, **67,** 41-46.

Kallassy, M., Toftgård, R., Ueda, M., Nakazawa, K., Vorechovský, I., Yamasaki, H. & Nakazawa, H. (1997). Patched (ptch)-associated preferential expression of smoothened (smoh) in human basal cell carcinoma of the skin. *Cancer Res.*, **57,** 4731-5.

Kaplan, E. & Meier, P. (1958). Non parametric estimation from incomplete observations. *J Am Stat Assoc*, **53**.

King, R. & Robins, M. (2006). Cancer biology. Pearson Education limited: Harlow.

Klaus, A. & Birchmeier, W. (2008). Wnt signalling and its impact on development and cancer. *Nat Rev Cancer*, **8,** 387-98.

Kleihues, P. & Cavenee, W.K. (2000). Tumours of the nervous system *World health Organization, classification of tumours. Lyon; IARC*.

Knudson, A.J. (1971). Mutation and cancer: statistical study of retinoblastoma. *Proc Natl Acad Sci U S A*, **68,** 820-3.

Koch, A., Hrychyk, A., Hartmann, W., Waha, A., Mikeska, T., Waha, A., Schuller, N., Sorcrsen, N., Berthold, F., Goodyer, C., G., Wiestler, O.D., Birchmeier, W., Behrens, J. & Pietsch, T. (2007). Mutations of the Wnt antagonist *AXIN2* (Conductin) result in TCF-dependent transcription in medulloblastomas. *Int J Cancer*, **121,** 284-291.

Koch, A., Waha, A., Hartmann, W., Milde, U. & Goodyer, C., G. (2004). No evidence for mutations or altered expression of the supperessor of fused gene (SUFU) in primitive neuroectodermal tumours. *Neuropathol. Appl. Neurobiol*, **30,** 532-39.

Koch, A., Waha, A., Tonn, J., Sörensen, N., Berthold, F., Wolter, M., Reifenberger, J., Hartmann, W., Friedl, W., Reifenberger, G., Wiestler, O.D. & Pietsch, T. (2001). Somatic mutations of WNT/wingless signaling pathway components in primitive neuroectodermal tumors *Int J Cancer*, **93,** 445-449.

Kool, M., Koster, J., Bunt, J., Hasselt, N., Lakeman, A., van Sluis, P., Troost, D., Meeteren, N., Caron, H., Cloos, J., Mrsić, A., Ylstra, B., Grajkowska, W., Hartmann, W., Pietsch, T., Ellison, D., Clifford, S. & Versteeg, R. (2008). Integrated genomics identifies five medulloblastoma subtypes with distinct genetic profiles, pathway signatures and clinicopathological features. *PLoS One.* , **3,** 1-14.

Koyama, M., Nagai, H., Bando, K., Matsumoto, S., Tajiri, T., Onda, M., Ito, M., Moriyama, Y. & Emi, M. (2000). New target region of allelic loss in hepatocellular carcinomas within a 1-cM interval on chromosome 6q23. *J. Hepatol*, **33,** 85-90.

Krischer, J., Ragab, A., Kun, L., Kim, T., Laurent, J., Boyett, J., Cornell, C., Link, M., Luthy, A. & Camitta, B. (1991). Nitrogen mustard, vincristine, procarbazine, and prednisone as adjuvant chemotherapy in the treatment of medulloblastoma. A Pediatric Oncology Group study. *J Neurosurg.* , **74,** 905-9.

Lamont, J., McManamy, C., Pearson, A., Clifford, S. & Ellison, D. (2004). Combined histopathological and molecular cytogenetic stratification of medulloblastoma patients. *Clin Cancer Res*, **10,** 5482-93.

Langdon, J., Lamont, J., Scott, D., Dyer, S., Prebble, E., Bown, N., Grundy, R., Ellison, D. & Clifford, S. (2006). Combined genome-wide allelotyping and copy number analysis identify frequent genetic losses without copy number reduction in medulloblastoma. *Genes Chromosomes Cancer*, **45,** 47-60.

Lee, A., Kessler, J., Read, T., Kaiser, C., Corbeil, D., Huttner, W., Johnson, J. & Wechsler-Reya, R. (2005). Isolation of neural stem cells from the postnatal cerebellum. *Nat Neurosci.*, **8,** 723-9.

Lee, S.E., Johnson, S.P., Hale, L.P., Li, J., Bullock, N., Fuchs, H., Friedman, A., Mclendon, R., Bigner, D.D., Modrich, P. & Friedman, H.S. (1998). Analysis of DNA mismatch repair proteins in human medulloblastoma. *Clin Cancer Res*, **4** 1415-1419.

Legoix, P., Bluteau, O., Bayer, J., Perret, C., Balabaud, C., Belghiti, J., Franco, D., Thomas, G., Laurent-Puig, P. & Zucman-Rossi, J. (1999). Beta-catenin mutations in hepatocellular carcinoma correlate with a low rate of loss of heterozygosity. *Oncogene.* **18,** 4044-4046.

Lindsey, J., Anderton, J., Lusher, M. & Clifford, S. (2005). Epigenetic events in medulloblastoma development. *Neurosurg Focus.*, **19,** E10.

Lo, K., Rossi, M., Eberhart, C. & Cowell, J. (2007). Genome wide copy number abnormalities in pediatric medulloblastomas as assessed by array comparative genome hybridization. *Brain Pathol.*, **17,** 282-96.

Louis, D., Ohgaki, H., Wiestler, O., Cavenee, W., Burger, P., Jouvet, A., Scheithauer, B. & Kleihues, P. (2007). The 2007 WHO classification of tumours of the central nervous system. *Acta Neuropathol.*, **114,** 97-109.

Makino, N., Yamato, T., Inoue, H., Furukawa, T., Abe, T., Yokoyama, T., Yatsuoka, T., Fukushige, S., Orikasa, S., Takahashi, T. & Horii, A. (2001). Isolation and characterization of the human gene homologous to the Drosophila headcase (hdc) gene in chromosome bands 6q23-q24, a region of common deletion in human pancreatic cancer. *DNA Seq.*, **11,** 547-53.

Malkin, D., Li, F., Strong, L., Fraumeni, J.J., Nelson, C., Kim, D., Kassel, J., Gryka, M., Bischoff, F. & Tainsky, M. (1990). Germ line p53 mutations in a familial syndrome of breast cancer, sarcomas, and other neoplasms. *Science*, **250,** 1233-8.

McDonald, J.D., Daneshvar, L.K., Willert, J.R., Matsumuea, K., Waldman, F. & Cogen, P.H. (1994). Physical mapping of chromosome 17p 13.3 in the region of putative tumour suppressor gene important in medulloblastoma. *Genomics*, **23,** 229-32.

McManamy, C., Lamont, J., Taylor, R., Cole, M., Pearson, A., Clifford, S. & Ellison, D. (2003). Morphophenotypic variation predicts clinical behavior in childhood non-desmoplastic medulloblastomas. *J Neuropathol Exp Neurol.*, **62,** 627-32.

McManamy, C., Pears, J., Weston, C., Hanzely, Z., Ironside, J., Taylor, R., Grundy, R., Clifford, S. & Ellison, D. (2007). Nodule formation and desmoplasia in medulloblastomas-defining the nodular/desmoplastic variant and its biological behavior. *Brain Pathol.* , **17,** 151-64.

Michiels, E., Weiss, M., Hoovers, J., Baak, J., PA, V., F, B. & Hermsen, M. (2002). Genetic alterations in childhood medulloblastoma analyzed by comparative genomic hybridization. *J Pediatr Hematol Oncol.*, **24,** 205-10.

Morin, P. (1999). Beta-catenin signaling and cancer. *Bioessays*, **21,** 1021-30.

Mullis, K.B., Faloona, F., Ascharf, S., Saiki, R.K., Horn, G.T. & Erlich, H.A. (1983). Specific enzymatic amplification of DNA in vitro: the polymerase chain reaction. *Quantitative biology*, **51,** 263-273.

Murphy, C. & Fornier, M. (2010). HER2-positive breast cancer: beyond trastuzumab. *Oncology*, **24,** 410-5.

Nhieu, J.T., Renard, C.A., Wei, Y., Cherqui, D., Zafrani, E.S. & Buendia, M.A. (1999). Nuclear accumulation of mutated beta-catenin in hepatocellular carcinoma is associated with increased cell proliferation. *Am J Pathol*, **155,** 703-710.

Offit, K., Levran, O., Mullaney, B., Mah, K., Nafa, K., Batish, S., Diotti, R., Schneider, H., Deffenbaugh, A., Scholl, T., Proud, V., Robson, M., Norton, L., Ellis, N., Hanenberg, H. & Auerbach, A. (2003). Shared genetic susceptibility to breast cancer, brain tumors, and Fanconi anemia. *J Natl Cancer Inst.* , **95,** 1548-51.

Packer, R., Cogen, P., Vezina, G. & Rorke, L. (1999). Medulloblastoma: clinical and biologic aspects. *Neuro Oncol.*, **1,** 232-50.

Packer, R., Gajjar, A., Vezina, G., Rorke-Adams, L., Burger, P., Robertson, P., Bayer, L., LaFond, D., Donahue, B., Marymont, M., Muraszko, K., Langston, J. & Sposto, R. (2006). Phase III study of craniospinal radiation therapy followed by adjuvant chemotherapy for newly diagnosed average-risk medulloblastoma. *J Clin Oncol.*, **24,** 4202-8.

Packer, R. & Vezina, G. (2008). Management of and prognosis with medulloblastoma: therapy at a crossroads. *Arch Neurol.*, **65,** 1419-24.

Pan, E., Pellarin, M., Holmes, E., Smirnov, I., Misra, A., Eberhart, C., Burger, P., Biegel, J. & Feuerstein, B. (2005). Isochromosome 17q is a negative prognostic factor in poor-risk childhood medulloblastoma patients. *Clin Cancer Res.*, **11,** 4733-40.

Paraf, F., Jothy, S. & Van Meir, E. (1997). Brain tumor-polyposis syndrome: two genetic diseases? *J Clin Oncol.* , **15,** 2744-58.

Pfister, S., Remke, M., Benner, A., Mendrzyk, F., Toedt, G., Felsberg, J., Wittmann, A., Devens, F., Gerber, N., Joos, S., Kulozik, A., Reifenberger, G., Rutkowski, S., Wiestler, O., Radlwimmer, B., Scheurlen, W., Lichter, P. & Korshunov, A. (2009). Outcome prediction in pediatric medulloblastoma based on DNA copy-number aberrations of chromosomes 6q and 17q and the MYC and MYCN loci. *J Clin Oncol.* , **27,** 1627-36.

Pietsch, T., Waha, A., Koch, A., Kraus, J., Albrecht, S., Tonn, J., Sörensen, N., Berthold, F., Henk, B., Schmandt, N., Wolf, H., von Deimling, A., Wainwright, B., Chenevix-Trench, G., Wiestler, O. & Wicking, C. (1997). Medulloblastomas of the desmoplastic variant carry mutations of the human homologue of Drosophila patched. *Medulloblastomas of the desmoplastic variant carry mutations of the human homologue of Drosophila patched*, **57,** 2085-8.

Pingoud-Meier, C., Lang, D., Janss, A., Rorke, L., Phillips, P., Shalaby, T. & Grotzer, M. (2003). Loss of caspase-8 protein expression correlates with unfavorable survival outcome in childhood medulloblastoma. *Clin Cancer Res.*, **9,** 6401-9.

Pizer, B. & Clifford, S. (2009). The potential impact of tumour biology on improved clinical practice for medulloblastoma: progress towards biologically driven clinical trials. *Br J Neurosurg.*, **23,** 364-75.

Potter, R., Czech, T., Diekmann, K., Slavc, I., Wimberger-Prayer, D. & Budka, H. (1998). *Tumours of the central nervous system*. Cancer in children. Oxford University Press: Oxford.

Ray, A., Ho, M., Ma, J., Parkes, R., Mainprize, T., Ueda, S., McLaughlin, J., Bouffet, E., Rutka, J. & Hawkins, C. (2004). A clinicobiological model predicting survival in medulloblastoma. *Clin Cancer Res.*, **10,** 7613.

Ridola, V., Grill, J., Doz, F., Gentet, J., Frappaz, D., Raquin, M., Habrand, J., Sainte-Rose, C., Valteau-Couanet & Kalifa, C. (2000). High-dose chemotherapy with autologous stem cell rescue followed by posterior fossa irradiation for local medulloblastoma recurrence or progression after conventional chemotherapy. *Cancer*, **110,** 156-63.

Rogers, H., Miller, S., Lowe, J., Brundler, M., Coyle, B. & Grundy, R. (2009). An investigation of WNT pathway activation and association with survival in central nervous system primitive neuroectodermal tumours (CNS PNET). *Br J Cancer.*, **21,** 1292-302.

Romer, J. & Curran, T. (2005). Targeting Medulloblastoma: small-molecule inhibitors of the Sonic Hedgehog pathway as potential cancer therapeutics *Cancer research*, **65,** 4975-78.

Rorke, L. (1983). The cerebellar medulloblastoma and its relationship to primitive neuroectodermal tumors. *J Neuropathol Exp Neurol.*, **42,** 1-15.

Rutkowski, S., Bode, U., Deinlein, F., Ottensmeier, H., Warmuth-Metz, M., Soerensen, N., Graf, N., Emser, A., Pietsch, T., Wolff, J., Kortmann, R. & Kuehl, J. (2005). Treatment of early childhood medulloblastoma by postoperative chemotherapy alone. *N Engl J Med.*, **352,** 978-86.

Rutkowski, S., Bueren, A.V., Hoff, K., Hartmann, W., Shalaby, T., Deinlein, F., Warmuth-Metz, M., Soerensen, N., Emser, A., Bode, U., mittler, U., Urban, C., Benesch, M., Kortmann, R.D., Schlegel, p.G., Kuehl, J., Pietsch, T. & Grotzer, M. (2007). Prognostic relevance of clinical and biological risk factors in childhood medulloblastoma: Results of patients treated in the prospective multicenter trial HIT'91 *Clin Cancer res*, **13,** 2651-2657.

Sadasivan, B., Lehner, P., Ortmann, B. & Spies, T. (1996). Roles for calreticulin and a novel glycoprotein, tapasin, in the interaction of MHC class I molecules with TAP. *Immunity*, **5,** 103-14.

Salaroli, R., Tomaso, T.D., Ronchi, A., Ceccarelli, C., Cammelli, S., Cappellini, A., Martinelli, G.N., Barbieri, E., Giangaspero, F. & G, C. (2008). Radiobiologic response of medulloblastoma cell lines: involvement of β-catenin? . *J Clin Oncol.*, **90,** 243-251.

Sambrook, J. & Russel, D. (2001). *Molecular Cloning: A Laboratory Manual*. Cold spring Harbor Laboratory. New York.

Sanger, F., Nicklen, S. & Coulson, A. (1977). DNA sequencing with chain-terminating inhibitors. *Proc Natl Acad Sci U S A*, **74,** 5463-5467.

Sarkar, C., Deb, P. & Sharma, M. (2005). Recent advances in embryonal tumours of the central nervous system. *Childs Nerv Syst.*, **21,** 272-93.

Scheurlen, W.G., Schwabe, G.C., Mollenhauer, I., Sorcrsen, N. & Kuhi, J. (1998). Molecular analysis of childhood primitive neuro-ectodermal tumors defines markers associated with poor outcome. *J. Clin. Oncol.*, **16,** 2478-85.

Schofield, D., West, D., Anthony, D., Marshal, R. & Sklar, J. (1995). Correlation of loss of heterozygosity at chromosome 9q with histological subtype in medulloblastomas. *Am J Pathol.*, **146,** 472-80.

Seliger, B., Maeurer, M. & Ferrone, S. (1997). TAP off--tumors on. *Immunol Today*, **18,** 292-9.

Shridhar, V., Staub, J., Huntley, B., Cliby, W., Jenkins, R., Pass, H., Hartmann, L. & Smith, D. (1999). A novel region of deletion on chromosome 6q23.3 spanning less than 500 Kb in high grade invasive epithelial ovarian cancer *oncogen*, **18,** 3913-3919.

Singh, S., Hawkins, C., Clarke, I., Squire, J., Bayani, J., Hide, T., Henkelman, R., Cusimano, M. & Dirks, P. (2004). Identification of human brain tumour initiating cells. *Nature*, **432,** 396-401.

Skowroska-Gardas, A. (1999). Radiotherapy of central nervous system tumors in young children: Benefits and pitfalls. *Medical Pediatric Oncology*, **33,** 572-76.

Smith, C., Santi, M., Rajan, E.J., Choi, M.R., Rood, B.R., Cornelison, R., MacDonald, T.J. & Vukmanovic, S.J. (2009). A novel role of HLA class 1 in the pathology of medulloblastoma. *Journal Transl Med.*, **12,** 59.

Srivastava, S.A., Zou, Z., Pirollo, K., Blatner, W. & Chang, E.H. (1990). Germ-line transmission of mutated *p53* gene in a cancer-prone family with Li-Fraumeni syndrome. *Nature*, **348,** 747-749.

Strachan, T. & Read, A. (2004). Human molecular genetics. Garland science: Oxon.

Tabori, U., Baskin, B., Shago, M., Alon, N., Taylor, M., Ray, P., Bouffet, E., Malkin, D. & Hawkins, C. (2010). Universal poor survival in children with medulloblastoma harboring somatic TP53 mutations. *J Clin Oncol.*, **28,** 1345-50.

Taipale, J. & Beachy, P. (2001). The Hedgehog and Wnt signalling pathways in cancer. *Nature*, **411,** 349-54.

Taylor, M., Mainprize, T. & Rutka, J. (2000). Molecular insight into medulloblastoma and central nervous system primitive neuroectodermal tumor biology from hereditary syndromes: a review. *Neurosurgery*, **47,** 888-901.

Taylor, R., Bailey, C., Robinson, K., Weston, C., Ellison, D., Ironside, J., Lucraft, H., Gilbertson, R., Tait, D., Walker, D., Pizer, B., Imeson, J. & Lashford, L. (2003). Results of a randomized study of preradiation chemotherapy versus radiotherapy alone for nonmetastatic medulloblastoma: The International Society of Paediatric Oncology/United Kingdom Children's Cancer Study Group PNET-3 Study. *J Clin Oncol.*, **21,** 1581-91.

Thomas, G.A. & Raffel, C. (1991). Loss of Heterozygosity on 6q, 16q, and 17p in Human Central Nervous System Primitive Neuroectodermal Tumors *Cancer Res.*, **51,** 639-643.

Thompson, M., Fuller, C., Hogg, T., Dalton, J., Finkelstein, D., Lau, C., Chintagumpala, M., Adesina, A., Ashley, D., Kellie, S., Taylor, M., Curran, T., Gajjar, A. & Gilbertson, R.

(2006). Genomics identifies medulloblastoma subgroups that are enriched for specific genetic alterations. *J Clin Oncol.*, **24,** 1924-31.

Tubergen, D., Gilchrist, G., O'Brien, R., Coccia, P., Sather, H., Waskerwitz, M. & Hammond, G. (1993). Improved outcome with delayed intensification for children with acute lymphoblastic leukemia and intermediate presenting features: a Childrens Cancer Group phase III trial. *J Clin Oncol.* , **11,** 527-37.

Umar, A., Boland, C., Terdiman, J., Syngal, S., de la Chapelle, A., Rüschoff, J., Fishel, R., Lindor, N., Burgart, L., Hamelin, R., Hamilton, S., Hiatt, R., Jass, J., Lindblom, A., Lynch, H., Peltomaki, P., Ramsey, S., Rodriguez-Bigas, M., Vasen, H., Hawk, E., Barrett, J., Freedman, A. & Srivastava, S. (2004). Revised Bethesda Guidelines for hereditary nonpolyposis colorectal cancer (Lynch syndrome) and microsatellite instability. *J Natl Cancer Inst.*, **96,** 261-8.

Vézina, L. & Packer, R. (1994). Infratentorial brain tumors of childhood. *Neuroimaging Clin N Am.*, **4,** 423-36.

Viana-Pereira, M., Almeida, I., Sousa, S., Mahler-Araújo, B., Seruca, R., Pimentel, J. & Reis, R. (2009). Analysis of microsatellite instability in medulloblastoma. *Neuro Oncol.*, **11,** 458-67.

Voute, P.A., Barrett, A., Stevens, M. & Caron, H.N. (2005). Molecular biology of childhood tumours. In *Cancer in children in clinical management* pp. 35-43. Oxford University Press.

Wang, V., Rose, M. & Zoghbi, H. (2005). Math1 expression redefines the rhombic lip derivatives and reveals novel lineages within the brainstem and cerebellum. *Neuron*, **48,** 31-43.

Wang, V.Y. & Zoghbi, H.Y. (2001). Genetic regulation of cerebellar development. *Nature Reviews Neuroscience*, **2,** 484-491.

Weil, M.D., Lamborn, K., Edwards, M.S.B. & Wara, W.M. (1998). Influence of a child's sex on medulloblastoma outcome. *JAMA*, **279** 1474-1476.

Woodburn, R., Azzarelli, B., Montebello, J. & Goss, I. (2001). Intense p53 staining is a valuable prognostic indicator for poor prognosis in medulloblastoma/central nervous system primitive neuroectodermal tumors. *J Neurooncol.*, **52,** 57-62.

Yoon, S. & Sege, R. (2006). The extracellular signal-regulated kinase: multiple substrates regulate diverse cellular functions. *Growth factors*, **24,** 21-44.

Zurawel, R., Allen, C., Chiappa, S., Cato, W., Biegel, J., Cogen, P., de Sauvage, F. & Raffel, C. (2000). Analysis of PTCH/SMO/SHH pathway genes in medulloblastoma. *Genes Chromosomes Cancer*, **27,** 44-51.

Zurawel, R.H., Chippa, S.A., Allen, C. & Raffel, C. (1998). Sporadic medulloblastomas contain oncogenic beta-catenin mutations. *Cancer Res*, **58,** 896-9.

Chapter 11

Appendices

Appendix 1

Molecular and IHC data for the PNET3

Preparation of the chemical reagents

Appendix

PNET3 ID	β-catenin nuclear localization	Pattern of IHC staining	*CTNNB1* status		Ch 6 status	Ch 17p status
			Codon/nucleotide alterations	Amino acid alterations		
2	Positive	F&S	33TCT>TTT	SER>PHE	RET	RET
9	Positive	F&S	37tct>tat	SER>TYR	LOH	RET
12	Negative		wild-type	wild-type	RET	RET
13	Negative		wild-type	wild-type	RET	LOH
15	Negative		wild-type	wild-type	RET	LOH
18	Negative		wild-type	wild-type	RET	RET
19	Negative		wild-type	wild-type	RET	RET
28	Positive	F&S	wild-type	wild-type	RET	LOH
30	Negative		wild-type	wild-type	RET	RET
31	Negative		wild-type	wild-type	RET	RET
32	Negative		wild-type	wild-type	RET	LOH
33	Negative		wild-type	wild-type	RET	RET
35	Negative		wild-type	wild-type	RET	RET
38	Negative		wild-type	wild-type	RET	LOH
39	Positive	F&S	wild-type	wild-type	LOH	RET
41	Negative		wild-type	wild-type	RET	RET
43	Negative		wild-type	wild-type	RET	LOH
44	Negative		wild-type	wild-type	RET	RET
47	Negative		wild-type	wild-type	RET	RET
48	Negative		wild-type	wild-type	RET	RET
51	Positive	W&S	34GGA>AGA	GLY>ARG	LOH	RET
52	Positive	W&S	32GAC>TAC	ASP>TYR	RET	RET
53	Negative		wild-type	wild-type		
54	Negative		wild-type	wild-type	RET	RET
62	Negative		wild-type	wild-type	RET	RET
63	Negative		wild-type	wild-type	9	9
65	Negative		wild-type	wild-type	RET	RET
66	Negative		wild-type	wild-type	RET	RET
69	Negative		wild-type	wild-type	RET	RET
72	Negative		wild-type	wild-type	RET	RET
75	Negative		wild-type	wild-type	RET	RET
77	Negative		wild-type	wild-type	RET	LOH
78	Positive	F&S	wild-type	wild-type	RET	LOH

(Table 11.1. to continued)

PNET3 ID	β-catenin nuclear localization	Pattern of IHC staining	*CTNNB1* status		Ch 6 status	Ch 17p status
			Codon/nucleotide alterations	Amino acid alterations		
81	Positive	F&S	34GGa>AGA	GLY>ARG	LOH	RET
82	Negative		wild-type	wild-type	RET	LOH
83	Negative		wild-type	wild-type	RET	RET
90	Negative		wild-type	wild-type	RET	RET
93	Negative		wild-type	wild-type		
95	Negative		wild-type	wild-type	RET	
101	Negative		wild-type	wild-type	RET	RET
102	Negative		wild-type	wild-type		
105	Negative		wild-type	wild-type	RET	RET
106	Negative		wild-type	wild-type	RET	RET
107	Negative		wild-type	wild-type	RET	LOH
111	Negative		wild-type	wild-type		
112	Positive	W&S	33TCT>CCT	SER>PRO	LOH	RET
113	Negative		wild-type	wild-type	RET	LOH
114	Negative					
116	Negative		wild-type	wild-type	RET	RET
119	Positive	W&S	34GG>GAA	GLY>GLU	LOH	RET
120	Negative		wild-type	wild-type	RET	RET
121	Negative		wild-type	wild-type	RET	LOH
124	Negative		wild-type	wild-type	RET	RET
126	Negative		wild-type	wild-type	RET	LOH
129	Negative		wild-type	wild-type	RET	LOH
131	Positive	W&S	32GAC>GTC	ASP>VAL	RET	LOH
132	Negative		wild-type	wild-type	RET	RET
134	Negative		wild-type	wild-type	RET	LOH
137	Positive	W&S	33TCT>TGT	SER>CYS	LOH	RET
139	Positive	W&S	32GAC>TAC	ASP>TYR	LOH	RET
141	Negative		wild-type	wild-type	RET	RET
145	Negative		wild-type	wild-type	RET	RET
146	Positive	W&S	32GAC>GTC	ASP>VAL	LOH	RET
147	Positive	W&S	33TCT>TAT	SER>TYR	LOH	RET
148	Negative		wild-type	wild-type	RET	RET
149	Negative		wild-type	wild-type	RET	RET
150	Negative		Wild-type	wild-type	RET	LOH

(Table 11.1. to continued)

PNET3 ID	β-catenin nuclear localization	Pattern of IHC staining	*CTNNB1* status		Ch 6 status	Ch17p status
			Codon/nucleotide alterations	Amino acid alterations		
152	Positive	W&S	wild-type	wild-type	RET	RET
157	Negative		wild-type	wild-type	RET	RET
160	Negative		wild-type	wild-type	RET	RET
161	Negative		wild-type	wild-type	RET	RET
164	Negative		wild-type	wild-type	RET	RET
165	Negative		wild-type	wild-type	RET	RET
166	Negative		wild-type	wild-type	RET	RET
169	Negative		wild-type	wild-type	RET	RET
171	Negative		wild-type	wild-type	RET	LOH
172	Positive	W&S	wild-type	wild-type	RET	RET
175	Negative		wild-type	wild-type	RET	RET
178	Positive	W&S			RET	RET
179	Negative		wild-type	wild-type	RET	RET
180	Positive	F&W	wild-type	wild-type	RET	LOH
182	Positive	W&S	wild-type	wild-type	RET	RET
183	Negative		wild-type	wild-type		
185	Negative		wild-type	wild-type	RET	RET
186	Negative		wild-type	wild-type	RET	LOH
189	Negative		wild-type	wild-type		
191	Negative		wild-type	wild-type	RET	RET
193	Negative		wild-type	wild-type	RET	RET
195	Negative		wild-type	wild-type	RET	RET
198	Negative		wild-type	wild-type	RET	LOH
199	Negative		wild-type	wild-type	RET	RET
200	Negative		wild-type	wild-type		
201	Negative		wild-type	wild-type	RET	RET
202	Negative				RET	RET
205	Negative		wild-type	wild-type		LOH
207	Negative		wild-type	wild-type	RET	RET
209	Positive	W&S	32GAC>TAC	ASP>TYR	LOH	RET
210	Negative		wild-type	wild-type	RET	RET
214	Negative		wild-type	wild-type	RET	LOH
216	Negative		wild-type	wild-type	RET	RET

(Table 11.1. to continued)

PNET3 ID	β-catenin nuclear localization	Pattern of IHC staining	*CTNNB1* status		Ch 6 status	Ch 17p status
			Codon/nucleotide alterations	Amino acid alterations		
217	Positive	W&S	34GGA>AGA	GLY>ARG	LOH	RET
50001	Negative		wild-type	wild-type	RET	RET
50010	Negative		wild-type	wild-type	RET	RET
50011	Negative		wild-type	wild-type	RET	RET
50012	Negative		wild-type	wild-type	RET	RET
50014	Negative		wild-type	wild-type	RET	RET
50015	Negative		wild-type	wild-type	RET	RET
50016	Negative		wild-type	wild-type	RET	RET
50017	Negative		wild-type	wild-type	RET	LOH
50018	Negative					
50019	Negative		wild-type	wild-type	RET	RET
50021	Positive	W&S	34GGA>GTA	GLY>VAL	RET	RET
50034	Negative		wild-type	wild-type	RET	RET
50035	Negative		wild-type	wild-type	RET	RET
50040	Negative		wild-type	wild-type	RET	LOH
50041	Negative		wild-type	wild-type	RET	RET
50044	Negative		wild-type	wild-type	RET	LOH
50045	Positive	W&S	wild-type	wild-type	RET	RET
50047	Negative		wild-type	wild-type	RET	LOH
50049	Negative		wild-type	wild-type	RET	RET
50056	Positive	W&S	33TCT>TTT	SER>PHE	LOH	RET
50057	Negative		wild-type	wild-type	RET	RET
50058	Negative		wild-type	wild-type	RET	RET
50060	Negative		wild-type	wild-type	LOH	RET
50063	Negative		wild-type	wild-type	RET	RET
50065	Negative					
50068	Negative		wild-type	wild-type	RET	RET
50072	Negative		wild-type	wild-type	RET	RET
50075	Negative				LOH	RET
50079	Negative		wild-type	wild-type	RET	RET
50080	Positive	F&S	32GAC>ACC	ASP>ASN	LOH	RET
50081	Negative					
50086	Positive	W&S	wild-type	wild-type	RET	RET

(Table 11.1. to continued)

PNET3 ID	β-catenin nuclear localization	Pattern of IHC staining	*CTNNB1* status		Ch 6 status	Ch 17p status
			Codon/nucleotide alterations	Amino acid alterations		
50088	Negative		wild-type	wild-type	RET	RET
50090	Positive	F&S	wild-type	wild-type	RET	RET
50091	Negative		wild-type	wild-type	RET	RET
50092	Negative		wild-type	wild-type	RET	LOH
50099	Negative		wild-type	wild-type	RET	LOH
50100	Negative		wild-type	wild-type	RET	RET
50101	Negative					
50104			wild-type	wild-type	RET	RET
50106	Negative		wild-type	wild-type		
50111	Negative		wild-type	wild-type	RET	RET
50113	Negative		wild-type	wild-type	RET	LOH
50116	Negative		wild-type	wild-type	RET	RET
50117	Positive	F&S	33TCT>TAT	SER>TYR	LOH	LOH
50120	Negative		wild-type	wild-type	RET	RET
50124	Negative		wild-type	wild-type	RET	LOH
50128	Negative		wild-type	wild-type	RET	LOH
50129	Positive	W&S			LOH	RET
50132	Negative		wild-type	wild-type	RET	LOH
50133	Negative		wild-type	wild-type	RET	LOH
50136	Negative		wild-type	wild-type	RET	LOH
50137	Negative		wild-type	wild-type	RET	RET
50142	Negative		wild-type	wild-type	RET	LOH
50145	Negative		wild-type	wild-type	RET	RET
50147	Negative		wild-type	wild-type	RET	RET
50150	Negative		wild-type	wild-type	RET	RET
50152	Negative		wild-type	wild-type		
50153	Negative		wild-type	wild-type	RET	RET
50154	Negative		wild-type	wild-type	RET	LOH
50158	Positive	W&S	32GAC>ACC	ASP>ASN		
50159	Positive	F&S	34GGA>GTA	GLY>VAL	LOH	RET
50161	Negative		wild-type	wild-type	RET	LOH
50163	Negative		wild-type	wild-type	RET	LOH
50165	Negative		wild-type	wild-type	RET	RET

(Table 11.1. to continued)

PNET3 ID	β-catenin nuclear localization	Pattern of IHC staining	*CTNNB1* status		Ch 6 status	Ch 17p status
			Codon/nucleotide alterations	Amino acid alterations		
50166	Negative		wild-type	wild-type	RET	RET
50167	Negative		wild-type	wild-type	RET	RET
50169	Negative		wild-type	wild-type	RET	RET
50170	Negative		wild-type	wild-type	RET	RET
50172	Negative		wild-type	wild-type	RET	LOH
50174	Negative		wild-type	wild-type	RET	RET
50176	Negative		wild-type	wild-type	RET	RET
50184	Negative		wild-type	wild-type	RET	RET
50189	Negative		wild-type	wild-type	RET	LOH
50193	Negative		wild-type	wild-type	RET	RET
50197	Negative		wild-type	wild-type	LOH	RET
50198	Negative		wild-type	wild-type	RET	RET
50204	Negative		wild-type	wild-type	RET	RET
50206	Negative		wild-type	wild-type	RET	LOH
50208	Negative		wild-type	wild-type	RET	RET
50209	Negative		wild-type	wild-type	RET	RET
50212	Negative		wild-type	wild-type	RET	RET
50217	Negative				RET	RET
50218	Negative		wild-type	wild-type	RET	RET
50224	Negative		wild-type	wild-type	RET	RET
50231	Negative					
50233	Negative		wild-type	wild-type	RET	LOH
50236	Negative		wild-type	wild-type	RET	LOH
50241	Negative		wild-type	wild-type	RET	LOH
50244	Negative		wild-type	wild-type	RET	LOH
50245	Negative		wild-type	wild-type	RET	RET
50248	Negative		wild-type	wild-type	RET	RET
50249	Negative		wild-type	wild-type	RET	LOH
50250	Negative		wild-type	wild-type	RET	RET
50251	Negative		wild-type	wild-type	RET	RET
50253	Negative		wild-type	wild-type	RET	RET
50254	Negative		wild-type	wild-type	RET	RET
50256	Positive	F&W	wild-type	wild-type	RET	RET

(Table 11.1. to continued)

PNET3 ID	β-catenin nuclear localization	Pattern of IHC staining	*CTNNB1* status		Ch 6 status	Ch 17p status
			Codon/nucleotide alterations	Amino acid alterations		
50259	Negative		wild-type	wild-type	RET	RET
50263	Negative		wild-type	wild-type	RET	RET
50268	Negative		wild-type	wild-type	RET	RET
50274	Positive	F&S	wild-type	wild-type	RET	RET
50276	Negative		wild-type	wild-type	RET	RET
50284	Negative		wild-type	wild-type	RET	RET
50290	Negative		wild-type	wild-type	RET	RET
50291	Negative		wild-type	wild-type	RET	RET
50292	Negative		wild-type	wild-type	RET	RET

Table 11.1. The molecular profile for the PNET3 cohort. IHC = immuno-histochemistry; F & S = focal and strong; W.S. = wide spread and strong, F & w = focal and weak; Ch = chromosome, RET = retention of heterozygosity, LOH = loss of heterozygosity.

TBE Buffer	
TBE	**1 Litre**
455 mM TRIS	**54g**
445 mM Boric acid	**27.5g**
10 mM EDTA	**20 ml**
dH20 make up to 1L	

Table 11.2. Composition of the TBE buffer

Appendix 2

Papers accepted for publication

The manuscript of the first paper has been submitted to the Journal of Clinical Oncology under the title “Definition of disease-risk stratification groups in childhood medulloblastoma using combined clinical, pathological and molecular variables” and is currently under review for publication (Revision acknowledgment- JCO/2010/302810).

The second letter to the author is also awaiting submission to the Journal of Clinical Oncology.

Definition of disease-risk stratification groups in childhood medulloblastoma using combined clinical, pathological and molecular variables

Running title: Risk stratification in medulloblastoma

David W. Ellison[a], Mehmet Kocat[b], James Dalton[a], Hisham Megahed[c], Meryl E. Lusher[c], Sarra L. Ryan[c], Wei Zhao[b], Sarah Leigh Nicholson[c], Roger E. Taylor[d], Simon Bailey[c], Steven C. Clifford[c]

[a] Department of Pathology, St. Jude Children's Research Hospital, 262 Danny Thomas, Memphis, Tennessee,38105, USA

[b] Department of Biostatistics, St. Jude Children's Research Hospital, 262 Danny Thomas, Memphis, Tennessee, 38105, USA

[c] Northern Institute for Cancer Research, University of Newcastle, Newcastle-upon-Tyne, UK

[d] South West Wales Cancer Centre, Singleton Hospital, Swansea, UK

Address for correspondence:

Dr. David W. Ellison, Dept. of Pathology MS# 250, St. Jude Children's Research Hospital, 262 Danny Thomas Place, Memphis, TN 38105, USA; David.Ellison@stjude.org
tel. 901 595 5438; fax. 901 595 3100

Prof. Steven C. Clifford, Northern Institute for Cancer Research, University of Newcastle, Newcastle-upon-Tyne, NE2 4HH, UK; s.c.clifford@ncl.ac.uk

Acknowledgements

The authors gratefully acknowledge support from the American Lebanese Syrian Associated Charities, the Samantha Dixon Brain Tumour Trust, and Cancer Research UK. Medulloblastomas investigated in this study were provided by the UK Children's Cancer and Leukaemia Group (CCLG) as part of CCLG-approved biological study BS-2007-04. This study was conducted with appropriate ethics committee approval; St. Jude XPD07-107/IRB & Newcastle / North Tyneside REC 07/Q0905/71.

Abstract

Purpose

Medulloblastomas are heterogeneous and include relatively good prognosis tumors characterized by Wnt-pathway activation, as well as cases that will fail conventional therapy. Developing a practical therapeutic stratification that allows accurate identification of disease-risk offers the potential to individualize adjuvant therapy and to minimize long-term adverse effects in a subgroup of survivors.

Methods

Using formalin-fixed paraffin-embedded (FFPE) tissue for immunohistochemistry, iFISH, and direct sequencing, to identify tumors with a Wnt-pathway signature and those harboring copy number abnormalities (CNAs) of potential prognostic significance (*MYC* / *MYCN* amplification, CNAs of chromosome 6 and 17), we evaluated clinical, pathological and molecular outcome indicators and stratification models in a large (n=207) cohort of medulloblastoma patients aged 3-16 years from the SIOP PNET3 trial.

Results

Metastatic disease and large cell / anaplastic (LC/A) phenotype were the clinicopathological variables associated with poor progression-free survival (PFS). Nuclear immunoreactivity for β-catenin, *CTNNB1* mutation, and monosomy 6 all identified a group of good prognosis patients. *MYC* amplification was associated with

poor outcome, but other CNAs were not. Low-risk medulloblastomas were defined as β-catenin nucleopositive tumors without metastasis at presentation, LC/A phenotype, or *MYC* amplification. High-risk medulloblastomas were defined as tumors with metastatic disease, LC/A phenotype, or *MYC* amplification. Low-risk, standard-risk, and high-risk categories of medulloblastoma had significantly ($P<0.0001$) different PFS and overall survival.

Conclusion

Integrating assays of molecular biomarkers, which can be undertaken on routinely collected diagnostic FFPE tissue, into stratification schemes for medulloblastoma alongside clinical and pathological outcome indicators can refine the current definition of disease risk and guide adjuvant therapy.

Introduction

Clinicopathological and biological studies have increasingly supported the hypothesis that medulloblastoma is a heterogeneous disease with diverse phenotypes and contrasting therapeutic outcomes.[1-5] Reduction of adjuvant therapy for a subgroup of patients with favorable disease that responds well to therapy has the potential to ameliorate long-term adverse effects; so the identification of this subgroup could become important for therapeutic stratification. Equally, identification of patients with high-risk disease provides an opportunity to intensify therapy with the aim of improving outcome. [6, 7]

Clinical factors, particularly metastatic disease at presentation, currently determine therapeutic stratification for medulloblastoma patients. However, data from clinical trial-based studies indicating distinct biological behaviors for pathological variants of medulloblastoma could potentially influence future schemes; large cell and anaplastic variants are increasingly regarded as high-risk disease, and desmoplastic tumors have a better outcome than other variants in infants. [4,8,9] Molecular markers have yet to be advanced for stratification. Despite many claims for their application in this context, few molecular abnormalities have been robustly associated with outcome in separate studies of large cohorts of uniformly treated patients. [2,10] In addition, the use of molecular markers will be adopted most readily if stratification shemes can be applied in any clinical laboratory using routine formalin-fixed paraffin-embedded (FFPE) tissue.

We first demonstrated that Wnt pathway activation in a subgroup of medulloblastomas characterized by nuclear immunoreactivity for β-catenin is associated with a good outcome, and this finding has since been replicated on several occasions. [11-13] Other abnormalities that characterize this subgroup of tumors, *CTNNB1* mutation and monosomy 6, may also be valuable indicators of a good outcome, but this hypothesis has not been robustly tested alongside β-catenin immunohistochemistry, and it remains to be determined which assay or combination of assays most appropriately identifies low-risk tumors alongside clinical and histological variables. [14-16] Further, a series of copy number abnormalities (CNAs), such as *MYC* or *MYCN* amplification and alterations on chromosomes 6q and 17, have been proposed as markers of poor outcome, but their relationship to favorable disease characterized by Wnt pathway activation and their clinical utility alongside identification of this favorable subgroup of medulloblastomas have not been adequately addressed in trial cohorts. [17-19]

In the present study of 207 children aged 3-16 years from the SIOP PNET3 trial, we report a comprehensive study of the utility of established Wnt subgroup markers and putative molecular markers of high-risk disease alongside clinicopathological disease features in risk stratification models of medulloblastoma. We establish validated clinical, histopathological, and molecular outcome indicators and demonstrate that these can be combined to delineate three distinct high-risk, standard-risk and low-risk groups among this cohort.

Methods

Patient cohort

Medulloblastoma samples (n=207) from children registered on the International Society for Pediatric Oncology (SIOP) PNET3 trial protocol (CNS9102) were provided by contributing centers. [5] Patients were randomized to 35Gy craniospinal radiotherapy and a 20Gy posterior fossa boost either alone or preceded by chemotherapy (carboplatin, cyclophosphamide, etoposide, vincristine). Cohort size for the present study was determined by tissue availability. The clinical characteristics of patients in the present study cohort matched those in the original PNET3 trial, with respect to both randomized and non-randomized patients. Furthermore, non-randomized patients were treated with identical chemotherapy and radiotherapy protocols and outcome data collected by the study center at the same frequency as randomized patients. Median age at diagnosis was 8.4 years (range 3.0 to 16.2 years), and males predominated (1.7:1). Slightly more patients received pre-radiotherapy chemotherapy than radiotherapy alone (109:98), and about half (101/207) had been part of the randomized trial, the remainder having been treated according to protocol. Central radiological review disclosed metastatic disease (Chang stage M2 / M3) at presentation in 38 patients (18%). Central histopathological review according to both WHO classification (2007) and current COG guidelines recorded 14 desmoplastic / nodular (6.8%), and 174 classic tumors (84%). Large cell and anaplastic variants were combined (n=19; 9.2%) into one category (LC/A).

Assays

Immunohistochemistry, interphase fluorescence in situ hybridization (iFISH), DNA extraction and *CTNNB1* mutation analysis were undertaken on FFPE tissue as previously described. [11, 16] Wnt-pathway medulloblastomas were identified by strong nuclear β-catenin immunoreactivity in one of two patterns, widespread or focal (Figure 1); either nuclear and cytoplasmic β-catenin staining combined to blanket almost all tumor cells (widespread), or nuclear β-catenin immunoreactivity was seen in cell clusters among others with weak or negligible nuclear immunoreactivity, but clearly amounting to more than 10% of tumor cells (focal). Rare tumors containing a few (<1%) scattered cells with β-catenin nuclear immunoreactivity among cells with no discernible nuclear staining were not regarded as Wnt-pathway tumors.

The following BACs were used to assess copy number (CN) by iFISH: chromosome 6p22, *DCDC2*, RP11-72O5; chromosome 6q23, *SGK1*, RP11-692B5; *MYC*, CTD-3056O22 / 2267H22 (8p control, RP11-1077A8 / RP11-867P15]; *MYCN*, RP11-355H10 / RP11-348M12 (2q control, RP11-296A19 / RP11-384O8); chromosome 17p13, *HIC1*, RP11-357O7 / RP11-806J5 (17q control, RP11-368A16 / RP11-661H23). Double minute patterns or homogeneously staining regions recorded at three frequencies (<5%, 5-50%, >50% of tumor cells) defined *MYC* and *MYCN* amplification, as previously described [17]. Tumors showing CN gains of *MYC* and *MYCN* (CN: 1-8 signals > control probe ≥2) were also recorded. Gain of 17q was defined as CN >2. Loss of 17p was evaluated in two ways: (i) CN <2, and (ii) CN <2 or CN 17q>17p≥2.

Statistical analysis

Events for progression free survival (PFS) were defined as time from start of therapy to date of progression or death on study. Events for overall survival (OS) were defined as time from start of therapy to date of death on study. Patients not experiencing an event were censored at the date of last-follow up. Survival distributions were estimated using the Kaplan-Meier method and compared between two or more groups of patients using the log-rank test. Associations between any two clinicopathological or molecular variables of interest were tested using Fisher's Exact test or Exact Chi-Square test. P values were not adjusted for multiplicity.

The classification and regression tree (CART) method was used to identify variables that best separate patients into different risk groups. [20] It is based on successively dividing the cohort into groups of similar response patterns using covariates, splitting a node into two subgroups using the covariate that best discriminates survival outcomes on the basis of likelihood ratio test. The process stops when no covariate can split subgroups further or when subgroups have reached a specified minimum size (n=5). The analysis was carried out using Rpart and Survival packages in R software. [21]

Results

Of 207 patients, 133 (64%) are currently alive without disease, median follow up being 8.8 years. Medical events have been recorded for 77/207 (37%), representing progressive disease in 71/77 children. Deaths were recorded in 74/207 (36%) cases, 68/74 being due to disease. Death was related to complications of therapy in one patient and to a high-grade glioma presumed secondary to radiotherapy in five, all of whom had no evidence of residual medulloblastoma.

Clinical and histopathological risk factors for outcome across the cohort

Outcome data for the cohort were: PFS (5yr) = 0.69±0.032, OS (5yr) = 0.75±0.030; PFS (10yr) = 0.63±0.046, OS (10yr) = 0.65±0.045 (Supp. Figure 1). Univariable survival analysis revealed that M stage, but not age, sex, or type of adjuvant therapy, was significantly associated with PFS and OS (Table 1; Supp. Figure 2a). Outcomes for children with classic and desmoplastic / nodular medulloblastomas were similar, but those with LC/A tumors had a significantly poorer survival, both PFS and OS (Table 1; Supp. Figure 2b). A combination of LC/A medulloblastoma and metastatic disease at presentation displayed a particularly aggressive behavior; 4/5 patients relapsed and died within three years.

Defining low-risk medulloblastomas – Wnt-pathway tumors

Immunohistochemistry with an anti-β-catenin antibody was undertaken in 206/207 cases. Of 33/206 (16%) tumors demonstrating nuclear immunoreactivity for β-catenin

(Table 2), 21 showed strong and widespread staining (Figure 1), while in the remaining 12 tumors this was patchy and either strong (n=10) or weak (n=2). *CTNNB1* mutation analysis was feasible in 31/33 β-catenin nucleopositive tumors and detected in 20/31 (65%). *CTNNB1* mutations were not detected in any β-catenin nucleonegative tumors tested (n=164). Nearly all (31/33) Wnt-pathway activated medulloblastomas had a classic morphology. Of 30/33 tested, 24/30 (80%) demonstrated monosomy 6, but few showed CNAs of chromosome 17, *MYC*, or *MYCN* (Table 2).

iFISH analysis of two loci (*DCDC2*, 6p22; *SGK1*, 6q23) on chromosome 6 revealed a balanced profile in 79/185 (43%) tumors, trisomy 6 in 12/185 (6%), polysomy 6 (3-5 copies/cell) in 64/185 (35%), and monosomy 6 in 27/185 (15%), but no evidence of specific *SGK1* gain. Heterozygous deletion of the 6q locus was detected in two tumors, and focal deletion of the 6p locus in one. Monosomy 6 was strongly associated with a Wnt-pathway immunohistochemical profile (Table 2); 24/27 (89%) tumors with monosomy 6 were β-catenin nucleopositive ($p<0.0001$). Three children with monosomy 6 / β-catenin nucleonegative tumors, which were all classic medulloblastomas without *MYC* or *MYCN* amplification (Table 2), are alive without disease, one despite presenting with M2 disease.

Analyzed as individual prognostic variables, nuclear immunoreactivity for β-catenin, *CTNNB1* mutation, and monosomy 6 all conferred a significantly improved prognosis (Table 1). Of 33 patients with β-catenin nucleopositive tumors only 5 (15%) have died (Supp. Figure 3). However, 2/5 did not die of disease; one died 11 years post-diagnosis

from a high-grade glioma, and the other died 2 months post-diagnosis from complications of therapy. Of the remaining three children, one presented with M3 disease, and one had a tumor with *MYC* amplification (Table 2). There was no significant difference in outcome between children with a medulloblastoma that showed widespread nuclear immunoreactivity for β-catenin and those with a tumor that showed patchy β-catenin nucleopositivity.

Survival analysis using these variables indicated that stratification by *CTNNB1* mutation, monosomy 6, or a combination of these with β-catenin immunohistochemistry did not identify a low-risk group with better outcome than immunohistochemistry for β-catenin alone (Supp. Figure 4). Other chromosome 6 CNAs were not outcome indicators. Multivariable survival analysis incorporating M status, pathological variant, and β-catenin immunoreactivity in a Cox proportional hazards model showed that all three were independent outcome indicators (Table 3).

Defining high-risk medulloblastomas - MYCN / MYC and chromosome 17 CNAs

With *MYCN* and *MYC* probes, iFISH detected groups of cells with a double-minute or HSR pattern (Figure 1) in 11/187 (5.8%) and 7/189 (3.7%) tumors, respectively (Table 4). *MYCN* or *MYC* gain (3-10 copies per cell) was recorded in 9/187 (4.8%) and 6/189 (3.2%) medulloblastomas, respectively. *MYC* amplification or gain was never detected alongside *MYCN* amplification or gain in any one tumor.

With chromosome 17 probes, iFISH revealed a balanced profile of chromosome 17 without ploidy change in 61/173 assessable tumors (35%). CNAs observed in 112/173 (65%) comprised: isodicentric 17q (n=29), polysomy (3-8 copies per cell; n=24), polysomy with imbalance (CN: 17q>17p≥2; n=47), isolated loss of 17p (n=5), isolated gain of 17q (n=5), monosomy 17 (n=2).

Across the entire cohort, only *MYC* amplification of the potential high-risk markers showed a significant association with outcome (Table 1). While *MYCN* amplification alone or *MYCN* amplification / gain was not significantly associated with poor outcome, we did note that, of 20 children with tumors characterized by a *MYCN* CNA, half of those dying of disease (4/8) had a tumor that combined *MYCN* amplification or gain with LC/A phenotype, and with M3 disease in 3/4 cases. All four children died within 2 years of diagnosis.

No chromosome 17 CNA was associated with PFS or OS. Although loss of 17p defined as CN <2 showed a trend towards poor outcome, this was not significant (PFS HR=1.45, p=0.14; OS HR=1.49, p=0.12).

Models of therapeutic stratification

Using a step-wise approach to risk-group identification, we first defined a low-risk group of β-catenin nucleopositive tumors that excluded cases with demonstrated high-risk factors: M+ disease, LC/A phenotype, or *MYC* amplification (Table 2; n=26). We then re-evaluated all variables for prognostic significance in a cohort without this low-risk

group (n=181). In univariable and multivariable analyses, M+ status, LC/A phenotype, and *MYC* amplification retained their association with poor outcome (Table 3), thus defining a high-risk group.

Defining low-risk and high-risk groups in this way produced three patient classes with significantly (P<0.0001) different PFS curves across the entire cohort (Figure 2). In a parallel analysis encompassing the entire cohort, we explored the prognostic value of clinical, pathological, and molecular markers with respect to PFS in a classification analysis and regression tree (CART) model, entering β-catenin immunoreactivity, pathological variant, M status, *MYC* amplification, *MYCN* amplification, and chromosome 17 CNAs (loss of 17p or gain of 17q). *MYCN* amplification, and chromosome 17 CNAs were not selected in any partitioning step, this alternative model supporting the selection of outcome indicators we had made according to LogRank analysis (Supp. Figure 5).

Discussion

Individualization of therapy for children with medulloblastoma represents a major goal in pediatric neuro-oncology. In recent years, histopathological and molecular disease features have been identified with the potential to provide a more refined stratification of disease-risk than current clinical indices. [4, 7-9] However, their clinical utility has often been limited by conflicting results and analysis of small single-center or heterogeneously treated cohorts. [22] We therefore undertook a comprehensive assessment of putative disease-risk biomarkers, alongside clinical and pathological indices, in a cohort of medulloblastomas from children aged 3 to 16 years on the SIOP PNET3 trial. Using this approach we report, for the first time in the context of an extensive trial cohort, the development of clinical stratification models based upon validated biomarkers, which can be assayed in FFPE tissue, and on clinicopathological features, for the assignment of patients to low-risk, standard-risk and high-risk disease groups.

We previously demonstrated that β-catenin nuclear immunoreactivity is an independent marker of favorable outcome in medulloblastoma patients from this trial cohort, a finding since validated in other independent trial cohorts. [11-13] β-catenin nucleopositivity characterizes a molecular subgroup of medulloblastomas associated with activation of the Wnt signaling pathway, *CTNNB1* mutations and distinct genomic (monosomy 6) and transcriptomic signatures. [11, 14-16] However, the relative prognostic significance of these different subgroup markers has not been assessed. β-catenin immunoreactivity,

CTNNB1 mutation and chromosome 6 status were therefore examined in the present study, which extends our investigations of this pathway in the SIOP PNET3 cohort from 109 to 207 cases. [11] β-catenin nucleopositivity was an over-arching marker of the Wnt subgroup, detected in every case with other molecular evidence of pathway activation. Chromosome 6 loss and *CTNNB1* mutation each characterized overlapping sub-sets of β-catenin nucleopositive cases (80% and 65%, respectively), and therefore have utility as corroborative surrogate markers of pathway activation, but they did not identify any group of patients with a more favorable prognosis than β-catenin nucleopositivity alone. Nuclear β-catenin immunoreactivity can be strong and widespread or patchy, the latter present in at least 10% of cells and usually accompanying weak nuclear immunoreactivity in surrounding cells. Both immunophenotypes were associated with *CTNNB1* mutation or monosomy 6 and did not show significant outcome differences.

Clinical variables associated with high-risk disease in univariate and multivariate analyses were LC/A phenotype and the presence of metastatic disease, validating both the expected clinical behavior of our cohort and data from other trail-based cohorts encompassing this age group. [8,9] *MYC* gene amplification present mainly as double minutes was the only biomarker to show an association with poor outcome. Previous studies, including our own, reporting data from small or non-uniformly treated cohorts have demonstrated an association between poor outcome and *MYC* or *MYCN* amplified cases in combination. [17-19] In our series, a particularly poor prognosis was noted for tumors with coincident LC/A phenotype and *MYC* amplification or *MYCN* amplification / gain, suggesting that *MYCN* amplification may have prognostic significance in certain

settings; however, the previously reported association between *MYC* or *MYCN* amplification and the LC/A variant was not validated in our cohort. [18,23]

Consistent with our previous report 11, cases with high-risk disease features (M+ disease (n=3) or LC/A pathology (n=2)) were observed within the favorable risk group defined by Wnt-pathway activation (n=33). However, their clinical behavior is less clear. Notably, of the three Wnt-positive cases that died of disease, two also displayed high-risk features. The observation of larger numbers of such cases will be required to establish their prognosis more accurately. Until such data are available, consideration of these cases as high-risk in any proposed clinical studies would appear prudent.

Previously reported prognostic associations in medulloblastoma could not be validated for all biomarkers presently tested in the PNET3 cohort, specifically gain of 6q at the *SGK1* locus, loss of 17p, and gain of 17q. [19, 24, 25] Such discrepancies may reflect differences in patient accrual or therapeutic factors and highlight the need for; (i) independent validation of findings from individual studies, and (ii) selection of prognostic indicators that demonstrate consistent associations across multiple clinical trial cohorts.

Patients in this study cohort were treated with conventional dose (35 Gy) craniospinal radiotherapy. It is essential that further studies be undertaken (i) to validate the prognostic role of these pathological and molecular markers in patient cohorts treated with reduced dose craniospinal radiotherapy and (ii) to determine whether the impact of these prognostic factors is influenced by the intensity of therapy. [3]

In summary, this study has validated a series of independent prognostic biomarkers for medulloblastomas from children aged 3-16 years at diagnosis utilizing FFPE tissue submitted for diagnostic histopathology. Biomarkers with potential prognostic significance were tested in multiple models, which consistently supported a stratification scheme encompassing the independent clinical, pathological and molecular indices identified in this study. Stratification models define three disease risk groups with significantly different outcomes, all of which can be readily defined by established radiological or tissue-based diagnostic tests: (i) low-risk medulloblastomas (13% of cases) defined as β-catenin nucleopositive tumors without metastatic disease at presentation, LC/A phenotype, or *MYC* amplification; (ii) high-risk medulloblastomas (28% of cases) defined as tumors with metastatic disease, LC/A phenotype, or *MYC* amplification; and (iii) standard risk medulloblastomas (59% of cases), which lack these discriminating features. Future studies must now focus on the prospective identification of these disease groups in clinical trials aimed towards the delivery of improved outcomes through the application of risk-tailored adjuvant therapies.

References

[1.] Ellison D: Classifying the medulloblastoma: insights from morphology and molecular genetics. Neuropathol Appl Neurobiol 28(4):257-82, 2002

[2.] Gilbertson RJ,Ellison DW: The origins of medulloblastoma subtypes. Annu Rev Pathol 3:341-65, 2008

[3.] Packer RJ, Gajjar A, Vezina G, et al: Phase III study of craniospinal radiation therapy followed by adjuvant chemotherapy for newly diagnosed average-risk medulloblastoma. J Clin Oncol 24(25):4202-8, 2006

[4.] Rutkowski S, Gerber NU, von Hoff K, et al: Treatment of early childhood medulloblastoma by postoperative chemotherapy and deferred radiotherapy. Neuro Oncol 11(2):201-10, 2009

[5.] Taylor RE, Bailey CC, Robinson K, et al: Results of a randomized study of preradiation chemotherapy versus radiotherapy alone for nonmetastatic medulloblastoma: The International Society of Paediatric Oncology/United Kingdom Children's Cancer Study Group PNET-3 Study. J Clin Oncol 21(8):1581-91, 2003

[6.] Ellison DW, Clifford SC, Gajjar A, et al: What's new in neuro-oncology? Recent advances in medulloblastoma. Eur J Paediatr Neurol 7(2):53-66, 2003

[7.] Pizer BL,Clifford SC: The potential impact of tumour biology on improved clinical practice for medulloblastoma: progress towards biologically driven clinical trials. Br J Neurosurg 23(4):364-75, 2009

[8.] McManamy CS, Lamont JM, Taylor RE, et al: Morphophenotypic variation predicts clinical behavior in childhood non-desmoplastic medulloblastomas. J Neuropathol Exp Neurol 62(6):627-32, 2003

[9.] Eberhart CG, Kepner JL, Goldthwaite PT, et al: Histopathologic grading of medulloblastomas: a Pediatric Oncology Group study. Cancer 94(2):552-60., 2002

[10.] Gilbertson RJ,Gajjar A: Molecular biology of medulloblastoma: will it ever make a difference to clinical management? J Neurooncol 75(3):273-8, 2005

[11]. Ellison DW, Onilude OE, Lindsey JC, et al: beta-Catenin status predicts a favorable outcome in childhood medulloblastoma. J Clin Oncol 23(31):7951-7, 2005

[12]. Gajjar A, Chintagumpala M, Ashley D, et al: Risk-adapted craniospinal radiotherapy followed by high-dose chemotherapy and stem-cell rescue in children with newly diagnosed medulloblastoma (St Jude Medulloblastoma-96): long-term results from a prospective, multicentre trial. Lancet Oncol 7(10):813-20, 2006

[13]. Fattet S, Haberler C, Legoix P, et al: Beta-catenin status in paediatric medulloblastomas: correlation of immunohistochemical expression with mutational status, genetic profiles, and clinical characteristics. J Pathol 218(1):86-94, 2009

[14]. Thompson MC, Fuller C, Hogg TL, et al: Genomics identifies medulloblastoma subgroups that are enriched for specific genetic alterations. J Clin Oncol 24(12):1924-31, 2006

[15]. Kool M, Koster J, Bunt J, et al: Integrated genomics identifies five medulloblastoma subtypes with distinct genetic profiles, pathway signatures and clinicopathological features. PLoS One 3(8):e3088, 2008

[16]. Clifford SC, Lusher ME, Lindsey JC, et al: Wnt/Wingless pathway activation and chromosome 6 loss characterize a distinct molecular sub-group of medulloblastomas associated with a favorable prognosis. Cell Cycle 5(22):2666-70, 2006

[17]. Lamont JM, McManamy CS, Pearson AD, et al: Combined histopathological and molecular cytogenetic stratification of medulloblastoma patients. Clin Cancer Res 10(16):5482-93, 2004

[18]. Eberhart CG, Kratz J, Wang Y, et al: Histopathological and molecular prognostic markers in medulloblastoma: c-myc, N-myc, TrkC, and anaplasia. J Neuropathol Exp Neurol 63(5):441-9, 2004

[19]. Pfister S, Remke M, Benner A, et al: Outcome prediction in pediatric medulloblastoma based on DNA copy-number aberrations of chromosomes 6q and 17q and the MYC and MYCN loci. J Clin Oncol 27(10):1627-36, 2009

[20]. Schmoor C, Ulm K,Schumacher M: Comparison of the Cox model and the regression tree procedure in analysing a randomized clinical trial. Stat Med 12(24):2351-66, 1993

[21]. Therneau T, Atkinson, EJ. An Introduction to Recursive Partitioning Using the RPart Routines. 1997. http://www.med.nyu.edu/biostatistics/people/Ilana%20Belitskaya-Levy/Courses/MAS/Handouts/RPART%20short.pdf.

[22]. Pizer B,Clifford S: Medulloblastoma: new insights into biology and treatment. Arch Dis Child Educ Pract Ed 93(5):137-44, 2008

[23]. Stearns D, Chaudhry A, Abel TW, et al: c-myc overexpression causes anaplasia in medulloblastoma. Cancer Res 66(2):673-81, 2006

[24]. Pan E, Pellarin M, Holmes E, et al: Isochromosome 17q is a negative prognostic factor in poor-risk childhood medulloblastoma patients. Clin Cancer Res 11(13):4733-40, 2005

[25]. Gilbertson R, Wickramasinghe C, Hernan R, et al: Clinical and molecular stratification of disease risk in medulloblastoma. Br J Cancer 85(5):705-12, 2001

Figure legends

Figure 1:

(a) Widespread nuclear and cytoplasmic immunoreactivity for β-catenin is seen in this Wnt pathway medulloblastoma. (b) Patchy variable nuclear immunoreactivity for β-catenin characterizes this tumor, which contained a *CTNNB1* mutation. (c-f) Interphase FISH demonstrates monosomy 6 (c), a 2x17p:6x17q profile (d), gain of *MYCN* (e), and amplification of *MYC* (f).

Figure 2:

PFS curves for patients split into (a) three or (b) four risk categories. Low-risk (green, a & b) = M0 classic tumors showing β-catenin nucleopositivity; high-risk (red, a & b) = LC/A tumors or tumors with M+ disease or *MYC* amplification; worst-risk (black, b) = LC/A tumors plus M+ disease or *MYC* amplification; standard risk (blue) = the remainder; LogRank tests, both datasets $P<0.0001$.

Figure legends

Supplementary Figure 1:

PFS (green) and OS (blue) curves for the entire cohort (n=207).

Supplementary Figure 2:

(a) PFS curves split by metastatic status: M0 (green), M+ (red); LogRank P=0.0014. (b) PFS curves split by histopathological variants: classic (blue), D/N (green), and LC/A (red); LogRank P=0.0004.

Supplementary Figure 3:

PFS curves for patients split by β-catenin nuclear immunoreactivity: nucleopositive (green), nucleonegative (red); LogRank P=0.0095.

Supplementary Figure 4:

PFS plots for markers of good outcome; *CTNNB1* status and chromosome 6 CNAs alone or in combination with β-catenin immunohistochemical status do not identify a group of patients with a better outcome than children with β-catenin nucleopositive medulloblastomas. (a) PFS curves split by *CTNNB1* status: mutation (green), wt (red), LogRank P=0.0325; (b) PFS curves split by chromosome 6 status: monosomy (green), not monosomy (red), LogRank P=0.0327; (c) PFS curves split by a combination of β-catenin nuclear immunoreactivity and chromosome 6 status: β-catenin nucleopositive plus monosomy 6 (green), other tumors (red), LogRank P=0.0382; (d) PFS curves split

by a combination of β-catenin nuclear immunoreactivity and *CTNNB1* status: β-catenin nucleopositive plus *CTNNB1* mutation (green), other tumors (red), LogRank P=0.0340.

Supplementary Figure 5:

CART analysis of outcome categories. Figures are hazard ratios.

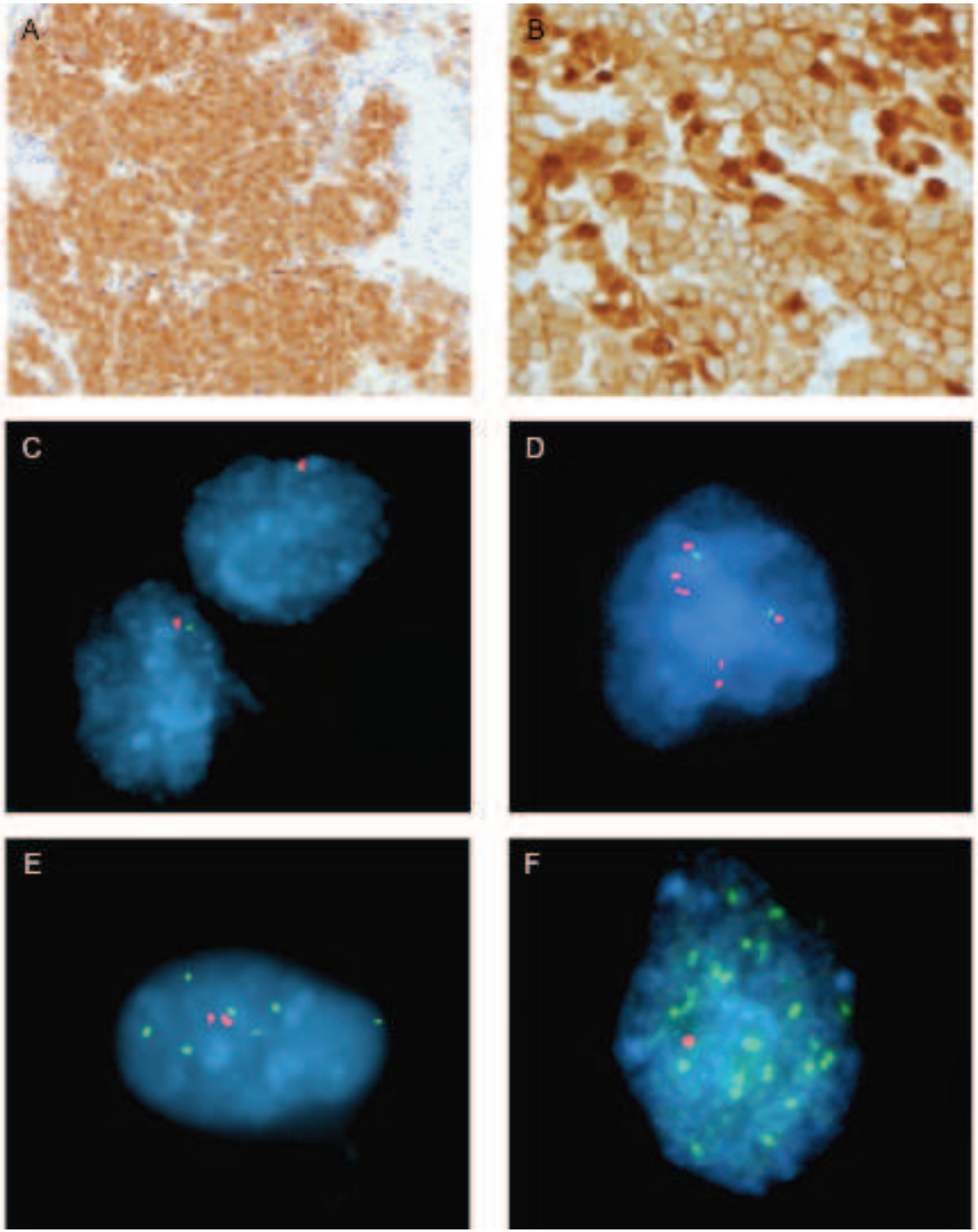
A
B
C
D
E
F

Figure 2a

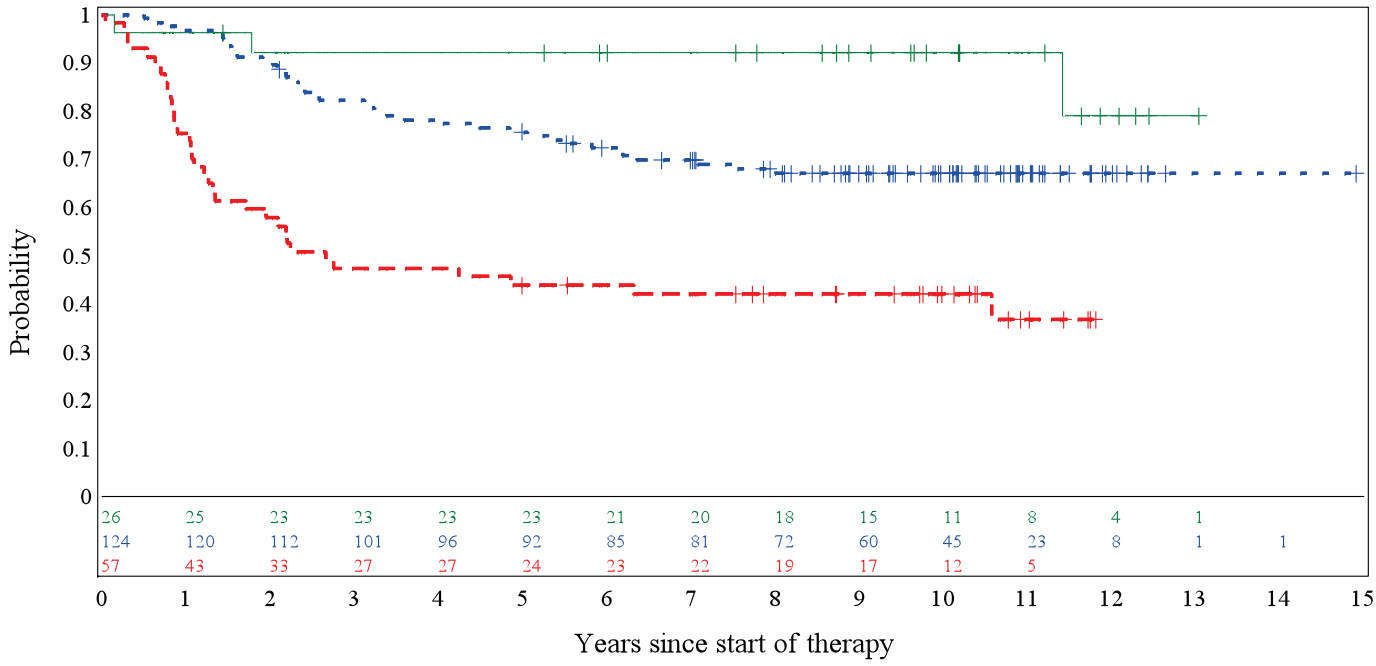

Figure 2b

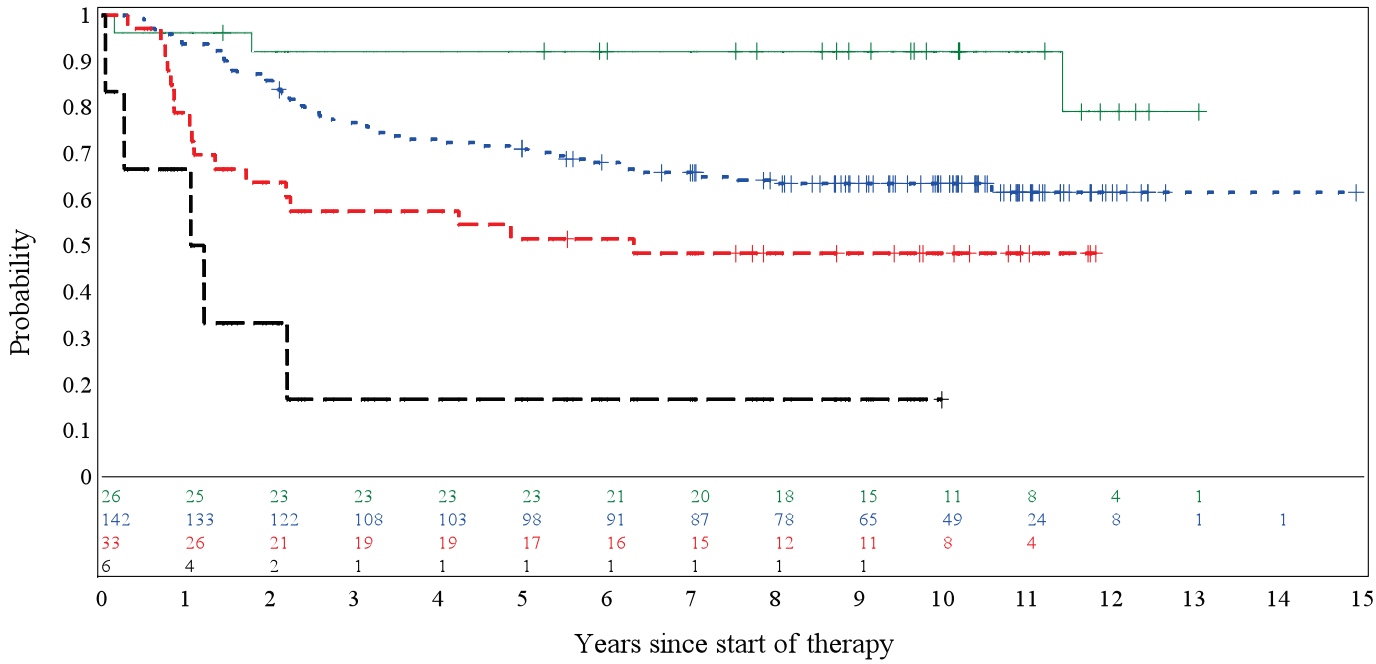

Table 1
Hazard ratios for progression-free and overall survival in a Cox model

Variable	Cox Proportional Hazards Model			
	PFS		OS	
	HR	P-value	HR	P-value
M Stage (M+ : M0)	2.22	0.0018	2.25	0.002
Age group (<8 : >12)	1.43	0.31	1.46	0.31
Age group (8-12 : >12)	0.98	0.95	1.04	0.92
Sex (male : female)	1.45	0.13	1.49	0.12
Therapy (RT/CT : RT)	1.26	0.32	1.33	0.22
Pathology (LC/A : classic)	3.08	0.0002	3.40	<0.0001
Pathology (D/N : classic)	0.80	0.67	0.88	0.80
β-catenin IHC (nuc-neg : nuc-pos)	3.12	0.014	2.89	0.022
CTNNB1 status (wt : mutant)	3.29	0.044	3.10	0.056
Chromosome 6 FISH (others : monosomy)	2.60	0.039	3.17	0.026
MYC FISH (amp : non-amp)	3.61	0.0058	3.61	0.0059
MYCN FISH (amp : non-amp)	1.11	0.84	1.20	0.73
Chromosome 17 FISH (17p loss : others)	1.45	0.14	1.49	0.12
Chromosome 17 FISH (17q gain : others)	1.13	0.62	1.16	0.57

PFS = progression-free survival
OS = overall survival
HR = hazard ratio
RT/CT = combined chemotherapy & radiotherapy
RT = radiotherapy
LC/A = large cell / anaplastic
D/N = desmoplastic / nodular
IHC = immunohistochemistry
nuc-neg = nucleonegative
nuc-pos = nucleopositive
wt = wild-type
amp = amplified
non-amp = not amplified

Table 2
Clinical, pathological, and cytogenetic characteristics of β-catenin nucleopositive medulloblastomas

β-catenin nuc IR	*CTNNB1* status	XO6 FISH	FISH *MYC* AMP/GAIN	FISH *MYCN* AMP/GAIN	XO17 FISH	Pathology	M stage	Status	Low-risk group
W&S	mut (32gac>tac)	monosomy	no	no	normal	classic	M0	DoD	Yes
W&S	mut (32gac>gtc)	monosomy	AMP 5-50%	no	normal	classic	M0	DoD	No
W&S	mut (33tct>cct)	monosomy	no	no	normal	classic	M0	Died¶	Yes
W&S	mut (34gga>aga)	monosomy	no	no	polysomy	classic	M0	ADF	Yes
W&S	mut (34gga>gaa)	monosomy	no	no	normal	classic	M0	ADF	Yes
W&S	mut (33tct>tgt)	monosomy	no	no	normal	LC/A	M0	ADF	No
W&S	mut (32gac>tac)	monosomy	no	no	normal	classic	M0	ADF	Yes
W&S	mut (34gga>aga)	monosomy	no	no	normal	classic	M0	ADF	Yes
W&S	mut (33tct>ttt)	monosomy	gain	no	ND	classic	M0	ADF	Yes
W&S	mut (34gga>gta)	polysomy	no	no	polysomy	classic	M2	ADF	No
W&S	mut (32gac>tac)	trisomy	no	gain	polysomy	classic	M0	ADF	Yes
W&S	mut (32gac>gtc)	ND	no	no	p loss-ploidy	LC/A	M0	ADF	No
W&S	mut (33tct>tat)	ND	no	no	normal	classic	M0	ADF	Yes
W&S	mut (32gac>aac)	ND	no	no	ND	classic	M0	ADF	Yes
W&S	wt	monosomy	no	no	monosomy	classic	M0	Died§	Yes
W&S	wt	monosomy	no	no	normal	classic	M0	ADF	Yes
W&S	wt	monosomy	no	no	normal	classic	M0	ADF	Yes
W&S	wt	monosomy	no	no	normal	classic	M3	ADF	No
W&S	wt	normal	no	no	normal	classic	M0	ADF	Yes
W&S	ND	monosomy	no	no	i17q	classic	M0	ADF	Yes
W&S	ND	monosomy	no	no	normal	classic	M0	ADF	Yes
P&S	mut (33tct>ttt)	monosomy	ND	ND	ND	classic	M0	ADF	Yes
P&S	mut (37tct>tat)	monosomy	no	no	normal	classic	M0	ADF	Yes
P&S	mut (34gga>aga)	monosomy	no	no	normal	classic	M0	ADF	Yes
P&S	mut (32gac>aac)	monosomy	no	no	normal	classic	M0	ADF	Yes
P&S	mut (33tct>tat)	monosomy	no	no	normal	classic	M0	ADF	Yes
P&S	mut (34gga>gta)	monosomy	no	no	normal	classic	M0	ADF	Yes
P&S	wt	monosomy	ND	ND	ND	classic	M3	ADF	No
P&S	wt	monosomy	no	no	normal	classic	M0	ADF	Yes
P&S	wt	monosomy	no	no	p loss	classic	M0	ADF	Yes
P&S	wt	normal	no	no	normal	classic	M0	ADF	Yes
P&W	wt	polysomy	no	no	polysomy	classic	M0	ADF	Yes
P&W	wt	normal	no	no	p loss	classic	M3	DoD	No

W&S = widespread strong immunoreactivity
P&S = patchy strong immunoreactivity
P&W = patchy weak immunoreactivity
mut = mutation
wt = wild type
AMP = amplification
DoD = died of disease
ADF = alive disease-free
Died¶ = died from high-grade glioma, 11 years post-diagnosis
Died§ = died from side-effects of therapy, 2 months post-diagnosis
ND = not done

Table 3

Hazard ratios for progression-free survival in a Cox model

Total cohort

Variable	Cox Proportional Hazards Model			
	PFS - univariate (n=206)		PFS - multivariate (n=206)	
	HR	P-value	HR	P-value
Pathology (LC/A : classic or D/N)	3.13	0.0002	2.78	0.0013
M Stage (M+ : M0)	2.22	0.0018	1.95	0.011
β-catenin IHC (nuc-neg : nuc-pos)	3.12	0.014	3.01	0.034

Patient cohorts with 'low-risk' β-catenin nucleopositive tumors omitted

Variable	Cox Proportional Hazards Model			
	PFS - univariate (n=181)		PFS - multivariate (n=164)	
	HR	P-value	HR	P-value
Pathology (LC/A : classic or D/N)	2.78	0.0008	2.46	0.0069
M Stage (M+ : M0)	1.96	0.0093	1.80	0.032
MYC FISH (amp vs non-amp)	3.20	0.013	3.16	0.015

PFS = progression-free survival

HR = hazard ratio

LC/A = large cell / anaplastic

D/N = desmoplastic / nodular

nuc-neg = nucleonegative

nuc-pos = nucleopositive

amp = amplified

non-amp = not amplified

Table 4
Clinical, pathological, and cytogenetic characteristics of medulloblastomas with *MYC* or *MYCN* amplification or gain

FISH *MYC* AMP/GAIN	FISH *MYCN* AMP/GAIN	β-catenin nuc IR	*CTNNB1* status	XO6 FISH	XO17 FISH	Pathology	M stage	Status
AMP >50%	gain	negative	wt	ND	p loss	LC/A	M0	DoD
AMP >50%	polysomy	negative	wt	other	polysomy	classic	M0	ADF
AMP >50%	ND	negative	ND	other	ND	classic	M0	DoD
AMP 5-50%	negative	negative	wt	other	monosomy	classic	M0	DoD
AMP 5-50%	ND	negative	wt	ND	polysomy with imbalance	classic	M3	ADF
AMP 5-50%	negative	W&S	mut (32gac>gtc)	monosomy	normal	classic	M0	DoD
AMP <5%	negative	negative	wt	other	isodicentric 17q	classic	M0	DoD
gain	negative	negative	wt	other	polysomy	classic	M0	DoD
gain	negative	W&S	mut (33tct>ttt)	monosomy	ND	classic	M0	ADF
gain	polysomy	negative	wt	other	polysomy with imbalance	classic	M3	DoD
gain	polysomy	negative	wt	other	q gain	classic	M0	ADF
gain	polysomy	negative	wt	other	polysomy with imbalance	classic	M0	ADF
gain	polysomy	negative	wt	other	polysomy with imbalance	classic	M0	ADF
polysomy	AMP >50%	negative	wt	other	polysomy with imbalance	classic	M0	ADF
monosomy	AMP >50%	negative	wt	other	polysomy with imbalance	LC/A	M0	DoD
negative	AMP >50%	negative	wt	other	polysomy with imbalance	classic	M0	ADF
negative	AMP >50%	negative	wt	other	normal	classic	M0	DoD
ND	AMP >50%	negative	wt	ND	ND	classic	M0	ADF
negative	AMP >50%	negative	wt	other	polysomy with imbalance	classic	M3	ADF
negative	AMP >50%	negative	wt	other	polysomy with imbalance	classic	M3	ADF
ND	AMP 5-50%	ND	wt	other	ND	LC/A	M3	DoD
polysomy	AMP 5-50%	negative	wt	other	polysomy with imbalance	classic	M0	ADF
negative	AMP <5%	negative	wt	other	normal	classic	M0	ADF
negative	AMP <5%	negative	wt	ND	normal	D/N	M0	DoD
negative	gain	negative	wt	other	normal	LC/A	M3	DoD
negative	gain	negative	wt	other	polysomy with imbalance	classic	M2	ADF
negative	gain	negative	wt	other	polysomy	classic	M0	ADF
polysomy	gain	W&S	mut (32gac>tac)	other	polysomy	classic	M0	ADF
polysomy	gain	negative	wt	other	polysomy with imbalance	classic	M0	DoD
polysomy	gain	negative	wt	other	ND	classic	M0	ADF
polysomy	gain	negative	wt	other	polysomy with imbalance	classic	M0	ADF
polysomy	gain	negative	wt	other	polysomy	LC/A	M3	DoD
polysomy	gain	negative	wt	other	polysomy	classic	M0	DoD

W&S = widespread strong nuclear immunoreactivity
mut = mutation
wt = wild type
AMP = amplification
DoD = died of disease
ADF = alive disease-free
ND = not done

TP53 mutations in favourable risk WNT subtype medulloblastomas

Janet C. Lindsey, Rebecca M. Hill, Hisham Megahed, Meryl E. Lusher, Ed Schwalbe, Michael Cole
Northern Institute for Cancer Research, Newcastle University, Newcastle upon Tyne, U.K.

Twala L. Hogg, Richard J. Gilbertson, David W. Ellison
St. Jude Children's Research Hospital, Memphis, TN, U.S.A.

Simon Bailey, Steven C. Clifford*
Northern Institute for Cancer Research, Newcastle University, Newcastle upon Tyne, U.K.

*Correspondence to:
Professor Steven C. Clifford, Northern Institute for Cancer Research, Newcastle University, Level 5, Sir James Spence Institute, Royal Victoria Infirmary, Newcastle upon Tyne, NE1 4LP, U.K. e-mail: s.c.clifford@ncl.ac.uk.

Acknowledgements
This work was supported by grants from the Samantha Dickson Brain Tumour Research Trust, Cancer Research UK and The Katie Trust. Medulloblastomas investigated in this study include samples provided by the UK Children's Cancer and Leukaemia Group (CCLG) as part of CCLG-approved biological study BS-2007-04.

TO THE EDITOR:

The accurate assignment of disease risk and the delivery of individualised risk-adapted therapies represent major goals in medulloblastoma, the most common malignant brain tumour of childhood. Such strategies have the potential to facilitate reduction of long-term therapy-associated morbidities in favourable risk cases, and therapeutic intensification in high-risk cases. Recent years have witnessed significant advances in our understanding of the molecular pathology of medulloblastoma; validated molecular and pathological prognostic biomarkers have been identified which have the potential to refine disease risk assessment, and are being advanced to define treatment groups in International clinical trials[1].

Aberrations of the TP53 pathway have been widely reported in medulloblastoma, however their prognostic relevance and relationships to other molecular disease features are not well understood[1]. We therefore read with interest the recent report by Tabori et al[2] describing a universally poor prognosis for medulloblastoma patients with tumours harbouring *TP53* gene mutations. In an institutional series of 49 cases from the Hospital for Sick Children, Toronto, this group reported *TP53* mutations in 8 (15%). All mutated cases recurred rapidly following initial therapy and a 5-year overall survival of 0% was reported, compared to 74% in non-mutated cases, which was highly significant in univariate and multivariate analyses ($p<0.003$).

Based on these data, *TP53* mutation status appears to have significant potential as a prognostic biomarker of adverse disease risk. We therefore sought to validate these findings in an independent series of medulloblastomas. We selected a cohort for analysis (n=50) which was representative of all major established clinical (36 classic, 6 large cell / anaplastic, 8 desmoplastic / nodular pathology; 8 metastatic (M2-3), 42 M0-1 disease; 25 male, 25 female; 7 infants <3 years of age at diagnosis, 43 non-infants) and molecular sub-types (see below) of the disease.

TP53 mutations were detected in five cases (10%) within our cohort by direct PCR-based DNA sequence analysis of exons 4-9 using standard methods (Figure 1A)[1,2]. The rate, nature and spectrum of mutations observed were consistent with the findings from Tabori et al[2] and other published studies[1]; all were missense substitutions previously been reported in the UMD *TP53* mutation database (http://p53.free.fr/Database/p53_database_distr.html), examples of homozygous and heterozygous mutations were observed, and mutations were not associated with genetic loss of the entire p-arm of chromosome 17 (assessed as previously described[3]). All *TP53* mutations were found in non-infant cases without evidence of metastatic disease, classified clinically as 'standard risk'. On clinical review of all mutated cases, one was identified as a germline mutation in the context of Li-Fraumeni syndrome (LFS), while all others were somatic mutations associated with sporadic tumours.

We did not observe an adverse prognosis associated with somatic *TP53* mutations (Figure 1B). Indeed, the opposite trend was observed ($p=0.09$; Log-rank test); all *TP53* mutated cases had a favourable outcome and are experiencing durable remissions (5.6 to 11.1 years). The single LFS *TP53* mutated case relapsed and died of disease within 1.1 year of diagnosis with medulloblastoma.

To provide context to these unexpected findings, we next investigated any relationships between *TP53* mutation and the molecular disease subgroups which have been consistently recognised in medulloblastoma. Major subgroups are characterised by mutational activation of the Sonic Hedgehog

(SHH subgroup; ~25% of cases in continuous cohorts) or Wnt/Wingless (WNT subgroup; 10-15% of cases) developmental signalling pathways, signature transcriptional and genomic profiles, and associations with specific clinical disease features and outcomes[3-5]. WNT subgroup cases (n=15) included in our cohort were identified by the presence of *CTNNB1* mutations and chromosome 6 defects (Figure 1C), while SHH subgroup cases (n=12) were identified by their characteristic transcriptional profiles (Figure 1D), using our previously described methods[3,5]. Evidence of *TP53* mutation was found in all disease subgroups (Figure 1E), but somatic mutations were apparently enriched in the WNT subgroup (mutation in 3/15 (20%) WNT vs. 1/34 non-WNT cases; p=0.08, Fisher's exact test). The WNT subgroup has been associated with a favourable prognosis (>90% overall survival) in multiple clinical trial-based studies[6,7]. The segregation of 3 of the 4 cases with somatic *TP53* mutations into the WNT group is therefore consistent with their good prognosis in the present study, and indicates strongly that *TP53* mutations which arise within this subgroup are not associated with a poor prognosis, although the analysis of increased numbers will be required to fully define these relationships.

In addition to the WNT-associated mutations, the *TP53* mutation detected in a LFS medulloblastoma was associated with a poor prognosis and the SHH subtype, and a further mutation was observed in a case outside the SHH and WNT groups. While these numbers do not allow assessment of the prognostic relevance of *TP53* mutations within these groups, they indicate that the impact of *TP53* mutations is dependent on the clinical (i.e. sporadic vs. familial disease) and molecular disease contexts in which they arise. Furthermore, they raise the possibility that undiagnosed LFS may account for a proportion of high-risk *TP53* mutated cases, which could be routinely assessed by parallel analysis of *TP53* mutation status in tumour and constituitional material. Such cohort-related factors are likely to underlie the different prognostic associations observed for *TP53* mutated medulloblastomas in the two cohorts reported to date, and it will be important to understand the molecular context of high-risk associated *TP53* mutations, as observed by Tabori et al[2].

In summary, these data demonstrate *TP53* mutations in medulloblastoma are not universally associated with a poor prognosis, and can occur in the context of favourable-risk WNT subtype cases. Our data reinforce the requirements for (i) independent confirmation of reported prognostic biomarkers, and (ii) a detailed understanding of their biological role and interaction with other molecular markers, prior to their consideration for clinical use. This is particularly the case for *TP53* mutations in medulloblastoma, where their contribution to disease development and utility as a biomarker appears to be pleiotropic and dependent upon the molecular and disease contexts in which mutations arise. While the present and published[2] studies highlight these issues well, both are limited numerically, and comprehensive biological studies involving larger continuous cohorts, ideally derived from uniformly-treated, multi-centre clinical trials, will be necessary for their resolution.

References

1. Pizer BL, Clifford SC: The potential impact of tumour biology on improved clinical practice for medulloblastoma: progress towards biologically driven clinical trials. Br J Neurosurg 23:364-75, 2009

2. Tabori U, Baskin B, Shago M, et al: Universal poor survival in children with medulloblastoma harboring somatic TP53 mutations. J Clin Oncol 28:1345-50, 2010

3. Clifford SC, Lusher ME, Lindsey JC, et al: Wnt/Wingless pathway activation and chromosome 6 loss characterize a distinct molecular sub-group of medulloblastomas associated with a favorable prognosis. Cell Cycle 5:2666-70, 2006

4. Kool M, Koster J, Bunt J, et al: Integrated genomics identifies five medulloblastoma subtypes with distinct genetic profiles, pathway signatures and clinicopathological features. PLoS ONE 3:e3088, 2008

5. Thompson MC, Fuller C, Hogg TL, et al: Genomics identifies medulloblastoma subgroups that are enriched for specific genetic alterations. J Clin Oncol 24:1924-31, 2006

6. Ellison DW, Onilude OE, Lindsey JC, et al: beta-Catenin status predicts a favorable outcome in childhood medulloblastoma: the United Kingdom Children's Cancer Study Group Brain Tumour Committee. J Clin Oncol 23:7951-7, 2005

7. Gajjar A, Chintagumpala M, Ashley D, et al: Risk-adapted craniospinal radiotherapy followed by high-dose chemotherapy and stem-cell rescue in children with newly diagnosed medulloblastoma (St Jude Medulloblastoma-96): long-term results from a prospective, multicentre trial. Lancet Oncol 7:813-20, 2006

Figure legend

Figure 1. Clinical and molecular features of *TP53* mutated medulloblastomas. A. Mutation and clinical characteristics of cases harbouring *TP53* mutations (5 of 50 cases analysed; Het, heterozygous; Hom, homozygous; LCA, large-cell / anaplastic; CLA, classic; M, male; N/A, data not available). **B.** Kaplan-Maier survival plots for cases harbouring spmatic *TP53* mutations versus other cases. **C.** WNT subtype medulloblastomas (15/50) identified by *CTNNB1* (encoding β-catenin) mutation (vertical stacked boxes represent amino acid substitutions detected in individual tumours, shown relative to the wild-type reference sequence) and chromosome 6 loss of heterozygosity (LOH, grey boxes; no LOH, white boxes) analysis. **D.** SHH subtype medulloblastomas (12/50; closed circles) identified using a three-gene mRNA expression signature. **E.** Relationships between *TP53* mutations and the WNT and SHH disease subtypes (*LFS case).

A

TP53 mutation					Clinical data					
Nucleotide	Protein	Mutation status	17p loss	*TP53* database	Li-Fraumeni syndrome	Age at diagnosis (years)	Pathology	Gender	M stage	Clinical disease risk
G 517 A	Val173Met	Het	No	Yes	No	13.4	LCA	M	0	Standard
G 542 A	Arg181His	Hom	N/A	Yes	No	12.7	CLA	M	0	Standard
G 733A	Gly245Ser	Het	No	Yes	No	10.8	CLA	M	0	Standard
G 775 T	Asp259Tyr	Het	No	Yes	No	5.1	CLA	M	0	Standard
C 844 T	Arg282Trp	Hom	No	Yes	Yes	6.0	LCA	M	0	Standard

B

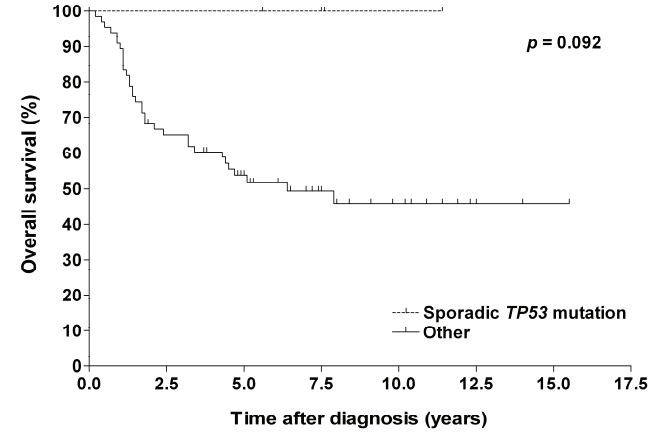

C

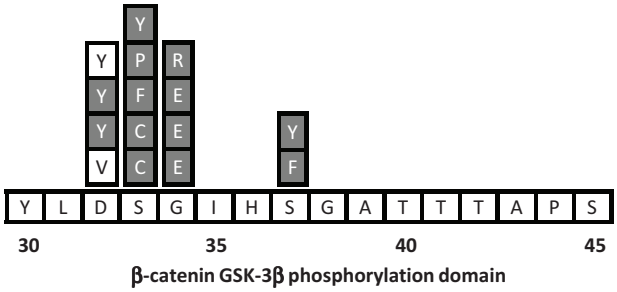

D

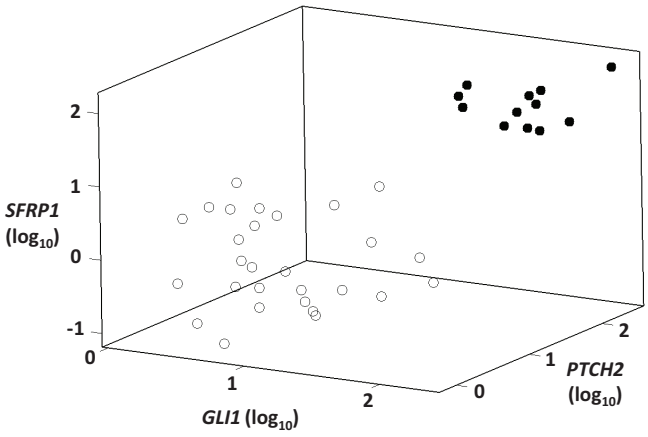

E